

**PHARMACOGENETICS OF
MONOCARBOXYLATE TRANSPORTERS**

LEAN CHOO BEE

NATIONAL UNIVERSITY OF SINGAPORE

2011

DECLARATION

I hereby declare that this thesis is my original work and it has been written by me in its entirety. I have duly acknowledged all the sources of information which have been used in the thesis.

This thesis has also not been submitted for any degree in any university previously.



Lean Choo Bee

10 November 2012

ACKNOWLEDGEMENTS

First of all, I would like to extend my utmost sincere gratitude to my supervisor, Professor Edmund Lee Jon Deoon for his excellent guidance, patience and advice on this project. I also thank him for his continuous moral encouragement and advice when in times of difficulties. Thank you for your unwavering support and kindness over the past five years.

I would like to express my sincere appreciation to all the staff and students of Pharmacogenetics Laboratory. Many thanks for all the invaluable technical assistance and support given to me during the conduct of this project. Thank you for all the kindness, support and laughs. It was my greatest pleasure working with you all.

I would like to thank Investigational Medicine Unit, National University Health System for supporting the clinical study. Besides, I would like to extend my gratitude to Eric Seow (Clinical Trial Coordinator), Grace Xie (Clinical Trial Coordinator) and Angeline Koh (Unit Manager) for their assistance and guidance on the trial matters.

Last but not least, I would like to express my deepest appreciation for my family, especially my late father, for their love and support.

| TABLE OF CONTENTS | Page |
|---|-------------|
| Title page | i |
| Declaration | ii |
| Acknowledgements | iii |
| Table of Contents | iv |
| Research Summary | ix |
| List of Tables | xi |
| List of Figures | xiv |
| List of Abbreviations and Symbols | xvi |
| List of Publications and Manuscripts | xviii |
| Chapter 1. Introduction – Literature Review | 1 |
| 1.1 Roles of Membrane Transporters in the Safety Profile of Drugs | 2 |
| 1.2 Transporter Superfamilies | 7 |
| 1.2.1 The ABC Transporters | 7 |
| 1.2.2 The SLC Transporters | 10 |
| 1.3 The Role of Transporters in Drug Absorption, Distribution, Metabolism and Excretion | 11 |
| 1.3.1 Transporters and Drug Absorption | 11 |
| 1.3.2 Transporters and Drug Metabolism | 15 |
| 1.3.3 Transporters and Renal Elimination | 14 |
| 1.3.4 Transporters and Tissue Distribution | 14 |
| 1.3.5 Food and Drug Interactions | 17 |
| 1.3.6 Summary of Role of Transporters in Drug Distribution | 20 |
| 1.4 Overview of Monocarboxylate Transporter Family | 23 |
| 1.4.1 Monocarboxylate Transporter 1-4 | 28 |
| 1.4.1.1 Monocarboxylate Transporter 1 (SLC16A1) | 28 |
| 1.4.1.2 Monocarboxylate Transporter 2 (SLC16A7) | 34 |
| 1.4.1.3 Monocarboxylate Transporter 3 (SLC16A8) | 34 |
| 1.4.1.4 Monocarboxylate Transporter 4 (SLC16A3) | 35 |
| 1.4.2 Tissue Distribution of MCTs | 36 |
| 1.4.3 Intracellular Lactate Shuttle | 41 |
| 1.4.4 Biochemical and Structural Aspects | 46 |
| 1.4.5 MCT Mutation and Genetic Syndromes | 49 |
| 1.4.6 Regulation of MCT Isoforms | 50 |

| | |
|--|-----|
| 1.4.7 Roles of MCTs in Drug and Xenobiotic Distribution | 53 |
| 1.5 Thesis Rationale | 54 |
| 1.6 Specific Aims of the Study | 57 |
| Chapter 2. Population Genotyping Data of PGL Study Population | 59 |
| Overview | 60 |
| 2.1 Materials and Methods | 62 |
| 2.1.1 Study Populations | 62 |
| 2.1.2 DNA Extraction | 62 |
| 2.1.3 Primer Selection | 64 |
| 2.1.3.1 Monocarboxylate Transporter 1 | 64 |
| 2.1.3.2 Monocarboxylate Transporter 4 | 64 |
| 2.1.4 Polymerase Chain Reaction Amplification | 69 |
| 2.1.5 Agarose Gel Electrophoresis | 69 |
| 2.1.6 DNA Sequencing | 70 |
| 2.1.6.1 PCR Product Clean Up | 70 |
| 2.1.6.2 Cycle Sequencing | 70 |
| 2.1.6.3 DNA Precipitation | 71 |
| 2.1.7 Mutational Analysis of DNA Sequences | 71 |
| 2.2 Results | 73 |
| 2.2.1 Genetic variations in the SLC16A1 gene in the Chinese and Indian populations of Singapore | 73 |
| 2.2.1.1 Overview of Genetic Screening Data | 73 |
| 2.2.1.2 Genetic Variants Detected in the Promoter and 5'-UTR Regions of SLC16A1 gene | 78 |
| 2.2.1.3 Genetic Variants Detected in the Exon, Intron and 3'-UTR Regions of SLC16A1 gene | 92 |
| 2.2.1.4 Linkage Disequilibrium (LD) Analysis | 105 |
| 2.2.1.5 Haplotype Construction and Frequency Estimation | 109 |
| 2.2.2 Genetic Variations in the MCT4 (SLC16A3) Gene in the Chinese and Indian Populations of Singapore | 113 |
| 2.2.2.1 Overview of Genetic Screening Data | 113 |
| 2.2.2.2 Genetic Variants Detected in the Promoter and 5'-UTR Regions of Transcript Variant 1 of SLC16A3 gene | 126 |
| 2.2.2.3 Genetic Variants Detected in the Promoter and 5'-UTR Regions of Transcript Variant 3 of SLC16A3 gene | 144 |

| | |
|--|-----|
| 2.2.2.4 Genetic Variants Detected in the Exon, Intron and 3'-UTR Regions of <i>SLC16A3</i> gene | 155 |
| 2.2.2.5 Linkage Disequilibrium (LD) Analysis | 177 |
| 2.2.2.6 Haplotype Construction and Frequency Estimation | 184 |
| 2.3 Discussion | 187 |
| 2.3.1 Genetic Variations in the MCT1 (SLC16A1) Gene in the Chinese and Indian Population of Singapore | 191 |
| 2.3.2 Genetic Variations in the MCT4 (SLC16A3) Gene in the Chinese and Indian Population of Singapore | 198 |
| Chapter 3. The Inhibitory Effects of Pharmaceutical Agents and Phytochemical Compounds on Human Monocarboxylate Transporter 1 | 206 |
| Overview | 207 |
| 3.1 Materials and Methods | 208 |
| 3.1.1 Materials | 208 |
| 3.1.2 Red Blood Cells Lactate Influx Assay | 208 |
| 3.1.2.1 Subjects | 208 |
| 3.1.2.2 Preparation of RBCs for Lactate Influx Assay | 208 |
| 3.1.2.3 Total Lactate Influx | 210 |
| 3.1.2.4 Time-dependent Total Lactate Influx | 210 |
| 3.1.2.5 MCT1-mediated Lactate Influx | 211 |
| 3.1.2.6 Calculation of Lactate Influx | 211 |
| 3.1.2.7 Data Analysis | 211 |
| 3.1.2.8 Statistical Analysis | 212 |
| 3.2 Results | 213 |
| 3.2.1 Time dependent Lactate Influx | 213 |
| 3.2.2 Human Erythrocyte Lactate Transport Activity | 215 |
| 3.2.3 Inhibitory Effects of Phytochemical and Pharmacological Agents on L-lactate Influx on Human Erythrocyte | 217 |
| 3.2.3.1 The inhibitory effects of various compounds on L-lactate uptake | 217 |
| 3.2.3.2 The Inhibitor Potencies of Selected Compounds | 217 |
| 3.2.4 Graphic Determination of Inhibitor Type | 225 |
| 3.3 Discussion | 233 |
| 3.3.1 Human Erythrocyte L-lactate Uptake | 234 |

| | |
|--|-----|
| 3.3.2 Inhibitory Effects of Dietary and Pharmacological Compounds on L-lactate Influx | 235 |
| 3.3.3 Summary | 241 |
| Chapter 4. Interindividual Variation in Total and Carrier-mediated Lactate Influx into Human Erythrocytes of Local Chinese Population | 242 |
| Overview | 243 |
| 4.1 Materials and Methods | 244 |
| 4.1.1 Subjects | 244 |
| 4.1.2 Erythrocytes Lactate Influx Assay | 244 |
| 4.1.2.1 Preparation of RBCs for Lactate Influx Assay | 244 |
| 4.1.2.2 Total Lactate Influx | 245 |
| 4.1.2.3 MCT1-mediated Lactate Influx | 246 |
| 4.1.2.4 Calculation of Lactate Influx | 246 |
| 4.1.2.5 Data Analysis | 247 |
| 4.1.3 DNA Amplification | 247 |
| 4.1.3.1 DNA extraction | 247 |
| 4.1.3.2 Polymerase Chain Reaction Amplification | 248 |
| 4.1.3.3 Agarose Gel Electrophoresis | 249 |
| 4.1.4 DNA Sequencing | 249 |
| 4.1.4.1 PCR Product Clean Up | 249 |
| 4.1.4.2 Cycle Sequencing | 249 |
| 4.1.4.3 DNA Precipitation | 250 |
| 4.1.4.4 Mutational Analysis of DNA Sequences | 250 |
| 4.1.5 Statistical Analysis | 251 |
| 4.2 Results | 252 |
| 4.2.1 RBC Lactate Transport Activity | 252 |
| 4.2.2 Polymorphism-phenotype association of SLC16A1 gene | 256 |
| 4.3 Discussion | 266 |
| 4.3.1 Interindividual variation in Total and MCT1-mediated lactate influx | 267 |
| 4.3.2 Polymorphism-phenotype association of MCT1 gene | 268 |
| 4.3.3 Summary | 270 |

| | |
|---|-----|
| Chapter 5. A Randomized Crossover Study to Evaluate the Potential Influence of MCT1 and Its Inhibitor, Diflunisal, on the Distribution of Lactate in Plasma and Erythrocyte in Healthy Male Adults | 271 |
| Overview | 272 |
| 5.1 Materials and Methods | 273 |
| 5.1.1 Study Design | 273 |
| 5.1.2 Subject Selection | 276 |
| 5.1.3 Sample Size Assumptions | 276 |
| 5.1.4 Blood Sampling | 277 |
| 5.1.5 Lactate Analysis | 277 |
| 5.1.6 Statistical analysis | 278 |
| 5.2 Results | 279 |
| 5.2.1 Plasma and Erythrocyte Lactate Levels | 279 |
| 5.2.2 Plasma to RBC Lactate Ratio | 283 |
| 5.3 Discussion | 285 |
| 5.3.1 The influence of diflunisal on L-lactate distribution in blood | 286 |
| 5.3.2 Summary | 291 |
| Chapter 6. Conclusion | 292 |
| 6.1 Conclusion | 297 |
| Chapter 7. Future work | 300 |
| 7.1 Future direction | 301 |
| References | 303 |
| Appendix I | 319 |
| Appendix II | 323 |
| Appendix III | 356 |

RESEARCH SUMMARY

In this study, we studied the effect of genetic polymorphism and drug/food interaction on members of SLC superfamily, *SLC16A* family of proton-linked membrane transport proteins known as monocarboxylate transporters (MCTs). The genetic polymorphism in *SLC16A1* and *SLC16A3* genes that may be present in the ethnic Chinese (n = 95) and Indian (n = 96) groups of Singapore population have been examined. The promoter, coding region and exon-intron junctions of the *SLC16A1* and *SLC16A3* genes encoding the MCT1 and MCT4 transporters were screened for genetic variations by DNA sequencing. A total of 21 genetic variations, including 14 novel ones, were found in *SLC16A1* gene. Of the 3 nonsynonymous variants, the 303T>G (Ile101Met) was predicted by PolyPhen and SIFT as having a potentially detrimental effect on MCT1 activity. In contrast, the 1282 G>A (Val428Ile) and 1470 T>A (Asp490) were speculated to be benign. A total of 46 genetic variants were detected in *SLC16A3* gene, of which 33 are novel. Among the 5 nonsynonymous variants, only 44 C>T (Ala15Val) was predicted by both bioinformatics algorithms as having damaging effect on MCT4 protein function, whereas 55 G>A (Gly19Ser), 574G>A (Val192Met) and 916G>A (Gly306Ser) had conflicting results between the SIFT and PolyPhen programs. Lastly, the 641C>T (Ser214Phe) was predicted to be a benign variant.

A common MCT1 polymorphism, 1470 T>A (Asp490Glu), has been identified in both ethnic Chinese and Indian groups. Given that MCT1 is the only MCT isoform found in the human erythrocyte and contributes up to 90% of lactate influx, we chose to study human erythrocytes to investigate the effect of this polymorphism in

the MCT1-mediated lactate influx. The 10-assay grouped data suggests that human MCT1 system exhibited a low affinity but high capacity transport mechanism for the transport of lactate into red blood cells. Besides, low interindividual variations were observed in the total- and MCT1-mediated lactate influx into human erythrocytes in the local Chinese population. In addition, the data shows that T allele of 1470 T>A (Asp490Glu) may have a defective effect in transport function and appear to have a lower transport activity. However, additional studies involving larger samples are required to verify the impact of 1470 T>A (Asp490Glu) polymorphism in MCT1 transporter activity.

The diet-interaction via MCT1 inhibition may affect lactate shuttling and drug disposition. Therefore, the effects of various dietary and pharmacological agents on MCT1 were examined on human erythrocyte lactate influx. Of these, diflunisal, diclofenac, mefenamic acid, meclofenamic acid, tolfenamic acid, luteolin, etodalac, phloretin and morin exhibited strong inhibition on MCT1-mediated L-lactate influx. The inhibitory concentrations of some of these tested NSAIDs are in the range of physiologically relevant concentrations that are achievable from the oral intake. Therefore, a clinical trial was designed to investigate the effect of one of the tested NSAIDs, diflunisal, on lactate distribution between plasma and erythrocytes. In this study, the subjects were pre-treated with 5 oral doses of placebo or diflunisal (500mg) followed by a single dose infusion of sodium lactate at the infusion rate of 5.6mg/kg/min for 30 min. We observed small differences between placebo- and diflunisal-treated groups. These differences, however, were not statistically significant. The data suggests that given dose of diflunisal was insufficient to inhibit lactate transport in the blood for this study.

LIST OF TABLES

| Table No. | Title | Page |
|-----------|---|------|
| 1 | The ten most highly expressed ABC and SCL transporters mRNAs in human tissues | 5 |
| 2 | The ratio of the concentrations in different tissues for various substrates, between mdr knockout (-/-) and wildtype (+/+) mice | 14 |
| 3 | Drug-drug interactions or toxicities involving drug transporters | 20 |
| 4 | Tissue-to-plasma concentration ratio (Kp) of drug substrates in wild-type (wt) and knockout mice (ko) | 22 |
| 5 | Human SLC16 family members | 26 |
| 6 | Substrate and inhibitor affinities for monocarboxylate transporter 1 in various expression systems | 31 |
| 7 | The effects of mutating charged residues in potential TM helices of MCT1 on its plasma membrane expression and activity | 48 |
| 8 | Primer sequences and PCR conditions used for the analysis of promoter, 5'-UTR, coding and 3'-UTR regions of SLC16A1 gene | 66 |
| 9 | Primer sequences and PCR conditions used for the analysis of promoter, 5'-UTR, coding and 3'-UTR regions of transcript variants of SLC16A3 gene | 67 |
| 10 | The description and frequency of SLC16A1 gene polymorphisms identified in the Chinese and Indian populations of Singapore | 74 |
| 11 | SLC16A1 data quality check: goodness of fit to Hardy Weinberg Equilibrium | 76 |
| 12 | SLC16A1 inter-ethnic difference in allele frequency | 77 |
| 13 | The predictive effects of SNPs on the transcription factor binding sites of SLC16A1 gene | 81 |
| 14 | Pair-wise linkage disequilibrium (D') coefficients between SLC16A1 bi-allelic promoter polymorphisms in ethnic Indian population | 106 |
| 15 | Pair-wise linkage disequilibrium (D') coefficients between SLC16A1 bi-allelic coding region polymorphisms in ethnic Chinese population | 107 |
| 16 | Pair-wise linkage disequilibrium (D') coefficients between SLC16A1 bi-allelic coding region polymorphisms in ethnic Indian population | 108 |
| 17 | Haplotype structure defined by 3 commonest SNPs in the SLC16A1 5' flanking coding region in Singapore population | 112 |
| 18 | The description and frequency of SLC16A3 polymorphisms detected in the promoter and 5'-UTR regions of three transcript variants identified in the Chinese and Indian populations of Singapore | 116 |
| 19 | The description and frequency of SLC16A3 variations detected in the coding and 3'-UTR regions of three transcript variants identified in the Chinese and Indian populations of Singapore | 118 |
| 20 | The SLC16A3 promoter transcript variant 1 population data quality check: goodness of fit to Hardy Weinberg Equilibrium | 120 |
| 21 | The SLC16A3 promoter transcript variant 3 population data quality check: goodness of fit to Hardy Weinberg Equilibrium | 121 |
| 22 | The SLC16A3 coding region population data quality check: goodness of fit to Hardy Weinberg Equilibrium | 122 |
| 23 | SLC16A3 inter-ethnic difference in allele frequency of polymorphisms in transcript variant 2 of promoter region | 123 |
| 24 | SLC16A3 inter-ethnic difference in allele frequency of polymorphisms in transcript variant 4 of promoter region | 124 |

| | | |
|----|---|-----|
| 25 | The inter-ethnic difference in allele frequency of polymorphisms in the coding region of SLC16A3 | 125 |
| 26 | The predictive effects of SNP on the transcription factor binding sites of MCT4 | 127 |
| 27 | Pair-wise linkage disequilibrium (D') coefficients between SLC16A3 bi-allelic promoter (transcript variant 1) polymorphisms in ethnic Chinese population | 178 |
| 28 | Pair-wise linkage disequilibrium (D') coefficients between SLC16A3 bi-allelic promoter (transcript variant 1) polymorphisms in ethnic Indian population | 179 |
| 29 | Pair-wise linkage disequilibrium (D') coefficients between SLC16A3 bi-allelic promoter (transcript variant 3) polymorphisms in ethnic Chinese population | 180 |
| 30 | Pair-wise linkage disequilibrium (D') coefficients between SLC16A3 bi-allelic promoter (transcript variant 3) polymorphisms in ethnic Indian population | 181 |
| 31 | Pair-wise linkage disequilibrium (D') coefficients between SLC16A3 bi-allelic coding region polymorphisms in ethnic Chinese population | 182 |
| 32 | Pair-wise linkage disequilibrium (D') coefficients between SLC16A3 bi-allelic coding region polymorphisms in ethnic Indian population | 183 |
| 33 | Haplotype structure defined by 3 commonest SNPs in the SLC16A3 5' flanking promoter region of transcript variant 1 in Singapore population | 188 |
| 34 | Haplotype structure defined by 3 commonest SNPs in the SLC16A3 5' flanking promoter region of transcript variant 3 in Singapore population | 189 |
| 35 | Reported SLC16A1 genetic polymorphism allele frequencies | 196 |
| 36 | Reported SLC16A3 genetic polymorphism allele frequencies | 203 |
| 37 | The inhibitory effects of various compounds on the uptake of L-lactate in human erythrocytes | 218 |
| 38 | The IC50 values of tested compounds on the uptake of L-lactate (5 mM) by human erythrocytes | 224 |
| 39 | The Ki values and mode of inhibitions of tested compounds on the uptake of L-lactate by human erythrocytes | 232 |
| 40 | The mode of inhibition of tested compounds determined by Prism mixed-model inhibition model. The mode of inhibition is determined by the Alpha value | 232 |
| 41 | The total lactate influx into RBC of local Chinese population | 254 |
| 42 | The Monocarboxylate transporter 1- mediated lactate influx into RBC of local Chinese | 255 |
| 43 | The Mann Whitney U tests were performed to analyze the differences between TA and AA genotypes of the 1470 T>A (Asp490Glu) polymorphism in total lactate influx | 259 |
| 44 | The Mann Whitney U tests were performed to analyze the differences between TA and AA genotypes of the 1470 T>A (Asp490Glu) polymorphism in MCT1-mediated lactate influx | 261 |
| 45 | The Mann Whitney U tests were performed to analyze the differences of the Km between TA and AA genotypes of the 1470 T>A (Asp490Glu) polymorphism | 263 |
| 46 | The Mann Whitney U tests were performed to analyze the differences of the Vmax between TA and AA genotypes of the 1470 T>A (Asp490Glu) polymorphism | 265 |

| | | |
|----|---|-----|
| 47 | Study Plan- Period 1 | 274 |
| 48 | Study Plan- Period 2 | 275 |
| 49 | The paired t tests were performed to test for the effect of diflunisal in L-lactate distribution in plasma and RBC | 281 |
| 50 | Pharmacokinetic parameters for L-lactate in placebo- and diflunisal-treated groups | 282 |
| 51 | The paired t tests were performed to analyze the differences of plasma to RBC lactate ratio between placebo and diflunisal groups | 284 |
| 52 | Summary of data | 297 |

LIST OF FIGURES

| Figure | Title | Page |
|--------|---|------|
| 1 | The proposed topology of the monocarboxylate transporter (MCT) family | 30 |
| 2 | Relative distribution of MCT1, MCT2 and MCT4 in 15 frozen human tissues | 39 |
| 3 | Hypothesized routes of lactate transportation and compartmentalization of lactate metabolism in human skeletal muscle cells | 40 |
| 4 | Schematic diagram of cell-to-cell lactate shuttle | 45 |
| 5 | Nucleotide sequence of the 5'-flanking region of the SLC16A1 gene and location of polymorphisms identified | 79 |
| 6 | Topological location of SLC16A1 non-synonymous mutations detected in this study and retrieved from the dbSNP database | 93 |
| 7 | Ethnic distribution of SLC16A1 haplotypes | 111 |
| 8 | Six transcripts have been described for SLC16A3 gene | 115 |
| 9 | Topological location of SLC16A3 non-synonymous mutations detected in this study and retrieved from the dbSNP database | 156 |
| 10 | Ethnic distribution of SLC16A3 haplotypes in the promoter region of transcript variant 1 | 186 |
| 11 | Ethnic distribution of SLC16A3 haplotypes in the promoter region of transcript variant 3 | 187 |
| 12 | Time course experiment depicting total lactate influx into RBCs into human red blood cells | 214 |
| 13 | Effect of lactate concentration and MCT inhibitor on the lactate influx into RBCs | 216 |
| 14 | Inhibitory effects of NSAIDs (a) statins (b) and phytochemicals (c) on L-lactate (5 mM) uptake by human erythrocytes | 219 |
| 15 | Lineweaver-Burk plots of uptake of L-lactate at several fixed concentrations of inhibitor of interest | 227 |
| 16a | Total lactate influx into RBC of local Chinese population | 253 |
| 16b | Monocarboxylate transporter 1- mediated lactate influx into RBC of local Chinese population | 253 |
| 17 | The total lactate influx into RBC at four external L-lactate concentration in TA and AA groups of SLC16A1 gene | 258 |
| 18 | The MCT1-mediated lactate influx into RBC at four external L-lactate concentration in TA and AA groups of SLC16A1 gene | 260 |
| 19 | The constant of Michaelis-Menten (Km) for the total and MCT1-mediated lactate influx in in TA and AA groups of SLC16A1 gene | 262 |
| 20 | The maximal lactate transport capacity (Vmax) for the total and MCT1-mediated lactate influx in in TA and AA groups of SLC16A1 gene | 264 |
| 21 | The change of plasma and RBC lactate levels in the subjects pretreated with placebo and diflunisal during lactate infusion | 281 |

| | | |
|----|--|-----|
| | and during recovery | |
| 22 | The total area under the curve (AUC) of plasma and RBC lactate levels in the subjects pretreated with placebo and diflunisal | 282 |
| 23 | Plasma to RBC lactate ratio during exogenous lactate infusion and during recovery period | 284 |
| 24 | The illustration figure of diflunisal in inhibiting the L-lactate influx into human RBC | 286 |

LIST OF ABBREVIATIONS AND SYMBOLS

| | |
|-------|--|
| ABC | ATP-binding cassette |
| ATP | Adenosine triphosphate |
| BCRP | Breast Cancer Resistance Protein |
| cAMP | Cyclic adenosine monophosphate |
| CHC | alpha-cyano-4-hydroxycinnamic |
| CsA | Cyclosporin-A |
| DIDS | 4,4'-Diisothiocyano-2,2'-stilbenedisulfonic acid |
| ELT | Leiomyoma-derived cell line |
| HIV | Human immunodeficiency virus |
| KO | Knockout |
| MCT | Monocarboxylate transporter |
| MDR | Multiple drug resistance |
| mRNA | messenger ribonucleic acid |
| MRP | Multidrug resistant protein |
| MsrA | Methicillin-resistant <i>Staphylococcus aureus</i> |
| NSAID | Nonsteroidal anti-inflammatory agents |
| OAT | Organic anion transporter |
| OATP | Organic anion-transporting polypeptide |
| OD | Optical density |
| pCMBS | 4-Chloromercuribenzoic acid |
| PCR | Polymerase chain reaction |
| PGL | Pharmacogenetics lab |
| P-gp | P-glycoprotein |
| PKA | Protein kinase A |

| | |
|------|---------------------------------|
| PKC | Protein kinase C |
| RD | Rhabdomyosarcoma cell line |
| SLC | Solute carrier family |
| SNP | Single nucleotide polymorphism |
| TAT1 | T-type amino acid transporter 1 |
| TMD | Transmembrane domain |
| UTR | Untranslated region |
| WT | Wildtype |

LIST OF PUBLICATIONS

1. Fock KM, Ang TL, Bee LC, Lee EJ. Proton pump inhibitors: do differences in pharmacokinetics translate into differences in clinical outcomes? *Clin Pharmacokinet.* 2008;47(1):1-6.
2. Edmund Jon Deon LEE, Choo Bee LEAN, Lie Michael George LIMENTA. Role of membrane transporters in the safety profile of drugs. *Expert Opin Drug Metab Toxicol.* 2009;5(11):1369-83.
3. Choo Bee LEAN, Edmund Jon Deon LEE. Genetic Variations of the MCT1 (SLC16A1) Gene in the Chinese Population of Singapore. *Drug Metab Pharmacokinet.* 2009;24(5):469-74.
4. Choo Bee LEAN, Edmund Jon Deon LEE. Genetic Variations of the MCT4 (SLC16A3) Gene in the Chinese Population of Singapore (Accepted)
5. Choo Bee LEAN, Edmund Jon Deon LEE. The Inhibitory Effects of Pharmaceutical Agents and Phytochemical Compounds on Human Monocarboxylate Transporter 1(submitted for publication)

CHAPTER 1
LITERATURE REVIEW AND STUDY OBJECTIVES

1.1 ROLES OF MEMBRANE TRANSPORTERS IN THE SAFETY PROFILE OF DRUGS

It has increasingly been recognized that few molecules move across the cell membrane without the assistance of transporter proteins. Singer and Nicholson (1972) conceptualized the idea of the plasma membrane being a fluid dynamic entity [1]. The cell membrane consists primarily of the amphipathic lipid bilayer, by which the arrangement of hydrophilic heads and hydrophobic tails of the lipid bilayer prevents polar solutes (e.g. monocarboxylates, carbohydrates, proteins, ions, nucleic acids and amino acids) from diffusing across the membrane, but generally allows for the passive diffusion of hydrophobic molecules. Therefore, the movement of polar molecules across the amphipathic lipid bilayer often involves interaction with some sort of active transport processes. Transmembrane transport is mediated by specific integral membrane proteins called transporters. Although non-polar solutes can diffuse across the lipid bilayer, it is now known that the transport of some hydrophobic molecules is mediated by transporters. For example, the cellular trafficking of cholesterol, phospholipid and other endogenous lipophilic substrates is mediated by ABCA1 transporter. Transporters are categorized into passive and active transporters. Passive transporters, also known as facilitated transporters, allow solutes to flow downhill with their electrochemical gradients. Active transporters, in contrast, allow the movement of solutes against their concentration gradients. The characterization of these transporters and their roles in cellular physiology and drug disposition has been the focus of intensive research for many years.

Crane was the first to formulate the cotransport concept to explain active transport in 1961 [2]. He demonstrated that sodium-glucose cotransport as the mechanism for intestinal glucose absorption and his findings eventually led to the cloning of the glucose transporter [3]. However, it was the discovery of the P-glycoprotein (ABCB1) that proved pivotal in our understanding of the vital role drug transporters play in drug disposition that largely determines the pharmacodynamics and pharmacokinetics of drugs [4]. ABCB1 is an ATP-dependent efflux pump with broad substrate specificity and is expressed primarily in certain cell types found in the liver, pancreas, kidney, colon, and blood brain barrier [5], and has likely evolved as a protective mechanism against harmful xenobiotic compounds. The P-glycoprotein transporter was first cloned and characterized by using its ability to confer cellular resistance to a wide range of chemotherapeutic drugs [4]. It causes decreased drug accumulation in multidrug-resistant cells and developed resistance to anticancer drugs. The discovery of P-glycoprotein's role in cellular resistance was the starting point to evaluate the role of transporters as important determinants of drug efficacy and toxicity.

The pharmacological compound must reach the target organ at sufficient concentrations in order for it to exert an effect. Since the discovery of the ABCB1, numerous similar transporters have been identified and gathered into a superfamily of ABC (ATP binding cassette) transporters. Meanwhile, another large superfamily of transporter called the SLC (solute carrier) transporters have also been identified since the discovery of the glucose transporter. These transporters are selectively expressed in many tissues and served a fundamental function in regulating the movement of endogenous and exogenous chemicals across both cellular and tissue

membranes, and play critical roles in determining drug efficacy and toxicity. Therefore, the assessment of the protein levels and transport capacity of each ABC and SLC transporter in target organs are therefore critical towards determining the drug disposition. Nishimura and Naito have done an excellent job in evaluating and detailing the levels of tissue-specific mRNA expression profiles of ABC and SLC transporters [6, 7]. A summary of the ten most highly expressed ABC and SLC transporter mRNAs in human tissues has been presented in **Table 1**. The studies conducted by Nishimura and Naito have comprehensively profiled the gene expression level of a large spectrum of transporters across various tissues and provided a framework for understanding the fundamental functions of transporters in regulating the movement of pharmaceutical compounds in and out of the cell.

Table 1. The ten most highly expressed ABC and SCL transporters mRNAs in human tissues (Adapted from Nishimura and Naito, 2005; Nishimura and Naito, 2008 [6, 7])

| Tissue | Expression of Human ABC Transporters in Various Tissues | Expression of Human SLC Transporters in Various Tissues |
|-----------------------|--|---|
| Adrenal gland | ABCA1, ABCC3, ABCB1, ABCD1, ABCA8, ABCG1, ABCF2, ABCF1, ABCA6, ABCD3 | SLC16A9, SLC40A1, SLC25A3, SLC25A37, SLC39A9, SLC24A6, SLC3A2, SLC30A1, SLC6A6, SLC25A44 |
| Bladder | NA | SLC25A6, SLC25A23, SLC25A3, SLC40A1, SLC25A5, SLC25A24, SLC8A1, SLC25A44, SLC25A37, SLC39A9 |
| Bone Marrow | ABCB10, ABCF1, ABCD3, ABCF2, ABCC4, ABCE1, ABCB2, ABCC1, ABCC10, ABCB8 | SLC25A37, SLC4A1, SLC40A1, SLC16A3, SLC25A6, SLC25A39, SLC2A3, SLC25A3, SLC25A5, SLC30A6 |
| Brain | ABCA2, ABCA5, ABCF2, ABCD2, ABCF1, ABCD3, ABCE1, ABCC5, ABCB9, ABCB8 | SLC22A17, SLC25A23, SLC39A10, SLC25A6, SLC17A7, SLC25A3, SLC1A2, SLC25A44, SLC25A5, SLC12A5 |
| Colon | ABCD3, ABCC3, ABCB2, ABCC7, ABCA1, ABCF2, ABCA5, ABCE1, ABCD1, ABCB10 | SLC25A6, SLC25A5, SLC25A3, SLC39A5, SLC25A23, SLC39A9, SLC25A24, SLC16A3, SLC25A44, SLC30A6 |
| Heart | ABCA8, ABCF2, ABCC9, ABCD3, ABCF1, ABCE1, ABCA9, ABCA5, ABCB1, ABCD1 | SLC25A3, SLC8A1, SLC16A7, SLC40A1, SLC25A30, SLC25A23, SLC25A11, SLC25A6, SLC25A37, SLC25A5 |
| Kidney | ABCD3, ABCC4, ABCF2, ABCF1, ABCB1, ABCC2, ABCE1, ABCA2, ABCC3, ABCB8 | SLC39A5, SLC25A6, SLC25A5, SLC5A12, SLC7A7, SLC12A1, SLC27A5, SLC34A1, SLC3A2, SLC25A3 |
| Liver | ABCA6, ABCG8, ABCB11, ABCB4, ABCG5, ABCA1, ABCD3, ABCC2, ABCC9, ABCF1 | SLC22A1, SLC40A1, SLC2A2, SLC25A5, SLC13A5, SLC39A5, SLC38A3, SLC22A7, SLC25A3, SLC39A9 |
| Lung | ABCA6, ABCA1, ABCB2, ABCF1, ABCC4, ABCA8, ABCF2, ABCD3, ABCG1, ABCE1 | SLC40A1, SLC34A2, SLC6A4, SLC25A6, SLC2A3, SLC39A8, SLC16A3, SLC25A37, SLC25A24, SLC25A3 |
| Mammary gland | NA | SLC25A3, SLC25A37, SLC25A6, SLC40A1, SLC25A39, SLC25A44, SLC37A3, SLC12A2, SLC20A2, SLC16A3 |
| Ovary | NA | SLC25A6, SLC40A1, SLC30A6, SLC25A37, SLC16A9, SLC25A3, SLC25A5, SLC25A23, SLC25A24, SLC24A6 |
| Pancreas | ABCC7, ABCF1, ABCA5, ABCD3, ABCE1, ABCF2, ABCC3, ABCD1, ABCC1, ABCC10 | SLC25A6, SLC25A5, SLC39A5, SLC40A1, SLC25A3, SLC39A9, SLC39A8, SLC30A6, SLC30A1, SLC39A6 |
| Peripheral leukocytes | ABCB2, ABCF1, ABCD1, ABCF2, ABCE1, ABCB3, ABCB10, ABCA2, ABCC1, ABCA1 | SLC25A37, SLC16A3, SLC25A6, SLC2A3, SLC25A3, SLC25A44, SLC25A5, SLC40A1, SLC30A6, SLC7A7 |
| Placenta | ABCD1, ABCF1, ABCA1, ABCB8, ABCF2, ABCG2, ABCG1, ABCB2, ABCD3, ABCC10 | SLC2A1, SLC40A1, SLC25A6, SLC3A2, SLC39A9, SLC7A2, SLC30A6, SLC39A6, SLC25A5, SLC39A8 |

The ten most highly expressed ABC and SCL transporters mRNAs in human tissues. The transporter expression level is ranked from highest to lowest.

NA= The mRNA expression level of transporters has not been analyzed in this target tissue.

ABC=ATP-binding cassette

SLC= Solute carrier

Table 1. (continue)

| | | |
|-----------------|---|--|
| Prostate | ABCC4, ABCF1, ABCD3, ABCF2, ABCA5, ABCE1, ABCB2, ABCC1, ABCA1, ABCB10 | SLC30A4, SLC39A10, SLC39A6, SLC25A6, SLC25A37, SLC39A9, SLC40A1, SLC14A1, SLC25A3, SLC25A23 |
| Retina | NA | SLC16A3, SLC25A6, SLC25A3, SLC23A2, SLC25A44, SLC25A5, SLC30A6, SLC16A14, SLC40A1, SLC25A23 |
| Salivary gland | ABCF1, ABCF2, ABCD3, ABCA6, ABCE1, ABCC7, ABCD1, ABCB2, ABCB10, ABCG1 | SLC25A6, SLC39A9, SLC25A5, SLC13A5, SLC25A3, SLC31A1, SLC5A5, SLC9A1, SLC25A23, SLC25A37 |
| Skeletal muscle | ABCF1, ABCF2, ABCA5, ABCD1, ABCD3, ABCC1, ABCC9, ABCA6, ABCB10, ABCA1 | SLC16A3, SLC25A3, SLC25A11, SLC25A4, SLC40A1, SLC25A23, SLC25A30, SLC19A2, SLC25A9, SLC25A6 |
| Small intestine | ABCD1, ABCD3, ABCF1, ABCG5, ABCB2, ABCF2, ABCG8, ABCB10, ABCC3, ABCG2 | SLC5A1, SLC25A6, SLC40A1, SLC25A5, SLC25A3, SLC39A5, SLC2A5, SLC39A9, SLC25A24, SLC13A2 |
| Smooth muscle | NA | SLC25A6, SLC25A23, SLC25A3, SLC8A1, SLC40A1, SLC25A5, SLC30A6, SLC12A2, SLC25A24, SLC25A37 |
| Spinal cord | ABCA2, ABCD3, ABCA8, ABCF1, ABCA6, ABCA1, ABCE1, ABCA5, ABCB2, ABCB8 | SLC22A17, SLC25A6, SLC39A10, SLC14A1, SLC16A9, SLC25A23, SLC39A9, SLC25A3, SLC39A6, SLC25A44 |
| Spleen | ABCB2, ABCF1, ABCF2, ABCG1, ABCA1, ABCD1, ABCE1, ABCC1, ABCD3, ABCB10 | SLC25A6, SLC16A9, SLC39A10, SLC25A5, SLC16A3, SLC25A3, SLC25A37, SLC30A6, SLC39A9, SLC40A1 |
| Stomach | ABCD3, ABCF1, ABCC3, ABCF2, ABCE1, ABCB2, ABCA6, ABCA5, ABCC1, ABCA8 | SLC25A6, SLC25A5, SLC25A3, SLC40A1, SLC25A37, SLC39A9, SLC16A3, SLC30A6, SLC25A23, SLC39A7 |
| Testis | ABCF1, ABCF2, ABCD1, ABCB9, ABCE1, ABCC1, ABCD3, ABCA5, ABCA8, ABCC12 | SLC25A37, SLC30A6, SLC16A3, SLC30A4, SLC30A1, SLC25A33, SLC40A1, SLC2A5, SLC16A9, SLC25A6 |
| Thymus | ABCF1, ABCA1, ABCB2, ABCD3, ABCF2, ABCC1, ABCG1, ABCD1, ABCA7, ABCC10 | SLC25A6, SLC25A5, SLC40A1, SLC25A3, SLC25A4, SLC25A8, SLC30A6, SLC39A9, SLC25A11, SLC16A3 |
| Thyroid gland | ABCF1, ABCA2, ABCF2, ABCA6, ABCD3, ABCA5, ABCE1, ABCA8, ABCC4, ABCA1 | SLC25A6, SLC5A3, SLC26A7, SLC5A5, SLC25A23, SLC26A4, SLC25A3, SLC30A6, SLC25A37, SLC40A1 |
| Trachea | ABCF1, ABCD3, ABCB2, ABCC1, ABCA1, ABCG1, ABCA5, ABCA8, ABCC4, ABCE1 | SLC25A6, SLC12A2, SLC16A3, SLC25A37, SLC40A1, SLC25A3, SLC25A5, SLC39A9, SLC16A9, SLC25A44 |
| Uterus | ABCF1, ABCF2, ABCA6, ABCD1, ABCD3, ABCA1, ABCG2, ABCB2, ABCE1, ABCB10 | SLC25A6, SLC40A1, SLC25A3, SLC25A5, SLC16A9, SLC39A9, SLC25A37, SLC25A23, SLC37A3, SLC30A6 |

The ten most highly expressed ABC and SCL transporters mRNAs in human tissues. The transporter expression level is ranked from highest to lowest.

NA= The mRNA expression level of transporters has not been analyzed in this target tissue.

ABC=ATP-binding cassette

SLC= Solute carrier

1.2 TRANSPORTER SUPERFAMILIES

1.2.1 The ABC Transporters

One of the largest and most ancient classes of transporters is the ATP-binding cassette (ATP) transporter superfamily [8-10]. This superfamily of transporters is identified not just by the presence of nucleotide binding domains but more specifically by a very characteristic and specific amino acid (LSGGQ) motif in the nucleotide binding domain [10]. It is the ability to bind ATP that allows these transporters to harness ATP as a source of energy to mediate active transport for molecules across the biological membranes. Members of the ABC transporter family are present in organisms from all kingdoms of life, with representatives in all extant phyla from prokaryotes to humans [8]. Transporters in this family have attracted considerable attention because they are involved in many crucial physiological functions, as well as being associated with human diseases including tumor resistance, cystic fibrosis and bacterial multidrug resistance [11]. So far there are 49 members of the ABC superfamily in humans which have been gathered into 7 families (Human Genome Organization) [12]. Of these, most studies have been done on ABCB1 (MDR1), ABCC1 (multidrug resistance-associated protein, MRP1), ABCC2 (MRP2) and ABCG2 (breast cancer resistance protein, BCRP), which are considered therapeutically important.

The variety of substrates handled by different ABC transporters is enormous: ranging from amino acids, sugars, inorganic ions, polysaccharides, peptides to proteins. These substrates are chemically different and vary greatly in size. However, each ABC transporter is relatively specific for a given substrate. The mechanism by which allows each transporter to retain a high degree of specificity

for a particular substrate, while achieving such diversity, is still being debated [8]. ABC transporters are divided into three main functional categories. In prokaryotes, importers provide an influx mechanism for essential nutrients. The ability of bacteria to grow and compete depends on the efficiency with which they can obtain and scavenge nutrients. The correlation in bacteria between the number of ABC transporters and the size of the bacterial genome suggest that the transporters are essential for normal bacterial metabolism and growth [13]. The ABC importers involved in uptake have yet been characterized in eukaryotic cells. The ABC exporters or effluxers are found in prokaryotes and eukaryotes [8]. In view of their ability to efflux molecules from the cytoplasm to the periplasm, the exporters are likely to serve as secretory mechanisms for cellular metabolic products. In bacteria, the effluxers are associated with bacterial antibiotic resistance by pumping the offending agents from the cell. An example of bacterial drug resistance is the erythromycin resistance of *Staphylococcus* which is mediated by the ABC protein MsrA [14]. The presence of these transporters in parasites and microorganisms, therefore, present challenges in the development of new anti-infectives, and in dealing with the emergence of drug resistant strains [15]. The third subgroup of ABC transporters involved in translation and DNA repair mechanisms, but do not function as transporters [16].

In humans, the ABC transporters function as part of the cellular defense mechanism, protecting the body against amphipathic xenotoxins. The ABC transporters have been found in every cell type studied so far. The P-glycoprotein is plentiful in the gut, liver and kidney, preventing entry of toxins into the body. In the blood-brain barrier, testis, bone marrow and placental trophoblasts,

P-glycoprotein provides protection of vital body parts. The wide xenobiotic substrate specificities handled by P-glycoprotein makes it the perfect candidate for this task. This broad specificity, however, could interfere with the delivery of drugs to the target organs. This challenges the development of new chemotherapeutic drugs.

1.2.2 The SLC Transporters

The solute-carrier gene (SLC) superfamily comprises 55 gene families, covering as much as 362 putatively functional protein-coding genes [17]. The gene products include passive transporters, symporters and antiporters. These transporters are found in all cellular and organelle membranes except the nuclear membrane. SLC transporters mediate the transport of a wide and diverse range of substrates including endogenous substrates (e.g. carboxylates, amino acids, peptides, glucose, neurotransmitters, vitamins, fatty acids and lipid), drugs, non-essential metals and other environmental xenobiotics. Unlike the ABC transporters, the SLC transporters do not have direct access to an energy source to power their activity. The passive transporters (also known as uniporters or facilitative transporters) transport solutes down a concentration gradient. Secondary active transporters, by contrast, allow solutes to move against concentration gradient by coupling to the transport of a second solute that flows down its concentration gradient. As such, the overall free energy change is still favorable. Although most of the SLC transporters function as influx mechanisms, they are not exclusively so and many can function as efflux or bidirectional transporters.

Contrary to gene nomenclature commonly assigned on the basis of evolutionary divergence, members within SLC superfamily has been named largely on functional rather than evolutionary relatedness. The homology between SLC families is very low to non-existent [17]. Furthermore, the properties of each family are often summarized based on just a few members that have been thoroughly characterized. One should bear in mind that some of the other members yet to be characterized will not adhere strictly to that specific moniker [17].

1.3 THE ROLE OF TRANSPORTERS IN DRUG ABSORPTION, DISTRIBUTION, METABOLISM AND EXCRETION

1.3.1 Transporters and Drug Absorption

In the past decades, membrane transporters have long been recognized as important determinants in the overall disposition of numerous pharmacological agents. In addition to the physicochemical properties (e.g. molecular size, charge distribution and hydrophobicity), drug interactions with membrane transporters determine the extent and direction of drug movement across organs.

In the small intestine, enterocytes express an array of carriers crucial for absorption of dietary compounds and pharmacological compounds. Both ABC and SLC transporters show considerable variability in expression along the gastrointestinal tract [18, 19]. For example, the expression of BCRP is found throughout the entire small intestine and colon, while MDR1 is expressed in greater abundance towards the terminal ileum and colon. MRP2, on the other hand, is expressed preferentially in the duodenum. It remains unclear that how the various transporters are collectively regulated in their spatial distribution along the intestines. Besides, the clinical implication of differential expression of transporter on drug absorption is not entirely clear. The studies of knockout animals such as *mdr1a* (-/-) allow us an insight into potential tissue pharmacokinetic consequences of compromised transporter function (**Table 2**). MDR1 actively pumps drugs back into the intestinal lumen and thus effectively limiting the extent (bioavailability) of drug absorption. The oral bioavailability of ivermectin, vinblastine, digoxin, and some human immunodeficiency virus (HIV) 1 protease inhibitors is markedly increased in *mdr1a* knockout mice as compared to wildtype mice. Furthermore, studies showed

that the interindividual variation in the bioavailability of cyclosporine and digoxin could be explained by the extent of intestinal MDR1 expression and activity [20, 21]. The expression of transporters also varies considerably between individuals. This further supports the role of transporters in determining the bioavailability of orally administered drugs.

Table 2. The ratio of the concentrations in different tissues for various substrates, between *mdr* knockout (-/-) and wildtype (+/+) mice (Adapted from Lee et al., 2009 [15])

| | Ivermectin ^a | Vinblasatin ^a | Dexamethasone | Digoxin | Cyclosporin A | Nelfinavir | Nelfinavir | Indinavir | Saquinavir |
|-----------------|--|--|---|--|---|--|---|---|---|
| | <i>mdr1a</i> (-/-):(+/+) | <i>mdr1a</i> (-/-):(+/+) | <i>mdr1a</i> (-/-):(+/+) | <i>mdr1a</i> (-/-):(+/+) | <i>mdr1a</i> (-/-):(+/+) | <i>mdr1a/b</i> (-/-):(+/+) | <i>mdr1a</i> (-/-):(+/+) | <i>mdr1a</i> (-/-):(+/+) | <i>mdr1a</i> (-/-):(+/+) |
| Brain | 87.0 | 22.4 | 2.5* | 35.5* | 17.0* | 16.1 | 36.3* | 10.6* | 7.4* |
| Muscle | 5.0 | 6.7 | 1.0 | 1.5* | 1.8 | | | | |
| Heart | 4.0 | 3.4 | 0.8 | 1.9* | 1.6* | 1.9 | 1.2 | 1.0 | 2.5* |
| Kidney | 3.0 | 2.3 | 1.2 | 1.9 | 1.0 | 9.3 | 1.5 | 0.9 | 1.3 |
| Liver | 3.8 | 2.4 | 1.1 | 2.0 | 1.2 | 3.0 | 1.1 | 1.2 | 0.8 |
| Gall bladder | 9.4 | 1.4 | 1.7 | 1.7 | 0.6 | | | | |
| Lung | 4.0 | 2.1 | 0.8 | 2.2* | 1.2 | | 5.4 | 1.0 | 1.6 |
| Stomach | 1.7 | 1.8 | | 1.6* | 1.4 | | | | |
| Small intestine | 3.9 | 2.9 | | 1.1 | 1.9* | | 2.4 | 2.7* | 1.9 |
| Colon | 3.5 | 2.1 | 1.3 | 0.7* | 1.6* | | 1.4 | 0.8 | 0.7 |
| Testis | 7.4 | 2.5 | 1.2 | 2.8* | 2.6* | | | | |
| Penis | | | | | | | | | |
| Epididymus | 2.8 | 1.0 | | | | | | | |
| Spleen | 3.7 | 1.7 | 0.9 | 2.3* | 1.5* | 4.1 | 2.1 | 1.0 | 1.4 |
| Thymus | 2.8 | 1.4 | | 2.2* | 1.1 | | | | |
| Lymph nodes | - | 1.3 | | | 1.4 | | | | |
| Plasma | 3.3 | 2.0 | 1.0 | 1.9* | 1.4 | 1.0 | 1.26* | 1.1 | 1.1 |
| | 0.2mg/kg, 1 hr after oral administration | 1mg/kg, 1 hr after oral administration | 0.2mg/kg, 4 hr after intravenous injection | 1mg/kg , 4 hr after intravenous injection | 1mg/kg, 4 hr after intravenous injection | 10mg/kg, 2 hr after intravenous injection | 3mg/kg, 4 hr after intravenous injection | 1.5mg/kg, 4 hr after intravenous injection | 2mg/kg, 4 hr after intravenous injection |
| | [22] | [22] | [23] | [23] | [23] | [24] | [25] | [25] | [25] |

*Significantly different from wild-type mice at $P < 0.05$.

^aStatistic test has not been performance for the assays.

Table 2. (continue)

| | Morphine | Grepafloxin | Olanzapine | FK506 | Doxepin | Venlafexine | Paroxetine | Mirtazapine |
|-----------------|---|--|---|---|---|--|--|--|
| | mdr1a(-/-):(+/+) | mdr1a/b(-/-):(+/+) | mdr1a(-/-):(+/+) | mdr1a(-/-):(+/+) | mdr1a/b(-/-):(+/+) | mdr1a/b(-/-):(+/+) | mdr1a/b(-/-):(+/+) | mdr1a/b(-/-):(+/+) |
| Brain | 1.7* | 2.8* | 3.0* | 33.0* | 1.2* | 2.3* | 2.1* | 1.3 |
| Muscle | 1.3 | | | | | | | |
| Heart | 1.1 | 1.0 | | 3.0* | | | | |
| Kidney | 0.8 | 1.4 | 1.8* | 2.4* | 1.1 | 1.1 | 0.9 | 1.1 |
| Liver | 1.1 | 1.0 | 2.6* | 5.0* | 1.3 | 1.4* | 0.9 | 1.2 |
| Gall bladder | 2.2* | | | | | | | |
| Lung | 1.1 | 1.0 | | 4.2* | | | | |
| Stomach | 0.8 | | | 2.4* | | | | |
| Small intestine | 0.7 | 0.9 | | | | | | |
| Colon | 0.6 | | | | | | | |
| Testis | 0.7 | 0.6 | | | | | | |
| Penis | | | 0.9 | | | | | |
| Epididymus | | | | | | | | |
| Spleen | 1.1 | | 1.0 | 2.2* | 1.0 | 1.1 | 1.0 | 1.0 |
| Thymus | 0.8 | | | | | | | |
| Lymph nodes | | | | | | | | |
| Plasma | 1.1 | 1.1 | 1.1 | | 1.1 | 1.3* | 1.4 | 1.3 |
| | 0.2mg/kg, 4 hr after intravenous injection [23] | 10mg/kg, 1 hr after intravenous injection [26] | 2.5mg/kg, 1 hr after intraperitoneal injection [27] | 2mg/kg, 5 hr after intravenous injection [28] | 10mg/kg, 1 hr after subcutaneous injection [29] | 5mg/kg, 1 hr after subcutaneous injection [29] | 1mg/kg, 1 hr after subcutaneous injection [29] | 1mg/kg, 1 hr after subcutaneous injection [29] |

*Significantly different from wild-type mice at $P < 0.05$.

^aStatistic test has not been performance for the assays.

1.3.2 Transporters and Drug Metabolism

Although a wide variety of biological tissues are able to metabolize drugs, the main organ responsible for the drug metabolism is the liver. Classical drug metabolism has been divided into Phase I and Phase II [30]. Phase I represents the oxidation, reduction and hydrolyses of foreign compounds. Phase II reaction involves conjugation (e.g. glucuronidation and glutamylation) of the partially detoxified metabolites. Two additional steps, called Phase 0 and Phase III of drug disposition have recently been described. These phases modulate the entry and existence of the unmodified or metabolized compounds, which mediated by various transporters on cell membranes. The hepatocyte is populated by large numbers of both ABC efflux and SLC influx transporters. These transporters are differentially expressed on the sinusoidal and bile canalicular surfaces of the hepatocytes. The differential expression profiles of transporters not only have major influences on the influx and efflux of drug molecules across the hepatocyte sinusoidal membrane, but they also determine the extent of drug elimination into the bile.

These developing ideas of transporter-mediated drug disposition have mounted challenges to the previous concepts based on passive diffusion of unbound drugs. Although these processes can be described, it remains unclear how transporter-mediated movement of drug molecules will eventually affect our concepts of drug disposition and eventually our expectations of drug efficacy and toxicity [15].

1.3.3 Transporters and Renal Elimination

The renal elimination of drug molecules involves three main processes in the nephron: glomerular filtration, reabsorption and secretion. Of these processes, glomerular filtration is the only process that is truly dependent on the circulating unbound fraction of drug. Most drug molecules, however, can only enter and exit the renal tubules through influx and efflux transporters. Because drug molecules traverse the entire depth of the renal tubular cells during reabsorption and secretion, both processes require the actions of influx and efflux transporters acting in concert to produce vectorial movements of drug molecules across the tubular epithelium [15]. The OAT transporters are important renal carriers for uptake of organic anions. OAT mediates the transportation of pharmacologically important drugs including β -lactam antibiotics, nonsteroidal anti-inflammatory drugs (NSAIDs), diuretics, nucleoside antiviral drugs, and anticancer agents [31]. The members of MRP and OATP families are localized on the apical membrane of proximal tubular cells and responsible to the urinary elimination of drug molecules.

1.3.4 Transporters and Tissue Distribution

The distribution of drug molecules throughout the body largely depends on the ability of the molecule to traverse across lipophilic membranes and into the various tissue compartments and volumes. The movement may be envisaged to be driven by the concentration of unbound molecule in the circulation when a molecule is fully permeable. This paradigm influenced our understanding in drug disposition and also how drug disposition affects therapeutic efficacy and toxicity [15]. The volume of distribution of a drug is thought to be largely determined by a balance between plasma protein binding and tissue binding. Notably, it is the unbound

fraction which exhibits pharmacologic effects. It is also the fraction that may be metabolized and/or excreted. The common plasma proteins that drug molecules bind to are human serum albumin, glycoprotein, lipoprotein, α , β , and γ globulins. However, what tissue binding actually represents has never been entirely clear. The pharmacodynamic responses of a drug are thought to be related to central compartment concentration of either unbound or total drug. The basic premise for this paradigm is assuming that the unbound drug molecules equilibrate freely across efficacy and toxicity compartments; thus central compartment concentrations of the drug provide a reasonable approximation of drug responses throughout the body. This paradigm is a simple and mechanistic model that relates central compartment concentration of drug molecules to drug efficacy and toxicity. However, there is no compelling evidence that the model is accurate [15].

An increase understanding of how extensively involved transporters are with drug disposition has revealed the inadequacies of the previously working paradigm. Drug distribution is now being determined by the dynamic interplay between uptake and efflux transporters within any given epithelial cells. Grover and Benet reviewed the effects of transporters in different compartments [32]. The complexity of the situation is reflected in the inability of the review to go beyond looking at central compartment measurements of distributional effects. The review concludes that the primary location of the transporter interaction, either at liver or kidneys, serves as the chief predictor of distributional volume changes [32]. This analysis provides a framework for understanding potential pharmacokinetic interactions rooted in drug transporters as they modify drug distribution.

1.3.5 Food and Drug Interactions

There is a growing recognition that transporters are not just mediators of an isolated physiological process, but rather part of an extended cellular and whole body mechanism for protection against unwanted xenobiotic effects. In addition, transporters also have roles in the disposition of pharmacologically active compounds. The complex actions of transporters during drug-transporter or food-transporter interactions may have far-reaching consequences.

Serious drug-drug interactions have contributed to a number of United States market withdrawals of approved drugs and also to recent rejections of a few new molecular entities [33]. Many of these interactions involved induction or inhibition of metabolizing enzymes and transporters, resulting in increased or reduce systemic exposure and subsequently altering the efficacies and side effects of pharmacological compounds. In addition to drug-transporter interaction, the popular use of dietary supplements and herbal medicines has raised awareness of the potential dietary-transporter interactions. A recent survey indicated that in United States, the use of prescription drugs continue to increase over the past 10 years [34]. The percentage of Americans who took at least one prescription drug in the past month increased from 44% to 48%. The use of two or more drugs increased from 25% to 31% and the use of five or more drugs increased from 6% to 11% [34]. Besides, it has been reported that over 40% used supplements in 1988-1994, and over 50% in 2003-2006 [35]. Furthermore, it is very common that prescribed drugs are taken together with herbal dietary products. Therefore, detailed information about potential transporter interactions between drugs and dietary supplements is needed.

It is reasonably expected that transporters will naturally have complex and multivariate interactions with both xenobiotics found in the diet and pharmaceuticals. Several studies have already documented the *in vitro* and clinical potential for such interactions [36, 37]. A summary of drug-transporter interactions or toxicities involving drug transporters is presented in **Table 3**. Transporter-based drug interactions may be inhibitory, inductive or both. Such interactions may alter the efficacy-toxicity profile of the affected drug. The transporter-based interactions will be clinically significant if such interaction alters the concentration of said affected drug at the site of action such that it falls outside of the therapeutic window [36]. Evidence shows that such transporter based interactions may result in changes in tissue concentration of affected drug without significantly affect the plasma concentration of the substrate [36]. For example, Cyclosporine (CsA) alters verapamil's distribution to the brain by inhibiting the P-gp transporter without affecting the plasma concentration-time profile of the substrate [38]. The transporter-based drug interactions may exert beneficial effects. For example, inhibition of human organic anion transport (hOAT) by probenecid reduced the nephrotoxicity of cidofovir [39, 40].

Table 3. Drug-drug interactions or toxicities involving drug transporters (Adapted from Ho and Kim, 2005 [41])

| Drug | Inhibitor/inducer | Measured effect/toxicity | Putative mechanism | References |
|-----------------|--------------------------|--|------------------------------|-------------------|
| Penicillin | Probenecid | Decreased renal clearance, prolonged half-life | Inhibition of OATs | [42] |
| ACE inhibitors | Probenecid | Decreased renal clearance, prolonged half-life | Inhibition of OATs | [42] |
| Antiviral drugs | Probenecid | Decreased renal clearance, prolonged half-life | Inhibition of OATs | [42] |
| Procainamide | Cimetidine | Decreased renal clearance, increased AUC | Inhibition of OCT, OAT, OATP | [42] |
| Levofloxacin | Cimetidine | Decreased renal clearance, increased AUC | Inhibition of OCT, OAT, OATP | [42] |
| Dofetilide | Cimetidine | Decreased renal clearance, increased AUC | Inhibition of OCT, OAT, OATP | [42] |
| Fexofenadine | Fruit juices | Decreased plasma levels | Inhibition of OATPs | [43] |
| Methotrexate | NSAIDs | Decreased renal clearance | Inhibition of OAT3 | [44] |
| Methotrexate | Probenecid | Decreased renal clearance | Inhibition of OAT3 | [44] |
| Loperamide | Quinidine | Increased CNS adverse effects | Inhibition of MDR1 | [45] |
| Talinolol | Verapamil | Decreased plasma levels | Inhibition of MDR1 | [46] |
| Fexofenadine | Erythromycin | Increased plasma levels | Inhibition of MDR1 | [47] |
| Fexofenadine | Rifampin | Decreased plasma levels | Inhibition of MDR1 | [48] |
| Digoxin | Quinidine | Increased plasma levels, decreased renal clearance | Inhibition of MDR1 | [49] |
| Digoxin | Verapamil | Increased plasma levels, decreased renal clearance | Inhibition of MDR1 | [50] |
| Digoxin | Talinolol | Increased plasma levels, decreased renal clearance | Inhibition of MDR1 | [51] |
| Digoxin | Clarithromycin | Increased plasma levels, decreased renal clearance | Inhibition of MDR1 | [52] |
| Digoxin | Statins | Increased plasma levels, decreased renal clearance | Inhibition of MDR1 | [53] |
| Digoxin | Rifampin | Decreased plasma levels | Inhibition of MDR1 | [54] |
| Digoxin | Troglitazone | Hepatotoxicity | Inhibition of BSEP | [55] |
| Digoxin | Bosentan | Cholestasis | Inhibition of BSEP | [56] |
| Digoxin | Estrogens | Cholestasis | Inhibition of BSEP | [57] |
| Digoxin | Cyclosporine | Cholestasis | Inhibition of BSEP | [57] |
| Digoxin | Cidofovir | Nephrotoxicity | Inhibition of OAT1 | [58] |
| Digoxin | Adefovir | Nephrotoxicity | Inhibition of OAT2 | [58] |
| Digoxin | Cephaloridine | Nephrotoxicity | Inhibition of OAT3 | [59] |

ACE, Angiotensin-converting enzyme; AUC, area under plasma concentration-time curve; NSAIDs, nonsteroidal anti-inflammatory drugs.

1.3.6 Summary of Role of Transporters in Drug Distribution

There is a growing recognition that transporters are not just mediators of an isolated physiological process but rather part of an extended cellular and whole body mechanism for protection against unwanted xenobiotic effects. Transporters are involved in almost every part of the therapeutic process from absorption, distribution and elimination of drug molecule to their efficacy and toxicity sites. The complex actions of transporters across various tissue and cell membranes during disease [60-62] or various drug-drug [63, 64] or food-drug interactions [65, 66] may potentially lead to large shifts in compartment: plasma concentration ratios at efficacy and toxicity sites. The studies of knockout animals such as *mdr1a* (-/-) allow us an insight into potential tissue pharmacokinetic consequences of compromised transporter function (**Table 4**). As transporter-mediated drug disposition is the dynamic interplay between the uptake and efflux transporters, the changes in transporter kinetics (e.g. genetic polymorphism, drug/food interaction, disease-altered expression) may shift the efficacy-toxicity relationship of a drug. Therefore, it is important to evaluate the transporter activity and potential drug/food interaction of individual transporter. As mentioned above, drug transporters can be generally separated into 2 superfamilies – ABC and SLC transporters. In this project, we focus on members of SLC superfamily, *SLC16A* family of proton-linked membrane transport proteins known as monocarboxylate transporters (MCTs).

Table 4. Tissue-to-plasma concentration ratio (K_p) of drug substrates in wild-type (wt) and knockout mice (ko) (Adapted from Lee et al., 2009 [15])

| Tissue | Morphine [23] | | | Dexamethasone [23] | | | Digoxin [23] | | | Digoxin [67] | | |
|-----------------|---------------|------------|-------|--------------------|------------|-------|--------------|------------|-------|--------------|------------|-------|
| | mdr1a(+/+) | mdr1a(-/-) | ko/wt | mdr1a(+/+) | mdr1a(-/-) | ko/wt | mdr1a(+/+) | mdr1a(-/-) | ko/wt | mdr1a(+/+) | mdr1a(-/-) | ko/wt |
| Brain | 0.49 | 0.72 | 1.48 | 0.28 | 0.71 | 2.49 | 0.08 | 1.54 | 18.73 | | | |
| Muscle | 0.59 | 0.65 | 1.10 | 0.65 | 0.62 | 0.95 | 1.11 | 0.87 | 0.78 | 0.80 | 0.42 | 0.53 |
| Heart | 0.84 | 0.85 | 1.00 | 1.02 | 0.79 | 0.77 | 0.67 | 0.67 | 1.01 | 1.13 | 0.63 | 0.55 |
| Kidney | 4.45 | 3.03 | 0.68 | 2.21 | 2.66 | 1.20 | 0.91 | 0.92 | 1.01 | 1.07 | 0.80 | 0.74 |
| Liver | 2.80 | 2.65 | 0.95 | 47.91 | 52.56 | 1.10 | 1.41 | 1.51 | 1.07 | 1.87 | 2.09 | 1.12 |
| Gall bladder | 48.35 | 93.06 | 1.92 | 304.13 | 517.38 | 1.70 | 46.99 | 43.49 | 0.93 | | | |
| Lung | 1.72 | 1.66 | 0.97 | 1.26 | 0.97 | 0.77 | 0.54 | 0.62 | 1.15 | | | |
| Stomach | 1.99 | 1.48 | 0.74 | | | | 0.57 | 0.47 | 0.83 | | | |
| Small intestine | 4.52 | 2.94 | 0.65 | | | | 1.90 | 1.12 | 0.59 | 2.59 | 0.54 | 0.21 |
| Colon | 7.73 | 4.25 | 0.55 | 4.26 | 5.74 | 1.35 | 1.50 | 0.54 | 0.36 | | | |
| Testis | 1.93 | 1.13 | 0.59 | 0.68 | 0.84 | 1.23 | 0.32 | 0.47 | 1.48 | | | |
| Spleen | 1.27 | 1.22 | 0.96 | 0.90 | 0.85 | 0.94 | 0.32 | 0.39 | 1.21 | | | |
| Thymus | 1.27 | 0.84 | 0.66 | | | | 0.32 | 0.38 | 1.18 | | | |
| Lymph nodes | | | | | | | | | | | | |

| Tissue | Cyclosporin A [23] | | | Vinblastine [22] | | | Ivermectin [22] | | | Saquinavir [25] | | |
|-----------------|--------------------|------------|-------|------------------|------------|-------|-----------------|------------|-------|-----------------|------------|-------|
| | mdr1a(+/+) | mdr1a(-/-) | ko/wt | mdr1a(+/+) | mdr1a(-/-) | ko/wt | mdr1a(+/+) | mdr1a(-/-) | ko/wt | mdr1a(+/+) | mdr1a(-/-) | ko/wt |
| Brain | 0.28 | 3.30 | 11.93 | 1.67 | 18.67 | 11.20 | 0.09 | 2.52 | 26.87 | 0.13 | 0.88 | 6.67 |
| Muscle | 2.50 | 3.13 | 1.25 | 7.33 | 24.67 | 3.36 | 0.60 | 0.92 | 1.54 | | | |
| Heart | 7.95 | 8.91 | 1.12 | 21.33 | 36.50 | 1.71 | 1.56 | 1.92 | 1.23 | 1.00 | 2.32 | 2.32 |
| Kidney | 36.89 | 26.98 | 0.73 | 133.00 | 155.33 | 1.17 | 2.94 | 2.71 | 0.92 | 3.65 | 4.38 | 1.20 |
| Liver | 140.00 | 118.46 | 0.85 | 38.33 | 46.83 | 1.22 | 8.13 | 9.56 | 1.18 | 6.00 | 4.38 | 0.73 |
| Gall bladder | 172.42 | 67.06 | 0.39 | 114.00 | 77.67 | 0.68 | 9.19 | 26.46 | 2.88 | | | |
| Lung | 15.89 | 13.09 | 0.82 | 172.33 | 176.33 | 1.02 | 1.44 | 1.75 | 1.22 | 2.74 | 3.97 | 1.45 |
| Stomach | 22.42 | 22.20 | 0.99 | 106.67 | 93.83 | 0.88 | 3.94 | 2.06 | 0.52 | | | |
| Small intestine | 28.16 | 38.00 | 1.35 | 65.67 | 96.17 | 1.46 | 1.94 | 2.33 | 1.20 | 7.13 | 12.15 | 1.70 |
| Colon | 14.16 | 16.33 | 1.15 | 71.33 | 74.00 | 1.04 | 1.94 | 2.08 | 1.07 | 30.77 | 20.79 | 0.68 |
| Testis | 1.50 | 2.74 | 1.83 | 8.67 | 10.67 | 1.23 | 0.59 | 1.35 | 2.29 | | | |
| Penis | | | | | | | | | | | | |
| Epididymus | | | | 77.67 | 39.67 | 0.51 | 3.69 | 3.15 | 0.86 | | | |
| Spleen | 18.63 | 19.91 | 1.07 | 292.00 | 240.33 | 0.82 | 0.81 | 0.92 | 1.14 | 1.19 | 1.53 | 1.28 |
| Thymus | 12.71 | 10.13 | 0.80 | 105.33 | 71.00 | 0.67 | 2.69 | 2.33 | 0.87 | | | |
| Lymph nodes | 16.08 | 15.30 | 0.95 | 131.33 | 82.67 | 0.63 | | | | | | |

Table 4. (continue)

| Tissue | Indinavir [25] | | | Nelfinavir [25] | | | Nelfinavir [24] | | | Grepafloxacin [26] | | |
|-----------------|----------------|------------|-------|-----------------|------------|-------|-----------------|---------------|-------|--------------------|---------------|-------|
| | mdr1a(+/+) | mdr1a(-/-) | ko/wt | mdr1a(+/+) | mdr1a(-/-) | ko/wt | mdr1a/1b(+/+) | mdr1a/1b(-/-) | ko/wt | mdr1a/1b(+/+) | mdr1a/1b(-/-) | ko/wt |
| Brain | 0.08 | 0.81 | 9.61 | 0.09 | 2.65 | 30.88 | 0.92 | 14.88 | 16.19 | 0.30 | 0.80 | 2.67 |
| Muscle | | | | | | | | | | | | |
| Heart | 0.79 | 0.76 | 0.97 | 0.69 | 0.71 | 1.03 | 1.75 | 3.30 | 1.89 | 8.20 | 7.80 | 0.95 |
| Kidney | 7.11 | 6.00 | 0.84 | 1.79 | 2.12 | 1.19 | 1.42 | 13.27 | 9.31 | 15.00 | 18.70 | 1.25 |
| Liver | 20.89 | 21.81 | 1.04 | 61.00 | 53.18 | 0.87 | 5.40 | 15.99 | 2.96 | 16.1 | 13.90 | 0.86 |
| Gall bladder | | | | | | | | | | | | |
| Lung | 3.21 | 3.00 | 0.93 | 7.71 | 34.24 | 4.44 | | | | 16.80 | 14.80 | 0.88 |
| Stomach | | | | | | | | | | | | |
| Small intestine | 18.11 | 44.05 | 2.43 | 8.57 | 31.35 | 3.66 | | | | 10.00 | 8.50 | 0.85 |
| Colon | 72.74 | 53.67 | 0.74 | 39.64 | 44.94 | 1.13 | | | | | | |
| Testis | | | | | | | | | | 1.40 | 0.80 | 0.57 |
| Epididymus | | | | | | | | | | | | |
| Spleen | 1.05 | 1.00 | 0.95 | 3.00 | 5.24 | 1.75 | 5.22 | 21.22 | 4.06 | | | |
| Thymus | | | | | | | | | | | | |
| Lymph nodes | | | | | | | | | | | | |

| Tissue | Olanzapine [27] | | | Ezetimibe [68] | | | L-Carnitine [69] | | |
|--------------|-----------------|------------|-------|----------------|--------------|-------|------------------|------------|-------|
| | mdr1a(+/+) | mdr1a(-/-) | ko/wt | mdr1a/b(+/+) | mdr1a/b(-/-) | ko/wt | octn2(+/+) | octn2(-/-) | ko/wt |
| Brain | 0.90 | 2.00 | 2.60 | 0.82 | 0.55 | 0.67 | 0.53 | 0.48 | 0.91 |
| Muscle | | | | | | | 1.51 | 0.35 | 0.23 |
| Heart | | | | | | | 11.70 | 1.05 | 0.09 |
| Kidney | 2.60 | 4.40 | 1.70 | 12.20 | 10.70 | 0.88 | 11.60 | 6.6 | 0.58 |
| Liver | 2.50 | 5.50 | 2.40 | 151.00 | 188.00 | 1.25 | 5.47 | 5.47 | 1.00 |
| Gall bladder | | | | | | | | | |
| Lung | | | | | | | 17.90 | 33.50 | 1.87 |
| Stomach | | | | | | | 6.11 | 2.92 | 0.48 |
| Testis | | | | 8.44 | 4.54 | 0.54 | | | |
| Penis | 1.00 | 0.80 | 0.90 | | | | | | |
| Epididymus | | | | | | | | | |
| Spleen | 5.20 | 4.70 | 0.90 | | | | | | |
| Thymus | | | | | | | | | |
| Lymph nodes | | | | | | | | | |

1.4 OVERVIEW OF MONOCARBOXYLATE TRANSPORTER FAMILY

The monocarboxylate transporter (MCT) family currently comprises of 14 members related to each other by sequence homology. The first 4 members (MCT1-MCT4) have been proven experimentally to mediate the transport of metabolically important endogenous monocarboxylates such as lactate, pyruvate, acetate and ketone bodies [70]. It was originally thought that these monocarboxylates would diffuse across the membrane via non-ionic of the free acid. However, the uptakes of these monocarboxylates were inhibited by α -cyano-4-hydroxycinnamate (CHC) [71] and *p*-chloromercuribenzenesulphonate (*p*CMBS) [72], indicating that their uptakes into human erythrocytes were mediated by some sort of transporter systems. The pKa of L-lactate, pyruvate are 3.86 and 2.39, respectively [73], thus under physiological pH, these acids dissociate almost entirely to their anions. These monocarboxylate anions are highly charged chemical structures and are transported across the plasma membrane via facilitated MCT transporters down their concentration gradients. The contribution of passive diffusion on monocarboxylate transportation is thought to be insignificant.

MCT1-4 classically transport metabolites across plasma membranes with direction controlled by proton and metabolite concentrations. Its transport of monocarboxylate anions is coupled by 1:1 stoichiometry to the symport of a proton. This transport does not require ATP, and is controlled instead by hydrogen ion and substrate gradients, thus facilitating the movement of substrates in (influx) or out (efflux) of the cell [73-75]. Before considering each of the members in more detail, a number of points are worth making about the MCT family in general.

Firstly, the name of MCTs does not correspond to the gene number except for MCT1, MCT9 and MCTs11-14. This confusion has been further aggravated by the renaming of some of the MCTs in 1998 [76]. For clarification purpose, the original name of each MCT is presented in **Table 5**. Secondly, only the first four members of the family (MCT1-MCT4) have been experimentally demonstrated to transport aliphatic monocarboxylates, whereas the substrate specificities of MCTs 5-7, 9 and 11-14 are yet to be elucidated. MCT8 is the thyroid hormone transporter.

SLC16A10 was named T-type amino acid transporter 1 (TAT1) rather than MCT10 and it is involved in the transport of system-T aromatic amino acids [70]. Thirdly, the regulation of MCTs is at the transcriptional and translational levels. No convincing experimental data indicates that the MCTs are regulated by protein phosphorylation. Lastly, MCT1 [77], MCT3 [78] and MCT4 [77] require the co-expression of the accessory protein CD147 (also known as OX-47, basigin, extracellular matrix metalloproteinase inducer (EMM-PRIN) and HT7) for correct functional expression in the membrane. MCT2 requires a different accessory protein, gp70 (also known as embigin) for its expression in plasma membrane [79].

We focus here on the first four classic members of SLC16A family. This literature research will progress through the following sections: (1) The kinetic and modulation of MCT1-4; (2) Tissue distribution of MCTs; (3) Intracellular lactate shuttle (4) Biochemical and structural aspects; (5) MCT mutation and genetic syndromes; (6) Regulation of MCT Isoforms; and (7) Roles of MCTs in drug and xenobiotic distribution

Table 5. Human SLC16 family members (adapted from Meredith and Christian, 2008 [70])

| Protein | Human gene | Alternative name (previous name*) | Sequence accession ID/chromosomal location | Substrate | Tissue distribution | Key references |
|----------------|-------------------|--|---|---|--|-----------------------|
| MCT1 | SLC16A1 | | NM_003051/1p13.2 | Monocarboxylates (lactate, pyruvate, ketone bodies) | Ubiquitous | [80, 81] |
| MCT2 | SLC16A7 | | NM_004731/12q14.1 | Monocarboxylates | Kidney, brain, adipocytes | [82, 83] |
| MCT3 | SLC16A8 | REMP | NM_013356/22q13.1 | Monocarboxylates | RPE, choroid plexus | [84, 85] |
| MCT4 | SLC16A3 | (MCT3) | NM_004207/17q25.3 | Monocarboxylates | Skeletal muscle, chondrocytes, leukocytes, testis, lung, placenta, heart, corneal epithelium, adipocytes | [76, 83, 86, 87] |
| MCT5 | SLC16A4 | (MCT4) | NM_004696/1p13.3 | Unknown | Brain, muscle, liver, kidney, lung, ovary, placenta, heart | [86] |
| MCT6 | SLC16A5 | (MCT5) | NM_004695/17q25.1 | Unknown | Kidney, muscle, brain, heart, pancreas, prostate, lung, placenta | [86] |
| MCT7 | SLC16A6 | (MCT6) | NM_004694/17q24.2 | Unknown | Brain, pancreas, muscle | [86] |

| | | | | | | |
|-------|----------|----------------|--------------------|---|--|----------|
| MCT8 | SLC16A2 | XPCT (MCT7) | NM_006517/Xq13.2 | T3, T4 | Liver, heart, brain, thymus, intestine, ovary, prostate, pancreas, placenta | [88] |
| MCT9 | SLC16A9 | | BN000144/10q21.2 | Unknown | Endometrium, testis, ovary, breast, brain, kidney, adrenal, retina | [73] |
| TAT1 | SLC16A10 | MCT10 | NM_018593/6q21-q22 | Aromatic amino acids (W, Y, F, L-dopa) | Kidney, intestine, muscle, placenta, heart | [89, 90] |
| MCT11 | SLC16A11 | | NM_153357/17p13.2 | Unknown | Skin, lung, ovary, breast, pancreas, RPE, choroid plexus | [91] |
| MCT12 | SLC16A12 | | NM_213606/10q23.3 | Unknown | Kidney | [91] |
| MCT13 | SLC16A13 | | BN000145/17p13.1 | Unknown | Breast, bone marrow stem cells | [91] |
| MCT14 | SLC16A14 | | BN000146/2q36.3 | Unknown | Brain, heart, ovary, breast, lung, pancreas, RPE, choroid plexus | [91] |

Notes: *Before publication of Wilson et al. (1998).

RPE, retinal pigmented epithelium.

1.4.1 Monocarboxylate Transporter 1-4

MCT1-4 are the only members to date, which have been shown to mediate the transport of monocarboxylates, such as lactate, pyruvate and butyrate. All four isoforms mediate the transport of monocarboxylates in a proton-mediated manner, but the detailed mechanism of other isoforms has not been studied. The topology of the MCT family is shown in **Fig. 1** and will be discussed in detail under section “Biochemical and structural aspects”.

1.4.1.1 Monocarboxylate Transporter 1 (*SLC16A1*)

MCT1 is the most studied and functionally characterized member of the MCT family, largely due to the fact that it is the only monocarboxylate transporter expressed in human erythrocytes. MCT1 is found in the great majority of tissues of all species studied, with no evidence for splice variants. Recently, MCT1 has been found to be expressed in human white fat and in human adipocytes (and preadipocytes) [83]. It was the first isoform to be identified at the molecular level and from these studies, MCT1 substrate and inhibitor specificity has been characterized in various models (**Table 6**). MCT1 mediates the transport of a wide variety of monocarboxylates. Characterization of endogenous MCT1 in erythrocytes [72], and MCT1 expressed in *Xenopus oocytes* [92, 93] has revealed that it transports short chain (C-2 to C-5) unbranched aliphatic monocarboxylates such as acetate ($K_m = 3.5$ mM) and propionate ($K_m = 1.5$ mM). Three and four carbon atom substrates with C-2 substitutions are preferred, such as L-lactate ($K_m = 3-5$ mM), pyruvate ($K_m = 0.7$ mM), acetoacetate ($K_m = 4-6$ mM), and β -hydroxybutyrate (10-12 mM) [91]. MCT1 lactate transport is stereoselective. It has a ten-fold preference for

L-lactate over D-lactate [94]. However, this stereoselective preference is not observed in 2-chloropropionate and β -hydroxybutyrate. A large number of inhibitors of MCT1-mediated transport are known, including α -cyano-4-hydroxycinnamate, quercetin, phloretin and *p*-chloromercuribenzenesulphonate (**Table 6**).

Figure 1. The proposed topology of the monocarboxylate transporter (MCT) family. MCTs have 12 transmembrane domains (TMDs) with intracellular N- and C-termini and a large intracellular loop between TMDs 6 and 7. The N- and C- termini and the large loop between TMDs 6 and 7 show the greatest variation between family members, whilst the TMDs themselves are highly conserved. Critical residues identified in MCT1 and two highly conserved motifs characteristic of the MCT family are included. CD147, the ancillary protein that associates with MCT1, MCT3 and MCT4, is also shown. (Adapted from Halestrap and Meredith, 2004 [91])

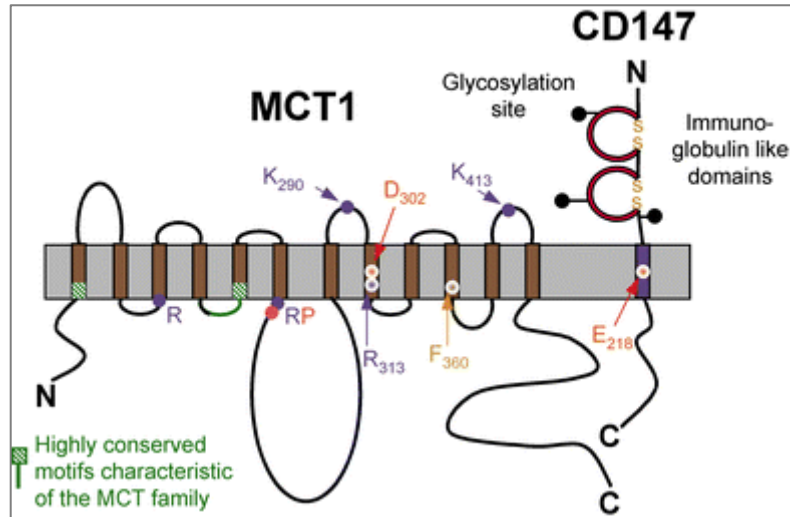


Table 6. Substrate and inhibitor affinities for monocarboxylate transporter 1 in various expression systems

| Substrate | Km | Transporter Source, Expression System | Ki | Transporter Source, Expression System |
|-------------------------------|---------|---------------------------------------|---------|---------------------------------------|
| Monocarboxylates | | | | |
| L-lactate | 8.3 mM | Hamster, Sf-9 cells [82] | 2.20 mM | Rat, erythrocytes [95] |
| | 6.0 mM | Human, oocyte [96] | | |
| | 5.6 mM | Rat, oocyte [97] | | |
| | 3.5 mM | Rat, oocyte [75] | | |
| | 1.19 mM | Human, RD cells [98] | | |
| | 6.4 mM | Mouse, ELT cells [99] | | |
| | 1.7 mM | Rat, TR-iBRB2 [100] | | |
| | 9.1 mM | Human, erythrocytes [101] | | |
| | 13.4 mM | Human, erythrocytes [102] | | |
| D-lactate | | | 51.0 mM | Rat, erythrocytes [95] |
| Acetate | | | 3.50 mM | Rat, erythrocytes [95] |
| Pyruvate | 3.1 mM | Hamster, Sf-9 cells [82] | 0.64 mM | Rat, erythrocytes [95] |
| | 2.5 mM | Human, oocyte [96] | | |
| | 2.1 mM | Mouse, ELT cells [99] | | |
| | 1.0 mM | Rat, oocyte [75] | | |
| | 2.0 mM | Human, erythrocytes [101] | | |
| Butyrate | 2.6 mM | Human, Caco2 cells [103] | | |
| Propionate | | | 1.50 mM | Rat, erythrocytes [95] |
| Glycolate | | | 6.60 mM | Rat, erythrocytes [95] |
| 4-Hydroxybutyrate | | | 7.20 mM | Rat, erythrocytes [95] |
| D,L- β -Hydroxybutyrate | 12.5 mM | Mouse, ELT cells [99] | | |
| Oxamate | | | 17.0 mM | Rat, erythrocytes [95] |
| Glyoxylate | | | 70.0 mM | Rat, erythrocytes [95] |
| 2-Oxobutyrate | | | 0.19 mM | Rat, erythrocytes [95] |
| 3-Oxobutyrate (Acetoacetate) | 5.5 mM | Rat, oocyte [75] | 3.50 mM | Rat, erythrocytes [95] |
| L-2-chloropropionate | | | 0.92 mM | Rat, erythrocytes [95] |
| D-2-chloropropionate | | | 0.98 mM | Rat, erythrocytes [95] |
| D/L-2-hydroxybutyrate | | | 1.30 mM | Rat, erythrocytes [95] |

| Substrate | K_m | Transporter Source, Expression System | K_i | Transporter Source, Expression System |
|---|------------------------|--|----------------------|--|
| D/L-3-hydroxybutyrate | | | 8.10 mM | Rat, erythrocytes [95] |
| Formate | | | >100 mM | Rat, erythrocytes [95] |
| Bicarbonate | | | >100 mM | Rat, erythrocytes [95] |
| 2-Hydroxy-2-methylpropionate | | | >100 mM | Rat, erythrocytes [95] |
| Pharmaceutical Compounds | | | | |
| Salicylic acid | | | 4.5 mM | Rat, TR-iBRB2 cells [100] |
| Valproic acid | | Human, BeWo cells [104] | 5.4 mM | Rat, TR-iBRB2 cells [100] |
| Atorvastatin | | Human, Caco-2 cells [105] | | |
| γ-Hydroxybutyric acid (GHB) | 2.07 mM | Human, HK-2 cells [106] | | |
| Inhibitor | IC₅₀ | Transporter Source, Expression System | K_i | Transporter Source, Expression System |
| Cyanocinnamate derivatives | | | | |
| α-Cyano-4-hydroxycinnamate (CHC) | | | 50 uM | Human erythrocytes [101] |
| | | | 425 uM | Rat, oocyte [75] |
| Cinnamic acid | | | 0.6 mM | Human erythrocytes [107] |
| α-Fluorocinnamate | | | 75 uM | Human erythrocytes [101] |
| α-Cyano-β-(1-phenylindol-3-yl) acrylate | | | 12 uM | Human erythrocytes [101] |
| NSAIDs | | | | |
| Diflunisal | 50 uM | Human, Caco-2 cells [108] | | |
| Diclofenac | 100 uM | Human, Caco-2 cells [108] | | |
| Ketoprofen ^c | 440 uM | Human, Caco-2 cells [108] | 380 uM | Human, Caco-2 cells [108] |
| Naproxen ^c | 250 uM | Human, Caco-2 cells [108] | 220 uM | Human, Caco-2 cells [108] |

| Inhibitor | IC50 | Transporter Source, Expression System | Ki | Transporter Source, Expression System |
|-------------------------|-------------|---|-----------|--|
| Flavonoids | | | | |
| Naringenin ^c | 23.4 uM | Human, Caco-2 cells [109] | 15.3 uM | Human, Caco-2 cells [109] |
| Silybin ^c | 30.2 uM | Human, Caco-2 cells [109] | 19.7 uM | Human, Caco-2 cells [109] |
| Luteolin ^c | 0.41 uM | Rat MCT1 gene-transfected MDA-MB231 cells [110] | | |
| Morin | 6.21 uM | Rat MCT1 gene-transfected MDA-MB231 cells [110] | | |
| Phloretin | 2.57 uM | Rat MCT1 gene-transfected MDA-MB231 cells [110] | 28 uM | Rat, oocyte[75] |

1.4.1.2 Monocarboxylate Transporter 2 (*SLC16A7*)

MCT2 was cloned from hamster liver and has 60% homology to MCT1 [82]. Northern blot analysis and inspection of human expressed sequence tag (EST) database suggests that MCT2 is expressed poorly in major tissues. There is no evidence for splice variants of the protein although splicing in the 5'- and 3'-untranslated region (UTR) has been reported [96, 111]. Human MCT2 was exogenously expressed in *Xenopus* oocyte. The kinetic studies revealed that MCT2 catalyzed the proton-coupled transport of monocarboxylates but with a higher affinity than MCT1. The K_m values of pyruvate and L-lactate are 0.1 mM and 0.7 mM, respectively [92]. Besides, MCT2 is also more sensitive than MCT1 to inhibition by inhibitors such as CHC and DIDS. However, MCT2 is not inhibited by pCMBS, an inhibitor that interferes with the accessory protein, CD147. This is because MCT2 has a different, pCMBS insensitive accessory protein, namely gp70 [79]. Interestingly, MCT2 is expressed in several cancer cell-lines although its expression was not found in the respective native tissue. This finding suggests that MCT2 plays a specific role in cancer cell metabolism [96].

1.4.1.3 Monocarboxylate Transporter 3 (*SLC16A8*)

The expression of MCT3 is restricted to the basal membrane of the retinal pigment epithelium [78, 112] and choroid plexus epithelia [84]. While MCT3 has not been extensively studied, chicken MCT3 transports L-lactate with a K_m value of 6 mM when it is expressed in yeast [113]. In contrast to MCT1, MCT3 is insensitive to CHC, phloretin and pCMBS [113]. CD147-null mice shown a reduction in MCT3 expression and the loss of polarized expression [114]. This indicates that CD147 accessory protein is required for functional expression of MCT3.

1.4.1.4 Monocarboxylate Transporter 4 (*SLC16A3*)

MCT4 expression is high in glycolytic tissue such as white skeletal muscle fibres, astrocytes, white blood cells and chondrocytes [76, 86, 115-119]. As glycolytic white tissues are the primary source of lactate formation via anaerobic glycolysis, it has been proposed that MCT4 may work as an efflux transporter to mediate the transport of lactic acid out into the interstitial fluid [91, 93, 98, 115, 117, 120].

Indeed, MCT4 is expressed in the rat neonatal heart, which is more glycolytic in its energy metabolism than the adult heart where MCT4 is absent [121].

Characterization of MCT4 transport in *Xenopus* oocyte system reveals that MCT4 has lower affinity for both MCT substrates and inhibitors than MCT1 [93, 117].

For example, the K_m for L-lactate were 3.5 mM and 28 mM for MCT1 and MCT4, respectively [93].

The properties of MCT4 are suitable for its proposed role in lactate efflux from muscle. The very low affinity of MCT4 for L-lactate may slow down the transport of lactic acid from the muscle and thus results in lactate accumulation during exercise. The drop in pH in myocytes inhibits the muscle contractile machinery and glycolysis and probably plays an important role in the development of muscle fatigue [93]. Although such accumulation of lactate within myocytes and consequent impairment of glycolysis may impair exercise performance, it serves as a feedback loop to limit the lactic acid production by muscle under extreme exercise conditions and thus prevents the risk of lactic acidosis occurrence [93].

1.4.2 Tissue Distribution of MCTs

The MCT expression profile varies among tissues within a single species, as examined at both mRNA and protein levels. As mentioned above, only MCT3 has a uniquely restricted distribution, while MCT1, MCT2 and MCT4 are expressed in many tissues. Fishbein *et al.* examined the human tissue distribution of MCT1, MCT2 and MCT4 at protein level by Western blot analysis [115] (**Fig. 2**). MCT1 was detected in all 14 tissues examined, with highest expression in heart. Furthermore, MCT1 is the only MCT isoform expressed in human erythrocytes. MCT2 was expressed in 13 tissues while MCT4 was detected in 7 tissues. It is worth noting that although MCT4 is hypothesized to work as efflux transporter in glycolytic cell, its expression has also been found in highly oxidative tissues like heart.

Although this data may reveal the tissue distribution of the expressed protein, it is more important to determine the cellular and subcellular localization of these proteins within the tissue. This can be achieved by using Western blot analysis and both immunofluorescence microscopy and immunogold electron microscopy with specific antipeptide antibodies [115]. Several studies have examined the localization of MCT1, 2 and 4 within the muscle and central nervous system [119, 122-124]. However, there is currently no published data for MCT5-MCT14.

In many tissues, more than one MCT isoform is expressed. The co-existence of several MCT isoforms may have physiological implication that is related to their unique properties and/or to their regulation. The differences in kinetic characteristics and tissue distribution of these isoforms allow for fine tuning as well

as differential regulation of the transport depending on the specific needs of a particular tissue [74]. One well-documented examples is skeletal muscle tissue (**Fig. 3**). MCT1 and MCT4 have been reported to be the major MCT isoforms expressed in skeletal muscle [91, 115, 117, 120] and this appears to correlate with either the influx or efflux of lactic acid into different muscle fibre types. MCT1 expression is the most predominant isoform in oxidative red fibres, whereas MCT4 expression is high in glycolytic white fibres [115, 116]. As glycolytic white fibres are the primary source of lactate formation via anaerobic glycolysis, MCT4 may work as an efflux transporter to mediate the transport of lactic acid out into the interstitial fluid, to be taken up by red oxidative fibres that express primarily MCT1 [91, 93, 98, 115, 117, 120].

MCT1 is expressed on the plasma membrane of cerebrovascular endothelial cells. It is the only known facilitator of lactic acid transport across the blood brain barrier [91, 125-129]. Cerebral lactate is a matter of great interest because lactate is an important brain energy substrate [130, 131]. Under pathological states such as diabetes, prolonged starvation or hypoglycemia, significant monocarboxylate utilization by the brain was reported [132-134]. Besides, systemic lactate is taken up by the brain during intensive exercise when circulating lactate level is elevated [135-138]. Therefore, MCT1 plays critical role in brain energy metabolism. Moreover, monocarboxylate transporters may involve in central nervous system disorders such as ischemia and stroke. Cerebral lactate is a key metabolite pathways leading to brain damaging during stroke and brain injury [139-141]. The level of lactic acidosis is thought to be the factor or key indicator of the severity of damage [142, 143]. Recently, the role of intracellular pH (pHi) in

controlling the transport of MCT1 was studied in cerebrovascular endothelial cells [144]. Under normal condition, brain lactate influx into cerebrovascular endothelial cell cytoplasm and subsequently release into the blood. During ischemic lactic acidosis, reduced oxygen delivery to the brain leads to anaerobic glycolysis resulting in lactic acid production in affected cerebrovascular endothelial cells in the parenchyma. The fall in endothelial intracellular pH prevents the movement of lactate from the brain into endothelial cells, thus blocks the brain-to-blood flux of lactic acid [144]. Therefore, the authors of this study concluded that acidic intracellular pH inhibits lactate transport by MCT1 in the cerebrovascular endothelial cell and MCT1 may contribute to the development of lactic acidosis in brain pathologies [144].

Figure 2. Relative distribution of MCT1, MCT2 and MCT4 in 15 frozen human tissues. For each MCT, the optical density or absorbance (A) per mg protein was averaged for several runs for each tissue, and its mean and standard error were normalized to that of the highest mean tissue value, which was set at 100. The tissues are listed here in ascending order for MCT 1 levels. Spleen gave smears rather than bands, and was therefore counted as zero, although they could represent degraded bands (Adapted from Fishbein et al. 2002 [115]).

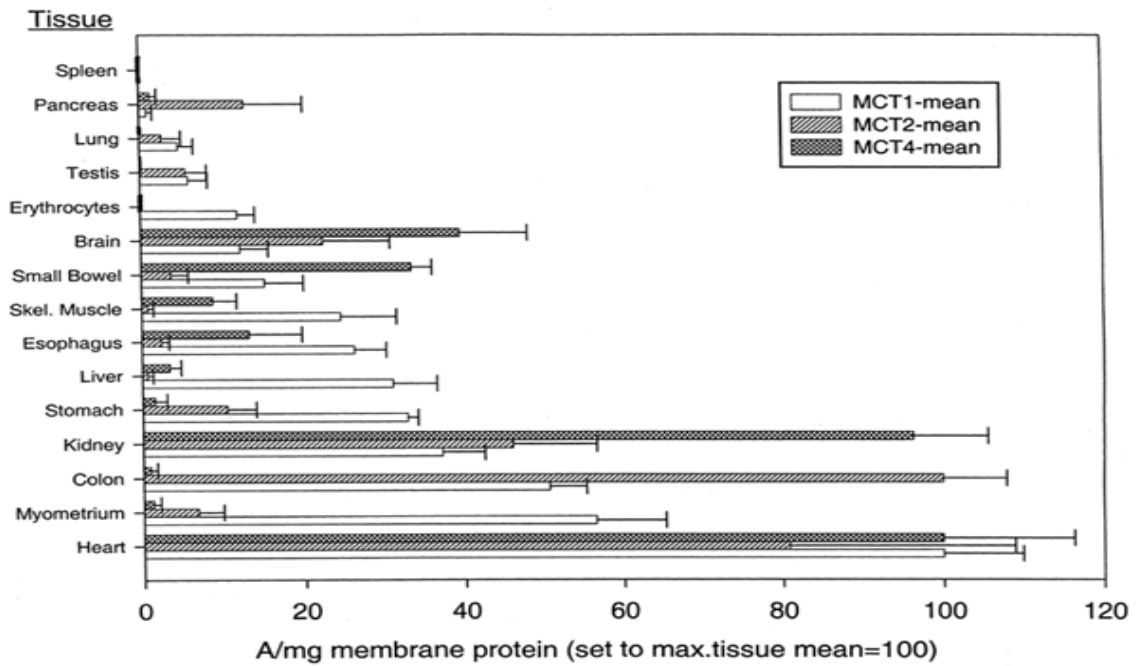
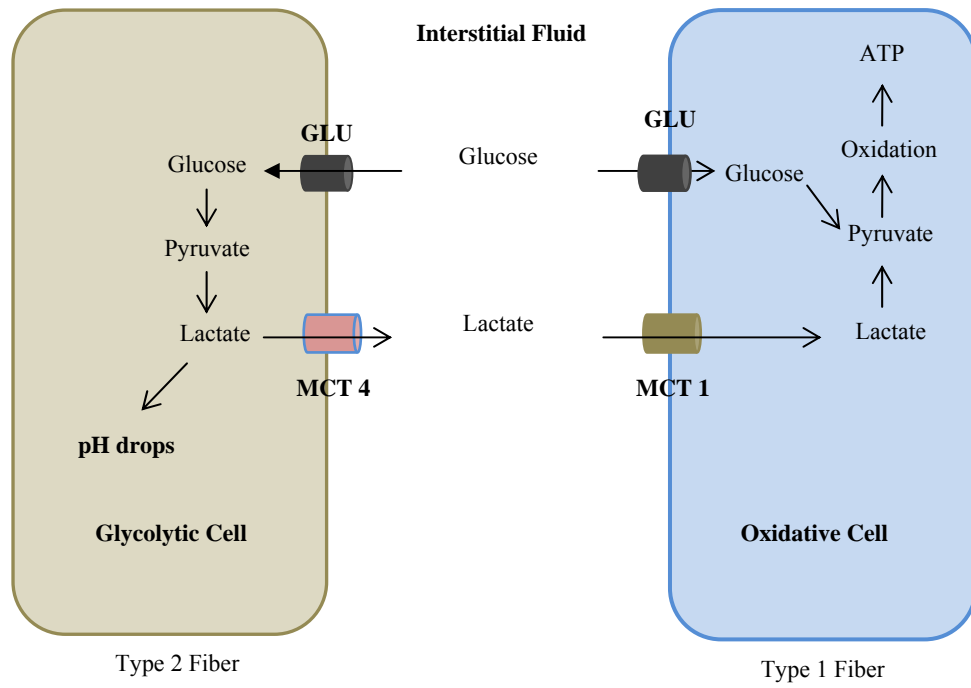


Figure 3. Hypothesized routes of lactate transportation and compartmentalization of lactate metabolism in human skeletal muscle cells [91, 93, 98, 115, 117, 120]



1.4.3 Intracellular Lactate Shuttle

Monocarboxylates such as lactate, pyruvate and ketone bodies are important in body energy metabolism. This is particularly true for lactate. For many centuries, lactate was largely considered as a dead-end waste product of glycolysis resulting from muscle hypoxia [145]. Lactic acid was thought to be the main cause of oxygen debt following exercise, an important factor in acidosis-induced tissue damage, and a major cause of muscle fatigue during intensive exercise [146]. Nonetheless, a new lactate paradigm has evolved since the early 1970s. Lactate is no longer considered as a dead-end waste product, but instead a central player in cellular, regional and whole body metabolism.

Over the past 40 years, considerable evidence suggests that lactate is an important intermediary in numerous metabolic processes and pathways. Lactate has been reported to be capable of inducing insulin resistance in muscle [147], of regulating energy homeostasis in the central nervous system [124], of inhibiting lipolysis in adipocytes [148], and of stimulating inflammatory pathways in L6 cells and in macrophages [149, 150]. Besides, lactate has even been shown to induce MCT1 expression in muscle cells [149]. The introduction of the lactate shuttle (cell-to-cell) hypothesis by George Brooks in 1984 has redefined the role of lactate in energy metabolism [151]. The cell-to-cell lactate shuttle provides the basic framework for interpretation of lactate metabolism. It posits that lactate formation and its subsequent distribution throughout the body is a major mechanism whereby the coordination of intermediary metabolism in different tissues, and cells within those tissues, can be accomplished [152]. Due to its large mass and metabolic capacity, the skeletal muscle is probably the major lactate producer as well as

consumer. During moderate- to high-intensity exercise, lactate is produced by glycolytic muscle fibres. Some of this lactate will be taken up by the neighbouring oxidative muscle fibres, and subsequently used as oxidative fuel [26, 153]. Part of this lactate escapes into the circulation, and is consumed by heart, and used for gluconeogenesis by the liver and kidney [154]. Lactate released into the blood can also be taken up by resting muscle and used as oxidative fuel [155, 156]. Furthermore, a recent study demonstrated that systemic lactate is an important substrate for the brain [138].

Blood is a key component in the lactate shuttle because it is the vehicle that distributes lactate to different tissues. It provides the route by which tissues throughout the body are linked together in the cell-to-cell lactate shuttle (**Fig. 4**) [157]. During exercise, lactate and protons move out from interstitial fluid of active muscles primarily through monocarboxylate transporter MCT1 and MCT4 and enter the plasma [73, 120, 158, 159]. From plasma, lactate is further transported into red blood cells (RBC) through MCT1 [73, 81, 82]. The cotransport of lactate and protons from lactate into RBC establishes a gradient between the plasma and interstitial fluid, which provides an additional space for lactate to be exported out from working muscles [157, 160]. This redistribution of lactate is crucial as the transport of lactate, together with its proton, out of contracting muscles and into blood may delay fatigue and hence improve exercise performance [161]. Furthermore, it has been calculated by Lindinger *et al.* that in human subjects lacking such transport, the lactate level in plasma would reach 162 mM after four 30s bouts of high intensity exercise [160]. Therefore, the role of MCT1 in transporting lactate into RBC is very important.

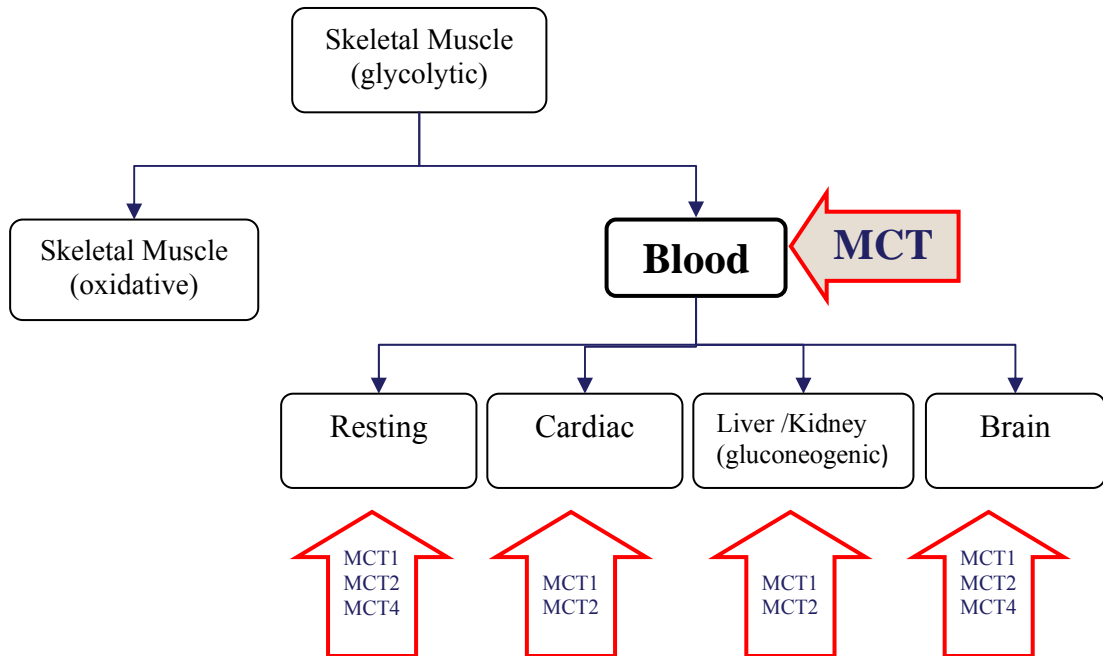
Three pathways mediate the transport of lactate across erythrocyte membrane: 1) nonionic diffusion of the undissociated acid; 2) an inorganic anion exchange system, often referred to as the band 3 system; and 3) a monocarboxylate-specific carrier mechanism [94, 162, 163]. The contribution of each of these systems in lactate transport is varying among species [94, 107]. In some mammals, monocarboxylate-specific transport system is the predominant pathway for lactate transport in the red blood cells, whereas the band 3 system is the preferred pathway for lactate transport in erythrocytes of other mammals. Deuticke has quantified the contributions of the three pathways in human erythrocytes and a few other species such as ox, rabbit, rat and guinea pig [107]. At a L-lactate concentration of 5 mM, transport via monocarboxylate system accounts for 90% of lactate flux across human erythrocyte membrane, while the band 3 system and nonionic diffusion contributed 6% and 4%, respectively. However, the band 3 system is the predominant pathway in ox's erythrocytes, which accounts for 53% of lactate transport. The monocarboxylate system and nonionic diffusion contributed 15% and 32% of lactate transport, respectively.

The roles of different carriers and the rate of total lactate influx vary among tissues and also among animal species. Previously, the RBC lactate transport capacities and pathways between athletic and non-athletic species have been studied. The study reported that lactate influx into the RBC of the athletic species was significantly greater than lactate influx into the RBC of the non-athletic species. The lactate influx into the RBC of athletic species (horses and dogs) is 3-65 times faster than lactate influx into the RBC of non-athletic species (cattle and goats). Differences in the influx of lactate into the RBC of the athletic species compared

with the nonathletic species correlate with the predominant pathway of transport. The monocarboxylate pathway was the primary pathway in RBC of the athletic species (~90% of total lactate influx), whereas the band 3 system was the primary pathway in RBC of nonathletic species (56-83% of total lactate influx) [164].

Human monocarboxylate transporters play important roles in shuttling of lactate among neighbouring cells, among tissues, between tissues, and among blood. At physiological pH, lactic acid is dissociated almost entirely to lactate anion [73]. Therefore, being highly charged, the contribution of passive diffusion on monocarboxylate transportation is thought to be insignificant. Previously, the inhibition of lactate transport mediated by MCTs has been suggested to be one of the factors that leads to apoptosis in skeletal muscle [165]. Given the current understanding of the roles of lactate as a central player in cellular, regional and whole body metabolism, any impairment in MCT activities may have greater impact in body's energy metabolism.

Figure 4. Schematic diagram of cell-to-cell lactate shuttle. Glucolytic muscle fibres produce lactate during exercise. Some of the lactate will be taken up by oxidative muscle fibres and be used as respiratory fuels. Part of the lactate enters blood circulation, and is consumed by heart, and used for gluconeogenesis by the liver. Systemic lactate can also be taken up by resting muscle and brain to be used as respiratory substrates.



1.4.4 Biochemical and structural aspects

The MCTs are generally predicted to have 12 α -helical transmembrane domains (TMDs), with the N- and C-termini located at the cytoplasm (**Fig. 1**). This has been confirmed experimentally for MCT1 in erythrocytes [166]. The main regions of sequence variation between isoforms are in the C- and N-termini regions and the large intracellular loop between TMD 6-7. There are two highly conserved sequences can be identified as characteristic of the MCT family; these are **[D/E]G[G/S][W/F][G/A]W** which traverses the lead into TMD1; and **YF**xK**[R/K][R/L]**xL**A**x**[G/A]**x**A**x**A**G which leads into TMD5 [73]. The residues in bold are totally conserved, while those in plain text are the consensus residue. These consensus regions are found in all 14 members of human MCTs and in the non-mammalian MCT family.

Knowledge of the molecular structure-function relationship of transporters is instrumental in producing accurate prediction of the effects of SNPs. Single-point mutations within these transmembrane domains have been shown to greatly affect the substrate specificity and transport activity of MCT1 transporter. The spontaneous nucleotide conversion of phenylalanine to cysteine at position 360 in TMD 10 of rat MCT1 converted major substrate specificity to mevalonic acid [167]. The roles of other residues have been investigated using site-directed mutagenesis (**Table 7**). A conversion of amino acid lysine to glutamine at position 290 (extracellular loop between TMD 7 and 8) or 413 (extracellular loop between TMD 11 and 12) abolished the irreversible inhibition of MCT1 by DIDS [70]. The substitution of arginine to threonine in TMD 8 (Arg306 in rat MCT1/Arg313 in human) resulted in the reduction of MCT1's substrate affinity as this arginine

residue was predicted to bind the carboxy group of the substrate [168]. Lastly, the amino acid substitution of Asp302 in rat (Arg 309 in human) MCT1 to glutamate completely abolished uptake despite normal surface expression [168].

Table 7. *The effects of mutating charged residues in potential TM helices of MCT1 on its plasma membrane expression and activity (Adapted from Manoharan et al. [169])*

| Mutation in rat MCT1 | Position in Human MCT1 | TM or loop | Plasma membrane expression | Activity | Reference |
|----------------------|------------------------|------------|----------------------------|----------|-----------|
| D15N | D15 | 1 | Yes | Yes | [170] |
| K38Q | K38 | 1 | Yes | Yes | [169] |
| K45Q | K45 | 1 | Yes | Yes | [169] |
| R86Q | R86 | 3 | Yes | Yes | [169] |
| R86E | R86 | 3 | Yes | Yes | [169] |
| K137Q | K137 | 4-5 | Yes | Yes | [170] |
| K141Q | K141 | 4-5 | Yes | Yes | [170] |
| K142Q | K142 | 4-5 | Yes | Yes | [170] |
| R143Q | R143 | 5 | Yes | No | [170] |
| R143H | R143 | 5 | Yes | Yes | [170] |
| R143K | R143 | 5 | Yes | No | [170] |
| R143E | R143 | 5 | Yes | No | [170] |
| R143E/E369R | R143 | 5/10 | Yes | No | [170] |
| R175Q | R175 | 5-6 | Yes | Yes | [169] |
| R196E | R196 | 6 | Yes | Yes | [169] |
| R196Q | R196 | 6 | Yes | Yes | [169] |
| K204E | K204 | 6, 6-7 | Yes | Yes | [169] |
| K282Q | K289 | 7-8 | Yes | Yes | [169] |
| K282R | K289 | 7-8 | Yes | Yes | [169] |
| K290Q | K297 | 7-8 | Yes | Yes | [169] |
| K290R | K297 | 7-8 | Yes | Yes | [169] |
| D302E | D309 | 8 | Yes | No | [168] |
| D302N | D309 | 8 | No | No | [168] |
| R306T | R313 | 8 | Low | ? | [168] |
| R306E | R313 | 8 | No | No | [169] |
| D302R/R306E | D309R/R313E | 8 | Yes | No | [169] |
| H337Q | H344 | 9 | Yes | Yes | [168] |
| E369R | E376 | 10 | Yes | No | [168] |
| E391Q | E398 | 11 | Yes | Yes | [168] |
| R404E | R410 | 11 | Yes | Yes | [169] |
| K413R | K420 | 11-12 | Yes | Yes | [169] |
| K413Q | K420 | 11-12 | Yes | Yes | [169] |

1.4.5 MCT mutation and genetic syndromes

Due to the importance of lactate transport in key metabolic processes, mutations in these transporters might provide an explanation for some pathophysiological conditions. In fact, the defects in MCT1 have already been associated with lactate transport deficiency in red blood cells and muscle tissues by Fishbein back in 1986 [171]. In 2000, Merezhinskaya *et al.* reported three missense mutations in MCT1 in five patients with symptomatic deficiency in lactate transport (SDLT) [172]. Of these, Lys204Glu and Glu472Gly were presumably responsible for the subnormal lactate transport, while Asp490Glu was proven to be a common polymorphism in the normal cohort. The Lys204Glu was subsequently expressed in *X. laevis* oocyte system and shown no effect on lactate transport [91]. However, the subject was revisited more recently, and expression of the mutant form in *X. laevis* oocytes was found to produce a marked decrease in maximum transport rate [74]. Although the study done by Merezhinskaya *et al.* did not comprehensively dissect the entire coding region of the gene and only selected SNPs (Lys204Glu, Glu472Gly and Asp490Glu) were screened in 79-90 normal subjects, Merezhinskaya *et al.* had nonetheless presented the first search for clinically relevant mutations in the MCT1 gene [172].

Recently, Otonkoski *et al.* identified two new mutations in the non-coding regions of MCT1 that leads to a dominantly inherited hypoglycemic disorder known as exercise-induced hyperinsulinism (EIHI) [173]. One group of patients had a mutation in the 5' untranslated promoter region and the other group had a mutation in the non-coding exon 1, each resulting in increased promoter binding and abnormally high transcript levels. MCT1 is not normally transcribed in pancreatic

cells. The increased transcription was presumed to lead to pyruvate uptake and metabolism upon exercise. This resulted in inappropriate insulin secretion despite the falling blood glucose [173].

1.4.6 Regulation of MCT Isoforms

MCT1 is ubiquitously expressed but is especially prominent in oxidative skeletal muscle, where it is up-regulated in response to chronic stimulation or exercise in rats and humans [75, 158, 174, 175]. Conversely, MCTs are down-regulated in response to denervation of muscle or spinal injury [158]. The mechanism of MCT1 regulation in skeletal muscle has not been established. Recently, Narumi *et al.* investigated the possible regulation of MCT1 by the major signaling pathways in human skeletal muscle rhabdomyosarcoma cells (RD cells) [176]. The effects of five major signaling pathways, namely protein kinase A, C, and G (PKA, PKC and PKG), protein tyrosine kinase (PTK) and Ca²⁺/calmodulin-mediated pathway on the regulation of MCT1 were examined. The data showed that the PKG-, PTK- and Ca²⁺/calmodulin-mediated pathway do not involve in the regulation of MCT1. The results showed that PMA, a PKC activator, increased the expression of MCT1 protein. In contrast, 8-Br-cAMP, a PKA activator, significantly decreased the MCT1 protein level in RD cells treated with 8-Br-cAMP for 24 hours. It has been reported that muscle contraction increase PKC activity [177]. Besides, there is information showing that muscle denervation leads to intracellular cAMP accumulation and stimulates PKA activity in muscle [178]. Therefore, these results indicate the possible involvement of a PKC- and PKA- mediated pathways associated with MCT1 expression in skeletal muscle [176]. The expression of MCT4 has been shown to be up-regulated by AMP-activated protein kinase

(AMPK) pathway [179]. In this study, the AMPK activation induced expression of MCT4 in RD cells and rat skeletal muscle in a fiber-type specific manner [179].

In human colon, there is evidence for up-regulation of MCT1 expression mediated by butyrate [180]. The basis of this regulation is a butyrate-induced increase in MCT1 mRNA level, resulting from the dual control of MCT1 gene transcription and stability of the MCT1 transcript. Borthakur *et al.* have cloned the promoter region of the MCT1 gene and identified the *cis* element for key transcription factors [181]. The results demonstrated the involvement of NF- κ B pathway in the regulation of MCT1 promoter activity by butyrate. In contrast, the PKC, PKA and tyrosine kinase pathways played no role in butyrate-induced MCT1 regulation [181]. Recently, the effects of somatostatin on butyrate absorption and MCT1 expression in intestinal Caco-2 cells have been examined [182]. Somatostatin is an important anti-inflammatory neuropeptide in the gastrointestinal tract, which is known to act as a neurotransmitter and hormone [183, 184]. The study showed that somatostatin increased the membrane levels of MCT1 and CD147 and enhanced association of MCT1 with CD147 in Caco-2 cells via the p38 MAPK-mediated pathway [182].

MCT1, MCT2 and MCT4 are expressed in human adipose tissue. A recent study reported that hypoxia results in increased lactate release and modulates the expression of specific MCTs by human adipocytes in a type-specific manner, with MCT1 and MCT4 expression being hypoxia-inducible transcription factor-1 (HIF-1) [83]. Hypoxia increased the mRNA levels of MCT1 and MCT4 in human adipocytes, but reduced the mRNA level of MCT2. MCT1 protein was increased

by 2.7-fold by 48 hours hypoxia, but the expression of MCT4 protein level remained unchanged. The changes in hypoxia-induced MCT gene expression was found to be reversible when the cells return to normoxia [83]. However, the result of this study was inconsistent with the finding of Ullah *et al.* [185]. Ullah *et al.* concluded that MCT4, but not MCT1, is regulated by hypoxia through a HIF-1 α -mediated mechanism. In addition, the HIF-1 transcription factor binding site is only found in the promoter region of MCT4, but not in the MCT1 and MCT2 genes. Therefore, the modulation of hypoxia in MCT1 and MCT2 expressions may be mediated through an indirect mechanism [83].

1.4.7 Roles of MCTs in drug and xenobiotic distribution

MCTs may also have a role in the transport of pharmacologically active compounds, which generally consist of weak organic monovalent acids, with a carboxyl attached to a relatively small R group [91]. These include statins such as lovastatin, simvastatin and atorvastatin. Nagasawa *et al.* have reported that lovastatin is taken up into bovine kidney NBL-1 cells and rat mesangial cells via MCT, with kinetic evidence suggesting that MCT4 is the isoform responsible for lovastatin uptake [186, 187]. However, the rat cultured mesangial cells and bovine kidney NBL-1 cells used by Nagasawa *et al.* were also shown to express other MCT isoforms; the involvement of other MCT isoforms cannot thus be excluded. MCTs might also mediate simvastatin uptake into the brain as simvastatin transport is competitively inhibited by acetate [105, 188]. Several weak organic acids have been experimentally proven to be transported by rat MCT1. The uptake of benzoic acid across intestinal and blood-brain barrier has been reported to be mediated by rat MCT1 [125, 189]. Furthermore, MCT1 has been reported to play a part in the uptake of gamma-hydroxybutyrate (GHB) across the blood-brain barrier [190], the absorption of nicotinic acid in the intestine [191], as well as the transportation of salicylic acid and valproic acid [100].

1.5 THESIS RATIONALE

Given that MCT1 and MCT4 have been implicated in lactate transport, any impairment in transporter activity may have far reaching consequences. One of the main objectives of this project was therefore to describe the genetic polymorphisms in the promoter, exons and exon-intron junctions of *SLC16A1* and *SLC16A3* genes that may be present in the ethnic Chinese and Indian groups of the Singapore population. The effects of SNPs reported in this study will be predicted using bioinformatics tools. To our knowledge, this is the first report on the comprehensive analysis of *SLC16A1* and *SLC16A3* genes in any population.

Although Merezhinskaya *et al.* had presented the first search of clinically relevant mutations in *SLC16A1* gene, the study done by Merezhinskaya *et al.* had screened only selected SNPs (Lys204Glu, Glu472Gly and Asp490Glu) in 79-90 normal subjects and did not comprehensively dissect the entire coding region of the gene.

The complex actions of transporters during drug-transporter or food-transporter interactions may have far-reaching consequences. Given the roles of MCT1 in transporting endogenous monocarboxylates as well as clinically important drugs [105, 192, 193], these interactions can cause serious consequences. The diet-drug interactions via MCT1 inhibition may affect lactate shuttling and drug disposition in the body. Several dietary and pharmacological compounds have been shown to serve as the substrate and/or inhibitor for MCT1 [108, 194, 195]. Therefore, the second objective of this study is to examine the effects of various dietary compounds and pharmacological agents on human monocarboxylate transporter 1 in mediating L-lactate transport across human red blood cells.

We are interested in the RBC lactate influx assay because it is an excellent model to study human MCT1 transporter. Unlike most cell-lines that express other MCT isoforms, MCT1 is the only isoform found in the human RBC and it accounts for 90% of lactate transport [72, 107]. Besides, RBC samples can be easily obtained and the techniques for preparation of RBCs and lactate influx measurement are well established [164, 196-200].

The role of different carriers and the rate of total lactate influx vary among tissues and also among animal species. However, variation in lactate transport within a single species has not been studied. It has been reported that the muscle-plasma lactate concentration gradients in human subjects vary widely between individual subjects [201]. However, it remained unknown whether the rate of lactate influx into the RBC exhibits similar interindividual variation. The third aim of this study was therefore to examine whether the rate of lactate influx into RBC varies among individual. We have previously screened the genetic variants in the *SLC16A1* gene in ethnic Chinese and Indian groups of the Singapore population and a common nonsynonymous SNP, 1470 T>A (Asp490Glu) had been identified in *SLC16A1* (**Table 10**). In light of this, it would be intriguing to explore the effect of this SNP on erythrocyte lactate transport.

We have previously examined the inhibitory effects of several drugs on MCT1-mediated L-lactate influx. Therefore, it will be beneficial to clinically examine the physiological effect of MCT1 in mediating lactate influx from plasma to erythrocyte. Hence, the fourth objective of this study was to evaluate the potential influence of MCT1 on distribution of lactate in plasma and erythrocyte and the

effect of MCT1 inhibitor, diflunisal, on lactate distribution in blood. The result of this study will increase our understanding of the clinical relevance of MCT1 transporter-based drug interactions.

1.6 SPECIFIC AIMS OF THE STUDY

- 1. To detect and describe the genetic polymorphisms in the *SLC16A1* and *SLC16A3* genes encoding MCT1 and MCT4 proteins that may be present in the ethnic Chinese and Indian groups of the Singaporean population**

The methods and approaches used to achieve this aim were:

- Genetic screening by PCR amplification of genomic DNA followed by direct sequencing
- Determination of genotype and allelic frequencies by gene counting
- Examine ethnic differences in allele frequencies by Chi Square analysis
- Reconstruction of haplotypes and estimation of population haplotype frequencies using SNPAnalyzer
- Examine ethnic differences in haplotype frequencies by Chi Square analysis

- 2. To examine the effects of pharmaceutical agents and phytochemical compounds on human erythrocyte MCT1**

The methods and approaches used to achieve this aim were:

- The inhibitory potencies of these compound were examined by determined the IC_{50} by making measurements over a broad range of inhibitor concentrations
- The inhibitor types were studied using the Lineweaver-Burk plots

3. To explore interindividual variation in erythrocyte lactate transport activity

The methods and approaches used to achieve this aim were:

- Performing human erythrocyte influx assay to measure transporter activity
- Genotyping of healthy volunteer using methods and approaches described in (1)
- Examine the relationship of 1470 T>A (Asp490Glu) variant with erythrocyte lactate transport activity

4. To evaluate the potential influence of MCT1 on the distribution of lactate in plasma and erythrocyte and the effects of the MCT1 inhibitor, diflunisal, on lactate distribution in blood

The methods and approaches used to achieve this aim were:

- This was a single-centre, randomized, 2 periods crossover drug interaction study conducted in 12 healthy adult male volunteers
- Sodium lactate infusion was used to raise the blood lactate level
- Diflunisal was selected as MCT1 inhibitor to block MCT1 activity
- The plasma, whole blood and erythrocyte lactate levels were measured in the absence or presence of diflunisal

CHAPTER 2

POPULATION GENOTYPING OF MCT1 AND MCT4

Part of this project has been published in:

Lean, C. B. and E. J. Lee (2009). "Genetic variations in the MCT1 (*SLC16A1*) gene in the Chinese population of Singapore." *Drug Metab Pharmacokinet* 24(5): 469-474.

The population genotyping of *SLC16A3* gene has been accepted for publication under manuscript entitled:

“Genetic Variations of the MCT4 (*SLC16A3*) Gene in the Chinese and Indian Populations of Singapore.”

OVERVIEW

MCT1 (*SLC16A1*) is the first member of monocarboxylate transporter (MCT) and its family is involved in the transportation of metabolically important monocarboxylates such as lactate, pyruvate, acetate and ketone bodies. This study aimed to identify genetic variations of *SLC16A1* in the ethnic Chinese (n = 95) and Indian (n = 96) groups of the Singaporean population. To our knowledge, this is the first report on the comprehensive analysis of *SLC16A1* gene in any population. The promoter, coding region and exon-intron junctions of the *SLC16A1* gene encoding the MCT1 transporter were screened for genetic variations in the study population by DNA sequencing. A total of 21 genetic variations of *SLC16A1*, including 14 novel ones, were found: 6 in the promoter region, 4 in the coding exons (3 nonsynonymous variations and 1 synonymous variation), 4 in the 5' untranslated region (5'UTR), 6 in the 3' untranslated region (3'UTR) and 1 in the intron. Of the 3 nonsynonymous variants, only 303T>G (Ile101Met) was predicted by PolyPhen and SIFT as having a potentially damaging effect on protein function, whereas 1282 G>A (Val428Ile) and 1470 T>A (Asp490Glu) were speculated to be benign. Genotyping data was in accordance to Hardy Weinberg Equilibrium for all loci, except for the -363-100 C>G SNP which showed departure from HWE in Chinese ($X^2=6.267$, $p=0.012$). Three reported SNPs, namely IVS3-17A>C, 1470T>A (Asp490Glu) and 2917(1414) C>T are the common polymorphisms found in the coding region of *SLC16A1* gene in Chinese and Indian populations. Linkage disequilibrium analysis revealed strong association between these common variants in both ethnic groups.

MCT4 (*SLC16A3*) is the third member of monocarboxylate transporter and is involved in the transportation of metabolically important monocarboxylates such as lactate, pyruvate, acetate and ketone bodies. This study aimed to identify genetic variations of *SLC16A3* in the ethnic Chinese (n = 95) and Indian (n = 96) groups of the Singaporean population. To our knowledge, this is the first report on the comprehensive analysis of *SLC16A3* gene in any population. The promoter, coding region and exon-intron junctions of the *SLC16A3* gene encoding the MCT4 transporter were screened for genetic variations in the study population by DNA sequencing. A total of 46 genetic variants were detected in *SLC16A3* gene, of which 33 are novel. Of these variants, 22 are located in the promoter regions, 2 in the 5' untranslated region (UTR), 10 in the coding exons (5 nonsynonymous and 5 synonymous variations), 6 in 3'UTR and 6 in the intron. Of the 5 nonsynonymous variants, only 44C>T (Ala15Val) was predicted by PolyPhen and SIFT as having a potentially damaging effect on protein function, whereas 55G>A (Gly19Ser), 574G>A (Val192Met) and 916G>A (Gly306Ser) had conflicting results between the SIFT and PolyPhen algorithms. Finally, 641C>T (Ser214Phe) was predicted to be tolerated variant. Genotyping data was in accordance to Hardy Weinberg Equilibrium for all loci, except for the IVS2-149 G>T SNP which showed departure from HWE in Chinese ($X^2=22.74$, $p<0.001$).

2.1 MATERIAL AND METHODS

2.1.1 Study Populations

Genetic materials used in this study were randomly selected from a previously-developed cell repository from healthy volunteers of Chinese and Indian descent. The fully anonymized white cell lines developed from 192 individuals of the ethnic Chinese and Indian of the Singaporean population were screened in this study (Chinese, n = 96; Indian, n = 96). However, the DNA sample of one Chinese individual was not sufficient for the screening of the entire gene. Hence this subject has been excluded out from the study and only 95 ethnic Chinese individuals were participated in this study. All donors had been recruited previously in accordance with the requirements of the local ethics requirements (Institutional Review Board, National University Hospital, Singapore) and had provided written informed consent. The mean age was 24.0 ± 5.2 (18-48) and 24.3 ± 7.6 (17-52) for Chinese and Indian, respectively. The male:female sex ratio was 48:47 for Chinese and 57:39 for Indians. All DNA samples were rendered anonymous by removing links with specific individual information, i.e., any ID, name, or address. Ethnicity was defined through self-declaration by the donors of similar ethnicity through three generations.

2.1.2 DNA extraction

Genetic materials used in this study were obtained from a previously-developed cell repository from healthy volunteers of Chinese and Indian descent. 45 ml of Buffer A (0.32 M sucrose, 10 mM Tris HCl pH 7.4, 5 mM MgCl₂, and 1 % Triton-X-100) was added to the white cell pellet and mixed by inversion. The solution was spun (4°C, 20 min, 1500 g) and the supernatant was removed by aspiration. The

same procedure was repeated once. The pellet was resuspended in 5 ml of Buffer B (25 mM EDTA pH 8.0 and 75 mM NaCl). This is followed by the addition of 250 μ l of 10 % Sodium Dodecyl Sulfate (SDS) and 20 μ l of 20 mg/ml proteinase K. The contents were vortexed briefly and incubated overnight at 37°C with shaking in an oven. At the end of incubation, 1.4 ml of saturated NaCl (6 M) was added to the mixture and the mixture was vortexed vigorously for 15 seconds. The solution was spun (15 min, 1500 g) and the supernatant was transferred to a new 50 ml falcon tube containing 15 ml of absolute ethanol. The mixture was mixed gently by inversion to precipitate DNA. The mixture was spun (20 min, 1500 g) and the supernatant was removed. The DNA pellet was washed with 5 ml of 70% ethanol and was spun (15 min, 1500 g). The supernatant was removed and the pellet for air-dried for 30 minutes. The recovered DNA was dissolved in 200 μ l of TE solution (10 mM Tris HCl pH 7.5 and 1 mM EDTA pH 7.5) and was dissolved at 4°C overnight. The DNA was transferred to an Eppendorf tube and stored at -20°C. The isolated DNA was quantified using μ Quant Universal Microplate Spectrophotometer (ITS) and absorbance readings were taken at 260 nm wavelength. Optical Density (OD), which determines the purity of the DNA, was obtained by measuring the ratio of 260 nm/280 nm (DNA maximum absorbance= 260 nm wavelength). OD readings between 1.7 – 1.8 were accepted as a lower or higher ratio indicates protein or ribonucleic acid contamination respectively. Finally, the DNA was diluted with DNase-free water to a concentration of 20 ng/ μ l.

2.1.3 Primer Selection

2.1.3.1 Monocarboxylate Transporter 1 (*SLC16A1*)

The *SLC16A1* gene spans approximately 44 kb and is mapped onto chromosome band 1p13.2-p12 in human. MCT1 comprises 5 exons and 4 introns, encoding an mRNA approximately 15,000 base pairs. The promoter and exonic fragments for the *SLC16A1* gene were generated using self-designed primer sequences. These primers were designed using Primer3 software (Whitehead Institute for Biomedical Research, Cambridge, MA, USA). A section between bases -1418 and + 217 was screened for *SLC16A1* promoter region (GenBank accession: NM_003051). The primer sequences and annealing temperatures for the promoters and exonic fragments of *SLC16A1* gene are summarized in **Table 8**.

2.1.3.2 Monocarboxylate Transporter 4 (*SLC16A3*)

SLC16A3 gene spans approximately 11 kb and is mapped onto chromosome band 17q25.3 in human. According to NCBI, six transcript variants have been described for this gene, of which all three transcripts have functional protein products (<http://www.ncbi.nlm.nih.gov/gene/9123>). The six transcript variants are created by alternative promoter usage and alternative splicing at the 5' end of the gene, therefore the protein products for all three transcript variants are identical. The promoter and exonic fragments for the *SLC16A3* genes were generated using self-designed primer sequences. These primers were designed using Primer3 software. The regions between bases -1534 and +159 of the *SLC16A3* transcript variant 2 (GenBank accession: NM_001042422.2), -531 and +14 of the *SLC16A3* transcript variant 3 (GenBank accession: NM_004207.3) and -1685 and +87 of the *SLC16A3* transcript variant 4 (GenBank accession: NM_001042423.2) were screened for

SLC16A3 promoter regions. The primer sequences and annealing temperatures for the promoters and exonic fragments of *SLC16A3* gene are summarized in **Table 9**.

Table 8. Primer sequences and PCR conditions used for the analysis of promoter, 5'-UTR, coding and 3'-UTR regions of *SLC16A1* gene

| Amplified or sequenced region | Forward primer (5' to 3') | Reverse primer (5' to 3') | Amplified region (NT_019273) | Length (bp) | Annealing temperature (°C) |
|-------------------------------|----------------------------|---------------------------|------------------------------|-------------|----------------------------|
| Promoter a | CTCAGTCGCTTCCCGCTAC | CTCGTTTGCTTGTTCCAGTACC | 9406444 - 9406939 | 496 | 60 |
| Promoter b | TCTTTAATACCCACCAGGCG | TCTGACGAGCTCTAGGCAATC | 9406789 - 9407242 | 454 | 58 |
| Promoter c | CGGGTCCCTTATTTACAAAATGT | GAAGTGGCGACAGTAGTAGAACC | 9407120 - 9407479 | 368 | 54 |
| Promoter d | AGCAGCAAGTGCTCAACAGAT | TCACCCGGATTATCCTCTCTAAT | 9407411 - 9407766 | 356 | 54 |
| Promoter e | CCTTTCTCCGTGTTTATCAAATG | AAGTTTTTGGGGGAGACTTAGG | 9407709 - 9408078 | 370 | 54 |
| Promoter f | CTGAGGACACAGAGCTGGTAAGT | TATTAGAAGACAGTGTGGCATCC | 9407990 - 9408349 | 397 | 58 |
| Exon 1 | CTGCAGTTCGGATGTCTGTGT | AAGGTCTCCTTCACCAGCACT | 9406154 - 9406622 | 469 | 58 |
| Exon 2 | TTCACAAAAGAGTTTTATAGGTGTGC | CTAATACAGACACTCTGGCTGCTTC | 9379337 - 9379723 | 387 | 50 |
| Exon 3 | CTTGTGTAGATGTGAGGGAGC | CAGGTAAATACAAAATAGCCAGCC | 9372234 - 9372500 | 266 | 55 |
| Exon 4a | GGATTTATATCCTATTCTTCCATTA | TCCAGCTTTCTCAAGGGATG | 9368059 - 9368449 | 390 | 56 |
| Exon 4b | CAGCCCTGTGTTCTCTGTGA | ACCAAAGGTGCAAAGAGTCC | 9367864 - 9368254 | 466 | 59 |
| Exon 4c | TGGAAGACACCCTAAACAAGAGA | CCAAAGAATCCCGCATAGAC | 9367622 - 9368011 | 390 | 50 |
| Exon 4d | TGGGACTGTAGCCAACACA | TTGCTTTCTGTCAGCATTCC | 9367410 - 9367766 | 357 | 55 |
| Exon 5a | GGATCCTTAAGCTTTGCTTGG | ATTTGCATTGAGCACCCTG | 9364101 - 9364551 | 451 | 50 |
| Exon 5b | CAAGGAGGAGGAAAGTCCAG | TCTTCCAGTGAAAATGTCTGAAA | 9363729 - 9364223 | 494 | 56 |
| Exon 5c | TGGGGGAAAGAAGTAGGTTC | CCTTAAGCACTTTACTTGGCTTC | 9363497 - 9363994 | 498 | 50 |

Table 9. Primer sequences and PCR conditions used for the analysis of promoter, 5'-UTR, coding and 3'-UTR regions of transcript variants of *SLC16A3* gene

| | Amplified or sequenced region | Forward primer (5' to 3') | Reverse primer (5' to 3') | Amplified region ^a | Length (bp) | Annealing temperature (°C) |
|----------------------|-------------------------------|---------------------------|------------------------------|-------------------------------|-------------|----------------------------|
| Transcript Variant 2 | Promoter 1a | CTCCTTTGTGTGTGAAGGCA | ACATCCTCCCTCTCTGAGGC | 400006 - 400558 | 493 | 60 |
| | Promoter 1b | GCACGGGCCAACTAAGTAGA | GTCTAGTTGTCAGGGCCACC | 399670 - 400123 | 527 | 58 |
| | Promoter 1c | CAGGCTCTCTGGCTCTGTCT | CCCAAACATCAAGATGAGGG | 399253- 399779 | 454 | 60 |
| | Promoter 1d | TCCTCTGGGTAACAACCTGG | ACCGAGACACCTTCCACATC | 398866 - 399358 | 553 | 58 |
| | Exon 1 | CATGTTGCAAATGAGAGAAAACA | AGGTCCCAACGTCTCCAG | 427045 - 427519 | 475 | 60 |
| Transcript Variant 4 | Promoter 3a | GTCTGCGGGGGTCAGAG | GTCTGCGGGGGTCAGAG | 430685 - 431181 | 497 | 60 |
| | Promoter 3b | CCTCCCGGTCTTCACCTT | AAGGAAGGAGCAGTGAGCAA | 430203 - 430826 | 624 | 60 |
| | Promoter 3c | GCCCTGTGGCTTCGAG | CCTCCACCCTAAAGCCAGT | 429804 - 430333 | 522 | 60 |
| | Promoter 3d | AGTGACCCTTATGCCAGGCT | GGACGCTACCGTAATTGCC | 429410 - 429898 | 489 | 60 |
| | Exon 1 | GAAACGAATTACCCTTTTCCTG | GGGACCTCTCCAGAAACCTC | 430980 - 431279 | 300 | 54 |
| | Exon 2 | CCACCAGACACCAGGTCAG | TTGCTGAGCCCAGCTACAC | 407812 - 408295 | 484 | 60 |
| | Exon 3 | GTTCTGAAAAGGTGGCTGTT | AAAGCCCGAGACCCTCATCT | 408478 - 409077 | 600 | 63 |
| | Exon 4a | AGATGAGGGTCTCGGGCTTT | GAAGACGCTCAGGTCTAGCAG | 409058 - 409422 | 365 | 60 |
| | Exon 4b | GTAGCCCTGTCTTCTGTGTG | AACATGGAGAAGCTGAAGAGG TAG | 409217 - 409661 | 445 | 60 |
| | Exon 4c | CTGGGCTTCATTGACATCTTC | CCAGCTCTGAGTCCCACACT | 409561 - 409994 | 434 | 60 |
| | Exon 5a | CACAAGCTCAGAGGCAGACAG | GAGCCAGTCCAGTTTGTA AAA | 410560 - 411043 | 484 | 60 |

| | | | | | |
|---------|------------------------|----------------------------|-----------------|-----|----|
| Exon 5b | GAGCATTTCCTGAAGGCTGAG | CATTAAAGTCACGTTGTCTCGA | 410891 - 411285 | 395 | 60 |
| Exon 5c | CAAGGTTACAAGGCATCCTCAC | AG GACAGAGCCACGGTAGGAAC | 411171 - 411558 | 388 | 67 |

2.1.4 Polymerase Chain Reaction Amplification

The polymerase chain reaction (PCR) amplifications were performed in a total volume of 30 μ l containing 1 X Master Mix (Promega, Madison, WI, USA), 0.4 μ M of each primer (Sigma-Aldrich, St. Louis, MI, USA) and 60 ng of DNA on the MJ Research Peltier Thermal Cycle (DNA Engine Dyad; MJ Research Inc, Waltham, MA, USA). The PCR conditions were pre-denaturation at 95°C for 5 min, followed by 35 cycles of denaturation at 95°C for 1 min, annealing for 1 min, and extension at 72°C for 1 min, and then a final extension at 72°C for 10 min. The annealing temperatures for the fragments of *SLC16A1* and *SLC16A3* genes are summarized in **Table 8** and **Table 9**, respectively. Cycle sequencing was performed on the MJ Research Peltier Thermal Cycler using the following conditions: initial denaturation at 96°C for 10 seconds, 50°C for 5 seconds, and 60°C for 4 minutes.

2.1.5 Agarose Gel Electrophoresis

After PCR amplifications, the PCR products obtained were verified by electrophoresis through 1% agarose gels stained with 0.2 μ g/ml ethidium bromide. They were subjected to electrophoresis at 100 V for 1 hour and visualized under UV illumination. PCR amplifications that were found to produce poor DNA yield were discarded and repeated because it would lead to downstream problems such as ambiguous results from DNA sequencing.

2.1.6 DNA Sequencing

2.1.6.1 PCR Product Clean Up

Prior to sequencing, PCR products were cleaned up to remove excess primers and unincorporated dNTPs. 12 µl of PCR products were being added to one unit of Shrimp Alkaline Phosphatase (Promega) and two units of Exonuclease I (New England Biolabs, Beverly, MA, USA). The reaction mix was incubated at 37°C for 15 minutes and followed by enzyme deactivation at 80°C for 20 minutes.

2.1.6.2 Cycle Sequencing

In this study, all PCR products were subjected to DNA sequencing. Mutational analysis of the candidate genes was performed using BigDye Terminator v3.1 Cycle Sequencing Kit. Extension reactions were performed in a total volume of 20 µl containing 10 µl of purified PCR products, 0.5 µl of BigDye Terminator reagent, 2 µl of 5x sequencing buffer, 2 µl of oligonucleotide primer (5 pmole/µl) and 3.5 µl of water. Primers for cycle sequencing were similar to the primers for PCR (**Table 8** and **Table 9**). Amplification of cycle sequencing products was generated using MJ Research Peltier Thermal Cycle with cycling profile: denaturation at 96°C for 1 min, 25 cycles of denaturation at 96°C for 10 seconds, annealing at 50°C for 5 seconds, extension at 60°C for 4 minutes. The extension products were stored at 4°C for maximum of 3 days or immediately proceed to DNA precipitation.

2.1.6.3 DNA Precipitation

After cycle sequencing, the 96-well reaction plate was removed from the thermal cycler and briefly spun. The sequencing products in each well were added with 2 μ l of 125 mM EDTA, followed by 2 μ l of 3 M sodium acetate. The contents were mixed and added with 50 μ l of absolute ethanol. The contents were gently mixed and incubated in the dark at room temperature for 25 minutes. After the incubation, the samples were spun at 3000 g for 30 minutes. The supernatant was discarded by inverting the plate and spun up to 185 g for 1 minute. This followed by added 70 μ l of 70 % ethanol to each well, and spun at 1650 g for 15 minutes. The supernatant was discarded and the DNA pellets were dried at 72°C for 10 minutes. To store, the plate was cover with aluminum foil and stored at 4°C for a period of 2 weeks prior to sequencing analysis. Alternatively, 12 μ l of HiDi was added to into each well containing DNA pellet and run on the automated ABI Prism Model 3100 Avant Genetic Analyzer (Applied Biosystems, Foster City, CA, USA).

2.1.7 Mutational Analysis of DNA Sequences

The sequences were analyzed with a Mutation SurveyorTM v2.61 (Softgenetics, State College, PA, USA) and Chromas (Techelysium software). All mutations flagged by the software were checked by visual inspection to avoid any false positives. PCR was repeated and bidirectional sequencing performed on all detected variants to rule out PCR-induced mutations and sequencing artefacts. SNPs detected were input into SNP analysis software, SNPAnalyser (http://snp.istech.info/istech/board/login_form.jsp, version 1.2A: Istech Corporation, Korea) to compute statistical calculations of Hardy-Weinberg

equilibrium, linkage disequilibrium and haplotype estimation. Putative transcription factor binding sites were identified using the MatInspector licensed software (Library version: Matrix Library 8.0). SNPInspector licensed software was used to identify transcription factor binding sites affected by SNPs. The PolyPhen (<http://genetics.bwh.harvard.edu/pph/>) and SIFT (<http://sift.jcvi.org/>) programs were used to predict the possible impact of amino acid substitution on structure and functions of a human protein.

2.2 RESULTS

2.2.1 Genetic variations in the *SLC16A1* gene in the Chinese and Indian populations of Singapore

2.2.1.1 Overview of Genetic Screening Data

This study identifies genetic variations in *SLC16A1* in the ethnic Chinese and Indian groups of the Singapore population (n = 191). The promoter, coding region and the exon-intron junctions of the *SLC16A1* gene encoding the MCT1 transporter were screened for genetic variation in the study population by direct DNA sequencing. A total of 21 genetic variations of *SLC16A1*, including 14 novel ones, were found: 6 in the promoter region, 4 in the coding exons (3 nonsynonymous variations and 1 synonymous variation), 4 in the 5' untranslated region (5'UTR), 6 in the 3' untranslated region (3'UTR) and 1 in the intron (**Table 10**). Of the 3 nonsynonymous variants, only 303T>G (Ile101Met) was predicted by PolyPhen and SIFT as having a potentially damaging effect on protein function, whereas 1282 G>A (Val428Ile) and 1470 T>A (Asp490Glu) were speculated to be benign.

The allele frequencies of each polymorphism are summarized in **Table 10**. The nucleotide numbering of polymorphisms reported in this study is according to the NCBI Genbank sequence accession NM_003051.3. The "A" of the translation initial codon ATG was numbered 1 and the transcription initiation site is designated as -363 as it is 363 bases upstream of translation start site. The outcomes of data quality check (goodness of fit to the Hardy Weinberg Equilibrium) are presented in **Table 11**. The inter-ethnic differences in allele frequency of each polymorphism are summarized in **Table 12**.

Table 10. The description and frequency of SLC16A1 gene polymorphisms identified in the Chinese and Indian populations of Singapore

| SNP ID | | Position | | | Allele frequency | | | | |
|--------------------|--------------|----------|--|--|-------------------|-----------------|------------|-----------------|-----------------|
| Name | dbSNP (NCBI) | Location | From the translational initiation site or from the end of the nearest exon | Nucleotide change | Amino acid change | PolyPhen | SIFT | Chinese (n=190) | Indians (n=192) |
| -363-855 T > C | Novel | Promoter | -363-885 | CTGGGCTGTCT T/C GGAAAGTTAC | | | | 0.005 | - |
| -363-345 G > T | rs73000320 | Promoter | -363-345 | TACAGCGCC GG/T CCCCAGCGT | | | | - | 0.016 |
| -363-307 C > T | Novel | Promoter | -363-307 | GCACCCGCAT C/T CATTCAAATG | | | | - | 0.005 |
| -363-289 T > G | Novel | Promoter | -363-289 | ATGCTGCCCA T/G TCCCCGCTCC | | | | - | 0.005 |
| -363-222 T > C | Novel | Promoter | -363-222 | TCTCGGTGACT T/C TTTCCTTTTT | | | | - | 0.005 |
| -363-100 C > G | rs60844753 | Promoter | -363-100 | TCTGGCAGGG C/G GTGGTAGCTC | | | | 0.068 | 0.005 |
| -298 G > C | Novel | 5'-UTR | -298 | GTGTGGCGGG G/C AGGGGGCGGC | | | | - | 0.01 |
| -297 A > C | Novel | 5'-UTR | -297 | TGTGGCGGG A/C GGGGGCGGCC | | | | - | 0.005 |
| del (-207-210)CAGA | Novel | 5'-UTR | -207 to -210 | CTGGCCCGGC del(CAGA) CAAAGTGGTG | | | | - | 0.005 |
| -136 A > G | Novel | 5'-UTR | -136 | GCAGCGAGCG A/G AGGACGGGAG | | | | - | 0.005 |
| 303 T > G | Novel | Exon 3 | 303 | GTGGCTTGAT T/G GCAGCTTCTT | Ile101Met | Possibly damage | Intolerant | - | 0.01 |

| | | | | | | | | | |
|--------------|------------|----------|-------------|---------------------------------------|-----------|--------|----------|-------|-------|
| IVS3 -17 A>C | rs74411643 | Intron 3 | E4 -17 | TTATTTATTT <u>A/C</u> TTTATTGTCT | | | | 0.621 | 0.427 |
| 1080 G>A | Novel | Exon 4 | 1080 | GTGTCTATG <u>C/G/A</u> GGATTCTTTG | | | | - | 0.005 |
| 1282 G>A | Novel | Exon 5 | 1282 | GGCATGTGG <u>C/G/A</u> TCGTCCTAAT | Val428Ile | Benign | Tolerant | 0.021 | - |
| 1470 T>A | rs1049434 | Exon 5 | 1470 | AAGACACAGAT <u>T/A</u> GGAGGGCCCA | Asp490Glu | Benign | Tolerant | 0.653 | 0.573 |
| 1748 T>G | rs11585690 | 3'UTR | 1748 (145) | TGATGGGATT <u>T/G</u> TTGTTTACT | | | | - | 0.021 |
| 1835 T>C | Novel | 3'UTR | 1835 (332) | CTTAAACCAT <u>T/C</u> TTTGCTGAATTC | | | | - | 0.016 |
| 2132 C>T | Novel | 3'UTR | 2132 (629) | GTTCTAGAC <u>A/C/T</u> AGTGTACTTG | | | | - | 0.005 |
| 2258 A>G | Novel | 3'UTR | 2258 (755) | ATGCATTTTGA <u>A/G</u> GTGTTTATAG | | | | 0.005 | - |
| 2917 C>T | rs7169 | 3'UTR | 2917 (1414) | CAGAAAGATA <u>C/T</u> AGACATTCAA | | | | 0.642 | 0.578 |
| 3445 T>C | rs9429505 | 3'UTR | 3445 (1942) | CTCTGCGTACT <u>T/C</u> TCTTCTCTCT | | | | - | 0.099 |

“A” of the translation codon ATG is numbered 1 (NM_003051.3 was used as the reference sequence).

The transcription initiation site is designated as -363 as it is 363 bases upstream of translation start site. The nucleotide upstream of transcription initiation site is designated as -363-n accordingly. n = number of nucleotide.

Table 11. *SLC16A1* data quality check: goodness of fit to Hardy Weinberg Equilibrium

| Polymorphisms | Chinese | | Indians | |
|------------------------|------------|---------------------|------------|---------------------|
| | Chi Square | HWE <i>p</i> -value | Chi Square | HWE <i>p</i> -value |
| -363-855 T > C | 0.003 | 0.959 | - | - |
| -363-345 G > T | - | - | 0.024 | 0.876 |
| -363-307 C > T | - | - | 0.003 | 0.959 |
| -363-289 T > G | - | - | 0.003 | 0.959 |
| -363-222 T > C | - | - | 0.003 | 0.959 |
| -363-100 C > G | 6.267 | 0.012* | 0.003 | 0.959 |
| -298 G > C | - | - | 0.011 | 0.918 |
| -297 A>C | - | - | 0.003 | 0.959 |
| del (-207-210) CAGA | - | - | 0.003 | 0.959 |
| -136 A>G | - | - | 0.003 | 0.959 |
| 303 T>G | - | - | 0.011 | 0.918 |
| IVS3 -17 A>C | 0.512 | 0.474 | 0.045 | 0.831 |
| 1080 G>A | - | - | 0.003 | 0.959 |
| 1282 G>A | 0.044 | 0.834 | - | - |
| 1470 T>A | 0.438 | 0.508 | 2.144 | 0.143 |
| 1748 T>G | - | - | 0.043 | 0.835 |
| 1835 T>C | - | - | 0.024 | 0.876 |
| 2132 C>T | - | - | 0.003 | 0.959 |
| 2258 A>G | 0.003 | 0.959 | - | - |
| 2917 C>T | 0.272 | 0.602 | 0.207 | 0.650 |
| 3445 T>C | - | - | 1.158 | 0.282 |

Departure of observed genotype distributions from expected frequencies were analyzed using Chi Square *goodness of fit* test. Expected genotype frequencies were calculated from allele frequencies (p, q) according to the HWE formula where $p^2 + 2pq + q^2$. For population genetics, the degree of freedom (d.f.) is determined by number of genotypes – number of alleles.

* *p* value is significant ($p < 0.05$)

Table 12. *SLC16A1* inter-ethnic difference in allele frequency

| Polymorphism | Allele Frequency | | Ethnic Difference | |
|--------------------|------------------|--------|-------------------|---------|
| | Chinese | Indian | Chi Sq | P-value |
| -363-855 T > C | 0.005 | - | - | - |
| -363-345 G > T | - | 0.016 | - | - |
| -363-307 C > T | - | 0.005 | - | - |
| -363-289 T > G | - | 0.005 | - | - |
| -363-222 T > C | - | 0.005 | - | - |
| -363-100 C > G | 0.068 | 0.005 | 0.621 | 0.427 |
| -298 G > C | - | 0.01 | - | - |
| -297 A > C | - | 0.005 | - | - |
| del (-207-210)CAGA | - | 0.005 | - | - |
| -136 A > G | - | 0.005 | - | - |
| 303 T > G | - | 0.01 | - | - |
| IVS3 -17 A > C | 0.621 | 0.427 | 14.4 | 0.0001* |
| 1080 G > A | - | 0.005 | - | - |
| 1282 G > A | 0.021 | - | - | - |
| 1470 T > A | 0.653 | 0.573 | 2.557 | 0.11 |
| 1748 T > G | - | 0.021 | - | - |
| 1835 T > C | - | 0.016 | - | - |
| 2132 C > T | - | 0.005 | - | - |
| 2258 A > G | 0.005 | - | - | - |
| 2917 C > T | 0.642 | 0.578 | 0.142 | 0.2 |
| 3445 T > C | - | 0.099 | - | - |

* p value is significant ($p < 0.05$)

2.2.1.2 Genetic Variants Detected in the Promoter and 5'-UTR Regions of *SLC16A1* gene

A total of 10 genetic variations were found: 6 in the promoter and 4 in the 5'UTR region. The location of each polymorphism and putative regulatory elements within the amplified 5' flanking region are presented in **Figure 5**. The predictive effects of SNPs on the transcription factor binding sites of *SLC16A1* gene are summarized in **Table 13**. The representative sequencing electropherograms and description of polymorphism distribution are discussed in section 2.2.1.2.1 to 2.2.1.2.10.

Figure 5 Nucleotide sequence of the 5'-flanking region of the *SLC16A1* gene and location of polymorphisms identified. The noncoding first exon sequence is shown in uppercase letters. Intron and flanking sequences are shown in the lowercase letters. The transcription start site (A) is designated as +1. Variant loci are highlighted. Underlined sequences correspond to the putative transcription factor binding sites.

-1800 taataaccct gaggtaggta ttatccttgt tttacagagt tgggagtgag gcttggaaag

-1740 gtaaaatgac ttgcttgagg acacagagct ggtaagtgca agaatcaaat ttggaactga

-1680 acagatctgg ctctcaggtc tatagtgtga atctaccacc ctatggggct ctataagcct

-1620 tcttttgagg tttcctggga ttcaccttat ttaaccactt ctactacat tccatagaac

-1560 aggcccttat atatttactt ctgaaccaga ctgaggatcc tgtctctcta acttaattct

-1500 ccttaccatc tacctgaatg ctgctgccac cctagcactg ctcttataag tcttagctgc

-1440 cccaatgacc cgaaatgcct tccctttctc cgtgtttatc aaatgtaaaa agcaattact

-1380 gtattactca ctagtagtac ttggccgtgg atgccacact gtcttctaata atactgaact

-1320 gttattggaa agcacatggg acctctcagg atctgatcct ccaatctcta ctcttcttca

-1260 atctcaggtt cttcatttgc aaaacagaaa ccataaggcc tacctcccag ggttgctgtg

-1200 agaattgagg gggagggtaa gtgaggggga gggtaagtga gggggtgagt cctggaaggg

-1140 aggaagacac gaggggaagg gcagggctct ggcaagcagc aagtgctcaa cagatgttgg

-1080 ttaatttgtg cctaagtctc ccccaaaaac ttgcaagctc tttgaaggca ggggccttgc
NF-κB

-1020 ctcatatttt tcggtatttc tcaaaagtcc tggacatcaa agacactcca tggttatttg

-960 atcacttcaa cacacacggt ggttatgcgg tcacagcggc tattatgtta aaaacaggct

-900 ctggagtgtg acttcaaatg ctggccgctg acgagctggg ctgtcggaa agttacttca
-363-855 T>C

-840 cctctctgag cctcgggtcc cttatttaca aaatgttcag ggcagtgcc acttcacagg

-780 gctgaggatt agagaggata atccgggtga ggagcatcag cccagcgcgc gcttgcacaa

-720 attctatccg gccccacata tgcacgtcc ataagcgtcc ggcctctgca ttctcgttt

-660 tccacgtggc cgaggtgcac accccaacc actgggccag tctccccacc ctcttacctg
USF

-600 ctcttctttc cggactcgtc ttaataacc accaggcgcc aaccgccgcg ggcttggtc

-540 tatggtggca agttgcatgg gttctcccat caggacctcc cgatgagcct acgaggtcgg

-480 ttctactact gtcgccactt cagagggagg aacaggccc ggagggttgg ggaacttccc
NF- κ B

-420 gaggtcactg aactggtgtc aggcccgat tggaatccaa acacatccca gcccatgccc

-360 ggctctacag cgccggcccc cagcgtcttc ccgggtgcca gcggcaccg catccattca
-363-345 G>T -363-307 C>T

-300 aatgctgccc attccccgct cctcagtcgc ttcccgtac tccgcacgcy catctcccc
-363-289 T>G

-240 acccgtcagg gtcaggcctc tcggtgactt ttccttttc tctggcagaa actgaggggt
AP1, -363-222 T>C

-180 gagaccgatg gttgtgtccc gaacgagggc agattgccta gagctcgtca gacagggacc
AP2

-120 caagggcgag tctggcaggg cgtggttagct ccgcgccgt cagcaggggc gcagcgcgcy
SP1, -363-100 C>G

-60 ggtcggactg ggacgccggt cacgtggcgg ggagggggcg ccggcgcgcy cgggcgagct
USF Sp1

1 AGAGGGCGCG CGCGGCTGAA AGCGTGTGGA GGC GCGGGCT GCAGTTCGGA TGTCTGTGTG
+1

61 GCGGGGAGGG GGCGGCGGCC GGGAGAGACG ACTCCGCCCC CTGCGCGCAT GCTCCGCCCC
Sp1, -297 A>C, -298 G>C

121 CGGCGGGTTA TAAGGCAGCC TCGCTGGCCC GGCCAGACAA AGTGGTGAGC TGCGACGTGA

181 CTGGCTAGCT GCGTGGGTAC TGGAACAAGC AAACGAGGCA GCGAGCGAAG GACGGGAGCC

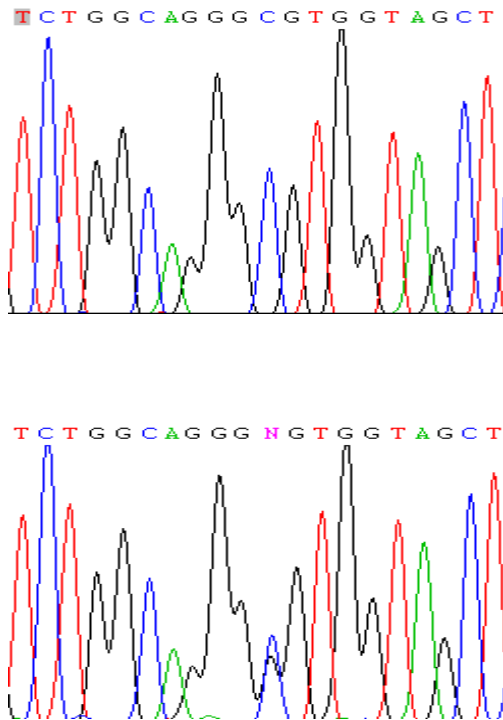
241 GGACCCTGGG CCCCCTGGAA CTCCAGCCTG CGCCACCACG TCACGCACAC GCTCGGCGCT

Table 13. The predictive effects of SNPs on the transcription factor binding sites of *SLC16A1* gene. For each SNP allele the transcription factor binding sites either deleted or generated by the nucleotide exchange.

| Polymorphism | Lost Family/Matrix | New Family Matrix |
|---------------------------------------|---|---|
| -363-855 T > C | - | Elk-1 |
| -363-345 G > T | Nuclear respiratory factor 1 (NRF1) | - |
| -363-307 C > T | Cut-like homeodomain protein (Cut Repeat III / homeodomain) | HMG box-containing protein 1 |
| | Homeobox protein engrailed (en-1) | Homeobox transcription factor Nanog |
| | Cellular and viral CCAAT box | HMG box-containing protein 1 |
| -363-289 T > G | Homeobox transcription factor Nanog | Core promoter-binding protein (CPBP) with 3 Krueppel-type zinc fingers |
| | LBP-1c (leader-binding protein-1c), LSF (late SV40 factor), CP2, SEF (SAA3 enhancer factor) | |
| | TEA domain-containing factors, transcriptional enhancer factors 1,3,4,5 | |
| -363-222 T > C | Nuclear factor of activated T-cells 5 | Retinoic acid receptor / retinoid X receptor heterodimer, DR5 sites |
| | | RAR-related orphan receptor alpha |
| | | HepG2-specific P450 2C factor-1, DR1 sites |
| | | Estrogen-related receptor beta |
| | | Monomers of the nur subfamily of nuclear receptors (nur77, nurr1, nor-1) |
| | | Peroxisome proliferator-activated receptor gamma, DR1 sites |
| | | Interferon regulatory factor 3 (IRF-3) |
| | | Gut-enriched Krueppel-like factor |
| -363-100 C > G | Aryl hydrocarbon / Arnt heterodimers, fixed core | Kruppel-like zinc finger protein 219 |
| | | Myogenic regulatory factor MyoD |
| | Basic transcription element (BTE) binding protein, BTEB3, FKLf-2 | Zinc finger transcription factor ZBP-89 |
| | | Zinc finger protein insulinoma-associated 1 (IA-1) functions as a transcriptional repressor |
| | Member of b-zip family, induced by ER damage/stress, binds to the ERSE in association with NF-Y | Kruppel-like factor 6 |
| | | Zic family member 2 |
| X gene core promoter element 1 | | |
| -298 G > C | Kidney-enriched kruppel-like factor, KLF15 | Myogenic regulatory factor MyoD (myf3) |
| | Myc associated zinc finger protein (MAZ) | |
| | Collagen krox protein (zinc finger protein 67 - zfp67) | |
| | Myeloid zinc finger protein MZF1 | |
| | Stimulating protein 1 | |
| | Kidney-enriched kruppel-like factor | |
| | MYC-associated zinc finger protein related transcription factor | |
| Purine-rich element binding protein A | | |
| -297 A>C | Myc associated zinc finger protein (MAZ) | Core promoter-binding protein (CPBP) with 3 Krueppel-type zinc fingers |
| | Collagen krox protein (zinc finger protein 67 - zfp67) | EGR1, early growth response 1 |
| | Myeloid zinc finger protein MZF1 | X gene core promoter element 1 |
| | Kruppel-like factor 6 | |
| | Purine-rich element binding protein A | EGR1, early growth response 1 |

2.2.1.2.1 -363-100 C>G

The -363-100 C>G single nucleotide polymorphism is located 100-bp upstream of the transcription start site. Representative sequencing electropherograms of AA and AB genotypes (homozygous wildtype and homozygous mutants respectively) are as below:



The genotypes distribution of CC, CG and GG amongst 95 Chinese sample are 84 (88.4%), 9 (9.5%) and 2 (2.1%) respectively. The genotypes distribution is departure from the HWE predicted distribution ($X^2 = 6.27, p = 0.012$). Amongst the 96 Indian samples, 95 (99%) samples were homozygous wildtype and 1 (1%) was heterozygous mutant. This observed distribution is in accordance to HWE ($X^2 = 0.003, p = 0.959$). The C nucleotide is the dominant allele in all two ethnic groups, which is consistent with the ancestral C allele reported in the NCBI SNP database (Reference SNP ID: rs60844753). The minor allele frequency (MAF)

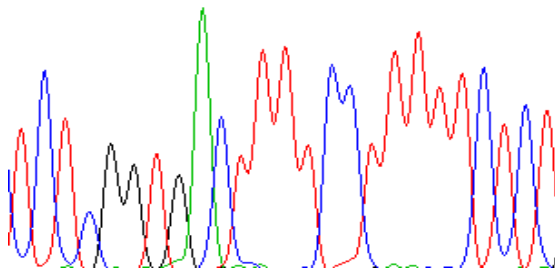
observed in the Chinese and Indian population was 0.068 and 0.005, respectively. Statistically significant inter-ethnic difference in allele frequency is observed when analyzed with Chi square test of independence ($X^2 = 10.81, p = 0.001$).

A substitution from C to G at position 100-bp upstream of the transcription start site may result in the loss and generation of several putative transcription factor binding sites (**Table 12**).

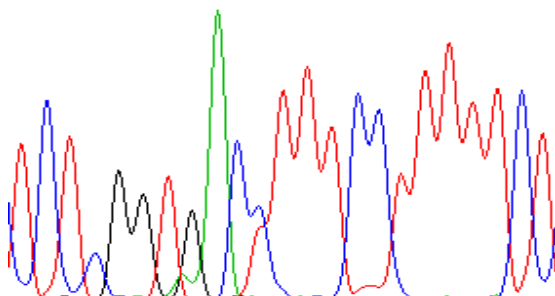
2.2.1.2.2 -363-222 T>C

The -363-222 T>C single nucleotide polymorphism is located 222-bp upstream of the transcription start site. Representative sequencing electropherograms of AA and AB genotypes are as presented:

■ C T C G G T G A C T T T T C C T T T T C T C T



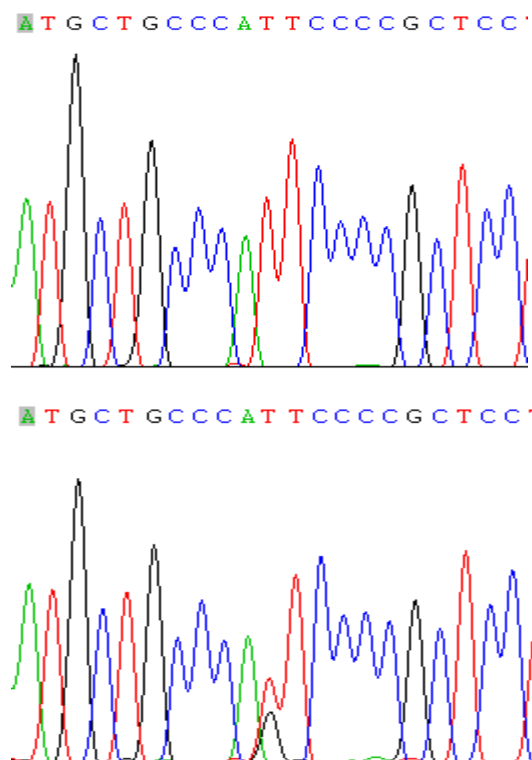
T C T C G G T G A C N T T T C C T T T T C T



The -363-222 T>C is a novel SNP and was found as heterozygotic in one Indian subject. The distribution of TT, TC and CC genotypes in Indian were 95 (99%), 1 (1%) and 0 (0%), respectively. The observed genotype distribution is in accordance to HWE ($X^2 = 0.003, p = 0.959$). This variant was not found in the ethnic Chinese group of Singapore population. The substitution was predicted to result in the loss of putative nuclear factor of activated T-cells 5 (NFAT5) binding site. It was also predicted that the substitution might lead to the generation of several putative transcription factor binding sites (**Table 13**).

2.2.1.2.3 -363-289 T>G

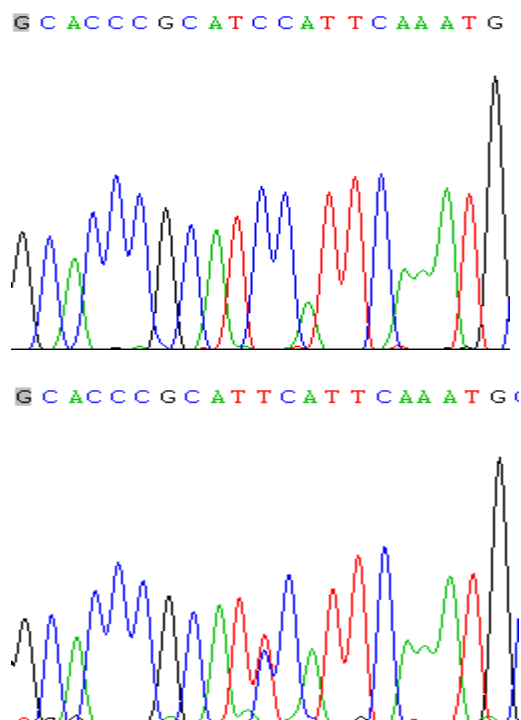
The -363-289 T>G SNP is located 289-bp upstream of the transcription start site. Representative sequencing electropherograms of AA and AB genotypes are as presented:



The -363-289 T>G is a novel SNP and was only detected in Indian population. The distribution of TT, TG and GG genotypes in Indian were 95 (99%), 1 (1%) and 0 (0%), respectively. No deviation from HWE was observed ($\chi^2 = 0.003$, $p = 0.959$). The substitution was predicted to result in the loss of homeobox transcription factor Nanog (NANOG) and TEA domain-containing factors (TEAD) binding sites. This SNP might also lead to the generation of new putative core promoter-binding protein (CPBP) with 3 Krueppel-type zinc fingers binding site.

2.2.1.2.4 -363-307 C>T

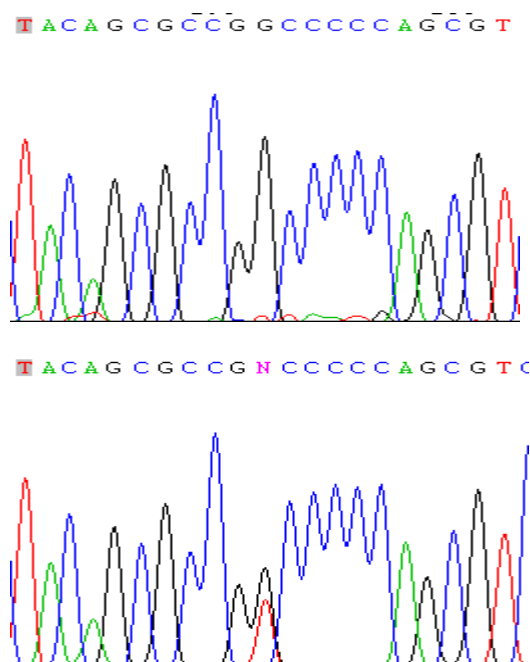
The -363-307 C>T SNP is located 307-bp upstream of the transcription start site. Representative sequencing electropherograms of AA and AB genotypes are as presented:



The -363-307 C>T is a novel SNP and was only detected in the Indian population. The distribution of CC, CT and TT genotypes in Indian were 95 (99%), 1 (1%) and 0 (0%), respectively. No deviation from HWE was observed ($X^2 = 0.003$, $p = 0.959$). The effects of SNP on transcription binding sites are summarized in **Table 13**.

2.2.1.2.5 -363-345 G>T

The -363-345 G>T SNP is located 345-bp upstream of the transcription start site. Representative sequencing electropherograms of AA and AB genotypes are as presented:

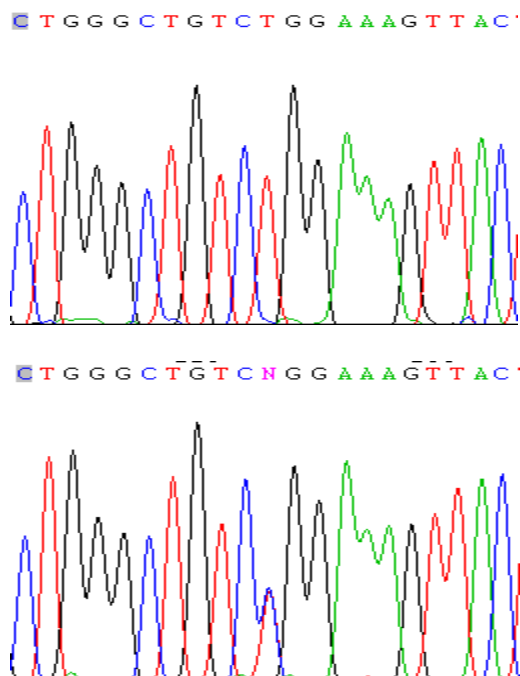


This variant was not found in the ethnic Chinese group of Singapore population. In the Indian population studied, 93 (96.8%) were GG, 3 (3.2%) were GT and 0 (0%) was TT. This distribution is in accordance to HWE ($X^2 = 0.024$, $p = 0.876$). The G nucleotide is the dominant allele in Indian population, consistent with the ancestral

G allele reported in the NCBI database (Reference SNP ID: rs73000320). The substitution was predicted to result in the loss of putative nuclear respiratory factor 1 (NRF1) transcription factor binding site.

2.2.1.2.6 -363-855 T>C

The -363-855 T>C SNP is located 855-bp upstream of the transcription start site. Representative sequencing electropherograms of AA and AB genotypes are as presented:

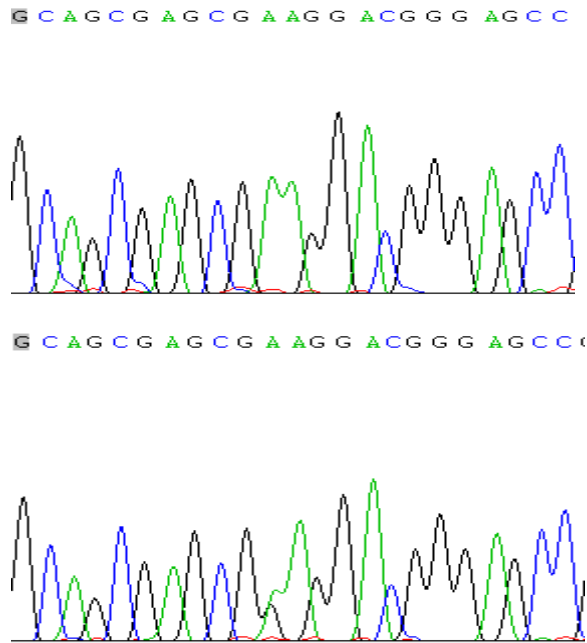


This SNP was found as heterozygotic in one Chinese subject. It is a novel SNP and was not detected in the ethnic Indian group of Singapore population. The distribution of TT, TC and CC genotypes in Indian were 95 (99%), 1 (1%) and 0 (0%), respectively. No deviation from HWE was observed for this polymorphism ($X^2 = 0.003, p = 0.959$). The substitution may lead to the generation of new putative Elk-1 transcription factor binding site.

2.2.1.2.7 -136 A>G

The -136 A>G SNP is positioned 136-bp upstream of the translational start site.

Representative sequencing electropherograms of AA and AB genotypes are as presented:

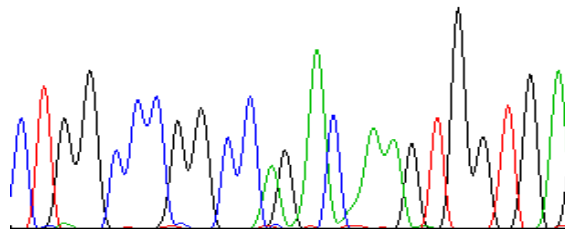


The -136 A>G is a novel polymorphism and 5'-UTR region of *SLC16A1* gene. It was found as heterozygotic in one Indian subject. The distribution of AA, AG and GG genotypes were 95 (99%), 1 (1%) and 0 (0%), respectively. This observed distribution is in accordance to HWE ($X^2 = 0.003$, $p = 0.959$).

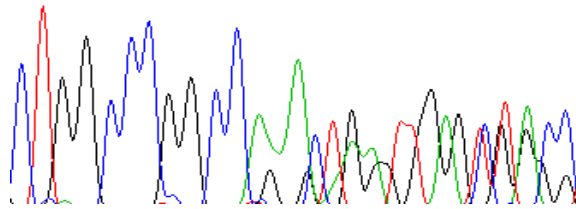
2.2.1.2.8 del (-207-210) CAGA

This novel polymorphism consisting of an CAGA sequence deletion is located 207 to 210-bp upstream of the translation start site and within the 5'-UTR of *SLC16A1* gene. Representative sequencing electropherograms of homozygous wildtype and heterozygous wildtype/deletion are presented:

■ T G G C C C G G C C A G A C A A A G T G G T G A



■ T G G C C C G G C C A A A C T N A T T G A G T T A C C



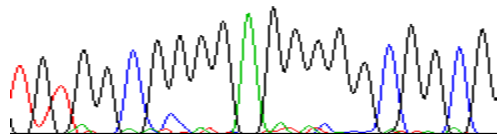
The del (-207-210) CAGA was found as heterozygotic in one Indian subject. The distribution of wildtype/wildtype, wildtype/deletion and deletion/deletion genotypes were 95 (99%), 1 (1%) and 0 (0%), respectively. No deviation from HWE was observed for this polymorphism ($X^2 = 0.003$, $p = 0.959$).

2.2.1.2.9 -297 A>C

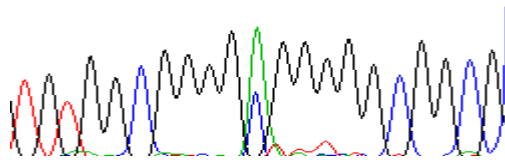
The -297 A>C SNP is positioned 297-bp upstream of the translational start site.

Representative sequencing electropherograms of AA and AB genotypes are as presented:

■ G T G G C G G G G A G G G G G C G G C G



■ G T G G C G G G G A G G G G G C G G C G

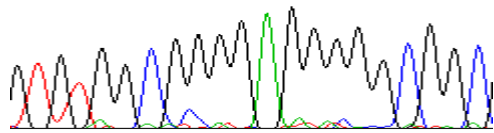


The -297 A>C is a novel polymorphism. It was found as heterozygotic in one Indian subject. The distribution of AA, AC and GG genotypes were 95 (99%), 1 (1%) and 0 (0%), respectively. This observed distribution is in accordance to HWE ($\chi^2 = 0.003$, $p = 0.959$). The effects of the substitution on transcription binding sites are summarized in **Table 13**.

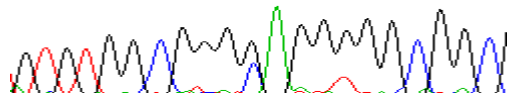
2.2.1.2.10 -298 G>C

The -298 G>C is a novel polymorphism and is located 298-bp upstream of the translational start site. Representative sequencing electropherograms of AA and AB genotypes are as presented:

GGTGTGGCGGGGAGGGGGCGGC



GGTGTGGCGGGGAGGGGGCGGC

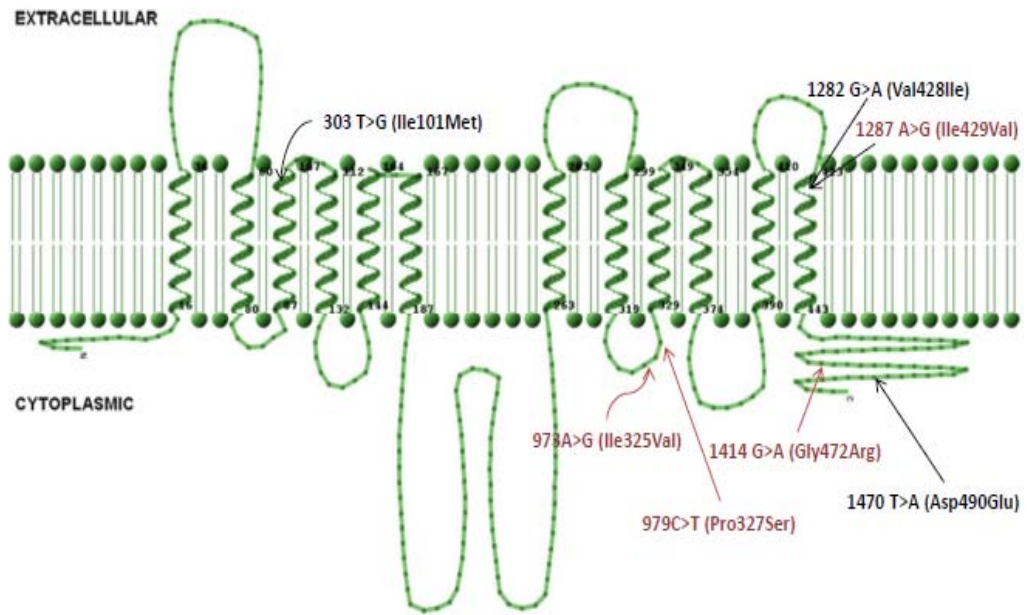


The distribution of AA, AC and GG genotypes in Indian population were 94 (97.9%), 2 (2.1%) and 0 (0%), respectively. This observed distribution is in accordance to HWE ($\chi^2 = 0.011$, $p = 0.918$). This SNP was not found in the Chinese group of Singapore population. It was also predicted that the substitution might lead to the loss and generation of several putative transcription factor binding sites (**Table 13**).

2.2.1.3 Genetic Variants Detected in the Exon, Intron and 3'-UTR Regions of *SLC16A1* gene

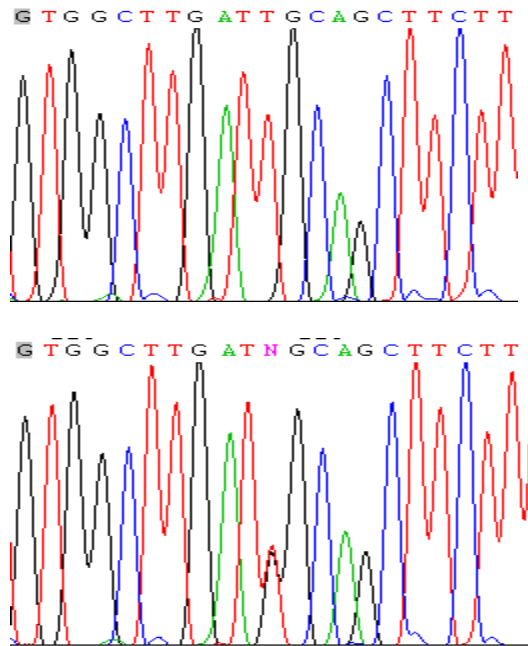
A total of 11 single nucleotide polymorphisms were detected: 4 in the exons (3 nonsynonymous and 1 synonymous variations), 1 in intron and 6 in the 3'-UTR region. The effects of nonsynonymous SNPs reported in this study were predicted using bioinformatics tools. The topological location of nonsynonymous SNPs is presented in **Figure 6**. The representative electropherograms showing the homozygous wildtype and heterozygous variants and the description of polymorphism are discussed in section 2.2.1.3.1 to 2.2.1.3.11.

Figure 6. Topological location of *SLC16A1* non-synonymous mutations detected in this study and retrieved from the dbSNP database (<http://www.ncbi.nlm.nih.gov/SNP/>). The mutations highlighted in black are the genetic variants found in the Chinese and Indian population of Singapore.



2.2.1.3.1 303 T>G (Ile101Met)

The 303 T>G (Ile101Met) and is located 303-bp downstream of the translational start site. Representative sequencing electropherograms of AA and AB genotypes are as presented:



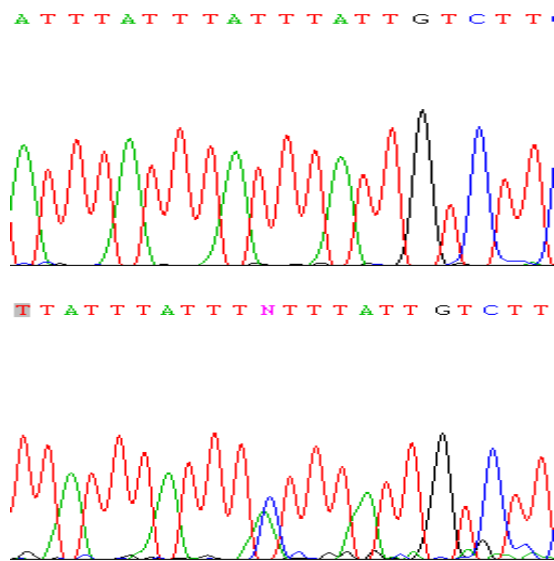
The 303 T>G (Ile101Met) polymorphism is a novel SNP that only detected in the Indian group of Singapore population. The distribution of TT, TG and GG genotypes in Indian were 94 (97.9%), 2 (2.1%) and 0 (0%), respectively. No deviation from HWE was observed for this polymorphism ($X^2 = 0.011$, $p = 0.918$).

Based on the putative protein topology, 303 T>G (Ile101Met) is located at the transmembrane (TM) 3 (**Fig.6**). A substitution from T to G at position 303 resulted in the conversion of amino acid isoleucine to methionine at position 101 of MCT1 protein. The PolyPhen and SIFT sequence homology-based tools were used to predict whether the amino acid substitution affects protein function based on

sequence homology and the physical property of amino acid. The 303 T>G (Ile101Met) variant was predicted to be probably damaging by both programs.

2.2.1.3.2 IVS3 -17 A>C

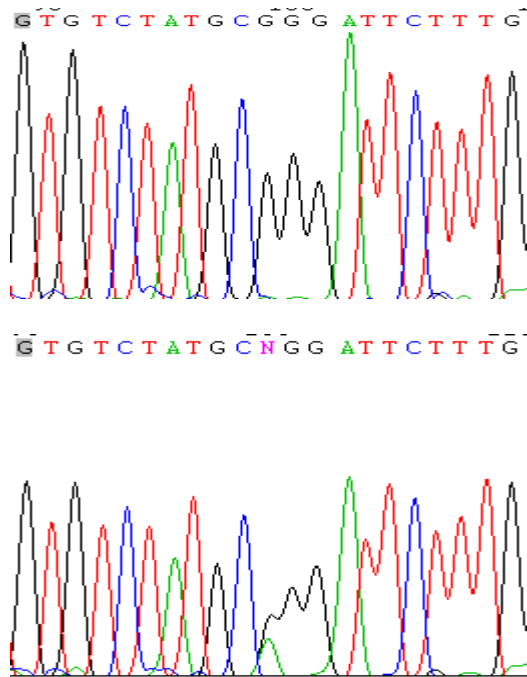
The IVS3 -17 A>C is a common polymorphism located in the intron 3 of *SLC16A1* gene. Representative sequencing electropherograms of AA and AB genotypes are as presented:



The distribution of AA, AC and CC genotypes in Chinese were 12 (12.5%), 48 (50.0%) and 35 (36.5%), respectively. In Indians, the frequencies of AA, AC and CC observed were 31 (32.3%), 48 (50%), and 17 (17.7%), respectively. No deviation from HWE were observed for all ethnic groups (Chinese $X^2 = 0.512$, $p = 0.474$; Indian $X^2 = 0.045$, $p = 0.831$). The A nucleotide is the dominant allele in Indians, consistent with the ancestral allele reported in the NCBI SNP database (Reference SNP ID: rs74411643). In contrast, the C allele is the dominant form in our Chinese population (0.621). The observed inter-ethnic difference in allele frequency is statistically significant ($X^2 = 14.4$, $p = 0.001$).

2.2.1.3.3 1080 G>A

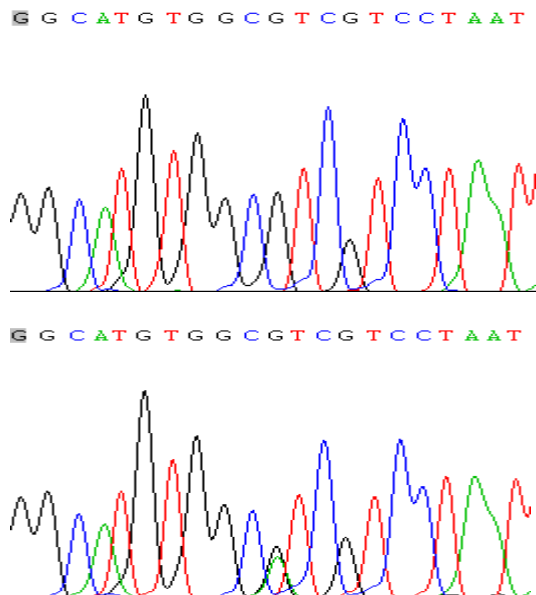
The 1080 G>A is a novel synonymous SNP that located at exon 4 of MCT1 protein. Representative sequencing electropherograms of AA and AB genotypes are as presented:



It was found as heterozygotic in one Indian subject. The distribution of GG, GA and AA genotypes were 95 (99%), 1 (1%) and 0 (0%), respectively. This observed distribution is in accordance to HWE ($\chi^2 = 0.003$, $p = 0.959$).

2.2.1.3.4 1282 G>A (Val428Ile)

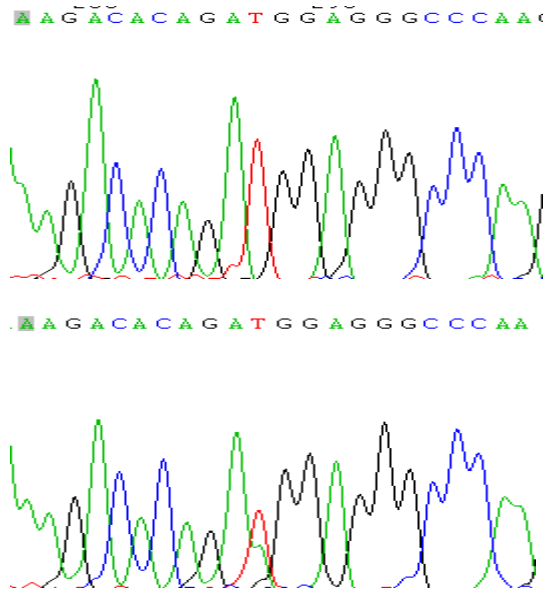
The 1282 G>A (Val428Ile) is a novel nonsynonymous variants that located at the exon 5 of *SLC16A1* gene. Representative sequencing electropherograms of AA and AB genotypes are as presented:



This variant was only detected in the Chinese group of Singapore population. The genotype distribution of GG, GA and AA amongst 95 Chinese samples were 91 (95.8%), 4 (4.2%), and 0 (0%), respectively. This is in accordance with the HWE distribution ($X^2 = 0.844$, $p = 0.834$). Based on putative protein topology, 1282G>A (Val428Ile) is located at the TM12 of MCT1 protein (**Fig. 6**). A substitution from G to A at position 1282 resulted in the conversion of amino acid valine to isoleucine at position 428 of MCT1 protein. Both amino acid residues are non-polar and thus this mutation is unlikely to affect the functions of the protein. This is consistent with the results obtained using the PolyPhen and SIFT programmes. The 1282 G>A (Val428Ile) variant was predicted to be benign by both programs.

2.2.1.3.5 1470 T>A (Asp490Glu)

The 1470 T>A (Asp490Glu) is a novel nonsynonymous variants that located at the exon 5 of *SLC16A1* gene. Representative sequencing electropherograms of AA and AB genotypes are as presented:



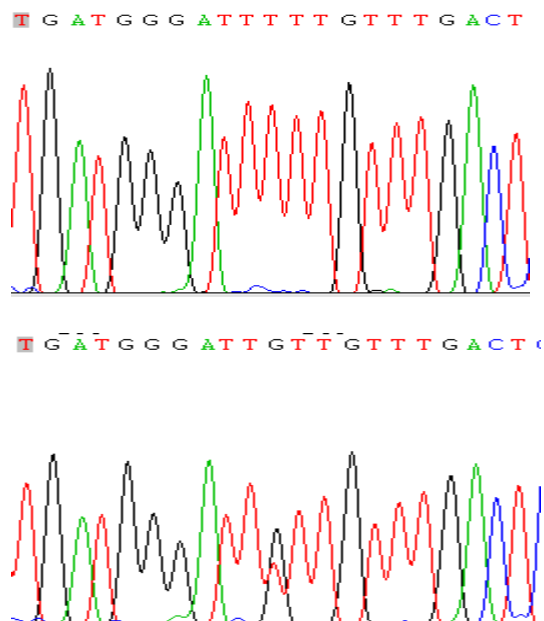
The 1470 T>A (Asp490Glu) polymorphism was detected as a common polymorphism in both ethnic Chinese and Indian groups of Singapore population. This SNP was previously reported by Merezhinskaya *et al.* Amongst the 96 Indian samples analyzed, 10 (10.4%) samples were homozygous wildtype, 46 (48%) samples were heterozygous mutants and 39 (40.6%) were homozygous mutants. This observed distribution is in accordance to HWE ($X^2 = 0.438$, $p = 0.508$). The genotype distribution of TT, TA and AA amongst 96 Indian samples were 14 (15%), 54 (56%) and 28 (29%). No deviation from HWE were observed for both ethnic groups (Chinese $X^2 = 0.438$, $p = 0.508$; Indian $X^2 = 2.144$, $p = 0.143$). The A allele is the dominant allele in Chinese and Indians, consistent with the ancestral A allele reported in the NCBI SNP database (Reference SNP ID:

rs1049434). No ethnic difference in allele frequency is observed in our study population ($X^2 = 2.557, p = 0.110$).

The 1470 T>A (Asp490Glu) is located at the cytoplasmic C-terminal end of MCT1 protein (**Fig. 6**). A substitution from T to A at position 1470 resulted in the conversion of amino acid aspartic acid to glutamic acid at position 490 of MCT1 protein. As glutamic acid and aspartic acid are both acidic amino acids with similar physicochemical properties, it is likely that substitution will not result in fundamental change. This is consistent with the results obtained using PolyPhen and SIFT which predicted this SNP to be benign and unlikely to have any significant effect on the protein function.

2.2.1.3.6 1748 T>G

The 1748 T>G SNP is located at the 3'-UTR of the *SLC16A1* gene. Representative sequencing electropherograms of AA and AB genotypes are as presented:

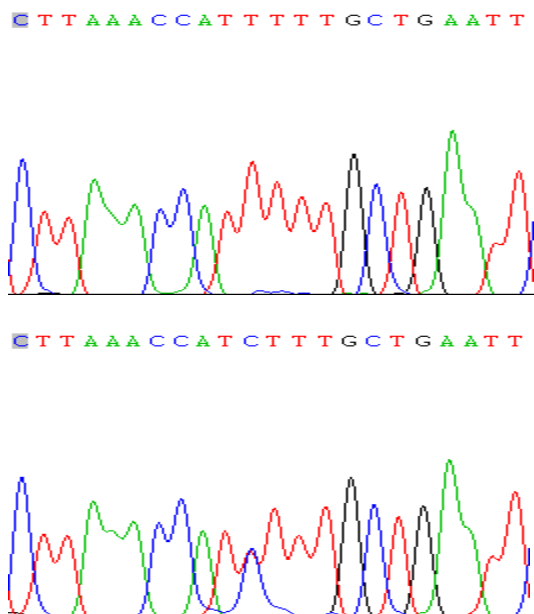


The 1748 T>G was found as heterozygotic in 4 Indians. The distribution of TT, TG and GG genotypes were 92 (95.8%), 4 (4.2%) and 0 (0%), respectively. This observed distribution is in accordance to HWE ($X^2 = 0.043$, $p = 0.835$). The A allele is the ancestral allele reported in the NCBI SNP database (Reference SNP ID: rs11585690).

2.2.1.3.7 1835 T>C

The 1835 T>C is a novel SNP locates at the 3'-UTR of MCT1 gene.

Representative sequencing electropherograms of AA and AB genotypes are as presented:



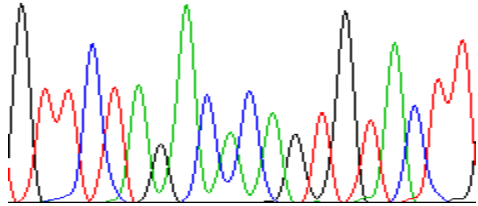
The 1835 T>C polymorphism was only found in the ethnic Indian group of Singapore population. The frequencies of TT, TC, and CC genotypes observed were 93 (96.9%), 3 (3.1%), 0 (0%), respectively. This observed distribution is in accordance to HWE ($X^2 = 0.024$, $p = 0.876$).

2.2.1.3.8 2132 C>T

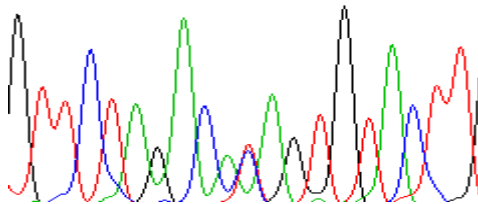
The 2132 C>T is a novel polymorphism locates at the 3'-UTR of *SLC16A1* gene.

Representative sequencing electropherograms of AA and AB genotypes are as presented:

GGTTCTAGACACAGTGTACTT



GGTTCTAGACACAGTGTACTT

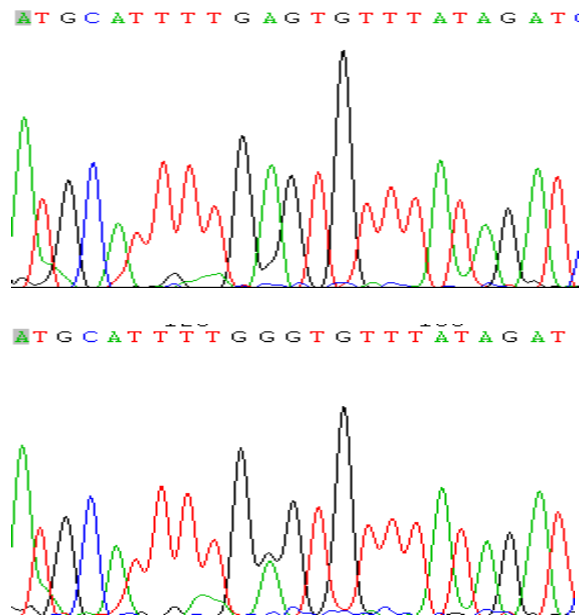


This variant was only detected in Indian group. The genotype distribution of CC, CT and TT were 95 (99%), 1 (1%) and 0 (0%), respectively. This observed distribution is in accordance to HWE ($\chi^2 = 0.003$, $p = 0.959$).

2.2.1.3.9 2258 A>G

The 2258 A>G is a novel variant locates at the 3'-UTR of *SLC16A1* gene.

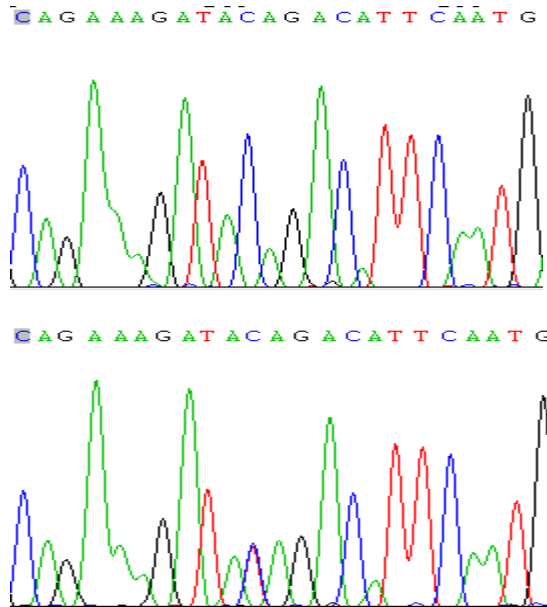
Representative sequencing electropherograms of AA and AB genotypes are as presented:



This SNP was found as heterozygotic in one Chinese subject. The frequencies of AA, AG and GG were 95 (99%), 1 (1%) and 0 (0%), respectively. No deviation from HWE was observed for this polymorphism ($\chi^2 = 0.003$, $p = 0.959$).

2.2.1.3.10 2917 C>T

The 2917 C>T SNP is located at the 3'-UTR of *SLC16A1* gene. Representative sequencing electropherograms of AA and AB genotypes are as presented:

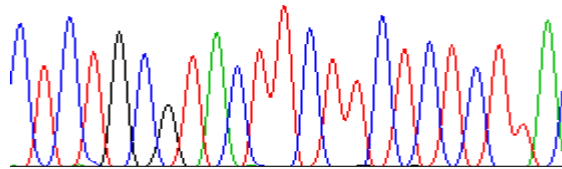


The 2917 C>T was found to be common polymorphism in the local Chinese and Indian populations. In Chinese, the frequencies of CC, CT, and TT genotypes were 11 (12%), 46 (48%), and 38 (40%). Amongst the 96 Indian samples analysed, 16 (17%) samples were homozygous wildtype, 49 (51%) samples were heterozygous mutants and 31 (32%) were homozygous mutants. No deviation from HWE were observed for both ethnic groups (Chinese $X^2 = 0.272$, $p = 0.602$; Indian $X^2 = 0.207$, $p = 0.650$). The NCBI SNP database (Reference SNP ID: rs7169) has reported this SNP as a C/T variant, and the ancestral allele is reported T nucleotide, which corresponds with the T nucleotide being the dominant allele in both ethnic groups. The minor C allele is occurring at a frequency of 0.422 Indians as compared to 0.358 in Chinese. No ethnic difference in allele frequency is observed in our study population ($X^2 = 0.142$, $p = 0.200$).

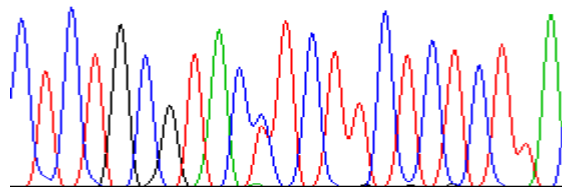
2.2.1.3.11 3445 T>C

The 3445 T>C is located at the 3'-UTR of *SLC16A1* gene. Representative sequencing electropherograms of AA and AB genotypes are as presented:

T C T G C G T A C T T C T T C T C T C T T A C



T C T G C C G T A C C T T C T T C C T C T C T T A



This SNP was only detected in the Indian group of Singapore population.

The observed frequencies of TT, TC and CC genotypes were 77 (80.2%),

19 (19.8%) and 0 (0%). No deviation from HWE was observed for this

polymorphism ($\chi^2 = 1.158, p = 0.282$).

2.2.1.4 Linkage Disequilibrium (LD) Analysis

Linkage disequilibrium (LD) refers to association between tightly linked SNPs.

Alleles at different loci are sometimes found together more or less often than expected based on their frequencies. Two alleles are said to be in LD if their alleles are in statistical association.

In this study, the significance of the associations was assessed by Chi square test.

The LD for each of the pairs of segregating sites was quantified by the D' . The $D' = 1$ is known as complete LD, which indicates that the two SNPs have not been separated by recombination, recurrent mutation or gene conversion. Detailed pair-wise LD coefficients for *SLC16A1* gene are presented in the **Tables 14 to 16**.

Table 14. Pair-wise linkage disequilibrium (D') coefficients between *SLC16A1* bi-allelic promoter polymorphisms in ethnic Indian population. The statistical significance of linkage disequilibrium was assessed by Chi-square test. Statistical significance was defined as $p < 0.05$. Site pairs that lack the power to detect significant association are indicated by ns. The number in bold represents LD value.

| Position | -363-345 G>T | -363-307 C>T | -363-289 T>G | -363-222 T>C | -363-100 C>G | -298 G>C | -297 A>C | del (-207-210) | -136 A>G |
|----------------|--------------|--------------|--------------|--------------|-------------------------|----------|----------|----------------|----------|
| -363-345 G>T | -- | ns | ns | ns | <0.0001 0.495 | ns | ns | ns | ns |
| -363-307 C>T | -- | -- | ns | ns | ns | ns | ns | ns | ns |
| -363-289 T>G | -- | -- | -- | ns | ns | ns | ns | ns | ns |
| -363-222 T>C | -- | -- | -- | -- | ns | ns | ns | ns | ns |
| -363-100 C>G | -- | -- | -- | -- | -- | ns | ns | ns | ns |
| -298 G>C | -- | -- | -- | -- | -- | -- | ns | ns | ns |
| -297 A>C | -- | -- | -- | -- | -- | -- | -- | ns | ns |
| del (-207-210) | -- | -- | -- | -- | -- | -- | -- | -- | ns |
| -136 A>G | -- | -- | -- | -- | -- | -- | -- | -- | -- |

Table 15. Pair-wise linkage disequilibrium (D') coefficients between *SLC16A1* bi-allelic coding region polymorphisms in ethnic Chinese population. The statistical significance of linkage disequilibrium was assessed by Chi-square test. Statistical significance was defined as $p < 0.05$. Site pairs that lack the power to detect significant association are indicated by ns. The number in bold represents LD value.

| Position | IVS -17 A>C | 1282 G>A | 1470 T>A | 2258 A>G | 2917 C>T |
|-------------|-------------|----------|-------------------------|----------|-------------------------|
| IVS -17 A>C | -- | ns | <0.0001 1.000 | ns | <0.0001 1.000 |
| 1282 G>A | -- | -- | ns | ns | ns |
| 1470 T>A | -- | -- | -- | ns | <0.0001 1.000 |
| 2258 A>G | -- | -- | -- | -- | ns |
| 2917 C>T | -- | -- | -- | -- | -- |

Table 16. Pair-wise linkage disequilibrium (D') coefficients between *SLC16A1* bi-allelic coding region polymorphisms in ethnic Indian population. The statistical significance of linkage disequilibrium was assessed by Chi-square test. Statistical significance was defined as $p < 0.05$. Site pairs that lack the power to detect significant association are indicated by ns. The number in bold represents LD value.

| Position | 303 T>G | IVS3 -17 A>C | 1080 G>A | 1470 T>A | 1748 T>G | 1835 T>C | 2132 C>T | 2917 C>T | 3445 T>C |
|--------------|---------|-----------------|----------|-------------------------|------------------------|----------|----------|-------------------------|-------------------------|
| 303 T>G | -- | ns | ns | ns | ns | ns | ns | ns | ns |
| IVS3 -17 A>C | -- | -- | | <0.0001 0.930 | ns | ns | ns | <0.0001 1.000 | <0.0001 1.000 |
| 1080 G>A | -- | -- | -- | ns | ns | ns | ns | ns | ns |
| 1470 T>A | -- | -- | -- | -- | 0.0103 1.000 | ns | ns | <0.0001 0.911 | <0.0001 1.000 |
| 1748 T>G | -- | -- | -- | -- | -- | ns | ns | 0.0091 1.000 | ns |
| 1835 T>C | -- | -- | -- | -- | -- | -- | ns | ns | ns |
| 2132 C>T | -- | -- | -- | -- | -- | -- | -- | ns | ns |
| 2917 C>T | -- | -- | -- | -- | -- | -- | -- | -- | <0.0001 1.000 |
| 3445 T>C | -- | -- | -- | -- | -- | -- | -- | -- | -- |

2.2.1.5 Haplotype Construction and Frequency Estimation

The single nucleotide polymorphisms identified in the 5'-flanking promoter and untranslated exon 1 region were regarded as a single block because of the high degree of linkage equilibrium and close physical distance of the loci. Several studies have interpreted the linkage disequilibrium pattern of polymorphisms in the *ABCA1* promoter as a region of low recombination probability and thus considered the 5'-flanking region to be a single haplotype to be analyzed separately from the coding region [202, 203]. The linkage disequilibrium between promoter and coding region is very weak. Therefore, the haplotype analysis was performed in the promoter and the coding region separately.

Haplotype structures were constructed from population genotype data separately for each ethnic group, and their respective frequencies were estimated using SNP analysis software, SNPAnalyser. The haplotype frequency was not performed in the promoter region of *MCT1* due to the low prevalence of SNPs identified in this region (**Table 10**). In the coding region of *SLC16A1*, three common polymorphisms (IVS-17 A>C, 1470 T>A and 2917 C>T) were identified in the ethnic Chinese and Indian of Singapore population. These SNPs were input into SNPAnalyser to compute statistical calculation of haplotype estimation. These variants comprised of 6 statistically inferred haplotypes, of which accounted for 100% of chromosomes analyzed. The haplotypes and the relative frequencies of three commonest SNPs in the coding region of *SLC16A1* are summarized in **Table 17**.

The six *SLC16A1* haplotypes in the ethnic Chinese and Indian group of Singapore population and their frequency distributions between ethnic groups are presented graphically in **Figure 7**. The distribution of haplotypes 1 and 3 were statistically significant different amongst the Chinese and Indian ethnic groups; haplotype 1 was estimated to be approximately 26% more common in Chinese than Indians (frequency of 0.621 versus 0.415; $X^2 = 15.98$, $p < 0.0001$). Haplotype 3 was estimated to occur in approximately 13.6% of Indians. In contrast, it had an estimated frequency of approximately 2% of Chinese ($X^2 = 17.26$, $p < 0.0001$). The haplotype that was most common in the Singapore population and predicted to occur at a relatively high frequency in both ethnic groups is haplotype 1; haplotype 1 had an estimated frequency of 0.621 and 0.415 in Chinese and Indians, respectively. The second common haplotype, haplotype 2, also occurred at similar frequencies of 0.348 and 0.400 in Chinese and Indians, respectively. Haplotype 3 was more common in Indians, but was considerably rare in Chinese (2% frequency). Haplotype 4, differing only at the 2917 C>T site, was occurred at relatively low frequencies at both ethnic groups (Chinese = 1.1% and Indians = 2.2%). Haplotype 5 and 6, were not detected in the ethnic Chinese group.

Figure 7. Ethnic distribution of *SLC16A1* haplotypes. The frequencies of six haplotypes identified in the ethnic Chinese and Indian of Singapore population.
* $p < 0.05$, frequency distribution is statistically significant.

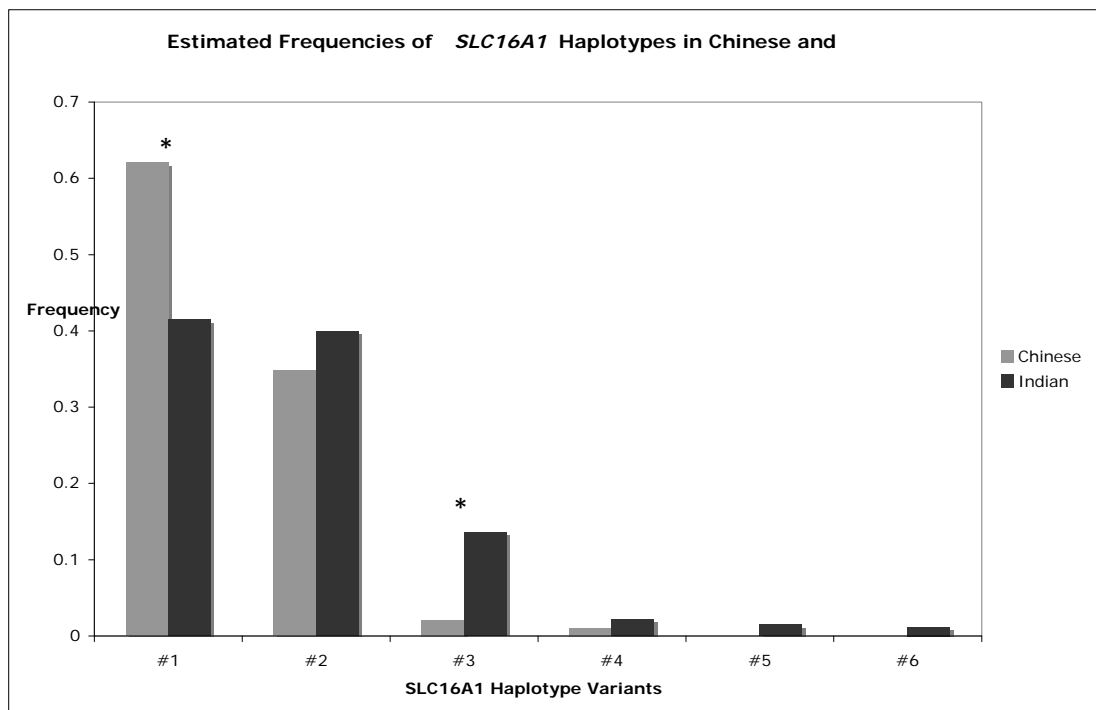


Table 17. Haplotype structure defined by 3 commonest SNPs in the *SLC16A1* 5'flanking coding region in Singapore population

| Haplotype No. | Polymorphisms | | | Estimated Haplotype Frequencies | | Chi sq value | p-value |
|---------------|---------------|----------|----------|---------------------------------|-------------------|--------------|-----------|
| | IVS -17 A>C | 1470 T>A | 2917 C>T | Chinese n = 190 | Indian n = 192 | | |
| 1 | C | A | T | 0.621 | 0.415 | 15.98 | < 0.0001* |
| 2 | A | T | C | 0.348 | 0.400 | 1.18 | 0.278 |
| 3 | A | A | T | 0.021 | 0.136 | 17.26 | < 0.0001* |
| 4 | A | A | C | 0.011 | 0.022 | 0.66 | 0.418 |
| 5 | A | T | T | 0.000 | 0.015 | - | - |
| 6 | C | T | T | 0.000 | 0.012 | - | - |

Haplotype structures were constructed and frequencies estimated using SNPAnalyser software. The six haplotypes listed here accounts for 100% of all chromosomes. Observed frequencies for haplotypes 5 and 6 are too small to be considered for chi square statistical test of independence.

* p < 0.05

2.2.2 GENETIC VARIATIONS IN THE MCT4 (*SLC16A3*) GENE IN THE CHINESE AND INDIAN POPULATIONS OF SINGAPORE

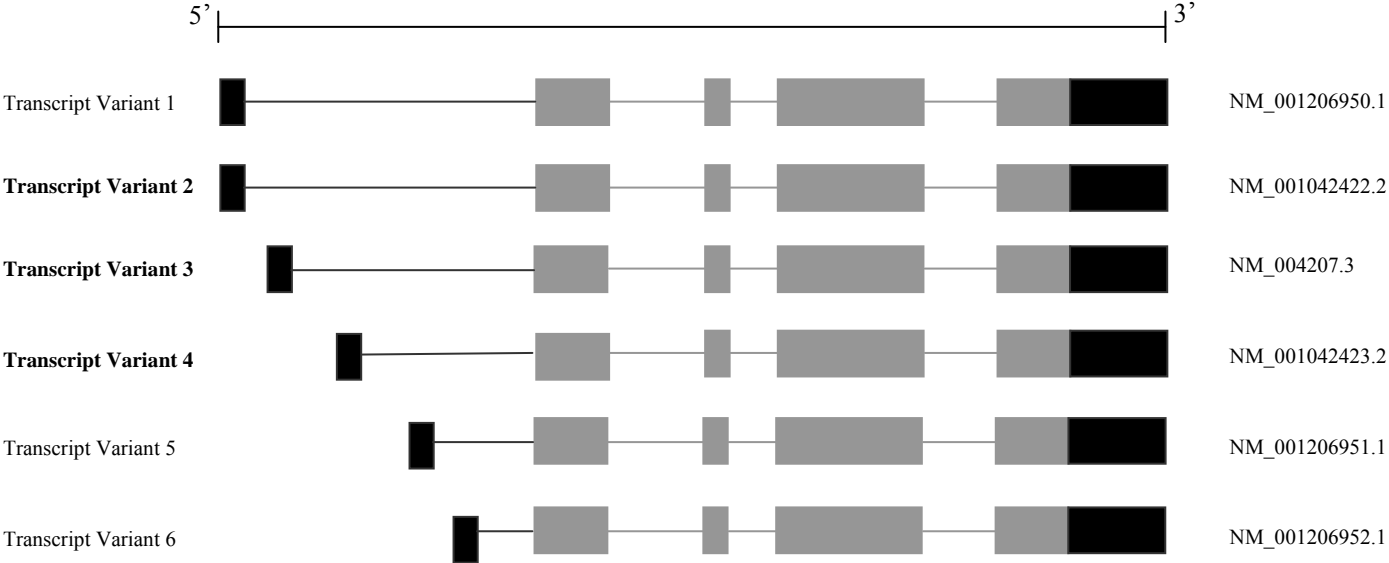
2.2.2.1 Overview of Genetic Screening Data

This study identifies genetic variations in *SLC16A3* in the ethnic Chinese and Indian groups of the Singapore population (n = 191). The promoter, coding region and the exon-intron junctions of the *SLC16A3* gene encoding the MCT4 transporter were screened for genetic variation in the study population by direct DNA sequencing. Sequencing analysis of *SLC16A3* from 191 Asian subjects resulted in the identification of 46 genetic variations, of which 33 are novel mutations (**Table 18 and Table 19**). Of these variants, 22 are located in the promoter region, 2 in the 5'-UTR, 10 in the coding exons (5 nonsynonymous and 5 synonymous variations), 6 in 3'-UTR and 6 in the intron. Of the 5 nonsynonymous variants, only 44C>T (Ala15Val) was predicted by PolyPhen and SIFT as having a potentially damaging effect on protein function, whereas 55G>A (Gly19Ser), 574G>A (Val192Met) and 916G>A (Gly306Ser) had conflicting results between the SIFT and PolyPhen algorithms. Finally, 641C>T (Ser214Phe) was predicted to be tolerated variant.

Previously, three transcript variants have been described for *SLC16A3* gene, of which three transcripts have functional protein products. However, the database has recently been updated and additional three transcript variants have been deposited (<http://www.ncbi.nlm.nih.gov/gene/9123>; **Fig. 8**). The six transcript variants are created by alternative promoter usage and alternative splicing at the 5' end of the gene, therefore the protein products for all six transcript variants are identical. As this project was performed prior to the update of *SLC16A3* gene sequence, we

intended to screen the promoter regions associated with the transcript variant 2, 3 and 4 of *SLC16A3* gene. However, we were unable to sequence the promoter region of transcript variant 3 because of the GC-rich content of this region. The amplification was unsuccessful despite several primer pairs were designed and commercial PCR kit was utilized to amplify this region. Therefore, the genotype information of this region is not included in this report. For transcript variant 2, the “A” of the translation initial codon ATG was numbered 1 and the transcription initiation site is designated as -139 as it is 139 bases upstream of translation start site (Reference ID: NM_001042422.2). For transcript variant 4, the transcription initiation site is designated as -118 as it is 118 bases upstream of translation start site (Reference ID: NM_001042423.2). The allele frequencies of each polymorphism are summarized in **Table 18** and **Table 19**. The outcomes of data quality check (goodness of fit to the Hardy Weinberg Equilibrium) are presented in **Table 20** to **22**. The inter-ethnic difference in allele frequencies of each polymorphism are summarized in **Table 23** to **25**.

Figure 8. Six transcripts have been described for SLC16A3 gene (<http://www.ncbi.nlm.nih.gov/gene/9123>). All transcript variants are created by alternative promoter usage and alternative splicing at the 5' end of the gene, therefore the protein products for all six transcript variants are identical.



| | | | | | | | |
|----------------------|----------------------|------------|----------|-----------------------------|-----------------------------------|-------|-------|
| Transcript variant 4 | -41 G > A | Novel | 5'UTR | -41 | CACCGGGACCC <u>G/A</u> GAGAGGAAGC | - | 0.005 |
| | IVS+100 C > T | Novel | Intron 1 | E1 +100 | GCGCGCACCT <u>C/T</u> CCCACCAAAG | - | 0.005 |
| | -118-115 G > A | Novel | Promoter | -118-115 ^b | TCCAGGAAG <u>G/A</u> AAAACGAATTA | 0.005 | - |
| | -118-130 A > C | rs3176828 | Promoter | -118-130 ^b | CAGGCAGCTC <u>A/C</u> TGGGATCCAG | 0.937 | 0.875 |
| | -118-249 C > T | rs79034755 | Promoter | -118-249 ^b | ACAGGGGCTG <u>C/T</u> TGGGGGAAGAA | 0.079 | 0.156 |
| | -118-331 G > A | rs60910743 | Promoter | -118-331 ^b | TGCAAGCTCG <u>G/A</u> CCCCGACACC | 0.163 | 0.161 |
| | -118del(-436-437) AG | rs58263941 | Promoter | -118(-436-437) ^b | GCGGACACAGdel(ag)CGGCAGGGCA | 0.105 | 0.146 |
| | -118-502 A > G | rs12450761 | Promoter | -118-502 ^b | GGAGTGGCCA <u>A/G</u> TCCGCAAATG | 0.147 | 0.146 |
| | -118-554 A > T | rs56043453 | Promoter | -118-554 ^b | GCCCAGCCCC <u>A/T</u> CTTGGGGCA | 0.926 | 0.875 |
| | -118-1131 C > A | Novel | Promoter | -118-1131 ^b | CCCCACGTCC <u>C/A</u> GCGGCTGGCG | - | 0.005 |
| | -118-1416 C > T | Novel | Promoter | -118-1416 ^b | TGGGCCACG <u>C/T</u> TGGGCAGCCGC | - | 0.01 |
| | -86 A > G | rs3176827 | 5'UTR | -86 | ACGGGCTGAC <u>A/G</u> GTCCAGCAGA | 0.926 | 0.875 |
| | IVS1+21 G > C | Novel | Intron 1 | E1 +21 | TGCAGGTCCAG <u>G/C</u> ACGCCTGAGG | 0.005 | - |

^a The transcription initiation site is designated as -139 as it is 139 bases upstream of translation start site. The nucleotide upstream of transcription initiation site is designated as -139-n accordingly. n= number of nucleotide (NM_001042422.2 was used as the reference sequence).

^b The transcription initiation site is designated as -118 as it is 118 bases upstream of translation start site. The nucleotide upstream of transcription initiation site is designated as -118-n accordingly. n= number of nucleotide (NM_001042423.2 was used as the reference sequence).

^c One of the heterogeneous deletion is deleted from 726 to 773 bp upstream of transcription initiation start site.

Search completed: August 2010

Table 19. The description and frequency of *SLC16A3* variations detected in the coding and 3'-UTR regions of three transcript variants identified in the Chinese and Indian populations of Singapore

| SNP ID | | Position | | | Allele frequency | | | | |
|----------------|--------------|----------|--|------------------------------|-------------------|-------------------|------------|-----------------|-----------------|
| Name | dbSNP (NCBI) | Location | From the translational initiation site or from the end of the nearest exon | Nucleotide change | Amino acid change | PolyPhen | SIFT | Chinese (n=190) | Indians (n=192) |
| 21 C > T | Novel | Exon 2 | 21 | CCGTGGTGGAC/T GAGGGCCCCA | | | | - | 0.005 |
| 44 C > T | Novel | Exon 2 | 44 | GCGTCAAGGC/T CCCTGACGGC | Ala15Val | Probably damaging | Intolerant | 0.011 | 0.042 |
| 55 G > A | Novel | Exon 2 | 55 | CCCTGACGGCG/A GCTGGGGCTG | Gly19Ser | Benign | Intolerant | - | 0.005 |
| 117 C > T | Novel | Exon 2 | 117 | ACGCCTTCCCC/T AAGGCCGTCAG | | | | - | 0.005 |
| IVS2-149 G > T | Novel | Intron 2 | E3 -149 | GCCTGCGCTCG/T GGGAGCCTGC | | | | 0.021 | - |
| IVS2-114 C > T | rs72634335 | Intron 2 | E3 -114 | TGGTGCCCCG/T GGGGGGAGGG | | | | 0.095 | - |
| IVS2-52 G > A | Novel | Intron 2 | E3 -52 | GAGCTCAGTCG/A GCTGGCGGGG | | | | 0.005 | - |
| IVS3+29 G > A | rs7215409 | Intron 3 | E3 +29 | TGGGCCGCACG/A TGCCAGGAGG | | | | 0.005 | 0.042 |
| 574 G > A | Novel | Exon 4 | 574 | CAACTGCTGCG/A TGTGTGCCGC | Val192Met | Benign | Intolerant | - | 0.005 |
| 609 G > A | Novel | Exon 4 | 609 | TGGTGGTCACG/A GCCAGCCGGG | | | | - | 0.005 |
| 641 C > T | Novel | Exon 4 | 641 | CCGCGACCCTC/T CCGGCGCCTG | Ser214Phe | Benign | Tolerant | 0.005 | 0.005 |
| 831 G > A | Novel | Exon 4 | 831 | ACATCTTCGCG/A CGGCCGCGCCG | | | | - | 0.031 |

| | | | | | | | | | |
|------------|------------|--------|------------|-------------------------------------|-----------|--------|------------|-------|-------|
| 916 G > A | Novel | Exon 4 | 916 | GTTCTTCAAC <u>G/A</u> GCCTCGCGGA | Gly306Ser | Benign | Intolerant | 0.005 | - |
| 1176 G > A | Novel | Exon 5 | 1176 | TCCTGGCGGG <u>G/A</u> GCCGAGGTGC | | | | 0.005 | - |
| 1494 C > T | Novel | 3'UTR | 1494 (96) | GGCAGGGCC <u>C/T</u> GGCTGGGCTC | | | | - | 0.005 |
| 1512 C > T | rs78825758 | 3'UTR | 1512 (114) | CTCCAGCTGC <u>C/T</u> GGCCCAGCGG | | | | 0.005 | - |
| 1594 C > T | Novel | 3'UTR | 1594 (196) | AGTGGATCTG <u>C/T</u> GGTGAAGCCA | | | | 0.058 | 0.005 |
| 1608 C > T | Novel | 3'UTR | 1608 (210) | GAAGCCAAGC <u>C/T</u> GCAAGGTTAC | | | | - | 0.005 |
| 1713 G > A | Novel | 3'UTR | 1713 (315) | TCGAGACAAC <u>G/A</u> TGACTTTAAT | | | | - | 0.005 |
| 1899 G > A | Novel | 3'UTR | 1899 (501) | TGGAGTGTT <u>A/G</u> GACCAACGGT | | | | 0.016 | - |

A of the translation initiation codon ATG is numbered 1 ((NM_001042422.2 was used as the reference sequence). Search completed: August 2010

Table 20. The SLC16A3 promoter transcript variant 2 population data quality check: goodness of fit to Hardy Weinberg Equilibrium

| Polymorphisms | Chinese | | Indians | |
|-------------------|------------|---------------------|------------|---------------------|
| | Chi Square | HWE <i>p</i> -value | Chi Square | HWE <i>p</i> -value |
| -139-1374 C > G | 0.003 | 0.959 | - | - |
| -139-1281 G > A | - | - | 0.793 | 0.373 |
| -139-1105 C > T | 0.188 | 0.664 | 0.218 | 0.641 |
| -139-845 G > A | | | 0.594 | 0.441 |
| -139-804 C > T | 2.501 | 0.114 | 0.261 | 0.610 |
| -139del(-727-795) | 0.698 | 0.403 | 1.500 | 0.221 |
| / | | | | |
| -139del(-727-773) | | | | |
| -139-540 C > T | 0.003 | 0.959 | - | - |
| -139-518 G > A | - | - | 0.003 | 0.959 |
| -139-477 G > T | 0.011 | 0.917 | - | - |
| -139-304 C > T | - | - | 0.003 | 0.959 |
| -139-246 C > G | - | - | 1.027 | 0.311 |
| -139-45 G > T | 0.003 | 0.959 | - | - |
| -139-40 C > G | 0.003 | 0.959 | - | - |
| -41 G > A | - | - | 0.003 | 0.959 |
| IVS+100 C > T | - | - | 0.003 | 0.959 |

Departure of observed genotype distributions from expected frequencies were analyzed using Chi Square *goodness of fit* test. Expected genotype frequencies were calculated from allele frequencies (p, q) according to the HWE formula where $p^2 + 2pq + q^2$. For population genetics, the degree of freedom (d.f.) is determined by number of genotypes – number of alleles.

* *p* value is significant ($p < 0.05$)

Table 21. The SLC16A3 promoter transcript variant 4 population data quality check: goodness of fit to Hardy Weinberg Equilibrium

| Polymorphisms | Chinese | | Indians | |
|-------------------|------------|---------------------|------------|---------------------|
| | Chi Square | HWE <i>p</i> -value | Chi Square | HWE <i>p</i> -value |
| -118-1416 C > T | - | - | 0.011 | 0.918 |
| -118-1131 C > A | - | - | 0.003 | 0.959 |
| -118-554 A > T | 0.235 | 0.628 | 0.113 | 0.737 |
| -118-502 A > G | 0.003 | 0.959 | 0.001 | 0.973 |
| -118del(-436-437) | 0.028 | 0.867 | 0.728 | 0.393 |
| -118-331 G > A | 0.158 | 0.691 | 0.144 | 0.705 |
| -118-249 C > T | 0.698 | 0.403 | 0.258 | 0.611 |
| -118-130 A > C | 0.432 | 0.511 | 0.218 | 0.641 |
| -118-115 G > A | 0.003 | 0.959 | - | - |
| -86 A > G | 0.601 | 0.438 | 0.218 | 0.641 |
| IVS1+21 G > C | 0.003 | 0.959 | - | - |

Departure of observed genotype distributions from expected frequencies were analyzed using Chi Square *goodness of fit* test. Expected genotype frequencies were calculated from allele frequencies (p, q) according to the HWE formula where $p^2 + 2pq + q^2$. For population genetics, the degree of freedom (d.f.) is determined by number of genotypes – number of alleles.

* *p* value is significant ($p < 0.05$)

Table 22. The SLC16A3 coding region population data quality check: goodness of fit to Hardy Weinberg Equilibrium

| Polymorphisms | Chinese | | Indians | |
|----------------|------------|---------------------|------------|---------------------|
| | Chi Square | HWE <i>p</i> -value | Chi Square | HWE <i>p</i> -value |
| 21 C > T | - | - | 0.003 | 0.959 |
| 44 C > T | 0.011 | 0.917 | 0.181 | 0.670 |
| 55 G > A | - | - | 0.003 | 0.959 |
| 117 C > T | - | - | 0.003 | 0.959 |
| IVS2-149 G > T | 22.74 | 0.000* | - | - |
| IVS2-114 C > T | 1.040 | 0.308 | - | - |
| IVS2-52 G > A | 0.003 | 0.959 | - | - |
| IVS3+29 G > A | 0.003 | 0.959 | 0.181 | 0.670 |
| 574 G > A | - | - | 0.003 | 0.959 |
| 609 G > A | - | - | 0.003 | 0.959 |
| 641 C > T | 0.003 | 0.959 | 0.003 | 0.959 |
| 831 G > A | - | - | 0.100 | 0.752 |
| 916 G > A | 0.003 | 0.959 | - | - |
| 1176 G > A | 0.003 | 0.959 | - | - |
| 1494 C > T | - | - | 0.003 | 0.959 |
| 1512 C > T | 0.003 | 0.959 | - | - |
| 1594 C > T | 0.359 | 0.549 | 0.003 | 0.959 |
| 1608 C > T | - | - | 0.003 | 0.959 |
| 1713 G > A | - | - | 0.003 | 0.959 |
| 1899 G > A | 0.024 | 0.876 | - | - |

Departure of observed genotype distributions from expected frequencies were analyzed using Chi Square *goodness of fit* test. Expected genotype frequencies were calculated from allele frequencies (p, q) according to the HWE formula where $p^2 + 2pq + q^2$. For population genetics, the degree of freedom (d.f.) is determined by number of genotypes – number of alleles.

* *p* value is significant ($p < 0.05$)

Table 23. *SLC16A3* inter-ethnic difference in allele frequency of polymorphisms in transcript variant 2 of promoter region

| Polymorphism | Allele Frequency | | Ethnic Difference | |
|-------------------|------------------|--------|-------------------|---------|
| | Chinese | Indian | Chi Sq | P-value |
| -139-1374 C > G | 0.005 | - | - | - |
| -139-1281 G > A | - | 0.083 | - | - |
| -139-1105 C > T | 0.916 | 0.875 | 1.695 | 0.193 |
| -139-845 G > A | - | 0.005 | - | - |
| -139-804 C > T | 0.853 | 0.673 | 13.89 | 0.001* |
| -139del(-727-795) | 0.921 | 0.833 | 6.81 | 0.009* |
| -139-540 C > T | 0.005 | - | - | - |
| -139-518 G > A | - | 0.005 | - | - |
| -139-477 G > T | 0.011 | - | - | - |
| -139-304 C > T | - | 0.005 | - | - |
| -139-246 C > G | - | 0.094 | - | - |
| -139-45 G > T | 0.005 | - | - | - |
| -139-40 C > G | 0.005 | - | - | - |
| -41 G > A | - | 0.005 | - | - |
| IVS+100 C > T | - | 0.005 | - | - |

* *p* value is significant ($p < 0.05$)

Table 24. *SLC16A3* inter-ethnic difference in allele frequency of polymorphisms in transcript variant 4 of promoter region

| Polymorphism | Allele Frequency | | Ethnic Difference | |
|----------------------|------------------|--------|-------------------|---------|
| | Chinese | Indian | Chi Sq | P-value |
| -118-115 G > A | 0.005 | - | - | - |
| -118-130 A > C | 0.937 | 0.875 | 4.279 | 0.039* |
| -118-249 C > T | 0.079 | 0.156 | 5.491 | 0.019* |
| -118-331 G > A | 0.163 | 0.161 | 0.002 | 0.964 |
| -118del(-436-437) AG | 0.105 | 0.146 | 1.065 | 0.302 |
| -118-502 A > G | 0.147 | 0.146 | 0.002 | 0.964 |
| -118-554 A > T | 0.926 | 0.875 | 2.807 | 0.094 |
| -118-1131 C > A | - | 0.005 | - | - |
| -118-1416 C > T | - | 0.01 | - | - |
| -86 A > G | 0.926 | 0.875 | 2.807 | 0.09 |
| IVS1+21 G > C | 0.005 | - | - | - |

* *p* value is significant ($p < 0.05$)

Table 25. The inter-ethnic difference in allele frequency of polymorphisms in the coding region of SLC16A

| Polymorphism | Allele Frequency | | Ethnic Difference | |
|----------------|------------------|--------|-------------------|---------|
| | Chinese | Indian | Chi Sq | P-value |
| 21 C > T | - | 0.005 | - | - |
| 44 C > T | 0.011 | 0.042 | 3.633 | 0.057 |
| 55 G > A | - | 0.005 | - | - |
| 117 C > T | - | 0.005 | - | - |
| IVS2-149 G > T | 0.021 | - | - | - |
| IVS2-114 C > T | 0.095 | - | - | - |
| IVS2-52 G > A | 0.005 | - | - | - |
| IVS3+29 G > A | 0.005 | 0.042 | 5.501 | 0.019* |
| 574 G > A | - | 0.005 | - | - |
| 609 G > A | - | 0.005 | - | - |
| 641 C > T | 0.005 | 0.005 | 0.000 | 1.000 |
| 831 G > A | - | 0.031 | - | - |
| 916 G > A | 0.005 | - | - | - |
| 1176 G > A | 0.005 | - | - | - |
| 1494 C > T | - | 0.005 | - | - |
| 1512 C > T | 0.005 | - | - | - |
| 1594 C > T | 0.058 | 0.005 | 8.712 | 0.003* |
| 1608 C > T | - | 0.005 | - | - |
| 1713 G > A | - | 0.005 | - | - |
| 1899 G > A | 0.016 | - | - | - |

* p value is significant ($p < 0.05$)

2.2.2.2 Genetic Variants Detected in the Promoter and 5'-UTR Regions of Transcript Variant 2 of *SLC16A3* gene

A total of 15 genetic variations were found in the 5'-flanking region of transcript variant 1: 13 in the promoter, 1 in the 5'-UTR region and 1 in the intron region.

The representative sequencing electropherograms and description of polymorphism distribution are discussed in section 2.2.2.2.1 to 2.2.2.2.15. The predictive effects of SNPs on the transcription factor binding sites of *SLC16A3* gene are summarized in **Table 26**.

Table 26. The predictive effects of SNP on the transcription factor binding sites of MCT4. For each SNP allele the transcription factor binding sites either deleted or generated by the nucleotide exchange.

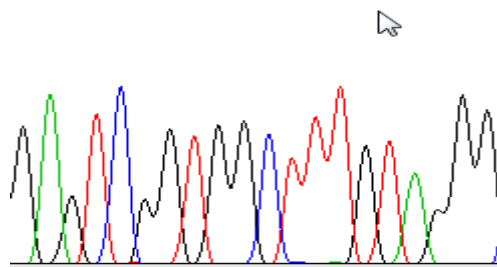
| | Name | Lost Family/Matrix | New Family Matrix |
|----------------------|-----------------|---|--|
| Transcript Variant 2 | -139-1374 C > G | Insulator protein CTCF (CCCTC-binding factor) Myeloid zinc finger protein MZF1 Myeloid zinc finger protein MZF1 Glial cells missing homolog 1 B-cell-specific activator protein | Olfactory neuron-specific factor |
| | -139-1281 G > A | Glial cells missing homolog 1 | PAX6 paired domain and homeodomain are required for binding to this site |
| | -139-1105 C > T | X-box binding protein RFX1 | Wilms Tumor Suppressor |
| | -139-845 G > A | MEL1 (MDS1/EVI1-like gene 1) DNA-binding domain 2 Myogenic bHLH protein myogenin (myf4) | Transcription factor yin yang 2 c-Rel |
| | -139-804 C > T | Stimulating protein 1 Carbohydrate response element binding protein (CHREBP) and Max-like protein X (Mlx) bind as heterodimers to glucose-responsive promoters | Egr-2/Krox-20 early growth response gene product Wilms Tumor Suppressor |
| | -139-540 C > T | Doublesex and mab-3 related transcription factor 4 Albumin D-box binding protein | Special AT-rich sequence-binding protein 1, predominantly expressed in thymocytes, binds to matrix attachment regions (MARs) |
| | -139-518 G > A | Binding sites for homodimers of large Maf-proteins | - |
| | -139-477 G > T | Neurogenin 1 and 3 (ngn1/3) binding sites | Meis homeobox 1 |
| | -139-304 C > T | - | - |
| | -139-246 C > G | Olfactory neuron-specific factor | - |
| | -139-45 G > T | - | - |
| | -139-40 C > G | - | Spermatogenic Zip 1 transcription factor |
| | -41 G > A | - | Neuron-restrictive silencer factor (11 bp spacer between half sites) |
| Transcript Variant 4 | -118-115 G > A | Nuclear factor of activated T-cells 5 | Interferon regulatory factor 7 (IRF-7) LIM homeobox 4, Gsh4 Homeobox and leucine zipper encoding transcription factor |
| | -118-130 A > C | - | - |
| | -118-249 C > T | Human zinc finger protein ZNF35 | Myeloid zinc finger protein MZF1 |
| | -118-331 G > A | - | - |
| | -118-502 A > G | Autoimmune regulator Transcriptional repressor CDP Nuclear factor Y (Y-box binding factor) FAST-1 SMAD interacting protein | - |
| | -118-554 A > T | H6 homeodomain HMX3/Nkx5.1 transcription factor | Kruppel-like factor 6 |
| | -118-1131 C > A | bHLH-PAS type transcription factors NXF/ARNT heterodimer | Activator protein 4 |
| | | Hypoxia induced factor-1 (HIF-1) | Myf5 myogenic bHLH protein |
| -118-1416 C > T | - | - | |
| -86 A > G | - | cAMP-responsive element binding protein Tax/CREB complex | |

2.2.2.2.1 -139-40 C>G

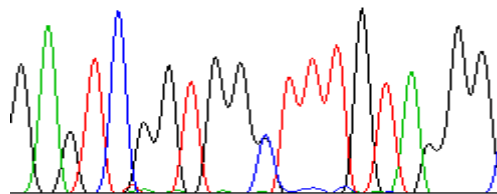
The -139-40 C>G single nucleotide polymorphism is located 40-bp upstream of the transcription start site and does not reside in any transcription factor binding site.

Representative sequencing electropherograms of AA and AB genotypes are as presented:

G A G T C G G T G G C T T T G T A G G G



G A G T C G G T G G N T T T G T A G G G



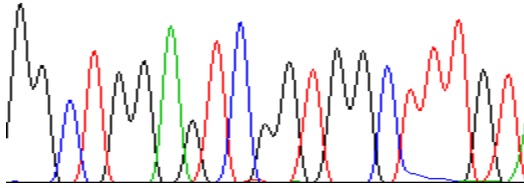
This is a novel SNP and was found as heterozygotic in one Chinese subject. The genotype distribution of CC, CG and GG were 94 (98.9%), 1 (1.1%) and 0 (0%), respectively. The observed genotype distribution is in accordance to HWE ($X^2 = 0.003$, $p = 0.959$). This variant was not found in the ethnic Indian group of Singapore population. A substitution from C to G at position 40-bp upstream of the transcription start site may result in the generation of new putative Spermatogenic Zip 1 transcription factor binding site (SPZ1).

2.2.2.2.2 -139-45 G>T

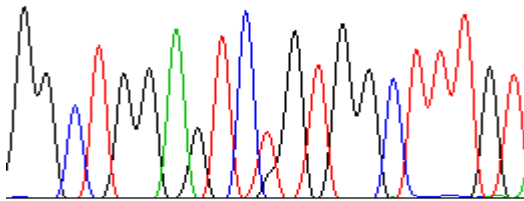
The -139-45 G>T is located 45-bp upstream of the transcription start site.

Representative sequencing electropherograms of AA and AB genotypes are as presented:

GGCTGGAGTCTGGTGGCTTTGT.



GGCTGGAGTCTTGTGGCTTTGT

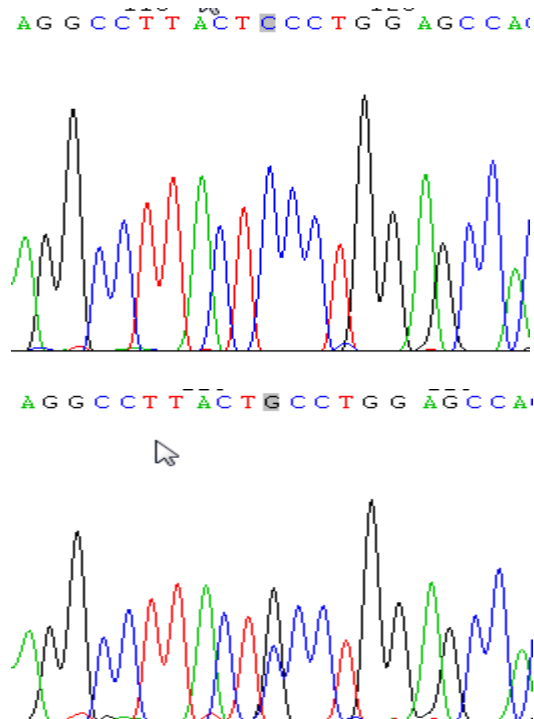


This variant was only detected in Chinese group. The genotype distribution of GG, GT and TT were 94 (98.9%), 0 (0%) and 1 (1.1%), respectively. This observed distribution is in accordance to HWE ($\chi^2 = 0.003$, $p = 0.959$). This SNP does not have any consequence on the transcription factor binding site.

2.2.2.2.3 -139-246 C>G

The -139-246 is located 246-bp upstream of the transcription start site.

Representative sequencing electropherograms of AA and AB genotypes are as presented:



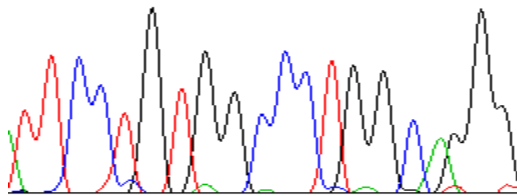
This variant was only detected in Indian group of Singapore population. Amongst the 96 Indian samples analyzed, the frequencies of CC, CG, and GG genotypes were 78 (81.3%), 18 (18.7%) and 0 (0%). This observed distribution is in accordance to HWE ($\chi^2 = 1.027, p = 0.311$). The ancestral allele is reported as “C” nucleotide, which corresponds with the C nucleotide being the dominant allele in both ethnic groups (Reference SNP ID: rs75888222). The minor G allele was occurring at a frequency of 0.094 in Indian while this G allele was not present in Chinese. A substitution from C to G at position 246-bp upstream of the

transcription start site may result in the loss of putative olfactory neuron-specific factor binding site (OLF1).

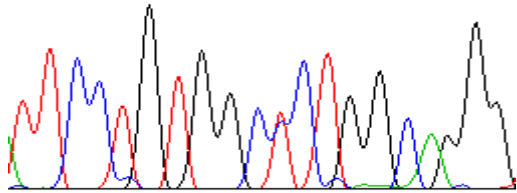
2.2.2.2.4 -139-304 C>T

The -139-304 C>T is located 304-bp upstream of the transcription start site. This SNP does not reside in any transcription factor binding site. Representative sequencing electropherograms of AA and AB genotypes are as presented:

. T T C C T G T G C C T G G C A G G G



T T C C T G T G G C T T G G C A G G G

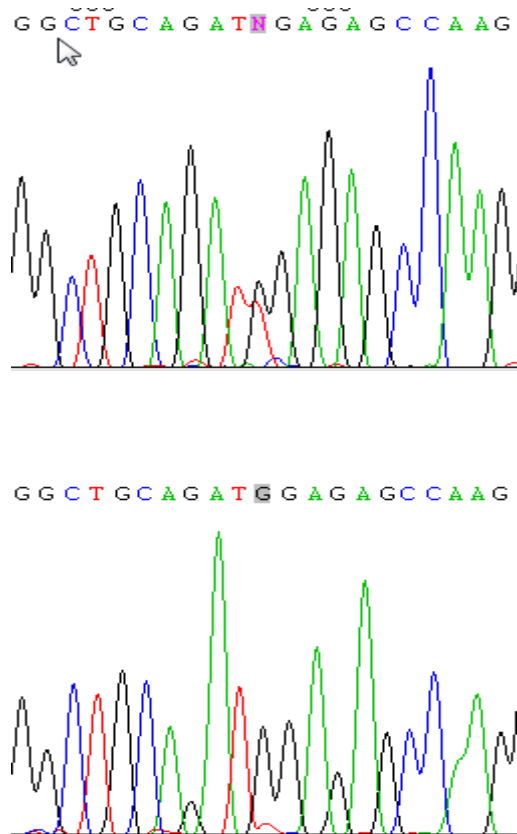


The -139-304 C>T is a novel SNP and was only found in Indian group. The genotype frequencies of the CC, CT and TT were 95 (99%), 1 (1%) and 0 (0%), respectively. No deviation from HWE was observed for this polymorphism ($X^2 = 0.003$, $p = 0.959$). This SNP does not have any consequence on the transcription factor binding site.

2.2.2.2.5 -139-477 G>T

The -139-477 G>T is located 477-bp upstream of transcription start site.

Representative sequencing electropherograms of AA and AB genotypes are as presented:

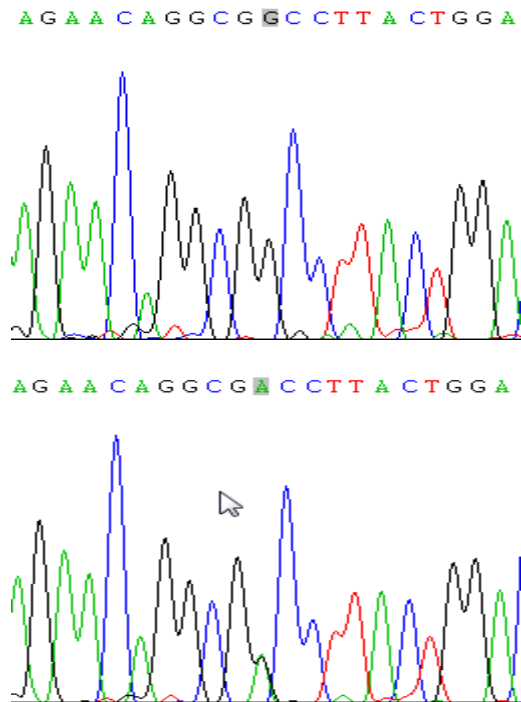


This SNP is novel and was only present in Chinese group. The genotype distribution of GG, GT and TT were 93 (97.9%), 2 (2.1%) and 0 (0%), respectively.

The observed genotype distribution is in accordance to HWE ($\chi^2 = 0.011$, $p = 0.917$). The substitution of G to T at position 477-bp upstream of the transcription start site may cause the loss of putative neurogenin 1 and 3 (ngn1/3) binding site (NEUROG) and the generation of new putative binding site for a Pbx1/Meis1 heterodimer (PBX1_MEIS1).

2.2.2.2.6 -139-518 G>A

The -139-518 G>A is located 518-bp upstream of transcription start site and within a putative androgene receptor binding site (ARE). Representative sequencing electropherograms of AA and AB genotypes are as presented:

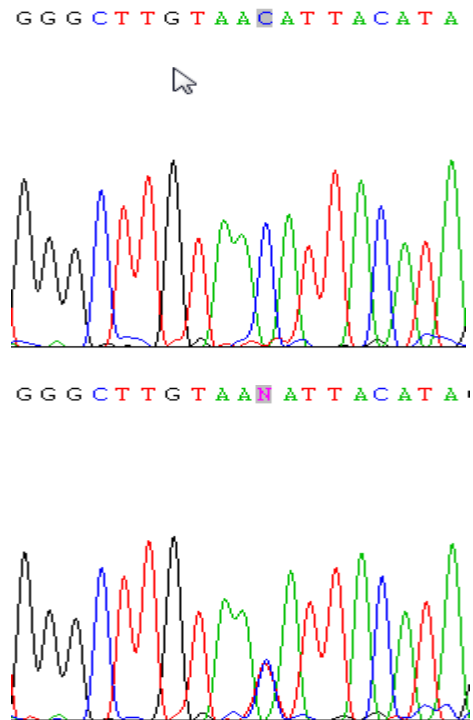


This SNP was found as heterozygotic in one Indian subject. The genotype frequencies of the GG, GA and AA were 95 (99%), 1 (1%) and 0 (0%), respectively. No deviation from HWE was observed for this polymorphism ($X^2 = 0.003$, $p = 0.959$). The substitution of nucleotide G to A at position 518-bp upstream of transcription start site was predicted to result in the loss of putative androgene receptor binding site (ARE).

2.2.2.2.7 -139-540 C>T

The -139-540 C>T is located 540-bp upstream of transcription start site.

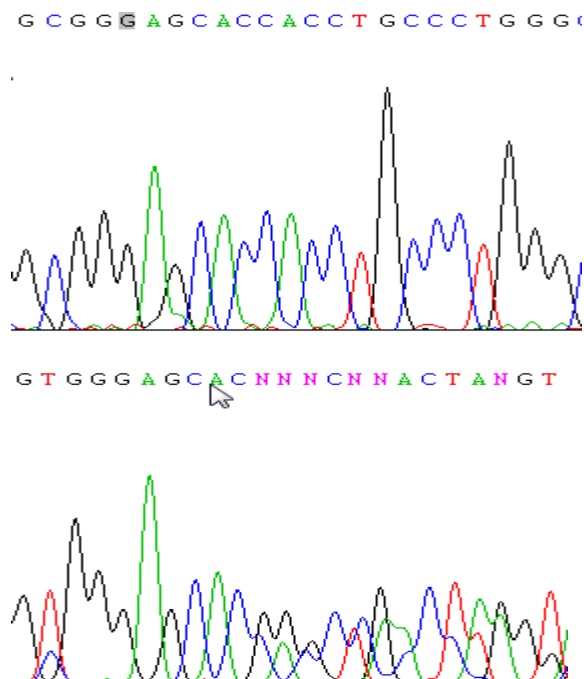
Representative sequencing electropherograms of AA and AB genotypes are as presented:



This SNP was found as heterozygotic in one Chinese subject but was not detected in Indian group. The genotype distribution of CC, CT and TT were 94 (98.9%), 1 (1.1%) and 0 (0%), respectively. This observed distribution is in accordance to HWE ($X^2 = 0.003, p = 0.959$). The substitution of nucleotide C to T at position 540-bp upstream of transcription start site may result in the loss of two putative transcription factor binding sites, doublesex and mab-3 related transcription factor 4 (DMRT4) and albumin D-box binding protein (DBP). The substitution may also lead to the generation of special AT-rich sequence-binding protein 1 (SATB) binding site.

2.2.2.2.8 -139- del (727-795)

The large deletion polymorphism consisting of an CACCTGCCCTGGGCGGGAGCAC tandem repeat sequence deletion is located 727 to 795-bp upstream of the transcription start site. Representative sequencing electropherograms of homozygous wildtype and heterozygous deletion genotypes are presented:



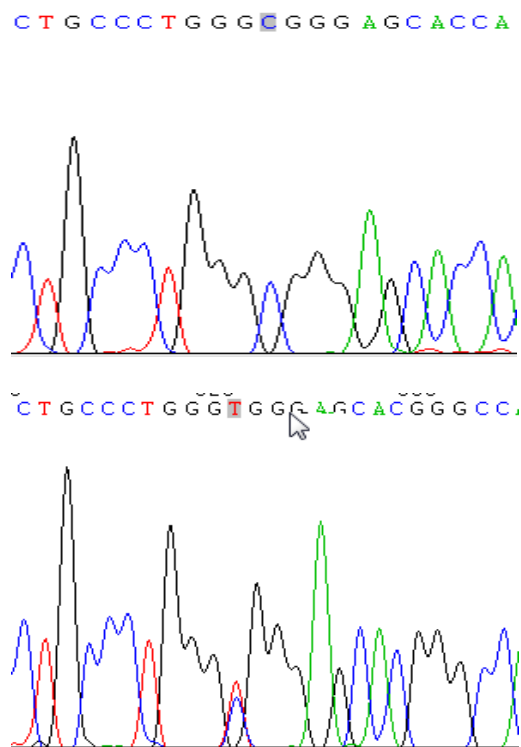
The distribution of homozygous wildtype, heterozygous deletion and homozygous deletion genotypes in Chinese were 0 (0%), 15 (15.8%) and 80 (84.2%), respectively. In Indians, the frequencies of homozygous wildtype, heterozygous deletion and homozygous deletion observed were 1 (1%), 30 (31.2%) and 65 (67.8%), respectively. No deviations from HWE were observed for all ethnic groups (Chinese $X^2 = 0.698$, $p = 0.403$; Indian $X^2 = 1.500$, $p = 0.221$). The large deletion form is the dominant allele in both ethnic groups. Ancestral allele information on this polymorphism is not available in the NCBI SNP database (Reference SNP ID: rs10704992). The homozygous wildtype was not found in

Chinese and only one sample was identified in Indians. Statistically significant inter-ethnic differences in allele frequency is observed when analysed with Chi square test of independence ($X^2 = 6.81, p = 0.009$).

2.2.2.2.9 -139-804 C>T

The -139-804 C>T is located 804-bp upstream of transcription start site.

Representative sequencing electropherograms of AA and AB genotypes are as presented:



This SNP was identified as a common polymorphism in the local Chinese and Indian populations. In Chinese, the frequencies of CC, CT, and TT genotypes were 4 (4.2%), 20 (20.8%), and 71 (75%). Amongst the 96 Indian samples analysed, the frequencies of CC, CT, and TT genotypes were 8 (8.3%), 43 (44.8%) and 45 (46.9%), respectively. No deviation from HWE were observed for both ethnic groups (Chinese $X^2 = 2.501, p = 0.114$; Indian $X^2 = 0.261, p = 0.610$). The NCBI

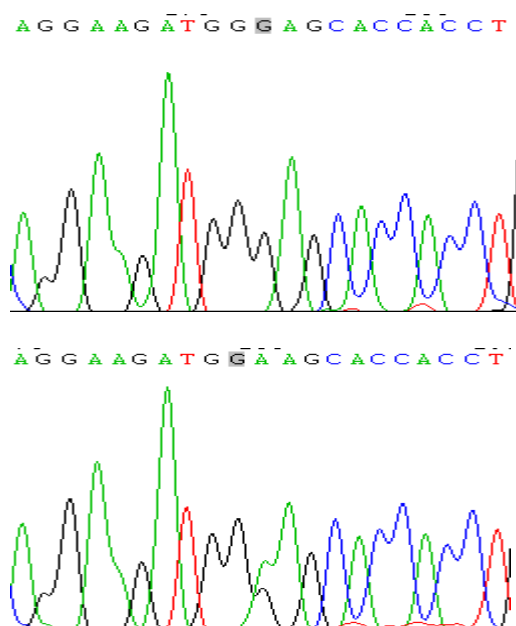
SNP database (Reference SNP ID: rs12453976) has reported this SNP as a C/T variant, and the ancestral allele is reported “T” nucleotide. However, the ancestral allele information on this polymorphism is not available. The observed inter-ethnic difference in allele frequency is statistically significant ($X^2 = 13.89, p < 0.001$).

The substitution of nucleotide C to T at position 804-bp upstream of transcription start site was predicted to result in the loss of putative stimulating protein 1 (SP1) and carbohydrate response element binding protein (CHREBP)/ Max-like protein X (Mlx) heterodimer (CHREBP_MLX) transcription factor binding sites. The substitution also leads to in the generation of putative Egr-2/Krox-20 early growth response (EGR2) and Wilms Tumor Suppressor (WT1) binding sites.

2.2.2.2.10 -139-845 G>A

The -139-845 C>T is located 845-bp upstream of transcription start site.

Representative sequencing electropherograms of AA and AB genotypes are as presented:

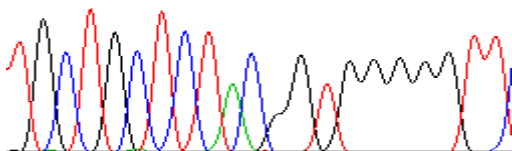


The -139-845 G>A is a novel SNP and only found as heterozygotic in one Indian sample. The genotype frequencies of the GG, GA and AA were 95 (99%), 1 (1%) and 0 (0%), respectively. No deviation from HWE was observed for this polymorphism ($X^2 = 0.003$, $p = 0.959$). The substitution of nucleotide G to A at position 845-bp upstream of transcription start site was predicted to result in the loss of putative MDS1/EVI1-like gene 1 DNA-binding domain 2 (MEL1) and Myogenic bHLH protein myogenin (myf4) (MYOGENIN) binding sites. The substitution was predicted to result in the generation of putative Transcription factor yin yang 2 (YY2) and c-Rel (CREL) binding sites.

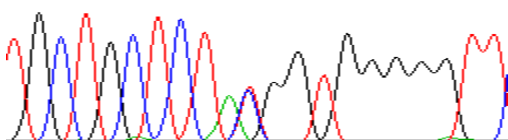
2.2.2.2.11 -139-1105 C>T

The -139-1105 C>T is located 1105-bp upstream of transcription start site. Representative sequencing electropherograms of AA and AB genotypes are as presented:

T G C T G C T C T A G G T G G G G G T T



T G C T G C T C T A T G G T G G G G G T T

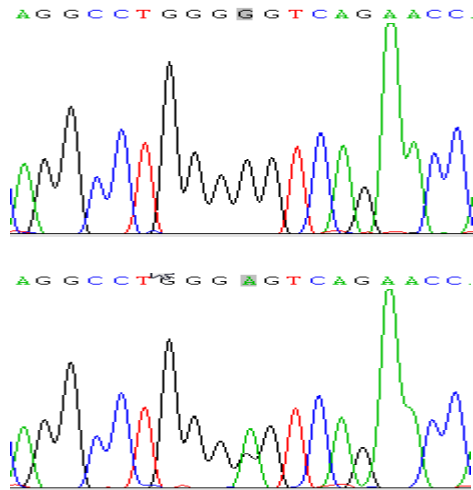


The -139-1105 C>T was found to be a common polymorphism in the local Chinese and Indian populations. The genotype distribution of CC, CT and TT amongst 95

Chinese samples were 1 (1.1%), 14 (14.7%) and 80 (84.2%), respectively. The distribution of CC, CT and TT in Indian were 2 (2.1%), 20 (20.8%) and 74 (77.1%), respectively. No deviation from HWE was observed for this polymorphism (Chinese $X^2 = 0.188$, $p = 0.664$; Indian $X^2 = 0.218$, $p = 0.641$). The T nucleotide is the dominant allele in both ethnic groups, which is consistent with the ancestral T allele reported in the NCBI SNP database (Reference SNP ID: rs11077983). The minor C allele is least frequent in Chinese (0.168) compared to the Indian (0.125) population. This difference was however not statistically significant within our study population ($X^2 = 1.695$, $p = 0.193$). The substitution of nucleotide C to T was predicted to result in the loss of putative regulatory factor X protein 1 (RFX1) and the generation of putative Wilms Tumor Suppressor (WT1) binding site.

2.2.2.2.12 -128-1281 G>A

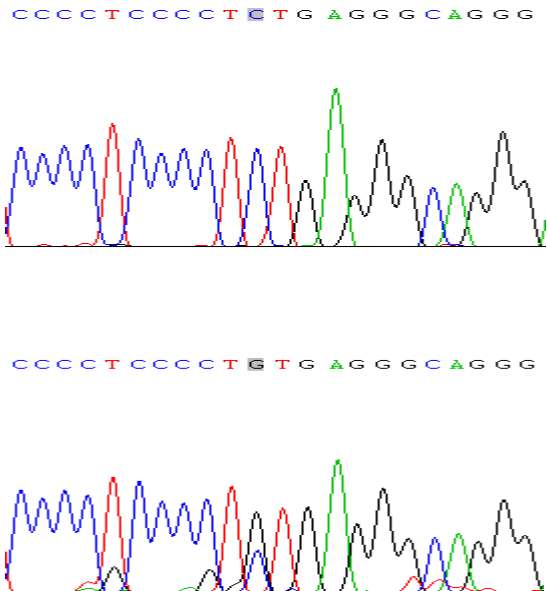
The -128-1281 G>A is a novel SNP locates at 1281-bp upstream of transcription start site. Representative sequencing electropherograms of AA and AB genotypes are as presented:



This SNP was only detected in the Indian group. The genotype distribution of GG, GA and AA were 80 (83%), 16 (17%) and 0 (0%), respectively. The observed distribution is in accordance to the HWE ($\chi^2 = 0.793$, $p = 0.373$). This substitution was predicted to result in the loss of Glial cells missing homolog 1 (GCM1) and the generation of PAX6 paired domain (PAX6) binding site.

2.2.2.2.13 -128-1374 C>G

The -128-1374 C>G is a novel SNP locates at 1374-bp upstream of transcription start site. Representative sequencing electropherograms of AA and AB genotypes are as presented:

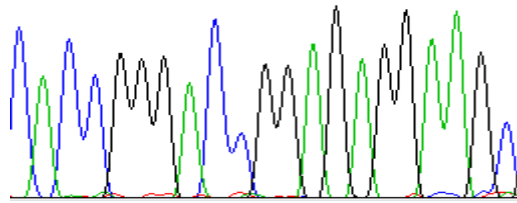


This SNP was only found in Chinese. The genotype distribution of CC, CG and GG were 94 (98.9%), 1 (1.1%) and 0 (0%), respectively. This observed distribution is in accordance to HWE ($\chi^2 = 0.003$, $p = 0.959$). The substitution of nucleotide C to G at position 1374-bp upstream of transcription start site was predicted to result in the loss and generation of several putative transcription factor binding sites (**Table 26**).

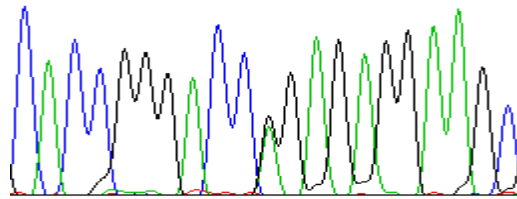
2.2.2.2.14 -41 G>A

The -41 G>A polymorphism is positioned 41-bp upstream of the translational start site. Representative sequencing electropherograms of AA and AB genotypes are as presented:

C A C C G G G A C C G G A G A G G A A G C



C A C C G G G A C C G A G A G G A A G C

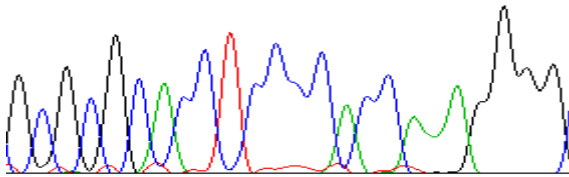


The -41 G>A is a novel polymorphism and 5'-UTR region of *SLC16A3* gene. It was found as heterozygotic in one Indian subject. The distribution of GG, GA and AA genotypes were 95 (99%), 1 (1%) and 0 (0%), respectively. This observed distribution is in accordance to HWE ($X^2 = 0.003$, $p = 0.959$). The nucleotide substitution was predicted to result in the generation of new putative neuron-restrictive silencer factor (NRSF) binding site.

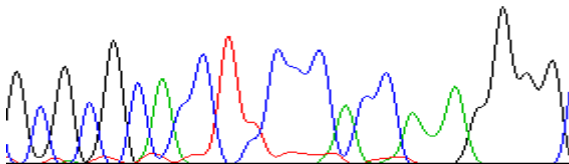
2.2.2.2.15 IVS +100 C>T

The IVS +100 C>T polymorphism is positioned at 100-bp downstream of exon 1 of transcript variant 1. Representative sequencing electropherograms of AA and AB genotypes are as presented:

G C G C G C A C C T C C C A C C A A A G G G G



G C G C G C A C C T C C C A C C A A A G G G G



The IVS +100 C>T is a novel SNP and was only identified in one Indian sample. The distribution of GG, GA and AA genotypes were 95 (99%), 1 (1%) and 0 (0%), respectively. This observed distribution is in accordance to HWE ($X^2 = 0.003$, $p = 0.959$).

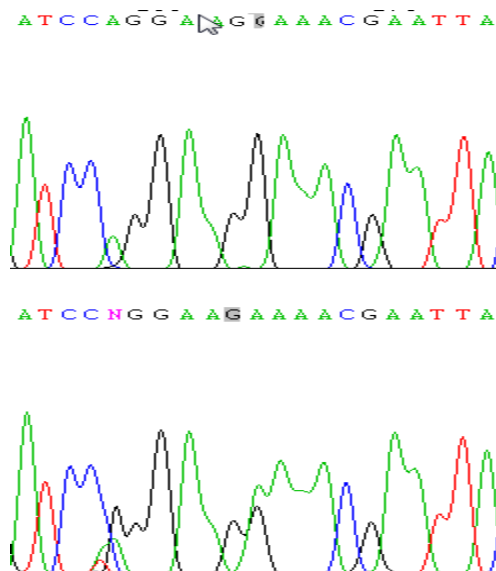
2.2.2.3 Genetic Variants Detected in the Promoter and 5'-UTR Regions of Transcript Variant 4 of *SLC16A3* gene

A total of 11 genetic variations were found in the 5'-flanking region of transcript variant 3: 9 in the promoter, 1 in the 5'-UTR and 1 in the intron region. The representative sequencing electropherograms and description of polymorphism distribution are discussed in section 2.2.2.3.1 to 2.2.2.3.11. The predictive effects of SNPs on the transcription factor binding sites of *SLC16A3* gene are summarized in **Table 26**.

2.2.2.3.1 -118-115 G>A

The -118-115 G>A is located 115-bp upstream of transcription start site.

Representative sequencing electropherograms of AA and AB genotypes are as presented:



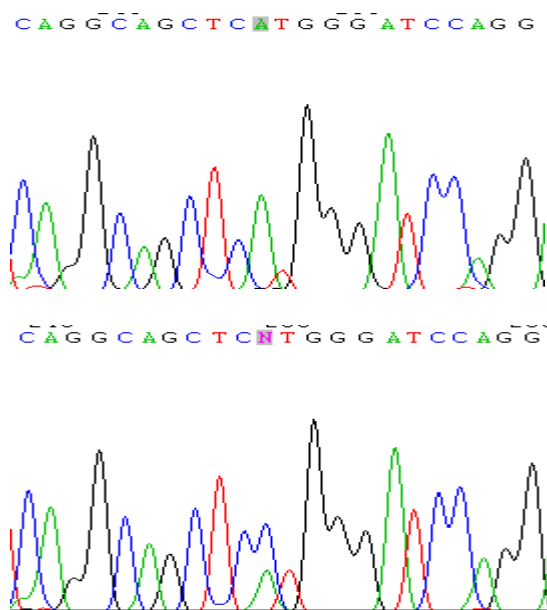
This SNP was found as heterozygous in one Chinese subject but was not detected in Indian group. The genotype distribution of GG, GA and AA were 94 (98.9%), 1 (1.1%) and 0 (0%), respectively. This observed distribution is in accordance to HWE ($X^2 = 0.003$, $p = 0.959$). The substitution of nucleotide G to A at position

115-bp upstream of transcription start site may result in the loss of a putative transcription factor binding sites, Nuclear factor of activated T-cells 5 (NFAT5). The substitution may also lead to the generation of three putative binding sites, namely Interferon regulatory factor 7 (IRF-7), LIM homeobox 4 (LHX4) and Homeobox and leucine zipper encoding transcription factor (HOMEZ).

2.2.2.3.2 -118-130 A>C

The -118-130 A>C is located 130-bp upstream of transcription start site.

Representative sequencing electropherograms of AA and AB genotypes are as presented:



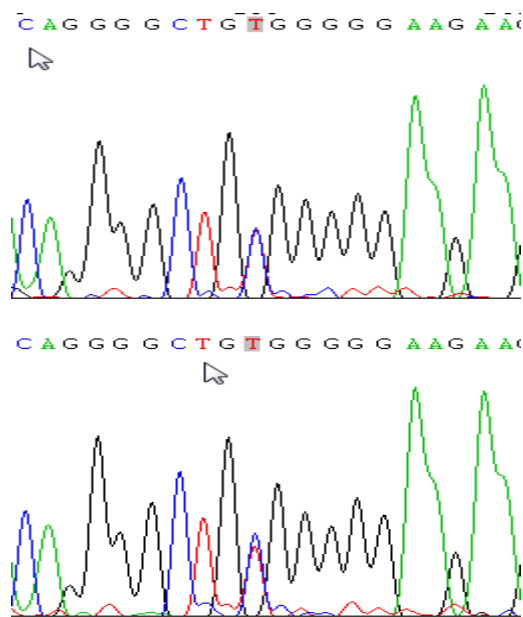
The -118-130 A>C was found to be common polymorphism in the local ethnic Chinese and Indian groups. The distribution of AA, AC and CC in Chinese were 0 (0%), 12 (12.6%) and 83 (87.4%), respectively. The genotype distribution of AA, AC and CC amongst 96 Indian samples were 2 (2.1%), 20 (20.8%) and 74 (77.1%), respectively. No deviation from HWE were observed for both ethnic groups (Chinese $X^2 = 0.432$, $p = 0.511$; Indian $X^2 = 0.218$, $p = 0.641$). The C

nucleotide is the dominant allele in both ethnic groups, which is consistent with the ancestral C allele reported in the NCBI SNP database (Reference SNP ID: rs3176828). The observed inter-ethnic difference in allele frequency is statistically significant ($X^2 = 4.279$, $p = 0.039$). This SNP does not have any consequence on the transcription factor binding site.

2.2.2.3.3 -118-249 C>T

The -118-249 C>T is located 249-bp upstream of transcription start site.

Representative sequencing electropherograms of AA and AB genotypes are as presented:



The -118-249 C>T is a reported SNP that detected in both ethnic groups. The genotype distribution of CC, CT and TT amongst 95 Chinese samples were 80 (84.2%), 15 (15.8%) and 0 (0%), respectively. The distribution of CC, CT and TT in Indian were 69 (71.9%), 24 (25%) and 3 (3.1%), respectively. No deviation from HWE was observed for this polymorphism (Chinese $X^2 = 0.698$, $p = 0.403$;

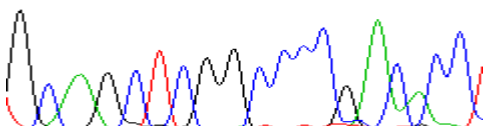
Indian ($X^2 = 0.258$, $p = 0.611$). The C nucleotide is the dominant allele in both ethnic groups, which is consistent with the ancestral C allele reported in the NCBI SNP database (Reference SNP ID: rs79034755). The observed inter-ethnic difference in allele frequency is statistically significant ($X^2 = 5.491$, $p = 0.019$). The nucleotide substitution was predicted to result in the loss of Human zinc finger protein ZNF35 (ZNF35) and the generation of new putative myeloid zinc finger protein (MZF1) binding site.

2.2.2.3.4 -118-331 G>A

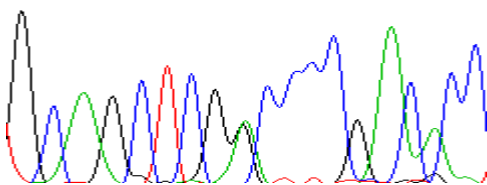
The -118-331 G>A is located 331-bp upstream of transcription start site.

Representative sequencing electropherograms of AA and AB genotypes are as presented:

G C A G C T C G G C C C G A C A C C



G C A G C T C G G C C C G A C A C C

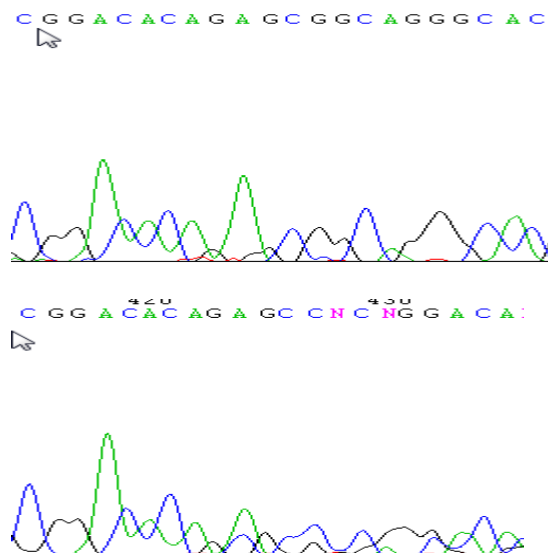


This SNP was detected in both ethnic groups. The distribution of GG, GA and AA in Chinese were 66 (69.5%), 27 (28.4%) and 2 (2.1%), respectively. The genotype distribution of GG, GA and AA amongst 96 Indian samples were 67 (69.8%),

27 (28.1%) and 2 (2.1%), respectively. No deviation from HWE were observed for both ethnic groups (Chinese $X^2 = 0.158$, $p = 0.691$; Indian $X^2 = 0.144$, $p = 0.705$). The G nucleotide is the dominant allele in both ethnic groups, which is consistent with the ancestral G allele reported in the NCBI SNP database (Reference SNP ID: rs60910743). The observed inter-ethnic difference in allele frequency is not statistically significant ($X^2 = 0.002$, $p = 0.964$). This SNP does not have any consequence on the transcription factor binding site.

2.2.2.3.5 -118 del (-436-437) AG

The deletion polymorphism consisting of an AG deletion is located 436 to 437-bp upstream of the transcription start site. Representative sequencing electropherograms of homozygous wildtype and heterozygous deletion genotypes are presented:



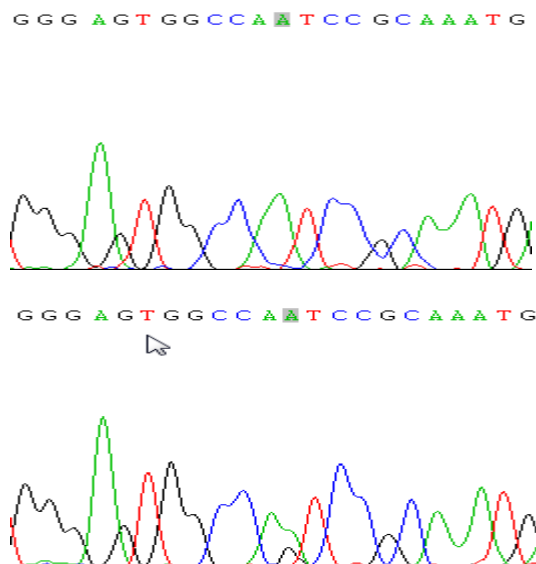
The distribution of homozygous wildtype, heterozygous deletion and homozygous deletion genotypes in Chinese were 75 (78.9%), 19 (20%) and 1 (1.1%), respectively. In Indians, the frequencies of homozygous wildtype, heterozygous deletion and homozygous deletion observed were 69 (71.9%), 26 (27.1%) and

1 (1%), respectively. No deviations from HWE were observed for all ethnic groups (Chinese $X^2 = 0.028$, $p = 0.867$; Indian $X^2 = 0.728$, $p = 0.393$). Ancestral allele information on this polymorphism is not available in the NCBI SNP database (Reference SNP ID: rs58263941). The observed inter-ethnic difference in allele frequency is not statistically significant ($X^2 = 1.065$, $p = 0.302$).

2.2.2.3.6 -118-502 A>G

The -118-502 A>G is located 502-bp upstream of transcription start site.

Representative sequencing electropherograms of AA and AB genotypes are as presented:



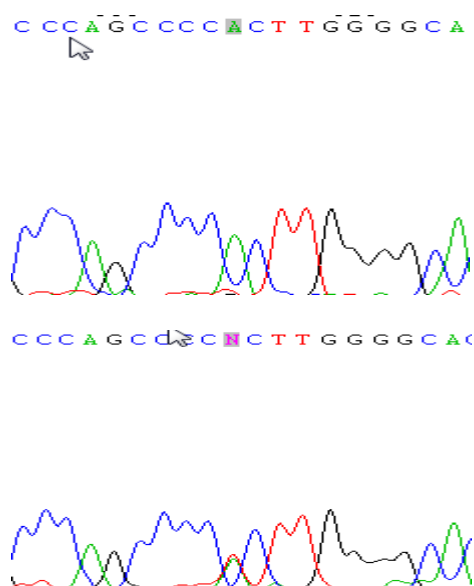
This reported SNP only found in both ethnic Chinese and Indian groups of Singapore population. The distribution of GG, GA and AA in Chinese were 69 (72.6%), 24 (25.3%) and 2 (2.1%), respectively. The distribution of AA, AG and GG in Indian were 70 (72.9%), 24 (25%) and 2 (2.1%), respectively. No deviations from HWE were observed for all ethnic groups (Chinese $X^2 = 0.003$, $p = 0.959$; Indian $X^2 = 0.001$, $p = 0.973$). The A nucleotide is the dominant allele in Indian, which is consistent with the ancestral A allele reported in the NCBI SNP

database (Reference SNP ID: rs12450761). The substitution of nucleotide from A to G at position 502-bp upstream of transcription start site may result in the loss of several transcription factor binding sites, namely autoimmune regulator (AIRE), transcription repressor CDP (CDP), nuclear factor Y (NFY) and FAST-1 SMAD interacting protein (FAST1).

2.2.2.3.7 -118-544 A>T

The -118-544 A>T is located 544-bp upstream of transcription start site.

Representative sequencing electropherograms of AA and AB genotypes are as presented:

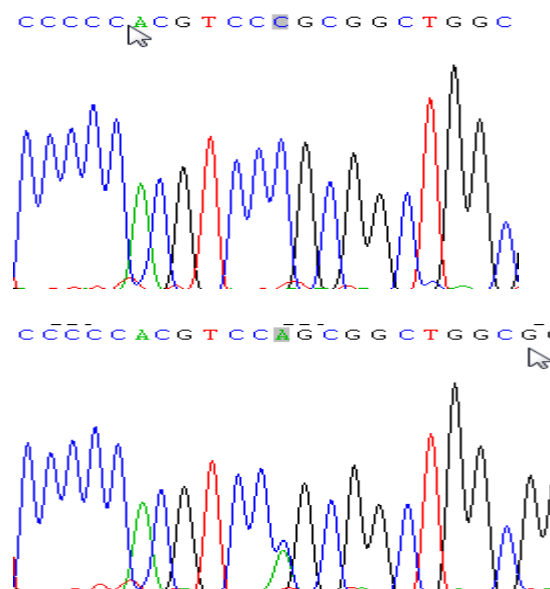


This SNP was found to be a common single nucleotide polymorphism present in the ethnic Chinese and Indian groups of Singapore population. Among the 95 Chinese samples studied, 0 (0%) samples were homozygous wildtype, 9 (9.5%) samples were heterozygous mutants and 86 (90.5%) were homozygous mutants. The genotype distribution of AA, AT and TT amongst 96 Indian samples were

2 (2.1%), 21 (21.9%) and 73 (76%), respectively. No deviation from HWE were observed for both ethnic groups (Chinese $X^2 = 0.235$, $p = 0.628$; Indian $X^2 = 0.113$, $p = 0.737$). The T nucleotide is the dominant allele in both ethnic groups, which is consistent with the ancestral T allele reported in the NCBI SNP database (Reference SNP ID: rs56043453). The observed inter-ethnic difference in allele frequency is statistically significant ($X^2 = 8.082$, $p = 0.004$). This SNP was predicted to result in the loss of putative H6 homeodomain HMX3/Nkx5.1 (HMX3) transcription factor and the generation of putative Kruppel-like factor 6 (KLF6) transcription factor.

2.2.2.3.8 -118-1131 C>A

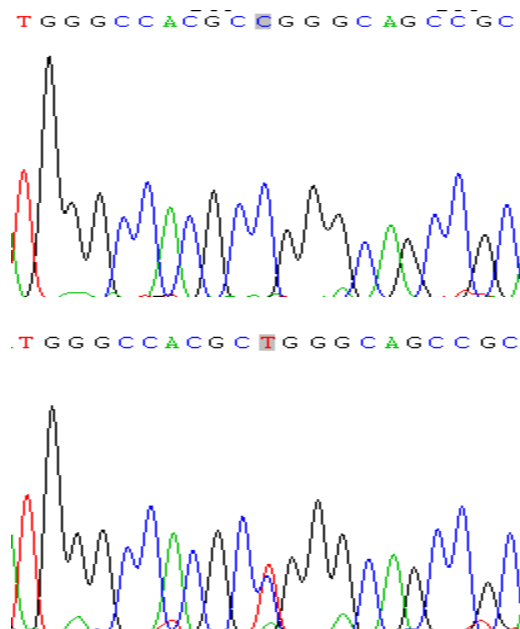
The -118-1131 C>A is located 1131-bp upstream of the transcription start site. Representative sequencing electropherograms of AA and AB genotypes are as presented:



The -139-1131 C>T is a novel SNP and was only found in Indian group. The genotype frequencies of the CC, CA and AA were 95 (99%), 1 (1%) and 0 (0%), respectively. No deviation from HWE was observed for this polymorphism ($X^2 = 0.003, p = 0.959$). This SNP may result in the loss of the putative bHLH-PAS type transcription factors NXF/ARNT heterodimer (NXF_ARNT) and Hypoxia induced factor-1 (HIF1) binding sites. Furthermore, this SNP may also lead to the generation of new putative activator protein 4 (AP4) and Myf5 myogenic bHLH protein (MYF5) transcription factor binding sites.

2.2.2.3.9 -118-1461 C>T

The -139-1461 C>T is located 1461-bp upstream of the transcription start site. Representative sequencing electropherograms of AA and AB genotypes are as presented:

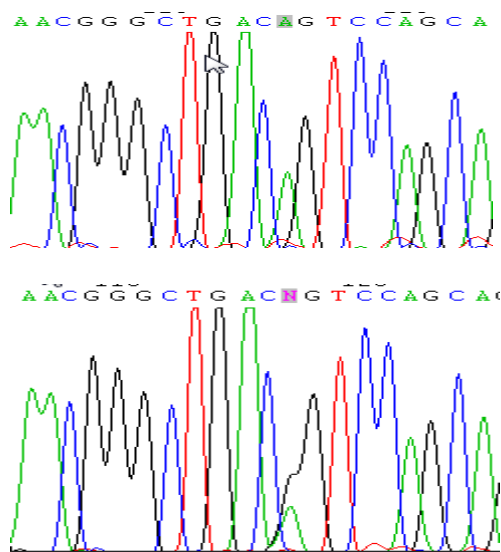


The -118-1461 C>T is a novel SNP and was only found in Indian group. The genotype frequencies of the CC, CT and TT were 94 (97.9%), 2 (2.1%) and 0 (0%), respectively. No deviation from HWE was observed for this polymorphism

($X^2 = 0.011, p = 0.918$). This SNP does not have any consequence on the transcription factor binding site.

2.2.2.3.10 -86 A>G

The -86 G>A polymorphism is positioned 86-bp upstream of the translational start site. Representative sequencing electropherograms of AA and AB genotypes are as presented:



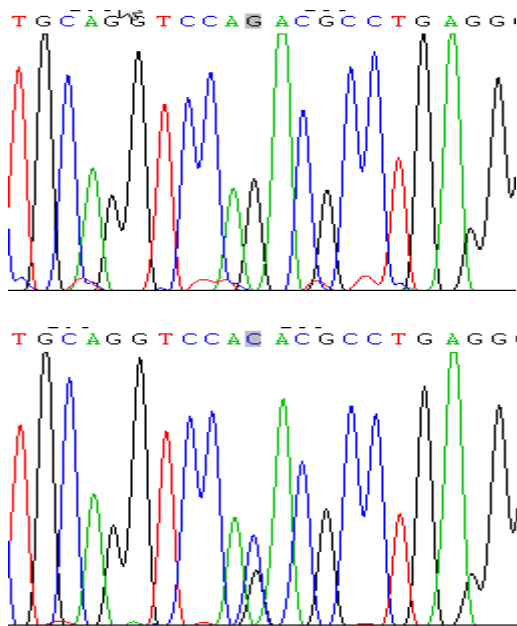
This SNP was found to be a common single nucleotide polymorphism present in the ethnic Chinese and Indian groups of Singapore population. Among the 95 Chinese samples studied, 0 (0%) samples were homozygous wildtype, 14 (14.7%) samples were heterozygous mutants and 81 (84.7%) were homozygous mutants. The genotype distribution of AA, AG and GG amongst 96 Indian samples were 2 (2.1%), 20 (20.8%) and 74 (77.1%), respectively. No deviation from HWE were observed for both ethnic groups (Chinese $X^2 = 0.601, p = 0.438$; Indian $X^2 = 0.218, p = 0.641$). The G nucleotide is the dominant allele in both ethnic groups.

However, the ancestral allele reported in the NCBI SNP database is A allele

(Reference SNP ID: rs3176827). The observed inter-ethnic difference in allele frequency is not statistically significant ($X^2 = 2.807, p = 0.090$).

2.2.2.3.11 IVS+21 G>C

The IVS+21 G>C polymorphism is positioned at 21-bp downstream of exon 1 of transcript variant 3. Representative sequencing electropherograms of AA and AB genotypes are as presented:

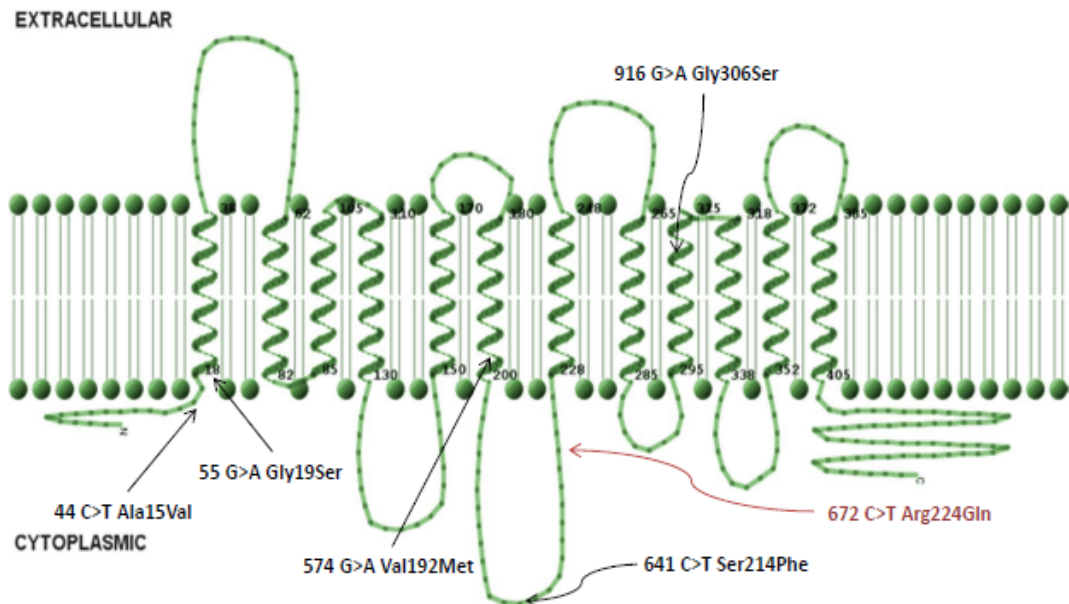


The IVS+21 G>C is a novel SNP and was only identified in one Chinese sample. The distribution of GG, GC and CC genotypes were 94 (98.9%), 1 (1.1%) and 0 (0%), respectively. This observed distribution is in accordance to HWE ($X^2 = 0.003, p = 0.959$).

2.2.2.4 Genetic Variants Detected in the Exon, Intron and 3'-UTR Regions of *SLC16A3* gene

A total of 20 variants were detected: 10 in the exons (5 nonsynonymous and 5 synonymous variations), 4 in introns and 6 in the 3'-UTR region. The effects of nonsynonymous SNPs reported in this study were predicted using bioinformatics tools, PolyPhen and SIFT. The representative electropherograms showing the homozygous wildtype and heterozygous variants and the description of polymorphism are discussed in section 2.2.2.4.1 to 2.2.2.4.20.

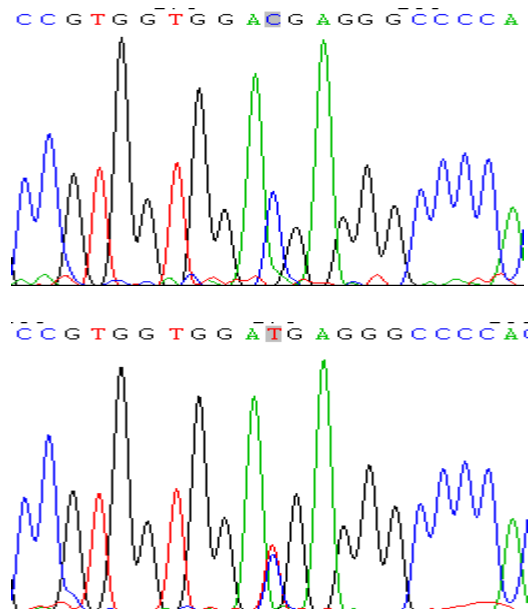
Figure 9. Topological location of *SLC16A3* non-synonymous mutations detected in this study and retrieved from the dbSNP database (<http://www.ncbi.nlm.nih.gov/SNP/>). The mutations highlighted in black are the genetic variants found in the Chinese and Indian population of Singapore.



2.2.2.4.1 21 C>T

The 21 C>T is a novel synonymous SNP that located at exon 2 of MCT4 protein.

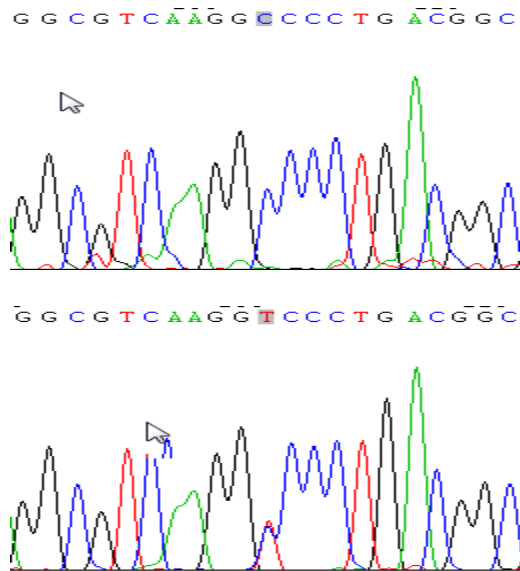
Representative sequencing electropherograms of AA and AB genotypes are as presented:



It was found as heterozygotic in one Indian subject. The distribution of CC, CT and TT genotypes were 95 (99%), 1 (1%) and 0 (0%), respectively. This observed distribution is in accordance to HWE ($X^2 = 0.003$, $p = 0.959$).

2.2.2.4.2 44C>T (Ala15Val)

The 44C>T (Ala15Val) is a novel nonsynonymous variant that located at exon 2 of MCT4 protein. Representative sequencing electropherograms of AA and AB genotypes are as presented:



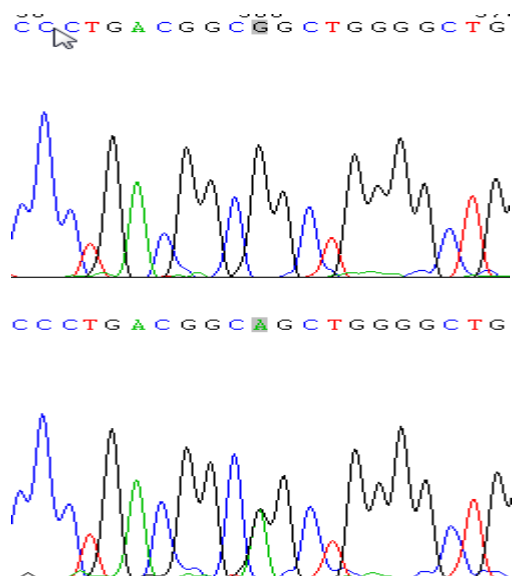
This SNP was identified in both ethnic Chinese and Indian groups of Singapore population. The distribution of CC, CT and TT genotypes in Chinese were 93 (97.9%), 2 (2.1%) and 0 (0%), respectively. In Indians, the frequencies of CC, CT and TT observed were 88 (91.7%), 8 (8.3%), and 0 (0%), respectively. No deviation from HWE were observed for all ethnic groups (Chinese $X^2 = 0.011$, $p = 0.917$; Indian $X^2 = 0.181$, $p = 0.670$). The observed inter-ethnic difference in allele frequency is not statistically significant ($X^2 = 3.633$, $p = 0.057$).

Based on putative protein topology, the 44C>T (Ala15Val) is located at the intracellular N-terminal of MCT4 protein (**Fig. 9**). A substitution from C to T at position 44 resulted in the conversion of amino acid alanine to valine at position 15 of MCT4 protein. Although both amino acid residues are non-polar, the 44C>T

(Ala15Val) was predicted to be probably damaging by PolyPhen and SIFT programs.

2.2.2.4.3 55G>A (Gly19Ser)

The 55G>A (Gly19Ser) is a novel nonsynonymous variant that located at exon 2 of MCT4 protein. Representative sequencing electropherograms of AA and AB genotypes are as presented:



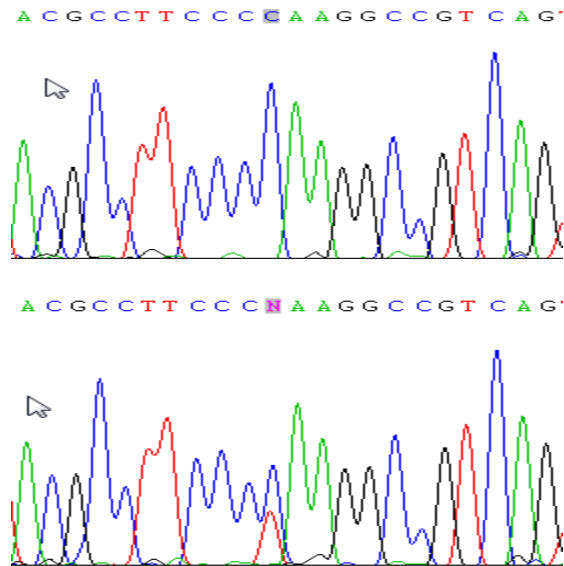
This variant was only present as heterozygotic in one Indian subject and was not found in Chinese population. The distribution of GG, GA and AA genotypes were 95 (99%), 1 (1%) and 0 (0%), respectively. This observed distribution is in accordance to HWE ($\chi^2 = 0.003$, $p = 0.959$).

The 55G>A (Gly19Ser) variant is located at the intracellular N-terminal of the MCT4 molecule (**Fig. 9**). The non-polar glycine is replaced by the polar serine. Although SIFT program predicted this substitution is intolerant, it was inconsistent with the results obtained using PolyPhen program which predicted this mutation was expected to be benign.

2.2.2.4.4 117 C>T

The 117 C>T is a novel synonymous SNP that located at exon 2 of MCT4 protein.

Representative sequencing electropherograms of AA and AB genotypes are as presented:

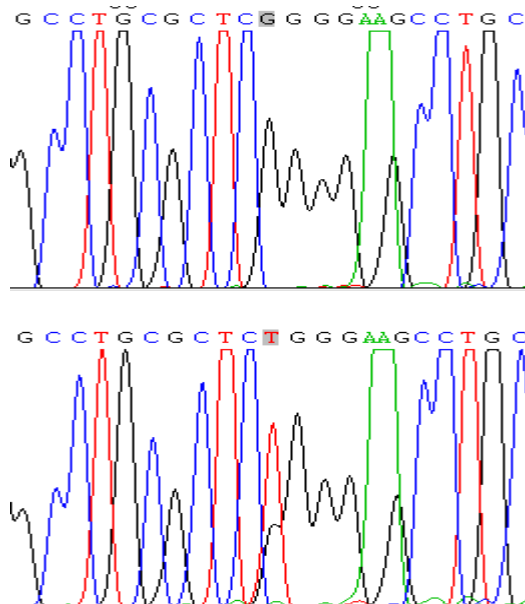


It was found as heterozygotic in one Indian subject. The distribution of CC, CT and TT genotypes were 95 (99%), 1 (1%) and 0 (0%), respectively. This observed distribution is in accordance to HWE ($X^2 = 0.003$, $p = 0.959$).

2.2.2.4.5 IVS-149 G>T

The IVS-149 G>T located at 149-bp upstream of exon 3 of MCT4 molecule.

Representative sequencing electropherograms of AA and AB genotypes are as presented:

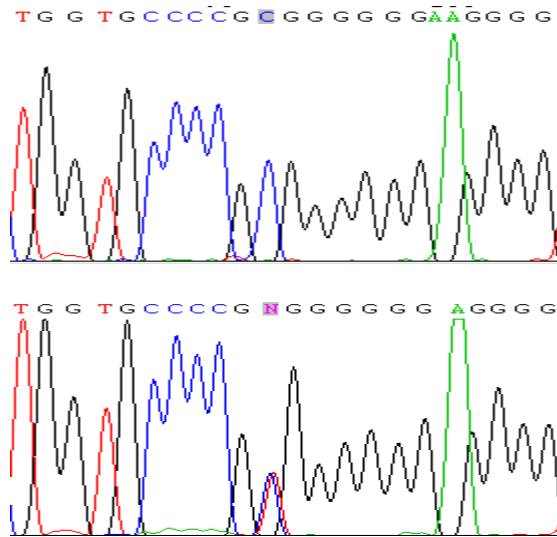


This variant was only found in Chinese. The genotype distribution of GG, GT and TT were 92 (96.8%), 2 (2.1%) and 1 (1.1%), respectively. This observed distribution is not in accordance to HWE ($\chi^2 = 22.74$, $p = 0.001$)

2.2.2.4.6 IVS-114 C>T

The IVS-114 G>T located at 114-bp upstream of exon 3 of MCT4 molecule.

Representative sequencing electropherograms of AA and AB genotypes are as presented:



This SNP was only identified in the Chinese subjects. The distribution of CC, CT and TT in Chinese were 77 (81.1%), 18 (18.9%) and 0 (0%), respectively. No deviation from HWE was observed for this polymorphism ($\chi^2 = 1.040$, $p = 0.308$).

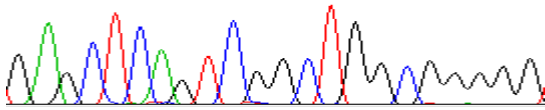
The C nucleotide is the dominant allele in ethnic Chinese group, which is consistent with the ancestral C allele reported in the NCBI SNP database (Reference SNP ID: rs72634335).

2.2.2.4.7 IVS-52 G>A

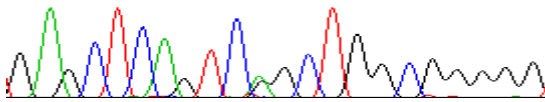
The IVS-52 G>A located at 52-bp upstream of exon 3 of MCT4 molecule.

Representative sequencing electropherograms of AA and AB genotypes are as presented:

G A G C T C A G T C G G C T G G C G G G G G



G A G C T C A G T C A G C T G G C G G G G G



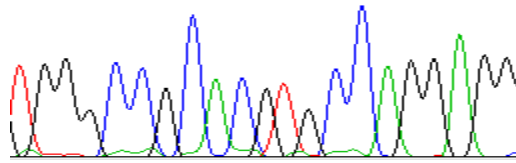
This variant was only found in Chinese. The genotype distribution of GG, GA and AA were 94 (98.9%), 1 (1.1%) and 0 (0%), respectively. This observed distribution is in accordance to HWE ($\chi^2 = 0.003$, $p = 0.959$).

2.2.2.4.8 IVS+29 G>A

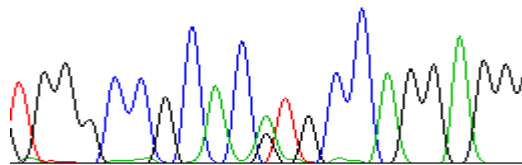
The IVS+29 G>A located at 29-bp downstream of exon 3 of MCT4 molecule.

Representative sequencing electropherograms of AA and AB genotypes are as presented:

T G G G C C G C A C G T G C C A G G A G G



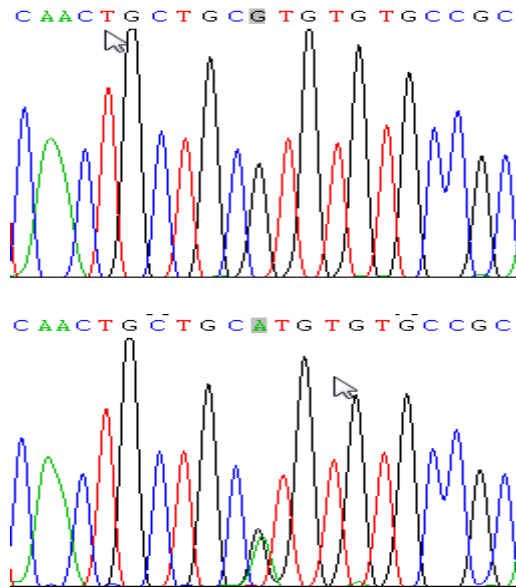
T G G G C C G C A C G T G C C A G G A G G



The IVS+29 G>A is a reported SNP that was found in both ethnic Chinese and Indian groups of Singapore population. The distribution of GG, GA and AA genotypes in Chinese were 94 (98.9%), 1 (1.1%) and 0 (0%), respectively. In Indians, the frequencies of GG, GA and AA observed were 88 (91.7%), 8 (8.3%), and 0 (0%), respectively. No deviation from HWE were observed for all ethnic groups (Chinese $\chi^2 = 0.003$, $p = 0.959$; Indian $\chi^2 = 0.181$, $p = 0.670$). The G nucleotide is the dominant allele in Indians. However, the ancestral allele reported in the NCBI SNP database is A allele (Reference SNP ID: rs7215409).

2.2.2.4.9 574 G>A (Val192Met)

The 574 G>A (Val192Met) is a novel nonsynonymous variant that located at exon 4 of MCT4 protein. Representative sequencing electropherograms of AA and AB genotypes are as presented:



This variant was only present as heterozygotic in one Indian subject and was not found in Chinese population. The distribution of GG, GA and AA genotypes were 95 (98.9%), 1 (1.1%) and 0 (0%), respectively. This observed distribution is in accordance to HWE ($\chi^2 = 0.003$, $p = 0.959$).

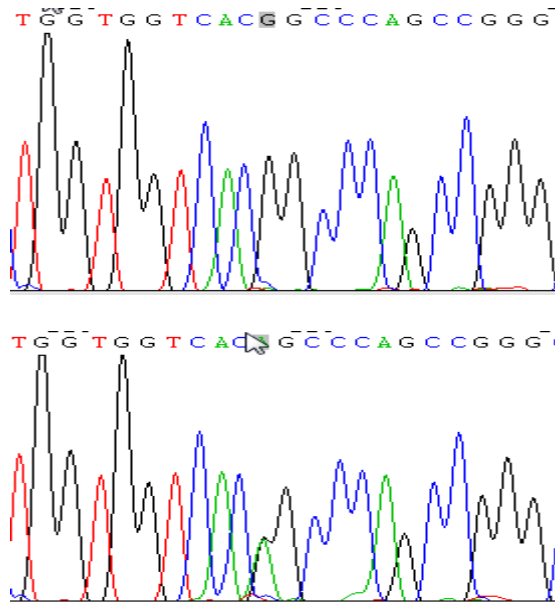
The 574 G>A (Val192Met) polymorphism is located at the TM6 of the MCT4 protein. A substitution from G to A at position 574 resulted in the conversion of amino acid valine to methionine at position 192 of MCT4 protein (**Fig. 9**).

Although both amino acid residues are non-polar, this variant has conflicting results between the SIFT and PolyPhen algorithms. PolyPhen program predicted that this substitution is benign while SIFT algorithm predicted this variant is intolerant.

2.2.2.4.10 609 G>A

The 609 C>T is a novel synonymous SNP that located at exon 4 of MCT4 protein.

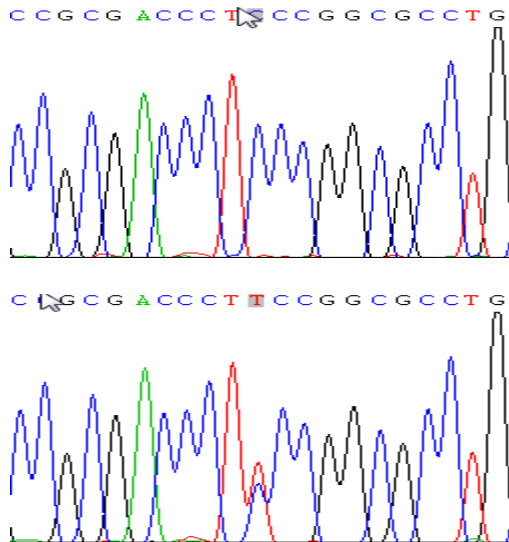
Representative sequencing electropherograms of AA and AB genotypes are as presented:



It was found as heterozygotic in one Indian subject. The distribution of GG, GA and TA genotypes were 95 (99%), 1 (1%) and 0 (0%), respectively. This observed distribution is in accordance to HWE ($X^2 = 0.003$, $p = 0.959$).

2.2.2.4.11 641 C>T (Ser214Phe)

The 641 C>T (Ser214Phe) is a novel nonsynonymous variant that located at exon 4 of MCT4 protein. Representative sequencing electropherograms of AA and AB genotypes are as presented:



It was found as heterozygotic in one Chinese and one Indian. The distribution of CC, CT and TT in Chinese were 94 (98.9%), 1 (1.1%) and 0 (0%), respectively. The distribution of AA, AG and GG in Indian were 95 (99%), 1 (1%) and 0 (0%), respectively. No deviations from HWE were observed for all ethnic groups (Chinese $X^2 = 0.003$, $p = 0.959$; Indian $X^2 = 0.003$, $p = 0.959$).

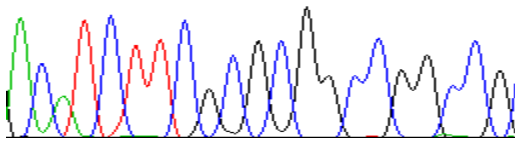
The 641 C>T (Ser214Phe) variant is located at the large intracellular loop between TM segments 6 and 7, which is least conserved among family members (**Fig. 9**). The polar serine is replaced by the non-polar phenylalanine. However, 641 C>T (Ser214Phe) was predicted to have mildest effect on the protein function by both algorithms.

2.2.2.4.12 831 G>A

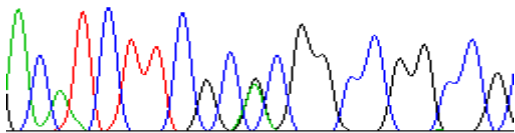
The 831 G>A is a novel synonymous SNP that located at exon 4 of MCT4 protein.

Representative sequencing electropherograms of AA and AB genotypes are as presented:

A C A T C T T C G C G C G G C C G G C C G



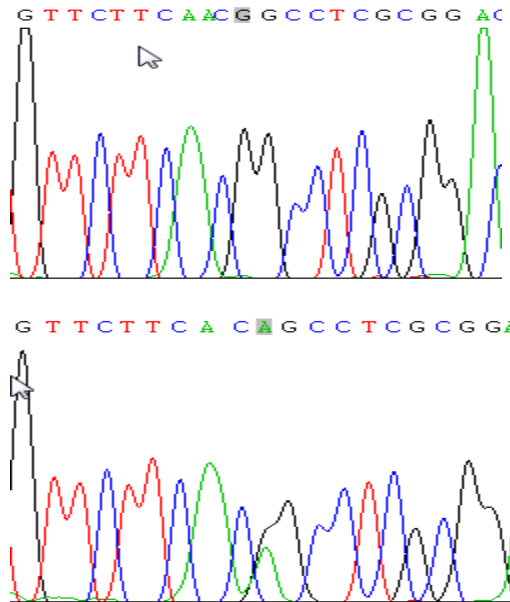
A C A T C T T C G C A C G G C C G G C C G



This SNP only detected in Indian subjects. The distribution of GG, GA and AA genotypes were 90 (93.8%), 6 (6.2%) and 0 (0%), respectively. This observed distribution is in accordance to HWE ($X^2 = 0.100, p = 0.752$).

2.2.2.4.13 916 G>A (Gly306Ser)

The 916 G>A is a novel nonsynonymous SNP that located at exon 4 of MCT4 protein. Representative sequencing electropherograms of AA and AB genotypes are as presented:

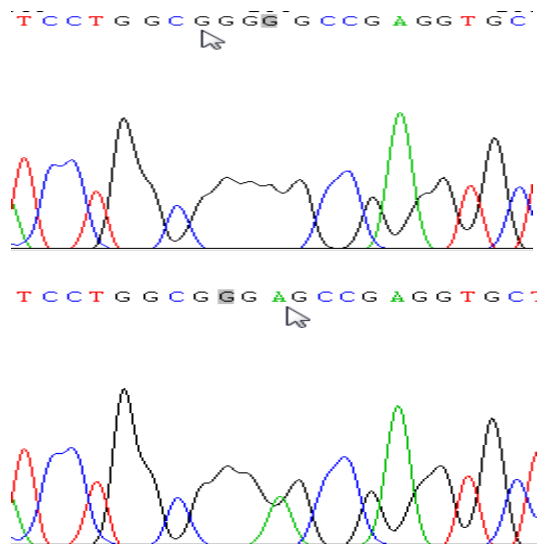


This variant was found as heterozygotic in one Chinese sample. The distribution of GG, GA and AA genotypes were 94 (98.9%), 1 (1.1%) and 0 (0%), respectively. No deviations from HWE were observed (Chinese $\chi^2 = 0.003$, $p = 0.959$).

The 916 G>A (Gly306Ser) variant is located at the TM9 of the MCT4 protein (**Fig. 9**). The non-polar glycine is replaced by the polar serine. This variant has conflicting results between the PolyPhen and SIFT programs. It was predicted by PolyPhen program that this substitution might not affect the transporter activity. However, SIFT program predicted that this substitution is intolerant.

2.2.2.4.14 1176 G>A

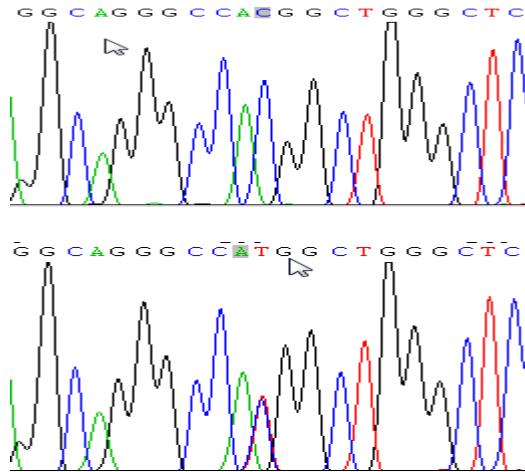
The 1176 G>A is a novel synonymous SNP that located at exon 5 of MCT4 protein. Representative sequencing electropherograms of AA and AB genotypes are as presented:



This SNP only detected in Chinese. The distribution of GG, GA and AA genotypes were 94 (98.9%), 1 (1.1%) and 0 (0%), respectively. This observed distribution is in accordance to HWE ($\chi^2 = 0.003, p = 0.959$).

2.2.2.4.15 1494 C>T

The 1494 C>T is located at the 3'-UTR of *SLC16A3* gene. Representative sequencing electropherograms of AA and AB genotypes are as presented:

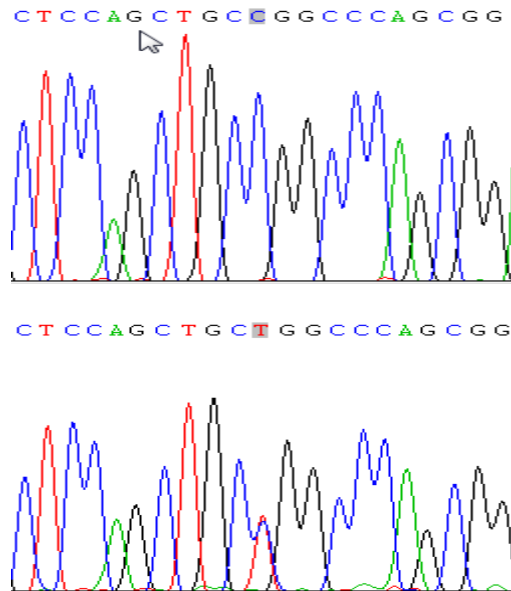


This SNP was only detected in the Indian group of Singapore population. The observed frequencies of CC, CT and TT genotypes were 95 (99%), 1 (1%) and 0 (0%). No deviation from HWE was observed for this polymorphism ($\chi^2 = 0.003$, $p = 0.959$).

2.2.2.4.16 1512 C>T

The 1512 C>T is a reported SNP locates at the 3'-UTR of *SLC16A3* gene.

Representative sequencing electropherograms of AA and AB genotypes are as presented:

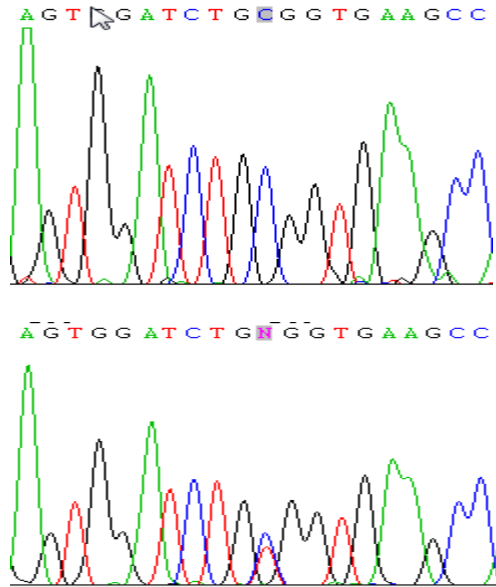


This SNP was only detected in the Chinese group of Singapore population. The observed frequencies of CC, CT and TT genotypes were 95 (99%), 1 (1%) and 0 (0%). No deviation from HWE was observed for this polymorphism ($X^2 = 0.003$, $p = 0.959$). The ancestral allele reported in the NCBI SNP database is C allele (Reference SNP ID: rs78825758).

2.2.2.4.17 1594 C>T

The 1594 C>T is a reported SNP locates at the 3'-UTR of *SLC16A3* gene.

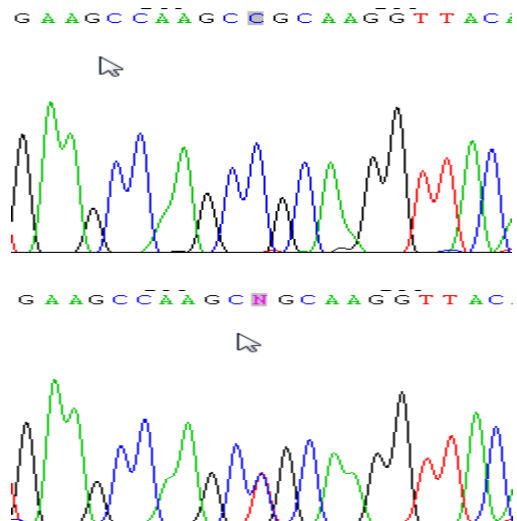
Representative sequencing electropherograms of AA and AB genotypes are as presented:



The distribution of CC, CT and TT genotypes in Chinese were 84 (88.4%), 11 (11.6%) and 0 (0%), respectively. In Indians, the frequencies of CC, CT and TT observed were 95 (99%), 1 (1%), and 0 (0%), respectively. No deviation from HWE were observed for all ethnic groups (Chinese $X^2 = 0.359$, $p = 0.549$; Indian $X^2 = 0.003$, $p = 0.959$).

2.2.2.4.18 1608 C>T

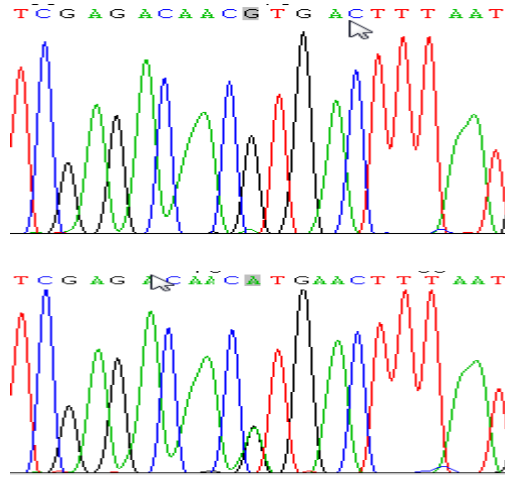
The 1608 C>T is located at the 3'-UTR of *SLC16A3* gene. Representative sequencing electropherograms of AA and AB genotypes are as presented:



This SNP was only detected in the Indian group of Singapore population. The observed frequencies of CC, CT and TT genotypes were 95 (99%), 1 (1%) and 0 (0%). No deviation from HWE was observed for this polymorphism ($X^2 = 0.003$, $p = 0.959$).

2.2.2.4.19 1713 G>A

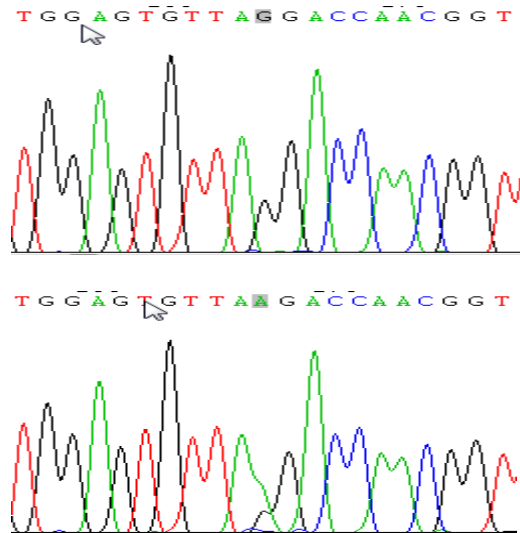
The 1713 G>A is located at the 3'-UTR of *SLC16A3* gene. Representative sequencing electropherograms of AA and AB genotypes are as presented:



This SNP was only detected in the Indian group of Singapore population. The observed frequencies of GG, GA and AA genotypes were 95 (99%), 1 (1%) and 0 (0%). No deviation from HWE was observed for this polymorphism ($X^2 = 0.003, p = 0.959$).

2.2.2.4.20 1899 G>A

The 1899 G>A is located at the 3'-UTR of *SLC16A3* gene. Representative sequencing electropherograms of AA and AB genotypes are as presented:



This SNP was only detected in the Chinese group of Singapore population. The observed frequencies of GG, GA and AA genotypes were 92 (96.8%), 3 (3.2%) and 0 (0%). No deviation from HWE was observed for this polymorphism ($X^2 = 0.024, p = 0.876$).

2.2.2.5 Linkage Disequilibrium (LD) Analysis

Linkage disequilibrium (LD) refers to association between tightly linked SNPs.

Alleles at different loci are sometimes found together more or less often than expected based on their frequencies. Two alleles are said to be in LD if their alleles are in statistical association.

In this study, the significance of the associations was assessed by Chi square test.

The LD for each of the pairs of segregating sites were quantified by the D' . The $D' = 1$ is known as complete LD, which indicates that the two SNPs have not been separated by recombination, recurrent mutation or gene conversion. Detailed pair-wise LD coefficients for SLC16A3 gene are presented in the **Tables 27 to 32**.

Table 27. Pair-wise linkage disequilibrium (D') coefficients between *SLC16A3* bi-allelic promoter (transcript variant 2) polymorphisms in ethnic Chinese population. The statistical significance of linkage disequilibrium was assessed by Chi-square test. Statistical significance was defined as $p < 0.05$. Site pairs that lack the power to detect significant association are indicated by ns. The number in bold represents LD value.

| POSITION | -139-1374 C>G | -139-1105 C>T | -139-804 C>T | -139 del (-727-795) | -139-477 G>T | -139-540 C>T | -139-45 G>T | -139-40 C>G |
|---------------------|------------------|------------------|-------------------------|-------------------------|-----------------|-----------------|-------------|-------------|
| -139-1374 c>g | -- | ns | ns | ns | ns | ns | ns | ns |
| -139-1105 c>t | -- | -- | <0.0001 0.767 | <0.0001 1.000 | ns | ns | ns | ns |
| -139-804 c>t | -- | -- | -- | <0.0001 0.749 | ns | ns | ns | ns |
| -139 del (-727-795) | -- | -- | -- | -- | ns | ns | ns | ns |
| -139-477 g>t | -- | -- | -- | -- | -- | ns | ns | ns |
| -139-540 c>t | -- | -- | -- | -- | -- | -- | ns | ns |
| -139-45 g>t | -- | -- | -- | -- | -- | -- | -- | ns |
| -139-40 c>g | -- | -- | -- | -- | -- | -- | -- | -- |

Table 28. Pair-wise linkage disequilibrium (D') coefficients between *SLC16A3* bi-allelic promoter (transcript variant 2) polymorphisms in ethnic Indian population. The statistical significance of linkage disequilibrium was assessed by Chi-square test. Statistical significance was defined as $p < 0.05$. Site pairs that lack the power to detect significant association are indicated by ns. The number in bold represents LD value.

| Position | -139-1281 G>A | -139-1105 C>T | -139-845 G>A | -139-804 C>T | -139 del (-727-795) | -139-518 G>A | -139-304 C>T | -139-246 C>G | -41 G>A | IVS +100 C>T |
|---------------------|------------------|------------------|-------------------------|-------------------------|-------------------------|-----------------|-----------------|-------------------------|---------|-----------------|
| -139-1281 G>A | -- | ns | <0.0001 0.921 | <0.0001 1.000 | ns | ns | ns | <0.0001 1.000 | ns | ns |
| -139-1105 C>T | -- | -- | ns | <0.0001 0.926 | <0.0001 0.947 | ns | ns | ns | ns | ns |
| -139-845 G>A | -- | -- | -- | 0.0008 1.000 | ns | ns | ns | <0.001 1.000 | ns | ns |
| -139-804 C>T | -- | -- | -- | -- | <0.001 0.891 | ns | ns | <0.001 1.000 | ns | ns |
| -139 del (-727-795) | -- | -- | -- | -- | -- | ns | ns | 0.0373 1.000 | ns | ns |
| -139-518 G>A | -- | -- | -- | -- | -- | -- | ns | ns | ns | ns |
| -139-304 C>T | -- | -- | -- | -- | -- | -- | -- | ns | ns | ns |
| -139-246 C>G | -- | -- | -- | -- | -- | -- | -- | -- | ns | ns |
| -41 G>A | -- | -- | -- | -- | -- | -- | -- | -- | -- | ns |
| IVS +100 C>T | -- | -- | -- | -- | -- | -- | -- | -- | -- | -- |

Table 29. Pair-wise linkage disequilibrium (D') coefficients between *SLC16A3* bi-allelic promoter (transcript variant 4) polymorphisms in ethnic Chinese population. The statistical significance of linkage disequilibrium was assessed by Chi-square test. Statistical significance was defined as $p < 0.05$. Site pairs that lack the power to detect significant association are indicated by ns. The number in bold represents LD value.

| Position | -118-554 A>T | -118-502 A>G | -118 del -(436-437) | -118-331 G>A | -118-249 C>T | -118-130 A>C | -118-115 G>A | -86 A > G | IVS1+21 G > C |
|--------------------|--------------|--------------|-------------------------|-------------------------|-------------------------|-------------------------|--------------|-------------------------|------------------|
| -118-554 A>T | -- | ns | ns | ns | ns | <0.0001 0.876 | ns | <0.0001 1.000 | ns |
| -118-502 A>G | -- | -- | <0.0001 0.823 | <0.0001 0.956 | <0.0001 0.652 | ns | ns | ns | ns |
| -118del- (436-437) | -- | -- | -- | <0.0001 0.816 | ns | ns | ns | ns | ns |
| -118-331 G>A | -- | -- | -- | -- | <0.0001 0.911 | ns | ns | ns | ns |
| -118-249 C>T | -- | -- | -- | -- | -- | ns | ns | ns | ns |
| -118-130 A>C | -- | -- | -- | -- | -- | -- | ns | <0.0001 0.816 | ns |
| -118-115 G>A | -- | -- | -- | -- | -- | -- | -- | ns | ns |
| -86 A>G | -- | -- | -- | -- | -- | -- | -- | -- | ns |
| IVS1 +21 G>C | -- | -- | -- | -- | -- | -- | -- | -- | -- |

Table 30. Pair-wise linkage disequilibrium (D') coefficients between *SLC16A3* bi-allelic promoter (transcript variant 4) polymorphisms in ethnic Indian population. The statistical significance of linkage disequilibrium was assessed by Chi-square test. Statistical significance was defined as $p < 0.05$. Site pairs that lack the power to detect significant association are indicated by ns. The number in bold represents LD value.

| Position | -118-1416 C>T | -118-1131 C>A | -118-554 A>T | -118-502 A>G | -118del- (436-437) | -118-331 G>A | -118-249 C>T | -118-130 A>C | -86 A>G |
|--------------------|------------------|------------------|-----------------|-----------------|-------------------------|-------------------------|-------------------------|-------------------------|-------------------------|
| -118-1416 C>T | -- | ns | ns | ns | ns | ns | ns | ns | ns |
| -118-1131 C>A | -- | -- | ns | ns | ns | ns | ns | ns | ns |
| -118-554 A>T | -- | -- | -- | ns | ns | 0.0097 1.000 | 0.0121 1.000 | <0.0001 0.952 | <0.0001 1.000 |
| -118-502 A>G | -- | -- | -- | -- | <0.0001 0.785 | <0.0001 1.000 | <0.0001 1.000 | 0.0215 1.000 | 0.0215 1.000 |
| -118del- (436-437) | -- | -- | -- | -- | -- | <0.0001 0.823 | <0.0001 0.780 | 0.0215 1.000 | 0.0215 1.000 |
| -118-331 G>A | -- | -- | -- | -- | -- | -- | <0.0001 0.919 | 0.0127 1.000 | 0.0126 1.000 |
| -118-249 C>T | -- | -- | -- | -- | -- | -- | -- | 0.0153 1.000 | 0.0153 1.000 |
| -118-130 A>C | -- | -- | -- | -- | -- | -- | -- | -- | <0.0001 0.952 |
| -86 A>G | -- | -- | -- | -- | -- | -- | -- | -- | -- |

Table 31. Pair-wise linkage disequilibrium (D') coefficients between *SLC16A3* bi-allelic coding region polymorphisms in ethnic Chinese population. The statistical significance of linkage disequilibrium was assessed by Chi-square test. Statistical significance was defined as $p < 0.05$. Site pairs that lack the power to detect significant association are indicated by ns. The number in bold represents LD value.

| Position | 44 C >T | IVS2-149 G>T | IVS2-114 C>T | IVS2-52 G>A | IVS3+29 G>A | 641C >T | 916G >A | 1176G>A | 1512C >T | 1594C >T | 1899G>A |
|---------------|---------|--------------|--------------|-------------|-------------------------|---------|---------|---------|----------|------------------------|-------------------------|
| 44 C >T | -- | ns | ns | ns | <0.0001 0.497 | ns | ns | ns | ns | ns | ns |
| IVS2 -149 G>T | -- | -- | ns | ns | ns | ns | ns | ns | ns | ns | ns |
| IVS2 -114 C>T | -- | -- | -- | ns | ns | ns | ns | ns | ns | ns | ns |
| IVS2 -52 G>A | -- | -- | -- | -- | ns | ns | ns | ns | ns | ns | ns |
| IVS3 + 29 G>A | -- | -- | -- | -- | -- | ns | ns | ns | ns | ns | <0.0001 0.495 |
| 641C >T | -- | -- | -- | -- | -- | -- | ns | ns | ns | 0.0362 0.472 | ns |
| 916G >A | -- | -- | -- | -- | -- | -- | -- | ns | ns | ns | ns |
| 1176G>A | -- | -- | -- | -- | -- | -- | -- | -- | ns | ns | ns |
| 1512C >T | -- | -- | -- | -- | -- | -- | -- | -- | -- | ns | ns |
| 1594C >T | -- | -- | -- | -- | -- | -- | -- | -- | -- | -- | ns |
| 1899G>A | -- | -- | -- | -- | -- | -- | -- | -- | -- | -- | -- |

Table 32. Pair-wise linkage disequilibrium (D') coefficients between *SLC16A3* bi-allelic coding region polymorphisms in ethnic Indian population. The statistical significance of linkage disequilibrium was assessed by Chi-square test. Statistical significance was defined as $p < 0.05$. Site pairs that lack the power to detect significant association are indicated by ns. The number in bold represents LD value.

| Position | 21C>T | 44C>T | 55G>A | 117C>T | IVS3+29 G>A | 574G>A | 609G>A | 641C>T | 831G>A | 1494C>T | 1594C>T | 1608C>T | 1713G>A |
|---------------|-------|-------|-------|--------|-------------------------|------------------------|--------|--------|--------|---------|-------------------------|---------|---------|
| 21 C>T | -- | ns | ns | ns | ns | ns | ns | ns | ns | ns | ns | ns | ns |
| 44 C>T | -- | -- | ns | ns | <0.0001 1.000 | 0.0045 0.481 | ns | ns | ns | ns | ns | ns | ns |
| 55 G>A | -- | -- | -- | ns | ns | ns | ns | ns | ns | ns | ns | ns | ns |
| 117 C>T | -- | -- | -- | -- | ns | ns | ns | ns | ns | ns | ns | ns | ns |
| IVS3 + 29 G>A | -- | -- | -- | -- | -- | 0.0045 0.481 | ns | ns | ns | ns | ns | ns | ns |
| 574 G>A | -- | -- | -- | -- | -- | -- | ns | ns | ns | ns | ns | ns | ns |
| 609 G>A | -- | -- | -- | -- | -- | -- | -- | ns | ns | ns | ns | ns | ns |
| 641 C>T | -- | -- | -- | -- | -- | -- | -- | -- | ns | ns | <0.0001 1.000 | ns | ns |
| 831 G>A | -- | -- | -- | -- | -- | -- | -- | -- | -- | ns | ns | ns | ns |
| 1494 C>T | -- | -- | -- | -- | -- | -- | -- | -- | -- | -- | ns | ns | ns |
| 1594 C>T | -- | -- | -- | -- | -- | -- | -- | -- | -- | -- | -- | ns | ns |
| 1608 C>T | -- | -- | -- | -- | -- | -- | -- | -- | -- | -- | -- | -- | ns |
| 1713 G>A | -- | -- | -- | -- | -- | -- | -- | -- | -- | -- | -- | -- | -- |

2.2.2.6 Haplotype Construction and Frequency Estimation

Haplotype structures were constructed in the promoter regions of transcript variant 2 and 4 of *SLC16A3* gene. The haplotype frequency was not performed in the coding region of *SLC16A3* due to the low prevalence of SNPs identified in this region (**Table 18**). Three commonest polymorphisms were detected in the promoter regions of both transcripts. These SNPs were input into SNPAnalyser to compute statistical calculation of haplotype estimation. The haplotypes and relative frequencies of the three commonest SNPs in the promoter of transcript variant 2 and 4 of *SLC16A3* gene are summarized in **Table 33 and 34**.

The six possible haplotypes with frequencies greater than 0.01 (1%) and accounting for approximately 99% of all chromosomes were estimated in the promoter of transcript variant 2 of MCT4. The frequency distributions between ethnic groups are presented graphically in **Figure 10**. Haplotypes 4 and 6 were not predicted in the Chinese population. In contrast, haplotype 5 was not predicted in Indians. The distribution of haplotypes 1, 2 and 4 are statistically significant difference in ethnic Chinese and Indian groups. Of the two ethnic groups, haplotype 5 is predicted to be least common in the Chinese population while haplotype 6 is the least common haplotype in Indians. The most common haplotype is haplotype 1. Haplotype 1 predicted to occur at a relatively high frequency in both ethnic groups, with an estimated frequency of 0.836 and 0.674 in Chinese and Indians, respectively.

In transcript variant 4 of *SLC16A3* gene, five promoter haplotypes were estimated from the population genotype data. The frequency distributions between ethnic

groups are presented graphically in **Figure 11**. All five promoter haplotypes were predicted in the Chinese population. In contrast, haplotype 3 and 5 were not estimated in Indians. The distribution of haplotype 1, 3, 4 and 5 are not statistically significant difference amongst Chinese and Indians. Haplotype 1 predicted to occur at a relatively high frequency in both ethnic groups, with an estimated frequency of 0.916 and 0.865 in Chinese and Indians, respectively.

Figure 10. Ethnic distribution of SLC16A3 haplotypes in the promoter region of transcript variant 2. The frequencies of six haplotypes identified in the ethnic Chinese and Indian of Singapore population. * $p < 0.05$, frequency distribution is statistically significant.

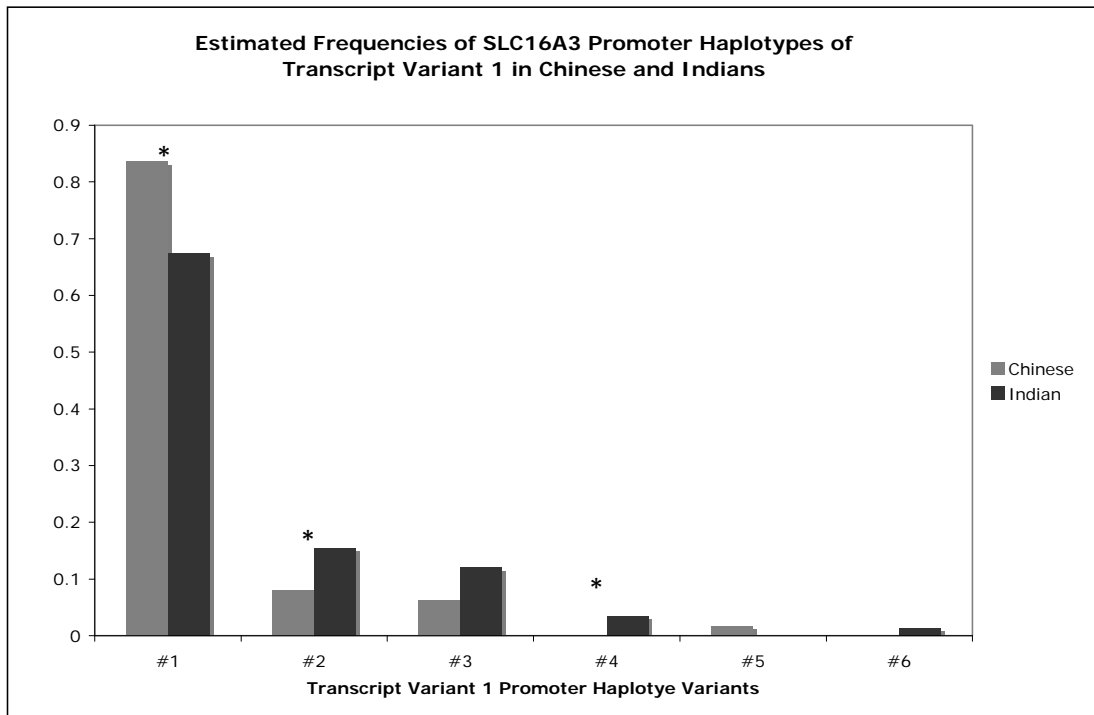


Figure 11. Ethnic distribution of SLC16A3 haplotypes in the promoter region of transcript variant 4. The frequencies of six haplotypes identified in the ethnic Chinese and Indian of Singapore population. * $p < 0.05$, frequency distribution is statistically significant.

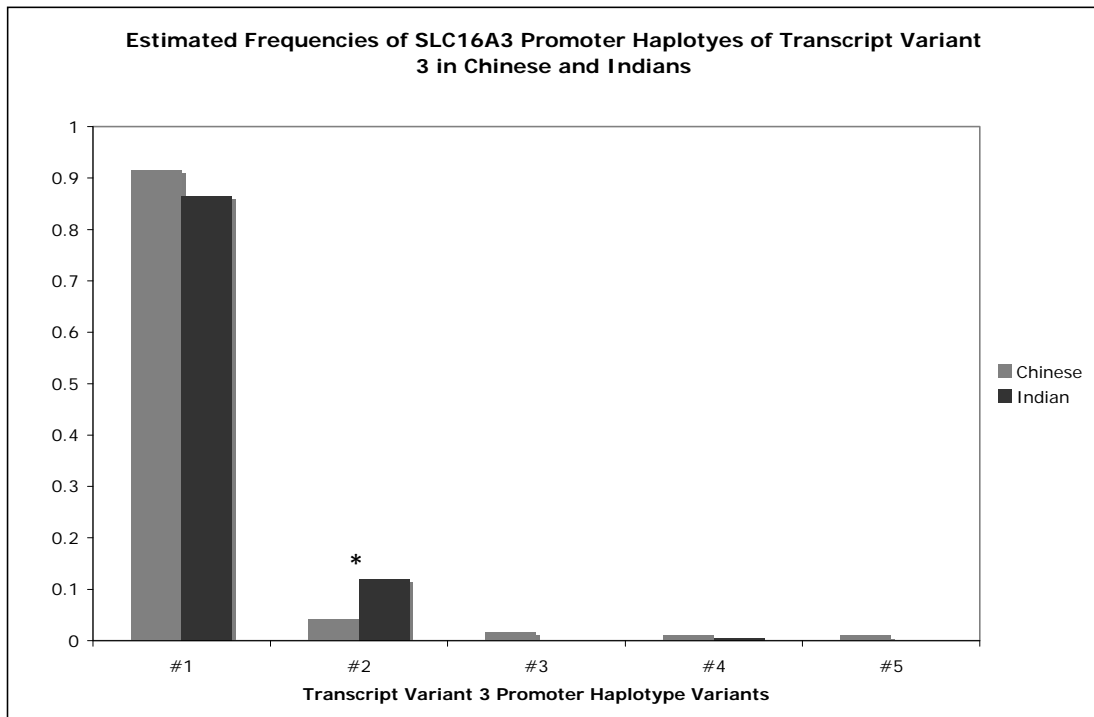


Table 33. Haplotype structure defined by 3 commonest SNPs in the SLC16A3 5'flanking promoter region of transcript variant 2 in Singapore population

| Haplotype No. | Polymorphisms | | | Estimated Haplotype Frequencies | | Chi sq value | p-value |
|---------------|-----------------|--------------|---------------------|---------------------------------|----------------|--------------|---------|
| | -139-1105 C > T | -139-804 C>T | -139 del (-727-795) | Chinese n = 190 | Indian n = 192 | | |
| 1 | T | T | Deletion | 0.836 | 0.674 | 14.01 | 0.000* |
| 2 | T | C | Deletion | 0.080 | 0.154 | 4.87 | 0.027* |
| 3 | C | C | Wildtype | 0.062 | 0.120 | 3.68 | 0.055 |
| 4 | T | C | Wildtype | 0.000 | 0.034 | 7.06 | 0.008* |
| 5 | C | T | Wildtype | 0.017 | 0.000 | | |
| 6 | T | T | Wildtype | 0.000 | 0.013 | | |
| | | | Total | 0.995 | 0.995 | | |

Haplotype structures were constructed and frequencies estimated using SNPAnalyser software. The haplotypes listed here accounts for 99.5% of all chromosomes. Observed frequencies for haplotypes 5 and 6 are too small to be considered for chi square statistical test of independence. * $p < 0.05$

Table 34. Haplotype structure defined by 3 commonest SNPs in the SLC16A3 5'flanking promoter region of transcript variant 4 in Singapore population

| Haplotype No. | Polymorphisms | | | Estimated Haplotype Frequencies | | Chi sq value | p-value |
|---------------|---------------|--------------|-----------|---------------------------------|----------------|--------------|---------|
| | -118-554 A>T | -118-130 A>C | -86 A > G | Chinese n = 190 | Indian n = 192 | | |
| 1 | T | C | G | 0.916 | 0.865 | 2.56 | 0.110 |
| 2 | A | A | A | 0.042 | 0.120 | 7.73 | 0.005* |
| 3 | T | C | A | 0.016 | 0.000 | | |
| 4 | T | A | G | 0.011 | 0.005 | | |
| 5 | T | A | A | 0.010 | 0.000 | | |
| | Total | | | 0.995 | 0.990 | | |

Haplotype structures were constructed and frequencies estimated using SNPAnalyser software. The haplotypes listed here accounts for > 99% of all chromosomes. Observed frequencies for haplotypes 3, 4 and 5 are too small to be considered for chi square statistical test of independence. * $p < 0.05$

2.3 DISCUSSION

Monocarboxylates such as L-lactate, pyruvate and acetate are important intermediaries in body energy metabolism. The anions of these monocarboxylates are highly charged and transported across the plasma membrane via human MCT1-4 in a proton-mediated manner. MCT1 is found in a great majority of tissues in all species studied and it is the only MCT isoform expressed on the plasma membrane of human erythrocyte. Human MCT4 is highly expressed in glycolytic tissues such as white skeletal muscle fibres, in which MCT4 may work as an efflux transporter to mediate the transport of lactate out into the interstitial. Given the current understanding of the roles of lactate as a central player in cellular and whole body metabolism, mutations in MCT1 and MCT4 have been hypothesized to affect normal L-lactate homeostasis leading to altered body energy metabolism and exercise intolerance. In fact, mutations in MCT1 have been associated with lactate transport deficiency in red blood cells and muscle tissues [171]. Therefore, one of the objectives of this study was to describe the single nucleotide polymorphisms in the *SLC16A1* and *SLC16A3* genes that may be present in the ethnic Chinese and Indian groups of the Singapore population. In the context of global genetic diversity, Singapore Chinese, the HapMap Han Chinese in Beijing and HapMap Japanese in Tokyo were virtually indistinguishable, while Singapore Malays were observed to be highly similar to the East Asian populations in general [204]. Singapore Indians, on the other hand, are genetically closer to the samples with European ancestries than to the East Asian samples from Human Genome Diversity Project (HGDP) [204]. Therefore, with cost and time constraints, only the ethnic Chinese and Indian groups were studied in this thesis.

2.3.1 Genetic Variations in the MCT1 (*SLC16A1*) Gene in the Chinese and Indian Population of Singapore

This study identified genetic variations in *SLC16A1* in the ethnic Chinese and Indian groups of the Singapore population (n = 191). The promoter, coding region and the exon-intron junctions of the *SLC16A1* gene encoding the MCT1 protein were screened for genetic variation in the study population by direct DNA sequencing. A total of 21 genetic variations of *SLC16A1*, including 14 novel ones, were found: 6 in the promoter region, 4 in the coding exons (3 nonsynonymous variations and 1 synonymous variation), 4 in the 5' untranslated region (5'UTR), 6 in the 3' untranslated region (3'UTR) and 1 in the intron (**Table 10**). The full review of reported allele frequencies in *SLC16A1* gene are summarized in **Table 35**. The locations of nonsynonymous SNPs detected in *SLC16A1* are presented in **Figure 6**.

SLC16A1 gene spans approximately 44 kb and is mapped onto chromosome band 1p13.2-p12 in humans [80]. MCT1 has 5 exons and 4 introns and is predicted to have 500 amino acids and 12 transmembrane spanning regions (**Fig. 6**) [70]. Of the three non-synonymous mutations detected, the 303 T>G (Ile101Met) and 1282 G>A (Val428Ile) are novel SNPs, while the 1470 T>A (Asp490Glu) variant was found to be a common polymorphism in this study. The 303 T>G (Ile101Met) was only detected in the Indian group of Singapore population. Based on putative protein topology, 303 T>G (Ile101Met) is located at TM3 of MCT1 protein. A substitution from nucleotide T to G at position 303 resulted in the conversion of amino acid isoleucine to methionine at position 101 of MCT1 protein. The Polyphen and SIFT sequence homology-based tools were used to predict the effects

on amino acid substitution on protein function based on sequence homology and the physical property of amino acid. Although both amino acids are nonpolar in nature, the 303 T>G (Ile101Met) variant was predicted to be probably damage by both programs. The physiological role of this polymorphism is still indeterminate.

The 1282 G>A (Val428Ile) was found as heterozygotic in four Chinese subjects. Based on putative protein topology, the 1282 G>A (Val428Ile) is located at the TM12 [70]. A substitution from G to A at position 1282 resulted in the conversion of amino acid valine to isoleucine at position 428 of MCT1 protein. Both amino acid residues are non-polar and thus this mutation is unlikely to affect the functions of the protein. This is consistent with the results obtained using the PolyPhen and SIFT programs which predicted this SNP to be benign and unlikely to have any significant effect on protein function.

Sequence analysis of MCT1 gene also revealed a common SNP, 1470 T>A (Asp490Glu). This SNP was previously reported by Merezhinskaya *et al* [172]. In this study, the allele frequencies of T and A are 34.7% and 65.3% for Chinese, and 42.6% and 57.3%, respectively. No ethnic difference in allele frequency is observed in our study population when analyzed with Chi square test of independence. Besides, the observed allele frequencies in our populations are similar to the observed allele frequencies in the Han Chinese, Japanese and Utah populations (**Table 35**). The glutamate residue at position 490 is located in the signal sequence (asp-x-glu; aa 488-490) for release from the endoplasmic reticulum when downstream from a tyr-x-x-φ motif (aa 445-448) [205]. As glutamic acid and aspartic acid are both acidic amino acids with similar physico-chemical properties,

it is likely that aspartate may be as effective as the preferred glutamate. This is consistent with the results obtained using PolyPhen and SIFT which predicted this SNP to be benign and unlikely to have any significant effect on the protein function. Although this SNP has been predicted to have no detrimental effect on transporter activity by bioinformatics tools, a 40% reduction of lactate transport rate has been identified in the erythrocytes of both individual homozygous and heterozygous for this polymorphic variant [172]. Recently, Cupeiro *et al.* has performed a pilot study to examine the influence of this SNP in high intensity exercise performance [206]. In this study, ten men aged 20-26 performed three controlled circuit training (CWT) sessions at 60%, 70% and 80% of the 15 repetition maximum (15RM), in non-consecutive days. The lactate measurements were performed immediately after each set had been completed. The carriers for MCT1 1470 T>A polymorphism showed higher lactate accumulation and higher maximal lactate concentration than non-carriers during the 80% CWT. The carriers of the 1470 T>A polymorphism seem to exhibit impaired functionality in MCT1, which would lead to impaired lactate transport into other cells for oxidation, thus resulted in the increased of blood lactate concentration [206].

Two reported non-synonymous SNPs, 973A>G (Val325Ile) and 979C>T (Ser327Pro) are not detected in the ethnic Chinese and Indian groups of Singapore population. The 973A>G (Val325Ile) variant was predicted to be benign by PolyPhen and SIFT programs and unlikely to have any significant effects on the protein function. The 979C>T (Ser327Pro) variant, however, may have detrimental effect on the transporter activity. Both Polyphen and SIFT algorithms predicted

that the amino acid substitution from serine to proline is intolerant and probably damaging.

A total of 10 genetic variations were found in the 5' flanking region of MCT1, of which -363-222 T>C, -363-289 T>G, -363-307 C>T, -363-855 T>C, -298 G>C, -297 A>C, del(-207-210)CAGA and -136 A>G are novel. Recently, the promoter region of MCT1 has been characterized [207]. Analysis of a 1.5 kb fragment (-1525/+213) of the MCT1 5'-flanking region, shows an absence of the classical TATA-Box element found in many eukaryotic promoters. Secondly, the sequence is GC-rich, with the 200-bp upstream and downstream of the transcription initiation site having a 72% of GC-content. Thirdly, the -70/+213 region of the promoter contains the essential *cis*-acting elements necessary for basal transcription of MCT1. Lastly, several putative transcription factor binding sites were identified using the MatInspector (Library version: Matrix Library 2.2) (**Fig. 5**). The GC-rich sequence is a characteristic of TATA-less promoters that usually contain stimulating protein 1 (Sp1) binding sites. These Sp1 binding sites interact with the GC-box and play crucial roles in start site selection [208, 209]. In this study, three Sp1 binding sites were detected within the GC-rich region of the transcription initiation site. As the -363-100 C>G mutation is located at the consensus sequence of the Sp1 binding site, it is likely to affect the transcription regulation of the MCT1 gene. The SNPInspector licensed software was used to identify transcription factor binding sites affected by these SNPs (**Table 13**). For each SNP, the transcription factor binding sites are either deleted or generated by the nucleotide exchange. However, the prediction of the effects of SNPs on the putative transcription factor binding based on computational bioinformatics tools can only

be speculative at this moment. The actual role of SNPs can only be clarified through functional assays. Nevertheless, this information may provide a framework for understanding the fundamental functions of putative transcriptional factor binding sites in regulating the transcriptional regulation of MCT1.

Table 35. Reported *SLC16A1* genetic polymorphism allele frequencies

| | SNP | dbSNP | Location | Chromosome Position | Amino acid change | Allele | Reported Allele Frequencies | | |
|----|--------------|-------------|----------|---------------------|-------------------|--------|-----------------------------|-----------------------------|--|
| 1 | 1325+603 A>G | rs114357382 | Promoter | 113500947 | | A G | 0.966 ^a 0.034 | | |
| 2 | 1325+313 C>G | rs74929506 | Promoter | 113500657 | | C G | 0.966 ^a 0.034 | | |
| 3 | 1325+61G>A | rs75737835 | Promoter | 113500405 | | G A | 0.966 ^a 0.034 | | |
| 4 | 919A>T | rs74111374 | Promoter | 113499938 | | A T | 0.720 ^a 0.280 | | |
| 5 | 811A>G | rs117282659 | Promoter | 113499830 | | A G | 0.975 ^b 0.025 | | |
| 6 | 757C>A | rs115748179 | Promoter | 113499776 | | C A | 0.966 ^a 0.034 | | |
| 7 | 431G>A | rs6699036 | Promoter | 113499450 | | G A | 0.983 ^a 0.017 | | |
| 8 | 301C>A | rs73000320 | Promoter | 113499320 | | C A | 0.966 ^a 0.034 | | |
| 9 | 221C>T | rs115304077 | Promoter | 113499240 | | C T | 0.966 ^a 0.034 | | |
| 10 | 56G>C | rs60844753 | Promoter | 113499075 | | G C | 0.075 ^b 0.925 | 0.023 ^c 0.977 | |
| 11 | 973A>G | rs116216229 | Exon | 113460055 | Ile325Val | A G | 0.975 ^a 0.025 | | |
| 12 | 979C>T | rs77373295 | Exon | 113460049 | Pro327Ser | C T | 0.922 ^a 0.008 | 0.980 ^d 0.020 | |

| | | | | | | | | | |
|----|----------|-------------|-------|-----------|-----------|--------|-----------------------------|-----------------------------|-----------------------------|
| 13 | 1002G>A | rs114731222 | Exon | 113460026 | Ala334Ala | G A | 0.975 ^a 0.025 | | |
| 14 | 1470T>A | rs1049434 | Exon | 113456546 | Asp490Glu | T A | 0.367 ^c 0.633 | 0.322 ^f 0.678 | 0.364 ^g 0.636 |
| 15 | *145T>G | rs11585690 | 3'UTR | 113456368 | | T G | 1.000 ^e 0.000 | 1.000 ^f 0.000 | 0.965 ^g 0.035 |
| 16 | *1414C>T | rs7169 | 3'UTR | 113455099 | | C T | 0.337 ^h 0.663 | 0.327 ⁱ 0.673 | 0.398 ^j 0.602 |

References:

- a HapMap Yoruba in Ibadan, Nigeria(YRI), n = 59
- b HapMap Han Chinese in Beijing, China + Japanese in Tokyo, Japan, n = 60
- c PA151258406 study population from Pharmacogenomics Knowledge base, n = 514
- d HapMap Yoruba in Ibadan, Nigeria(YRI), n = 25
- e HapMap Han Chinese in Beijing, China, n=45
- f HapMap Japanese in Tokyo, Japan, n=45
- g Hapmap Utah residents with Northern and Western European ancestry from the CEPH collection, n=59
- h HapMap Han Chinese in Beijing, China, n=43
- i HapMap Japanese in Tokyo, Japan, n=84
- j Hapmap Utah residents with Northern and Western European ancestry from the CEPH collection, n=113

2.3.2 Genetic Variations in the MCT4 (*SLC16A3*) Gene in the Chinese and Indian Population of Singapore

Sequencing analysis of *SLC16A3* gene from 191 Asian subjects (Chinese, n = 95; Indian, n = 96) resulted in the identification of 46 genetic variations, of which 33 are novel mutations (**Table 18** and **Table 19**). Of these variants, 22 are located in the promoter regions, 2 in the 5'-UTR, 10 in the coding exons (5 nonsynonymous and 5 synonymous variations), 6 in 3'-UTR and 6 in the intron. The full review of reported allele frequencies in *SLC16A3* gene are summarized in **Table 36**. The locations of nonsynonymous SNPs detected in *SLC16A3* are presented in **Figure 9**.

SLC16A3 gene spans approximately 11 kb and is mapped onto chromosome band 17q25.3 in human. According to NCBI, three transcripts variants have been described for this gene, of which all three transcripts have functional protein products (<http://www.ncbi.nlm.nih.gov/geo/9123>). The three transcript variants are created by alternative promoter usage and alternative splicing at the 5' end of the gene, therefore the protein products for all three transcript variants are identical. Sequence analysis of promoter regions revealed 14 and 10 polymorphisms in transcript variant 2 and 4 of MCT4 gene, respectively. We intended to screen all three promoter regions associates with the transcript variants of *SLC16A3* gene. However, due to some technical problems, we are unable to sequence the promoter region of transcript variant 3. Therefore, the genotype information of this region is not included in this thesis.

The MCT4 protein product is predicted to have 465 amino acids and 12 transmembrane spanning regions. Among the novel nonsynonymous variations, the

44C>T (Ala15Val) polymorphism is located at the intercellular N-terminal of MCT4 protein. It has been proposed that the two halves of the monocarboxylate molecule (TM helices 1-6 and 7-12) have different functional roles (**Fig. 9**). The N-terminal domains may be involved in energy coupling, maintenance structural integrity, and membrane insertion, whereas the C-terminus may be important for the determination of substrate specificity [73]. Therefore, this mutation is likely to affect transporter function in term of energy coupling. This is consistent with the results obtained using the PolyPhen and SIFT sequence homology-based tools. The 44C>T (Ala15Val) polymorphism was predicted to be probably damaging by both algorithms. This allele was found in both ethnic Chinese and Indian subjects with a frequency of 1.1% and 4.2%, respectively. No inter-ethnic difference in allele frequency is observed for this variant.

The 55G>A (Gly19Ser) variant is also located at the intercellular N-terminal of the molecule. This variant was only presented as heterozygotic in on Indian subject and was not found in Chinese population. Although PolyPhen program predicted that the amino acid substitution is benign, it was inconsistent with the results obtained using SIFT program that predicted this mutation was expected to be intolerant. Recently, Meredith and Christian have aligned all 14 members of human MCT protein sequences using the DIALIGN sequence alignment program. The 55G>A (Gly19Ser) is located at the consensus region of the molecule [70]. Therefore, a substitution of nonpolar amino acid glycine to hydrophilic serine may have significant effect on protein function. Similarly, both 574G>A (Val192Met) and 916G>A (Gly306Ser) variants have conflicting results between the SIFT and PolyPhen algorithms. The 574G>A (Val192Met) variant is located at the

transmembrane 6 of the MCT4 protein. This novel SNP was only present as heterozygotic in one Indian subject and was not found in Chinese population. A substitution from G to A at position 574 resulted in the conversion of amino acid valine to methionine at position 192 of MCT4 protein. Although both amino acid residues are non-polar, this variant has conflicting results between the SIFT and PolyPhen algorithms. PolyPhen program predicted that this substitution is benign while SIFT algorithm predicted this variant is intolerant.

The SIFT algorithm uses sequence homology among related genes and domain across species to predict the impact of all 20 possible amino acids at a given position. SIFT relies solely on sequence for prediction, therefore it has the potential to analyze a large amount of non-synonymous SNPs than tools that use structures [210],[211],[212],[213],[214]. PolyPhen, on the other hand, uses a set empirical rules based on sequence, phylogenetic, and structural information characterizing a particular variant [215],[216]. One of the possible explanations as to why PolyPhen and SIFT have conflicting results could be that PolyPhen incorporates structural information of the protein to determine if a genetic polymorphism may have effect on protein function [214].

The 916G>A (Gly306Ser) is a novel nonsynonymous variant that located at transmembrane 9 of MCT4 protein. This variant was found as heterozygotic in one Chinese. It was predicted by PolyPhen program that this substitution might not affect the transporter activity. However, SIFT program predicted that this substitution is intolerant and may affect transporter function. The 641C>T (Ser214Phe) variant is located at the large intracellular loop between

transmembrane segments 6 and 7. The polar serine is replaced by the non-polar phenylalanine. This is also in agreement that 641C>T (Ser214Phe) variant is located at the large intracellular loop between transmembrane 6 and 7, which is least conserved among family members. Thus, it is likely that substitution may not result in fundamental change.

The promoter regions of transcript variant 2 and 4 of *SLC16A3* gene were screened for genetic variants. In the promoter and 5'-UTR regions of transcript variant 2, a total of 14 genetic variations were found. Of which, 10 are novel variants. The SNP profiles for promoter region of transcript variant 2 were found to be varied between the Chinese and Indians. Out of the 14 SNP detected, 11 variants was only detected in either Chinese or Indian ethnic group. Besides, these SNPs are rare and present in low frequencies. Three common SNPs, namely -139-1105 C>T, -139-804 C>T and -139del(-727-795), were detected in both ethnic groups (**Table 18**).

Statistically significant inter-ethnic differences in allele frequency is observed in -139-804 C>T and -139del(-727-795) variants when analyzed with Chi square test of independence.

A total of 10 genetic variants were detected in the promoter region of transcript variant 4 of *SLC16A3* gene, of which four are novel variants (**Table 18**). Three common polymorphisms, namely -118-554 A>T, -118-130 A>C and -86 A>G were detected in the promoter and 5'UTR region of transcript variant 4.

Statistically significant inter-ethnic differences in allele frequency is observed in -118-554 A>T and -118-130 A>C variants when analyzed with Chi square test of independence.

The SNPInspector licensed software was used to identify transcription factor binding sites affected by polymorphisms (**Table 26**). For each SNP, the transcription factor binding sites are either deleted or generated by the nucleotide exchange. However, the prediction of the effects of SNPs on the putative transcription factor binding based on computational bioinformatics tools can only be speculative at this moment. The actual role of SNPs can only be clarified through functional assays.

Table 36. Reported SLC16A3 genetic polymorphism allele frequencies

| | SNP | dbSNP | Location | Chromosome Position | Amino acid change | Allele | Reported Allele Frequencies | | | |
|----|-----------|-------------|----------|---------------------|-------------------|--------|-----------------------------|-----------------------------|-----------------------------|--|
| 1 | 425288G>A | rs73999811 | Promoter | 80184337 | | G A | 0.907 ^b 0.093 | | | |
| 2 | 425517G>A | rs7215447 | Promoter | 80184566 | | G A | 0.775 ^a 0.225 | 0.534 ^b 0.466 | 0.955 ^h 0.045 | |
| 3 | 425534C>T | rs74989597 | Promoter | 80184583 | | C T | 0.983 ^a 0.017 | | | |
| 4 | 425699C>T | rs78765689 | Promoter | 80184748 | | C T | 0.967 ^a 0.033 | | | |
| 5 | 425728G>T | rs73999812 | Promoter | 80184777 | | G T | 0.898 ^b 0.102 | | | |
| 6 | 425963G>A | rs117548183 | Promoter | 80185012 | | G A | 0.975 ^a 0.025 | | | |
| 7 | 426139C>T | rs11077983 | Promoter | 80185188 | | C T | 0.102 ^b 0.898 | 0.333 ^a 0.667 | 0.085 ^h 0.942 | |
| 8 | 425288G>A | rs116429000 | Promoter | 80185273 | | C T | 0.949 ^b 0.051 | | | |
| 9 | 425517G>A | rs117995894 | Promoter | 80185448 | | G A | 0.967 ^a 0.033 | | | |
| 10 | 425534C>T | rs73999813 | Promoter | 80185979 | | G C | 0.958 ^b 0.042 | | | |
| 11 | 425699C>T | rs116935257 | Promoter | 80185816 | | G T | 0.983 ^d 0.017 | | | |
| 12 | 425728G>T | rs114201274 | Promoter | 80185958 | | C T | 0.983 ^b 0.017 | | | |

| | | | | | | | | | | |
|----|-----------|-------------|----------|----------|-----------|--------|-----------------------------|-----------------------------|-----------------------------|-----------------------------|
| 13 | 425963G>A | rs114967601 | Promoter | 80186013 | | A C | 0.975 ^b 0.025 | | | |
| 14 | 426139C>T | rs75888222 | Promoter | 80186047 | | C G | 0.967 ^a 0.033 | | | |
| 15 | 425288G>A | rs112712439 | 5'UTR | 80193882 | | G A | 0.932 ^b 0.068 | | | |
| 16 | 425517G>A | rs117720229 | Exon | 80193953 | Ala23Ala | C G | 0.983 ^a 0.017 | | | |
| 17 | 425534C>T | rs114195476 | Exon | 80195317 | Arg224Gln | G A | 0.983 ^b 0.017 | | | |
| 18 | 425699C>T | rs79525659 | Exon | 80195339 | Tyr231Tyr | C T | 0.966 ^b 0.034 | | | |
| 19 | 1308G>A | rs61730223 | Exon | 80196762 | Ser436Ser | G A | 0.958 ^b 0.042 | 0.974 ^c 0.026 | | |
| 20 | 25C>T | rs114517919 | 3'UTR | 80196877 | | C T | 0.915 ^b 0.085 | | | |
| 21 | 114C>T | rs78825758 | 3'UTR | 80196966 | | C T | 0.992 ^d 0.008 | | | |
| 22 | 196C>T | rs116904469 | 3'UTR | 80197048 | | C T | 0.950 ^d 0.05 | | | |
| 23 | 438C>T | rs9916408 | 3'UTR | 80197290 | | C T | 0.915 ^b 0.085 | 1.000 ^e 0.000 | 1.000 ^f 0.000 | 1.000 ^g 0.000 |
| 24 | 497G>A | rs1131633 | 3'UTR | 80197349 | | G A | 0.746 ^b 0.254 | 1.000 ^e 0.000 | 1.000 ^f 0.000 | 1.000 ^g 0.000 |

References:

- a Hapmap Utah residents with Northern and Western European ancestry from the CEPH collection, n=60
b HapMap Yoruba in Ibadan, Nigeria(YRI), n = 59
c Coriell Apparently Healthy Collection AGI_ASP_population, n=38

- d HapMap Han Chinese in Beijing, China + Japanese in Tokyo, Japan, n = 60
- e HapMap Han Chinese in Beijing, China, n=41
- f HapMap Japanese in Tokyo, Japan, n=41
- g Hapmap Utah residents with Northern and Western European ancestry from the CEPH collection, n=57
- h HapMap Han Chinese in Beijing, China, n=45

CHAPTER 3

THE INHIBITORY EFFECTS OF PHARMACEUTICAL AGENTS AND

PHYTOCHEMICAL COMPOUNDS ON

HUMAN MONOCARBOXYLATE TRANSPORTER 1

This project has been submitted for publication under manuscript entitled:

“The Inhibitory Effects of Pharmaceutical Agents and Phytochemical Compounds on Human Monocarboxylate Transporter 1.”

OVERVIEW

The monocarboxylate transporter 1 (MCT1) has been thought to be responsible for the transportation of L-lactate across the human erythrocyte plasma membrane. According to the lactate shuttle hypothesis, lactate formation and its subsequent distribution throughout the body is a major mechanism whereby the coordination of intermediary metabolism in different tissues, and cells within those tissues, can be accomplished. During exercise, lactate and protons move out from exercising muscles and enter the plasma. From plasma, lactate is further transported into erythrocytes through MCT1. MCT1, the only MCT isoform found in the human erythrocyte, accounts for 80-90% of lactate transport. This study uses an erythrocyte model to characterize the kinetics of MCT1 mediated lactate transport and shows that MCT1 is a low affinity high capacity ($K_m = 123.9 \pm 24.6$ mM; $V_{max} = 12079.0 \pm 722.3$ nmol/mL of RBCs/min) process for the transport of lactate. Various drugs and dietary compounds interact with human erythrocytic monocarboxylate transporter 1. Several pharmacological agents and dietary compounds were screened for their inhibitory effects on MCT1 activity. Of these, diflunisal, diclofenac, mefenamic acid, meclofenamic acid, tolfenamic acid, luteolin, etodalac, phloretin and morin were the most potent with IC_{50} values of 40.24 ± 1.10 , 1.33 ± 1.17 , 11.83 ± 1.24 , 9.68 ± 1.10 , 5.95 ± 1.12 , 2.71 ± 1.28 , 13.30 ± 1.06 , 47.98 ± 1.11 and 44.53 ± 1.08 μ M, respectively.

3.1 MATERIALS AND METHODS

3.1.1 Materials

Sodium L-lactate, diflunisal, diclofenac, sulindac, indomethacin, etodolac, ibuprofen, naproxen, ketoprofen, mefenamic acid, meclofenamic acid, flufenamic acid, tolfenamic acid, piroxicam, luteolin, morin, naringin, phloretin, silibinin, caffeine, capsaicin and α -cyano-4-hydroxycinnamic acid were purchased from Sigma Chemical Co. (St Louis, MO, USA). [^{14}C]-L-lactate was purchased from PerkinElmer Inc. (Waltham, MA, USA). Cerivastatin, rosuvastatin, pravastatin and simvastatin were kindly donated by AstraZeneca (London, UK).

3.1.2 RED BLOOD CELLS (RBCS) LACTATE INFLUX ASSAY

3.1.2.1 Subjects

A total of 4 subjects participated in this study. All subjects had been recruited previously in accordance with requirements (Institutional Review Board, National University Hospital, Singapore). The mean age is 30 ± 2.5 (28 to 33). The male: female sex ratio is 1:3. All DNA samples were rendered anonymous by removing links with specific individual information, i.e., any ID, name, or address.

3.1.2.2 Preparation of RBCs for Lactate Influx Assay

Techniques for RBC preparation and lactate influx measurement were adopted from previously published methods [72, 107, 162, 164]. Five milliliters of venous blood were drawn from each subject into heparinized vacutainers. An initial hematocrit (Hct) and hemoglobin concentration were determined for all blood samples. Three milliliters of blood sample were transferred to a 50 ml conical tube. The remaining portion of the blood sample was refrigerated at 4°C and saved for

repeat measurements if required. The RBCs were isolated by centrifugation at room temperature (25°C, 10 min, 2000g). The plasma and buffy coat were removed by aspiration, leaving only the RBC pellet. The pellet was mixed by inversion with 30 volumes of chloride buffer (150 mM NaCl, 10 mM Na-tricine, pH 8.0 at 37°C, osmolality ~ 315 mosmol/kg H₂O) and incubation in water bath for 30 min at 37°C. This step was to ensure removal of endogenous lactate [102]. At the end of the incubation, the RBCs were sedimented at room temperature (25°C, 10 min, 2000g) and the supernatant was removed by aspiration. The cell pellet was then washed two times. For each washing, four volumes of chloride buffer were added to the cell pellets, the pellet was mixed by inversion and then centrifuged (25°C, 10 min, 2000g). The supernatant was removed after each wash. Lactate depletion from the RBCs (~0.20 mM in 30% hematocrit solution) was confirmed by analysis via the spectrophotometric technique (BioVison; MV, California). After the final wash, the RBC pellet was suspended in HEPES buffer (90 mM NaCl, 50 mM HEPES, pH 7.4, 37°C, osmolality ~267 mosmol/kgH₂O) equivalent to a 30% hematocrit (packed cell volume) to obtain the stock cell solutions for influx measurements. This suspension was divided into two aliquots, each containing one milliliter. One of the two stock cell suspensions contained no lactate transport inhibitors. Five millimolar α -cyano-4-hydroxycinnamic acid (CHC) was added to the second stock cell suspension to inhibit the MCT1-mediated pathway. The two aliquots were incubated in a water bath for 30 min at 37°C, and Hct was determined in a sample of each stock cell suspension.

3.1.2.3 Total Lactate Influx

A 25 µl sample of stock cell solution was incubated in 75 µl of HEPES influx buffer for 20 s at 37°C. The HEPES buffer containing [¹⁴C]-lactate (0.2 µCi/ml) at thirteen unlabeled [La] values of 1.2, 3.7, 12.3, 37.0, 123.3, 370.0, 616.7 and 986.7 mM. All HEPES influx buffers were adjusted to a pH 7.4. Because of dilution with the stock cell solution, the actual final [La] values were 1, 3, 10, 30, 100, 300, 500 and 800 mM, respectively. The incubation was stopped with 2 ml of ice-cold stop solution [150 mM NaCl, 10 mM MES, pH 6.5] and tubes were immediately iced. The sample was spun by centrifugation (4°C, 10 min, 2000 g) and was washed twice to eliminate extracellular radioactivity. After the final wash, the RBC pellet was lysed and deproteinized with 0.5 ml of 4.2% perchloric acid followed by centrifugation of the sample (4°C, 10 min, 2000 g). Finally, 0.4 ml of the supernatant was pipetted into scintillation vials containing 5 ml of scintillation liquid (Amersham Bioscience; Amersham, UK) and the radioactivity of the supernatant was measured with a liquid scintillation counter (Beckman Coulter, Kraemer Boulevard, USA). All measurements were made in triplicate.

3.1.2.4 Time-dependent Total Lactate Influx

A 25 µl sample of stock cell solution was incubated in 75 µl of HEPES influx buffer containing [¹⁴C]-lactate at three unlabeled [La] values of 5, 50 and 100 mM. Two milliliters of ice-cold stop solution were added to each tube to stop influx at 10, 20, 30, 40, 50, 60, and 120 s. A time-course curve was drafted by plotting lactate influx against time of influx. The time at which lactate influx rate vs. time became nonlinear was determined by regression analysis. A single time point well

within the linear portion of the lactate influx vs. time curve was selected for subsequent lactate influx measurement.

3.1.2.5 MCT1-mediated Lactate Influx

The cells were suspended in HEPES containing CHC to block the MCT1 pathway.

The samples were treated exactly as for the total lactate influx assay.

3.1.2.6 Calculation of Lactate Influx

To express the data as influx of lactate per milliliter of cells, the 25 μ l sample of stock solution was multiplied by its hematocrit fraction (0.30) to obtain a packed cell volume. The lactate influx per microliter is then mathematically converted to a per milliliter value. Lactate influx through MCT1 transport system was estimated as follows. The difference between the uninhibited flux and the CHC-inhibited flux was taken to estimate the flux through MCT1. Because CHC is not specific to the MCT only, this value somewhat overestimates the role of the MCT1.

3.1.2.7 Data Analysis

For kinetic studies, the Michaelis-Menten constant (K_m) and maximum uptake rate (V_{max}) of L-lactic acid were estimated using GraphPad Prism 5 software. IC_{50} is defined as the inhibitor concentration to achieve 50% inhibition on the uptake of L-lactate. The IC_{50} value was determined from the non-linear regression of a dose-response curve using GraphPad Prism 5 software.

3.1.2.8 Statistical Analysis

Unless otherwise indicated, all data are expressed as mean \pm SEM. Student's *t*-test was used to determine the significance of differences between two group means.

Statistical significance among means of more than two groups was determined by one-way analysis of variance (ANOVA). Statistical significance was defined as

$P < 0.05$.

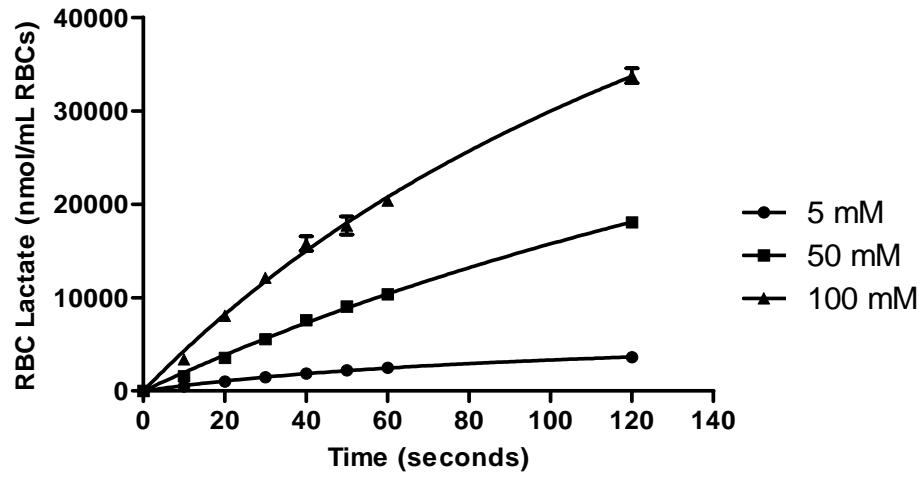
3.2 RESULTS

3.2.1 Time dependent Lactate Influx

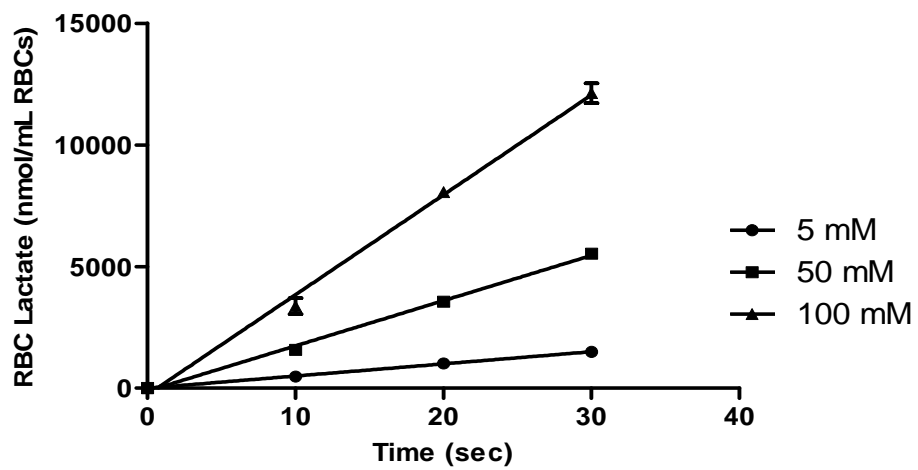
Figure 12a shows the uptake of L-lactate at three [La] values of 5, 50 and 100 mM. The reactions were stopped at 10, 20, 30, 40, 50, 60, and 120 s. The time at which lactate influx rate vs. time became nonlinear was determined by regression analysis. A single time point well within the linear portion of the lactate influx vs. time curve was selected for subsequent lactate influx measurement. Based on regression analysis time course of total lactate influx is linear up to 30 s at 5, 50 and 100 mM (**Figure 12b**). Therefore, 20 s was selected for subsequent lactate influx determination.

Figure 12. Time course experiment depicting total lactate influx in nanomoles/milliliter of RBCs into human red blood cells (RBCs) at 5, 50 and 100 mM lactate concentration (a). Based on regression analysis time course of total lactate influx is linear up to 30 s (b).

(a)



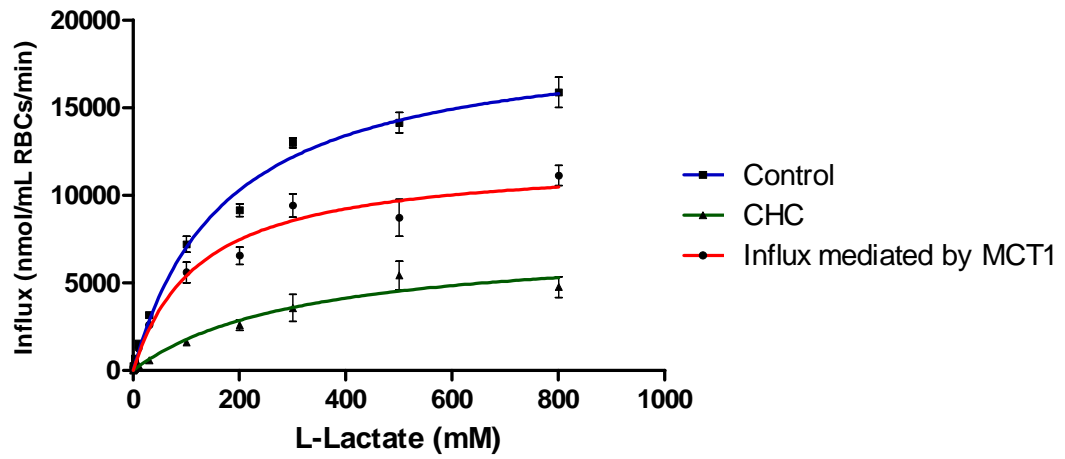
(b)



3.2.2 Human Erythrocyte Lactate Transport Activity

The effect of lactate concentration on the rate of influx is shown in **Fig. 13**. Total L-lactate influx into erythrocytes increased with increasing [La] values, and saturated at high lactate concentration. The apparent K_m and V_{max} for total lactate uptake were 174.0 ± 19.4 mM and 19228.0 ± 740.0 nmol/mL of RBCs/min, respectively. MCT1-mediated lactate influx was estimated by subtracting the total lactate influx from the uptake in the presence of CHC at various substrate concentrations. The apparent K_m and V_{max} for MCT1-mediated lactate influx were 123.9 ± 24.6 mM and 12079.0 ± 722.3 nmol/mL of RBCs/min, respectively.

Figure 13. Effect of lactate concentration and MCT inhibitor on the lactate influx into RBCs. Lactate influx was measured at eight external lactate concentration at 37 °C for 20 sec, in the presence or absence of CHC. Total lactate influx (blue) minus influx in the CHC-treated cells (green) represents influx via the monocarboxylate pathway (red).



3.2.3 Inhibitory Effects of Phytochemical and Pharmacological Agents on L-lactate Influx on Human Erythrocyte

3.2.3.1 The inhibitory effects of various compounds on L-lactate uptake

To investigate the effects of dietary and pharmacological compounds on L-lactate uptake, the uptakes of 100 mM of L-lactate were measured in the absence (control) or presence of 50 and 100 μ M of unlabeled test compounds (**Table 37**). L-lactate influx was significantly inhibited by several compounds tested in this study, namely diflunisal, diclofenac, mefenamic acid, meclofenamic acid, flufenami[102]c acid, tolfenamic acid, luteolin, morin, and phloretin. On the other hand, the inhibitory effects of pravastatin, rosuvastatin, simvastatin, naringin, capsaicin, coumorin, nicotine, salicylate and valproate on L-lactate influx were weak.

3.2.3.2 The Inhibitor Potencies of Selected Compounds

Several compounds exhibited inhibitory effects on the uptake of L-lactate (**Table 37**). The inhibitory potencies of these compounds were examined by determined the IC_{50} by making measurements over a broad range of inhibitor concentrations with substrate concentration fixed at 5 mM (**Fig.14**). The IC_{50} values of tested compounds was summarized in **Table 38**, of which diflunisal, diclofenac, mefenamic acid, meclofenamic acid, flufenamic acid, tolfenamic acid, etodalac, luteolin, phloretin and morin exhibited a strong inhibition effect on the uptake of L-lactate with an IC_{50} value of 2 to 40 μ M. On the other hand, the inhibitory effects of indomethacin, cerivastatin, rosuvastatin were weaker (**Table 38**).

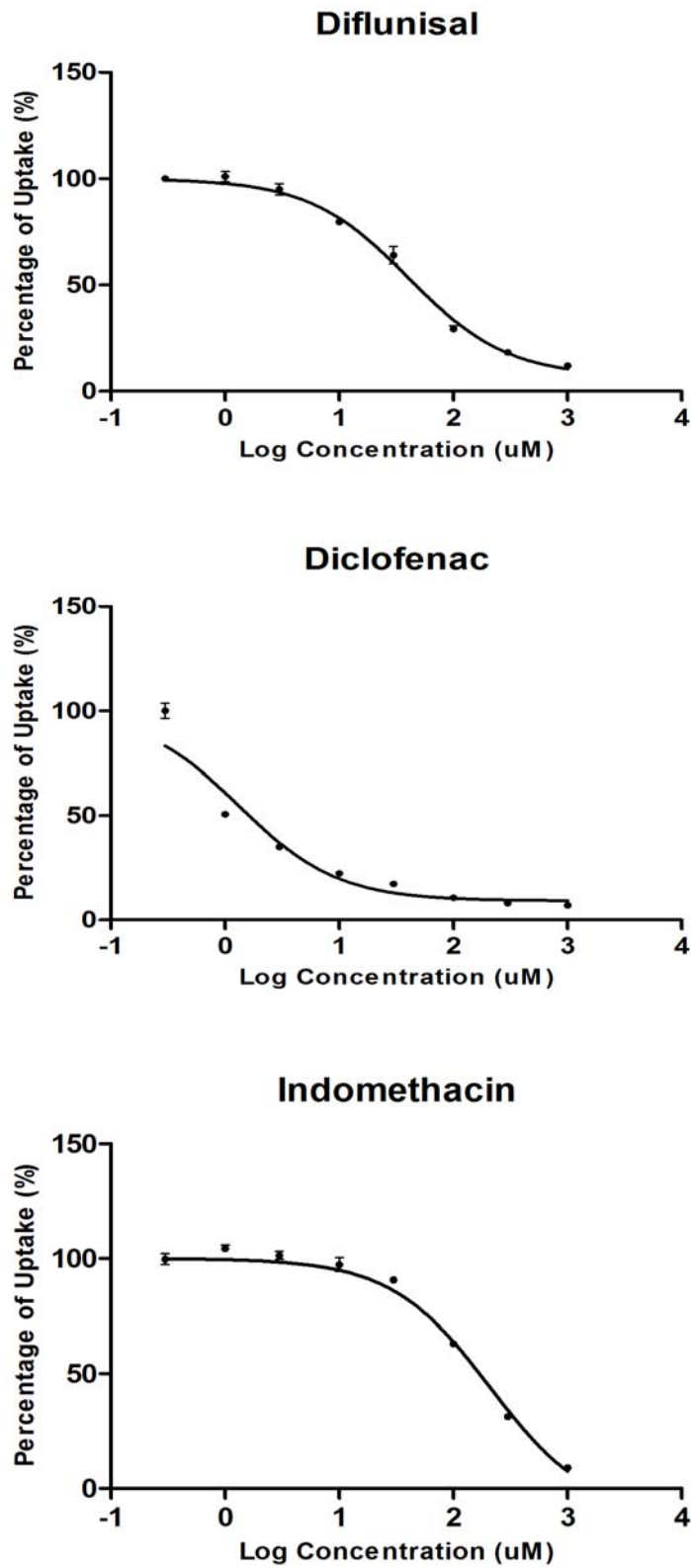
Table 37. The inhibitory effects of various compounds on the uptake of L-lactate in human erythrocytes. The uptakes of 100 mM of L-lactate were measured in the absence (control) or presence of 50 and 100 μ M of unlabeled test compounds.

* $p < 0.05$, ** $p < 0.01$, and *** $p < 0.001$; ns = not statistically significant

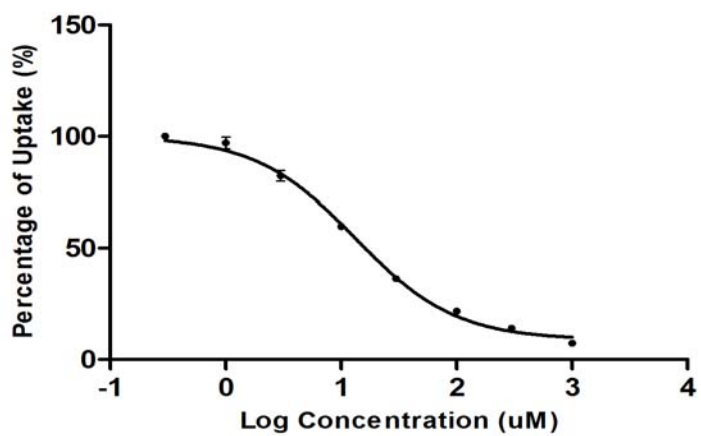
| Compounds | 50 μ M (% Control) | 100 μ M (% Control) |
|-----------------------|------------------------|-------------------------|
| NSAIDs | | |
| Diflunisal | 35.91 \pm 2.13 ** | 23.87 \pm 1.46 *** |
| Diclofenac | 33.52 \pm 2.41 ** | 28.77 \pm 1.21 ** |
| Sulindac | 80.89 \pm 2.77 * | 71.86 \pm 5.19 * |
| Indomethacin | 62.26 \pm 0.61 ** | 43.61 \pm 2.00 ** |
| Etodalac | 60.67 \pm 2.40 ** | 51.29 \pm 1.57 ** |
| Ibuprofen | 63.18 \pm 0.87 ** | 67.77 \pm 3.08 * |
| Naproxen | 73.71 \pm 6.97 * | 62.56 \pm 1.84 ** |
| Ketoprofen | 75.97 \pm 3.59 * | 70.92 \pm 2.49 * |
| Mefenamic acid | 26.38 \pm 2.72 ** | 17.20 \pm 6.02 ** |
| Meclofenamic acid | 18.15 \pm 1.19 ** | 12.68 \pm 2.35 ** |
| Flufenamic acid | 30.05 \pm 2.40 ** | 18.15 \pm 1.82 ** |
| Tolfenamic acid | 23.44 \pm 2.04 ** | 13.18 \pm 0.45 ** |
| Piroxicam | 72.9 \pm 2.12 ** | 58.86 \pm 1.35 ** |
| Statins | | |
| Cerivastatin | 71.66 \pm 0.59 ** | 59.74 \pm 1.42 *** |
| Pravastatin | 107.74 \pm 3.57 ns | 103.51 \pm 1.40 ns |
| Rosuvastatin | 89.34 \pm 4.53 ns | 75.04 \pm 1.92 ** |
| Simvastatin | 95.60 \pm 4.34 ns | 91.22 \pm 4.99 ns |
| Phytochemicals | | |
| Luteolin | 53.26 \pm 2.05 ** | 47.77 \pm 4.97 * |
| Morin | 72.79 \pm 0.79 ** | 45.02 \pm 3.42 ** |
| Naringin | 94.29 \pm 1.49 ns | 93.34 \pm 2.31** |
| Phloretin | 65.41 \pm 4.40 * | 47.74 \pm 2.68 ** |
| Silibinin | 77.87 \pm 1.44 * | 79.34 \pm 1.55 * |
| Caffeine | 86.83 \pm 2.85 ns | 80.68 \pm 3.78 ns |
| Capsaicin | 56.61 \pm 8.31 ns | 62.54 \pm 2.61 * |
| Coumorin | 94.94 \pm 6.66 ns | 92.63 \pm 0.16 ns |
| Nicotine | 82.65 \pm 10.30 ns | 80.77 \pm 5.38 ns |
| Others | | |
| Salicylate | 111.96 \pm 3.88 ns | 105.97 \pm 3.52 ns |
| Valproate | 100.89 \pm 0.94 ns | 107.72 \pm 1.65 ns |
| Probenecid | 60.92 \pm 4.47 * | 62.53 \pm 3.93 * |

Figure 14. Inhibitory effects of NSAIDs (a) statins (b) and phytochemicals (c) on L-lactate (5 mM) uptake by human erythrocytes

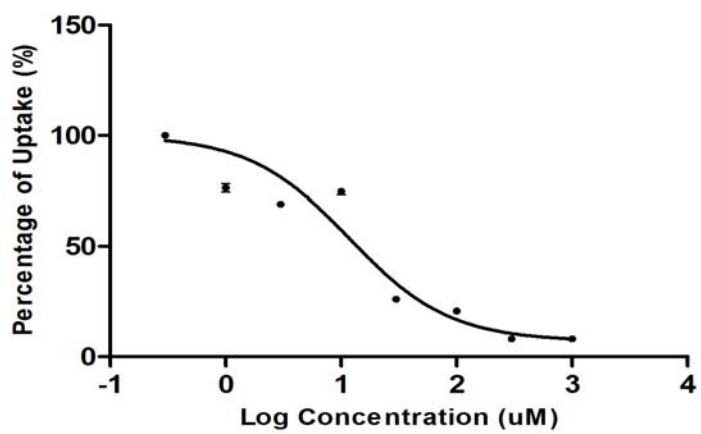
(a)



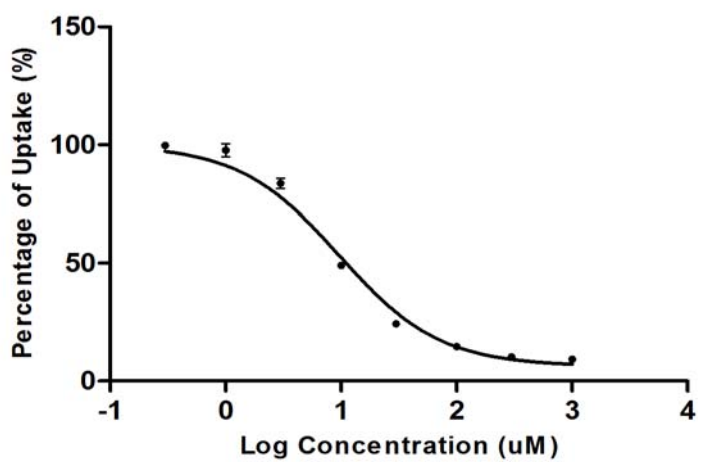
Etodalac



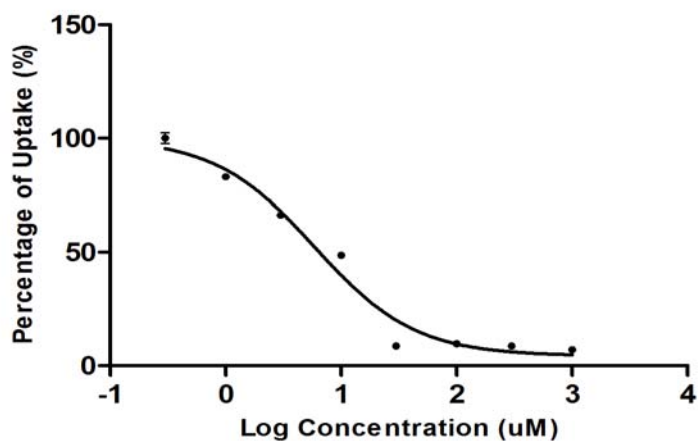
Mefenamic acid



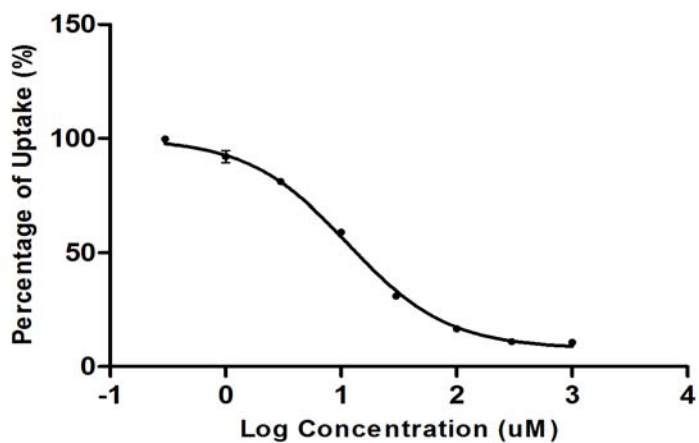
Meclofenamic acid



Tolfenamic acid

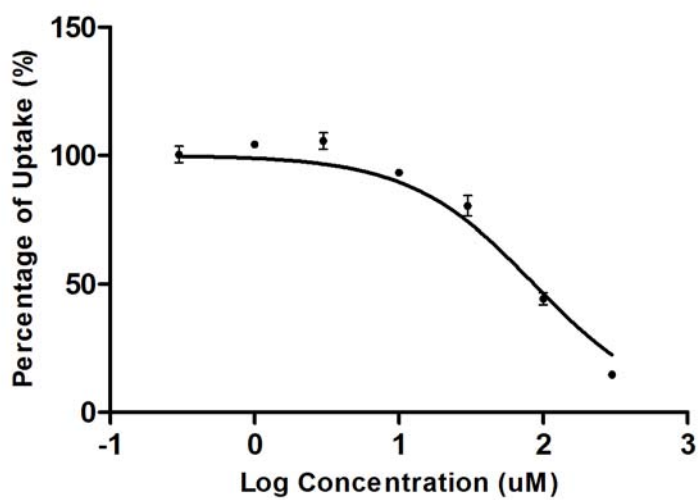


Flufenamic acid

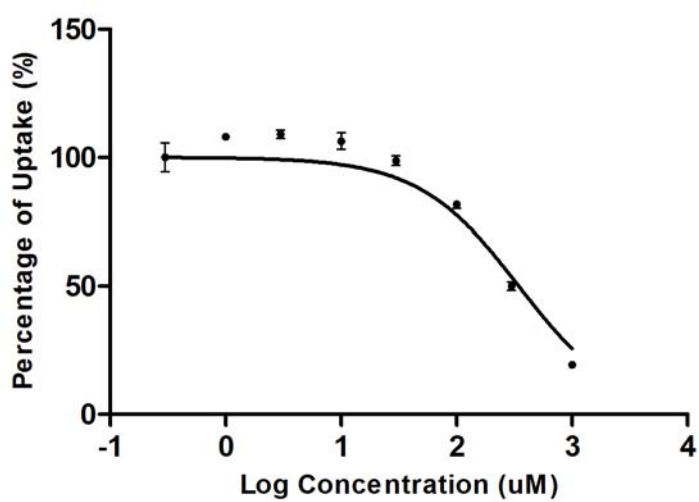


(b)

Cerivastatin



Rosuvastatin



(c)

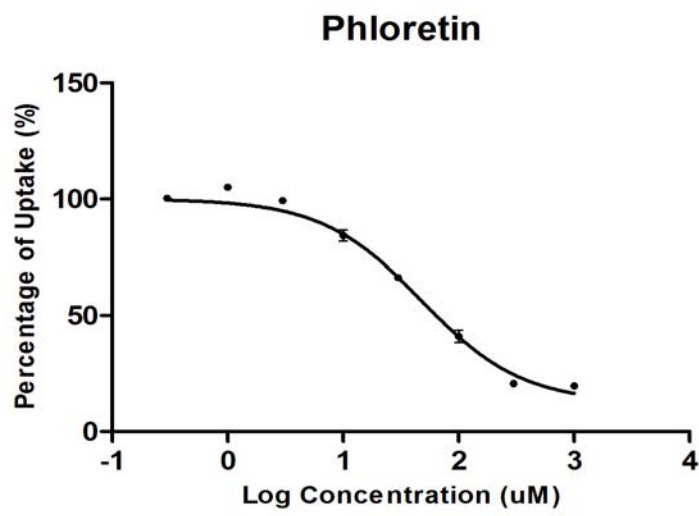
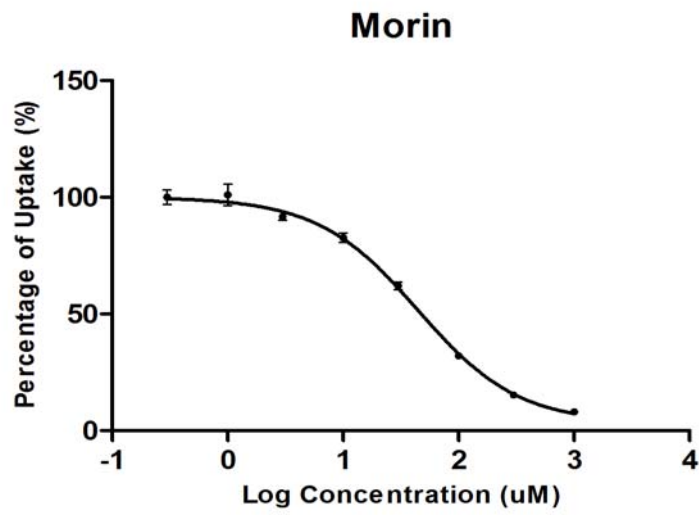
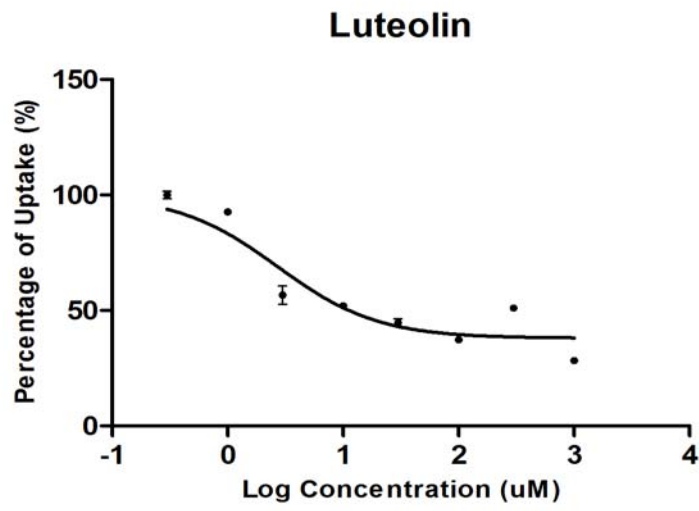


Table 38. The IC_{50} values of tested compounds on the uptake of L-lactate (5 mM) by human erythrocytes

| Compounds | IC_{50} values (μ M) |
|-----------------------|-----------------------------|
| NSAIDs | |
| Diflunisal | 40.24 ± 1.10 |
| Diclofenac | 1.33 ± 1.17 |
| Indomethacin | 210.0 ± 1.11 |
| Etodalac | 13.30 ± 1.06 |
| Mefenamic acid | 11.83 ± 1.24 |
| Meclofenamic acid | 9.68 ± 1.10 |
| Flufenamic acid | 11.42 ± 1.05 |
| Tolfenamic acid | 5.95 ± 1.12 |
| Statins | |
| Cerivastatin | 86.58 ± 1.28 |
| Rosuvastatin | 345.6 ± 1.26 |
| Phytochemicals | |
| Luteolin | 2.71 ± 1.28 |
| Morin | 44.53 ± 1.08 |
| Phloretin | 47.98 ± 1.11 |

3.2.4 Graphic and Software Determination of Inhibitor Type

The double reciprocal, or Lineweaver-Burk, plot is the most straightforward means of diagnosing inhibitor modality. To diagnose the inhibitor type, the initial velocity as a function of substrate concentration at several fixed concentrations of the inhibitor of interest was measured. To select the inhibitor concentrations, first measured the effect of a broad range of inhibitors concentrations with substrate concentration fixed at the K_m for MCT1-mediated L-lactate influx. From these results, the inhibitor concentrations that yielded between 30 and 75% inhibition were chosen. With the fixed inhibitor concentrations chosen, plot the data in terms of velocity as a function of substrate concentration for each inhibitor concentration. Finally, the reciprocal of initial velocity is plotted as a function of the reciprocal of substrate concentrations.

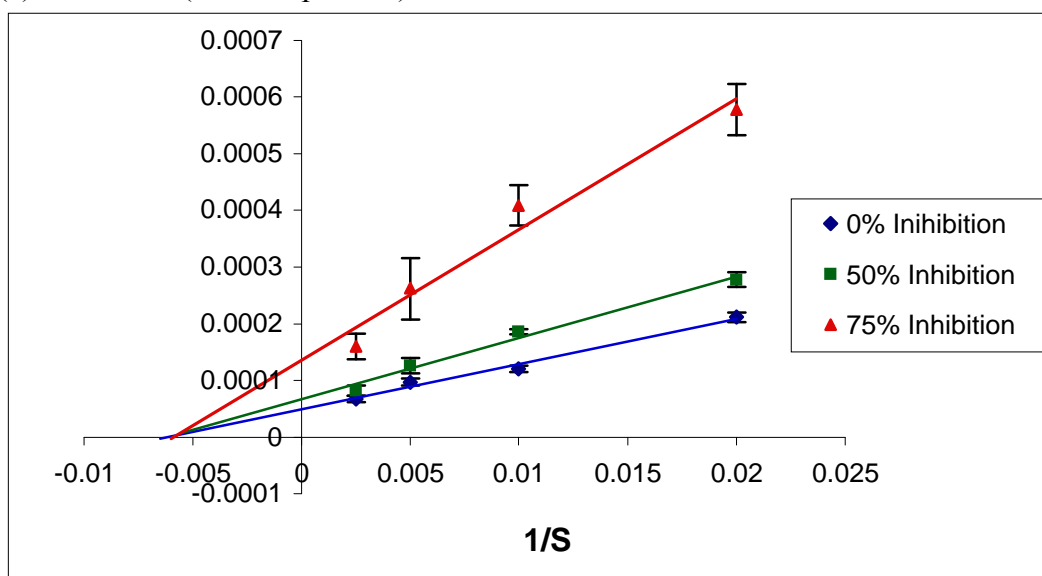
The Lineweaver-Burk double-reciprocal plots of the selected inhibitors are presented in **Figure 15**, of which diclofenac, etodalac, mefenamic acid, meclofenamic acid, flufenamic acid, tolfenamic acid, cerivastatin and luteolin are competitive inhibitors. Diflunisal, on the other hand, inhibits MCT1-mediated lactate uptake in a noncompetitive manner. The K_i values of selected inhibitors are summarized in **Table 39**.

The inhibitor modality of the tested compounds was verified using the mixed-model inhibition model of GraphPad Prism 5 software (**Table 40**). The mixed model is a general equation that includes competitive, uncompetitive and noncompetitive inhibition as special cases. The model has one additional parameter, Alpha, that diagnoses the mechanism of inhibition. The value of Alpha

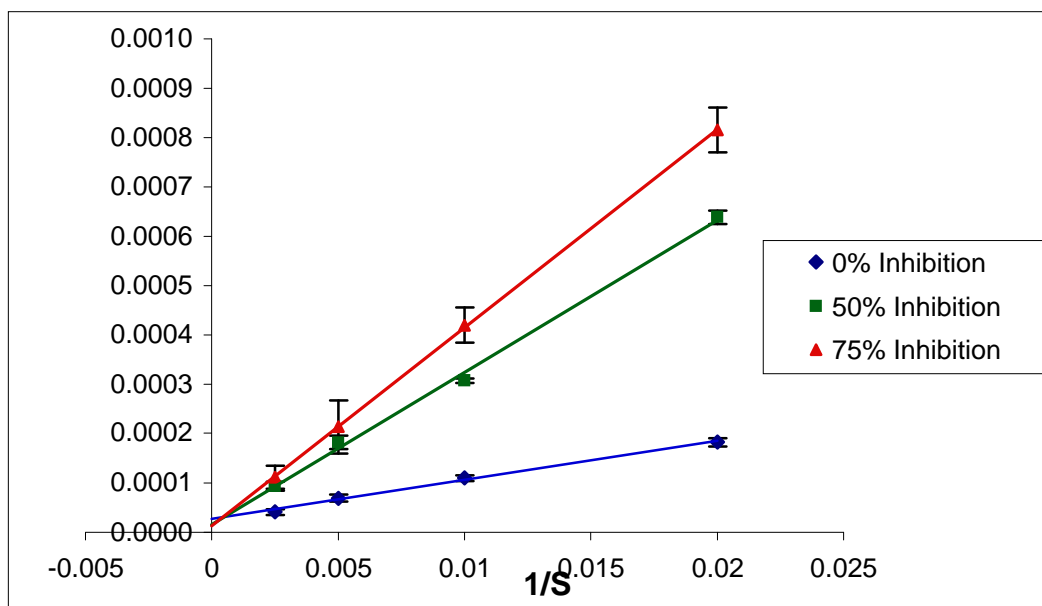
determines the degree to which the binding of inhibitor changes the affinity of the transporter to substrate. The value of Alpha is always greater than zero. When Alpha is equal to 1, the inhibitor does not alter the binding of transporter binding site to the substrate, and the mixed-model is identical to noncompetitive inhibition. When the value of Alpha is very large, the binding of inhibitor prevents binding of the substrate and the mixed model becomes identical to competitive inhibition. When Alpha is very small but greater than zero, the binding of inhibitor enhances transporter's affinity to the substrate, and the mixed model becomes nearly identical to an uncompetitive model. The Alpha values of the selected inhibitors are summarized in **Table 40**. Of which, diclofenac, etodolac, mefenamic acid, meclofenamic acid, flufenamic acid, tolfenamic acid, cerivastatin and luteolin appear to be competitive inhibitors. Diflunisal inhibits MCT1-mediated lactate uptake in an uncompetitive manner, which is inconsistent with the result of Lineweaver-Burk double-reciprocal plot. The inconsistency in inhibitor modality of diflunisal diagnosed by both methods is yet to be elucidated. Nonetheless, the Lineweaver-Burk double-reciprocal plot and mixed-model inhibition model show that diflunisal is not a competitive inhibitor.

Figure 15. Lineweaver-Burk plots of uptake of L-lactate at several fixed concentrations of inhibitor of interest

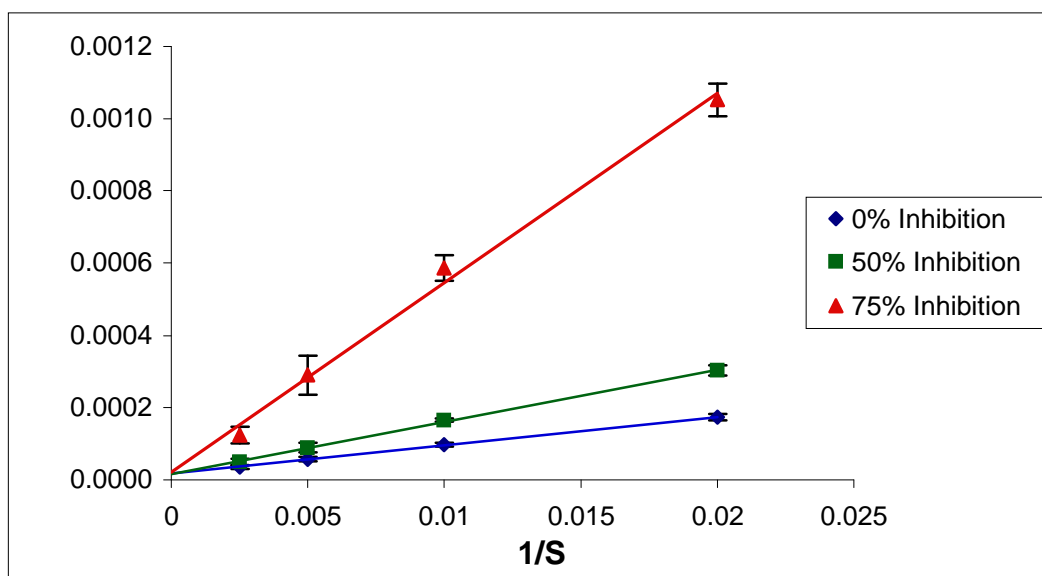
(a) Diflunisal (Noncompetitive)



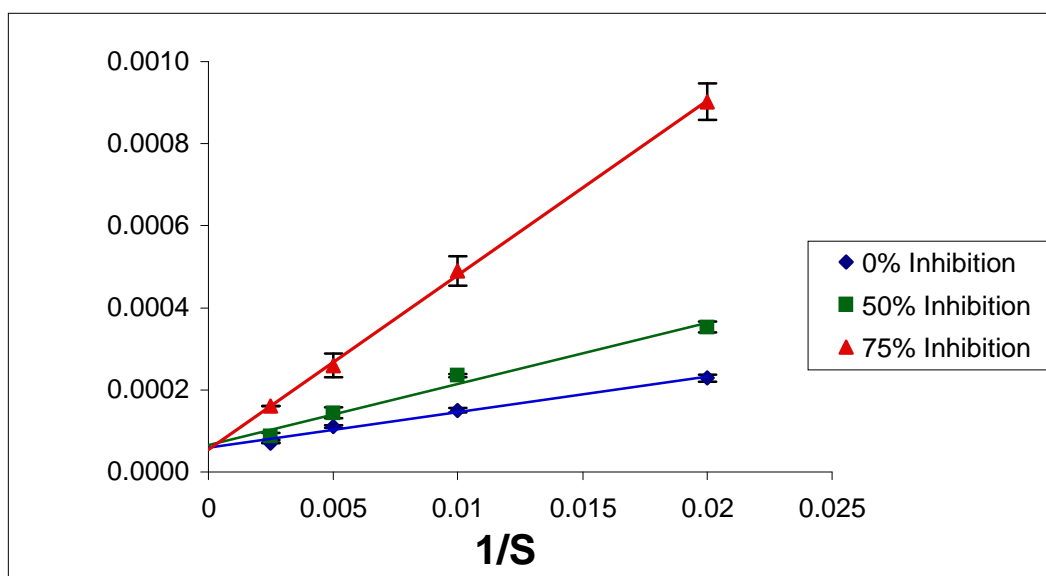
(b) Diclofenac (Competitive)



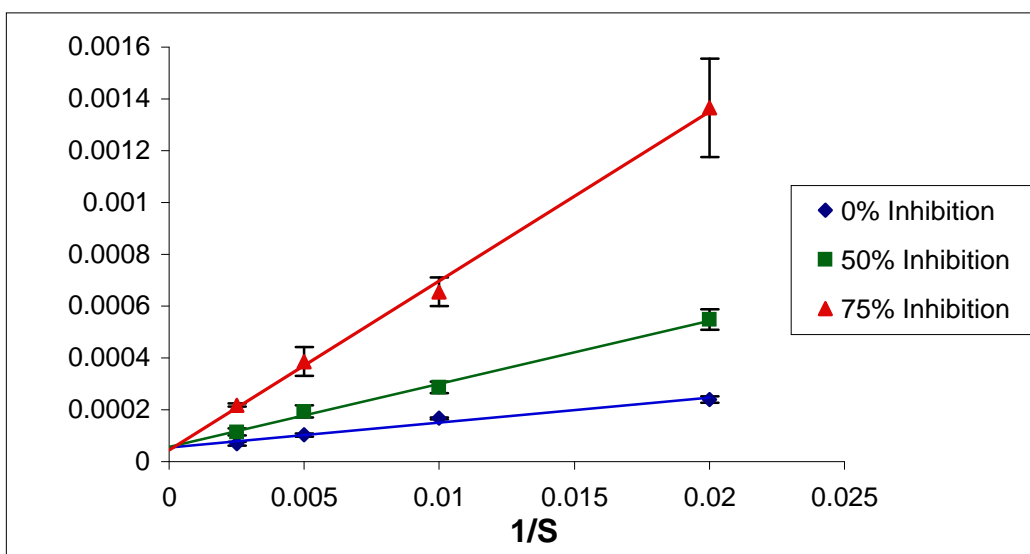
(c) Etodalac (Competitive)



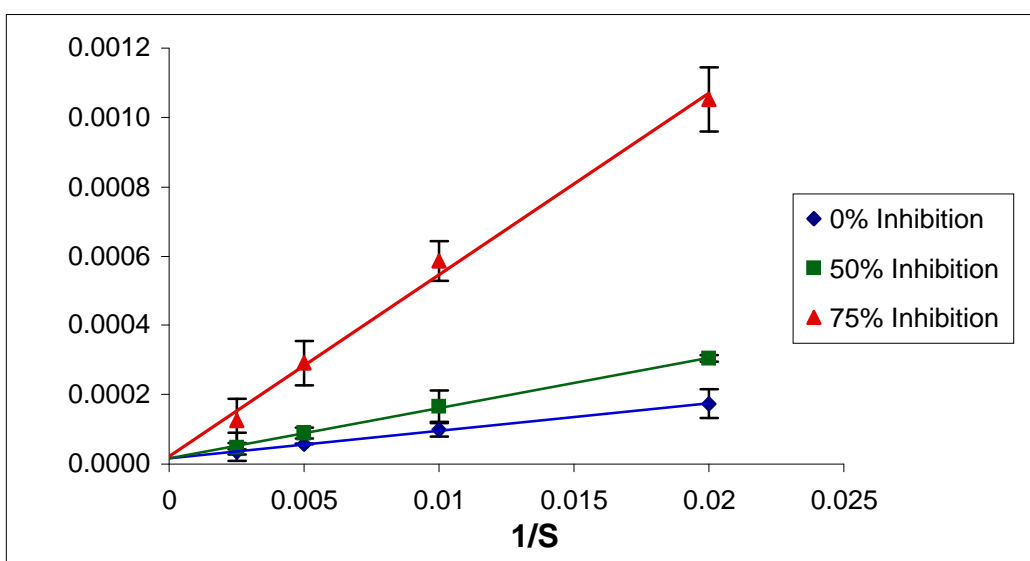
(d) Mefenamic acid (Competitive)



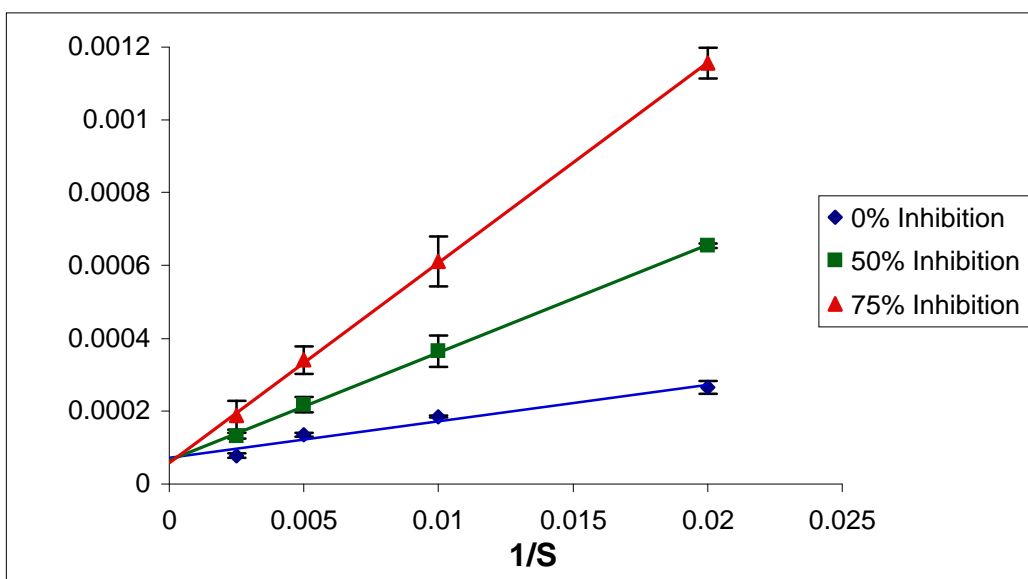
(e) Meclofenamic acid (Competitive)



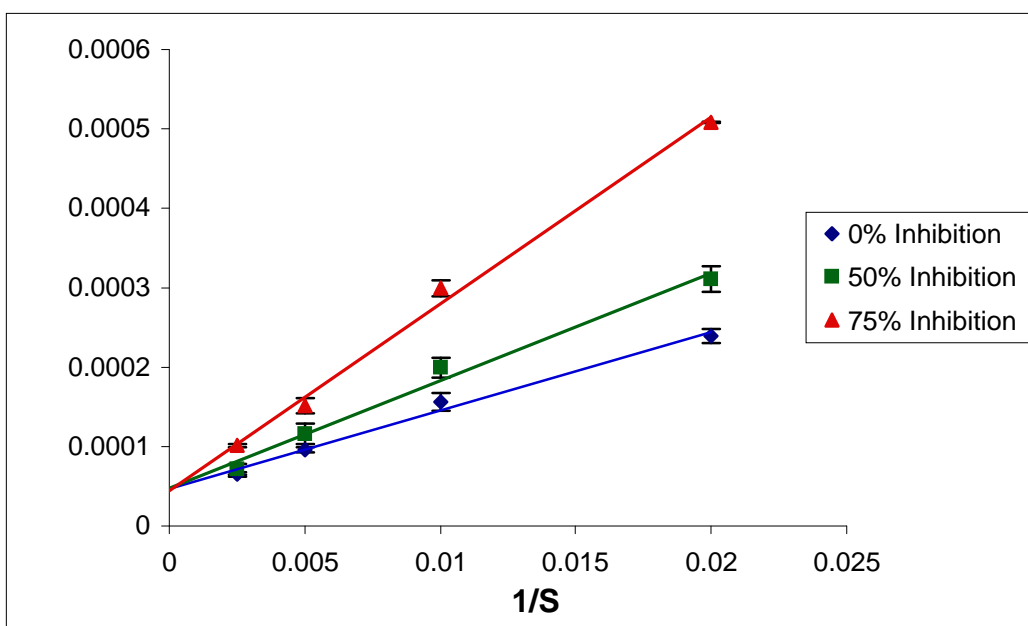
(f) Flufenamic acid (Competitive)



(g) Tolfenamic acid (Competitive)



(h) Cerivastatin (Competitive)



(i) Luteolin (Competitive)

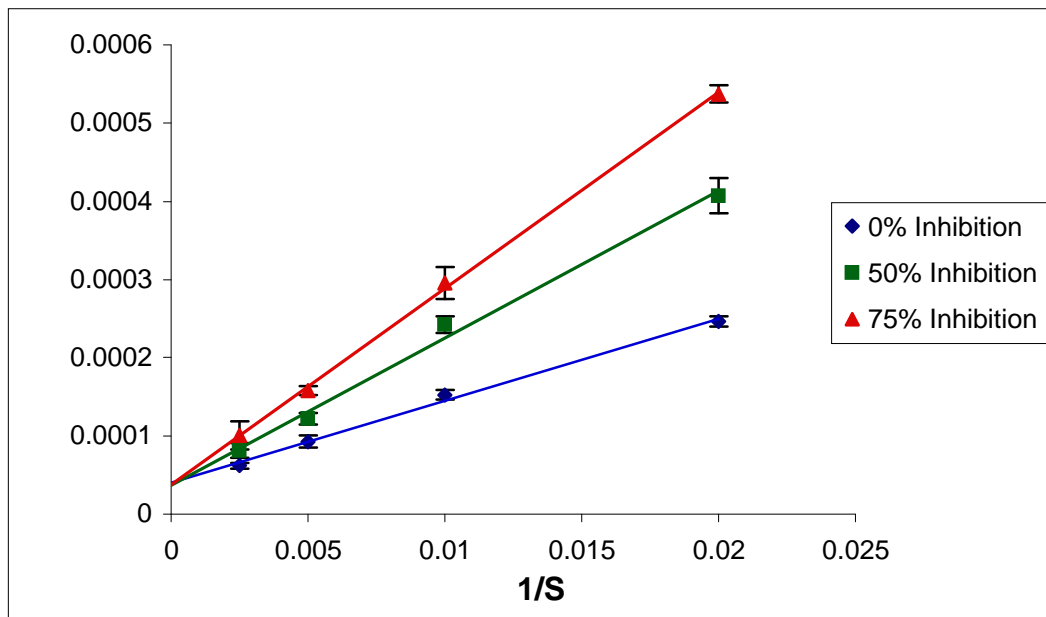


Table 39. The K_i values and mode of inhibitions of tested compounds on the uptake of L-lactate by human erythrocytes

| Compounds | K_i values (μM) | Mode of Inhibition |
|-----------------------|--------------------------------|--------------------|
| NSAIDs | | |
| Diflunisal | 29.56 ± 3.46 | Noncompetitive |
| Diclofenac | 6.17 ± 0.61 | Competitive |
| Etodalac | 341.7 ± 64.3 | Competitive |
| Mefenamic acid | 29.0 ± 3.82 | Competitive |
| Meclofenamic acid | 9.97 ± 2.04 | Competitive |
| Flufenamic acid | 23.29 ± 2.81 | Competitive |
| Tolfenamic acid | 8.95 ± 0.93 | Competitive |
| Statins | | |
| Cerivastatin | 89.07 ± 7.96 | Competitive |
| Phytochemicals | | |
| Luteolin | 75.68 ± 8.01 | Competitive |
| Morin | 42.63 ± 3.21 | Not done |
| Phloretin | 142.3 ± 15.9 | Not done |

Table 40. The mode of inhibition of tested compounds determined by Prism mixed-model inhibition model. The mode of inhibition is determined by the Alpha value

| | Goodness of fit, R_2 | Alpha | Mode of Inhibition |
|-------------------|------------------------|--------------------------|--------------------|
| Diflunisal | 0.9723 | 7.656 | Uncompetitive |
| Diclofenac | 0.9757 | $\sim 1.311\text{e}+018$ | Competitive |
| Etodalac | 0.7298 | $\sim 4.034\text{e}+014$ | Competitive |
| Mefenamic acid | 0.9669 | $\sim 6.706\text{e}+021$ | Competitive |
| Meclofenamic acid | 0.9472 | $\sim 2.273\text{e}+015$ | Competitive |
| Flufenamic acid | 0.9491 | $\sim 6.707\text{e}+011$ | Competitive |
| Tolfenamic acid | 0.9114 | $\sim 4.303\text{e}+017$ | Competitive |
| Cerivastatin | 0.9828 | $\sim 6.454\text{e}+015$ | Competitive |
| Luteolin | 0.9678 | $\sim 4.853\text{e}+018$ | Competitive |

3.3 DISCUSSION

There is a growing recognition that transporters are important mediators in physiological processes and drug disposition. Our understanding of the contribution of transporters in drug disposition has exploded with the creation of a variety of cell-line and transgenic mouse models. For example, the breakthrough in p-glycoprotein (P-gp) and Mdr1a/b (-/-) knockout mice has substantially influenced pre-clinical drug development and provided a good model in examining the role of these efflux proteins in drug disposition.

Food/drug-transporter interactions may be inhibitory, inductive, or both, and may involve influx and efflux transporters. Consequently, such interactions result in increased or decreased of systemic exposure and subsequently altered the efficacies and side effects of pharmacological compounds. Food/drug-interactions have increasingly been observed with increasing use of pharmacological agents, dietary supplements and herbal medicines. Therefore, detailed information about potential transporter interactions between drugs and dietary supplements is needed.

The monocarboxylate transporter 1 (MCT1) has been thought to be responsible for the transportation of L-lactate across the human erythrocyte plasma membrane. According to the lactate shuttle hypothesis, lactate formation and its subsequent distribution throughout the body is a major mechanism whereby the coordination of intermediary metabolism in different tissues, and cells within those tissues, can be accomplished. During exercise, lactate and protons move out from exercising muscles and enter the plasma. From plasma, lactate is further transported into erythrocytes through MCT1. MCT1, the only MCT isoform found in the human

erythrocyte, accounts for 80-90% of lactate transport. Given the roles of MCT1 in endogenous monocarboxylates and clinically important drugs, alter in transporter activity may have far-reaching consequences. The diet-drug interactions via MCT1 inhibition may affect lactate shuttling and drug disposition in the body. Several dietary and pharmacological compounds have shown to exhibit an inhibitory effect on human MCT1 activity [108, 110]. In this study, we further investigated the effects of various dietary and pharmacological agents on MCT1-mediated lactate influx into human erythrocytes.

3.3.1 Human Erythrocyte L-lactate Uptake

The apparent K_m and V_{max} for MCT1-mediated lactate influx found in this study were 123.9 ± 24.6 mM and 12079.0 ± 722.3 nmol/mL of RBC/min, respectively. The K_m value of this study was much higher than the K_m values reported by previous studies on human erythrocytes. On studying lactate influx into human erythrocytes, Dubinsky and Racker obtained a K_m of 13.4 mM [102]. However, this K_m value was estimated from experimental data where the transport activity was not assayed at saturation. The accuracy of K_m and V_{max} estimations are critically dependent on the range of substrate concentrations over which the initial velocity has been determined. If the measurements are made only at low substrate concentrations, the data will appear to be first-order. In this concentration range, the transporter binding sites never reach saturation and the K_m will be underestimated. In order to best characterize the steady state kinetic constants for a transport system, it is best to at least cover substrate concentration of 0.25-5.0 K_m [217]. Similar erroneous estimations have been observed in several studies that characterized the kinetics of MCT1. In these studies, the K_m of MCT1-mediated

transport lactate influx was estimated from uptake data measured at low substrate concentrations that had not reached saturation [87, 97, 100, 102, 161, 199]. The high K_m value of L-lactate has not been recognized before and may suggest that MCT1 may have other preferential substrates (such as pyruvate, ketone bodies and acetate) other than L-lactate. The data of this study suggests that MCT1 is a low affinity but high capacity transport process for the transport of L-lactate.

3.3.2 Inhibitory Effects of Dietary and Pharmacological Compounds on L-lactate Influx

A previous study had reported that several non-steroidal anti-inflammatory drugs (NSAIDs), namely diflunisal, diclofenac, ketoprofen and naproxen, exhibited a strong inhibition effect on human MCT transport activity [108]. In this study, we further investigated the effects of other NSAIDs on MCT1-mediated lactate influx. As summarized in **Table 38** and **Figure 14a**, diflunisal, diclofenac, mefenamic acid, meclofenamic acid, flufenamic acid, tolfenamic acid and etodalac exhibited a strong effect on the uptake of L-lactate with an IC₅₀ value of 2 to 40 μ M. In contrast to the study done by Choi *et al.*, the inhibitory effects of ketoprofen and naproxen on MCT1-mediated L-lactate uptake were weak (**Table 37**).

The inhibitory concentrations of tested NSAIDs (diflunisal, mefenamic acid, meclofenamic acid, flufenamic acid and tolfenamic acid) are in the range of physiologically relevant concentrations that are achievable from the oral intake. For example, the suggested dosage range of diflunisal is 500 mg to 1000 mg daily for osteoarthritis and rheumatoid arthritis. The peak plasma concentration of diflunisal achievable from single 500 mg oral dose was 87 μ g/mL, while the K_i of

diflunisal is 29.56 μM (equivalent to 7.40 $\mu\text{g/mL}$). Therefore, a strong inhibition of NSAIDs on MCT1 is achievable at the relevant plasma concentrations of diflunisal.

Three NSAIDs, namely diclofenac, meclofenamic acid and tolfenamic acid exhibited strong inhibitory effects on L-lactate transport, with a K_i value of 6.17 μM (~ 1.96 $\mu\text{g/mL}$), 9.97 μM (~ 3.35 $\mu\text{g/mL}$) and 8.95 μM (~ 2.34 $\mu\text{g/mL}$), respectively. The recommended dosage for diclofenac is 100-150 mg/day in divided doses for the relief of osteoarthritis. The peak plasma concentration of diclofenac achievable from single oral 50 mg dose is 0.8 $\mu\text{g/mL}$, while the peak plasma level of diclofenac achievable from multiple doses (oral 50 mg was administered 3 times daily for 7 days) was 2.3 $\mu\text{g/mL}$ [218]. The recommended dosage of meclofenamate sodium for pain relief, arthritis and osteoarthritis is 200 to 400 mg daily, administered in three or four equal doses. After the administration of 100 mg meclofenamate sodium for 18 days every 8 hours, the peak concentration was 4.8 $\mu\text{g/mL}$ for the parent compound on both day 1 and day 18. Lastly, tolfenamate is subscribed to patients suffering from acute migraine with a recommended dosage of 200mg. Pharmacokinetics data shows that a single oral dose of 200 mg, 400 mg and 800 mg of tolfenamic acid achieved a peak concentration of 2.97 $\mu\text{g/mL}$, 6.15 $\mu\text{g/mL}$ and 12.2 $\mu\text{g/mL}$ in the plasma, respectively [219]. Taking this data together, it suggests that strong inhibition of NSAIDs on L-lactate transport on human erythrocyte is expected at the therapeutically relevant plasma concentrations of tested NSAIDs.

Although inhibitory effects of tested NSAIDs are achievable at clinically relevant concentrations, we have to take into the consideration of protein binding property of the pharmaceutical compound. High protein binding ($\geq 99\%$) and small volume of distribution seem to be a common feature of the NSAIDs, namely diflunisal, diclofenac, mefenamic acid, meclofenamic acid and tolfenamic acid. A better comparison is with unbound plasma concentration. However, pharmacokinetics data reported the total plasma concentration rather than the unbound plasma concentration. The actual unbound plasma concentrations of tested NSAIDs may be below the K_i values reported in this study. The tested NSAIDs may not contribute significantly to the *in vivo* inhibition of MCT1 activity.

Interestingly, recent studies associated NSAID use with increased cardiovascular risk in healthy individuals and in patients with established cardiovascular disease [220-225]. A nationwide cohort study was carried out by Schjerning Olsen *et al.* to examine the association between NSAID treatment duration and risk of cardiovascular disease [220]. Overall, NSAID treatment was significantly associated with an increased risk of death and recurrent myocardial infarction. Analyses of individual NSAIDs showed that the traditional NSAID diclofenac was associated with the highest risk from the beginning of the treatment, while ibuprofen showed an increased risk when used for more than one week [220]. The selective COX-2 inhibitors, rofecoxib and celecoxib, were associated with increased risk of death after treatment. Naproxen, however, was not associated with an increased risk of death or myocardial infarction for the entire treatment duration. Lactate is an important fuel for myocardial energy. As MCT1 expression is abundant in heart tissue [7], one of the possible mechanism of NSAID-induced

cardiotoxicity could be due to inhibitory effect of NSAID on MCT1, which prevents the uptake of lactate by heart tissue. However, as the nature of NSAID-induced cardiotoxicity is unknown, this proposed mechanism is purely speculative.

The interaction of L-lactate and statins with MCT1 has also been examined in this study. Previously, Kobayashi *et al.* reported lipophilic statins significantly inhibited L-lactate uptake by MCT4 in a concentration-dependent manner [165]. However, the effects of statins on MCT1 transport system have yet to be evaluated. Out of the two hydrophilic (rosuvastatin and pravastatin) and two lipophilic (cerivastatin and simvastatin) statins examined in this study, only cerivastatin exhibited statistically significant inhibitory effect on MCT1. The inhibitory effects of simvastatin, pravastatin and rosuvastatin were very weak (**Table 37**). Statins are widely used cholesterol-lowering agents for prevention of cardiovascular diseases. Statins are well tolerated by most patients but can produce a variety of skeletal myopathies. One of the possible explanations of statin-induced cytotoxicity is associated with the inhibitory effects of statins on L-lactate mediated by MCT. It has been speculated that statins inhibit MCT-mediated efflux of L-lactate, resulting in induction of intracellular acidosis and apoptosis in myocytes [165, 226]. However, the finding in this study shows that rosuvastatin, simvastatin and pravastatin do not inhibit MCT1 transport activity. Besides, although cerivastatin exhibited certain degree of inhibition on MCT1, the peak plasma concentration of cerivastatin of multiple oral doses treatment (0.8 mg once daily for 10 days) was 0.0096 µg/mL. The plasma concentration of cerivastatin is far below the K_i value, which is 89.07 µM (~ 42.88 µg/mL). Therefore, impairment of MCT1 function is unlikely to contribute to statin-induced myotoxicity.

The popular use of dietary supplements and herbal medicine has raised the awareness of the potential diet-transporter interactions. Recently, Wang *et al.* reported that flavonoids, a class of polyphenolic compounds present in the diet and herbal products, are potent MCT1 inhibitors [110]. Therefore, the effects of several dietary compounds, including flavonoids on MCT1 were examined (**Table 37**). In this study, we demonstrated that luteolin, morin and phloretin were inhibitors of MCT1, whereas the effects of naringin, silibinin and coumorin on MCT1 were very weak. Our results are consistent with the results reported by Wang and Morris [110]. In their study, luteolin, morin and phloretin inhibited the uptake of γ -hydroxybutyrate (0.1 mM) by rat MCT1 gene-transfected MDA-MD231 cells with the IC₅₀ values of 0.41 ± 0.14 , 6.21 ± 2.01 and 2.57 ± 0.48 μ M, respectively. However, we demonstrated higher IC₅₀ values for luteolin, morin and phloretin, which were 2.71 ± 1.28 , 44.53 ± 1.08 and 47.98 ± 1.11 , respectively (**Table 38, Fig. 14c**). In addition, Shim *et al.* had reported that silibinin exhibited strong inhibitory effect on MCT1 in Caco-2 cells. However, silibinin showed little effect on MCT1-mediated L-lactate influx in this study. The discrepancy of results could be due to the differences in the experimental conditions, the nature of substrate and concentration of substrate present in the assay. Therefore, it is not rigorously correct to compare the relative potencies of inhibitors of different modalities by use of IC₅₀ values. Three dietary compounds were examined on their effects on MCT1. The *in vivo* inhibitory effects of these tested phytochemicals cannot be speculated as the pharmacokinetics data is not available. Nonetheless, the result found in this study suggests a potential diet-transporter interaction in human body.

The limitation of this study is SNP mutation analysis was not performed in the subjects involved in this study. This was because the *SLC16A1* gene is generally conserved in Singapore population and only one rare mutation was predicted to have detrimental effect on MCT1 transport activity (**Table 10**). Although 1470 T>A (Asp490Glu) was suggested to have a defective effect on MCT1 transport activity when the polymorphism-phenotype association was examined, this information was not yet available when this project was performance. Nonetheless, the individual variation was minimized by utilizing the erythrocytes samples from only four Chinese volunteers.

Three pathways mediate the transport of lactate across erythrocyte membrane. It has been reported that in human erythrocyte, MCT1 transport system accounts for 90% of lactate flux across membrane. The band 3 system and nonionic diffusion contributed 6% and 4%, respectively [107]. In this study, diflunisal, diclofenac, mefenamic acid, meclofenamic acid, flufenamic acid, tolfenamic acid, indomethacin, etodalac and morin inhibited approximately 90-93 % of lactate influx at external L-lactate concentration of 5 mM. The observation demonstrates reliability and specificity of the model in studying MCT1 transport kinetics.

3.3.3 Summary

Food/drug-transporter interactions have increasingly been observed with increasingly use of pharmacological agents, dietary supplements and herbal medicines. Given the roles of MCT1 in transporting endogenous monocarboxylates as well as clinically important drugs [105, 192, 193, 227], these interactions can cause serious consequences. The diet-drug interactions via MCT1 inhibition may affect lactate shuttling and drug disposition in the body. On the other hand, these interactions can have favourable effects. Recent studies reported that certain tumor cells up-regulated the expression of MCT1 to prevent cellular acidosis, these inhibitors could be the potential candidate drugs in cancer therapy by promoting cellular acidosis via MCT1 inhibition [228-232]. Taken together, several pharmacological agents and dietary compounds exhibited strong inhibition on MCT1-mediated L-lactate influx. Given that the inhibitory concentrations of some of the tested compounds are in the range of physiologically relevant concentrations that are achievable from the daily intake, the study raises the awareness of the potential diet-drug interaction via MCT1 inhibition. However, due to high protein binding of the tested NSAIDs, the actual unbound plasma concentrations of tested NSAIDs may be below the K_i values reported in this study. The tested NSAIDs may not contribute significantly to the *in vivo* inhibition of MCT1 activity. Therefore, it will be beneficial to examine the inhibitory effects of NSAID on MCT1 *in vivo*.

CHAPTER 4

INTERINDIVIDUAL VARIATION IN

TOTAL AND CARRIER-MEDIATED LACTATE INFLUX INTO

HUMAN ERYTHROCYTES OF LOCAL CHINESE POPULATION

OVERVIEW

The objective of this study was to examine the interindividual variation in total and MCT1-mediated lactate influx into human erythrocytes in the local Chinese population. A total of 10 healthy Chinese volunteers were recruited in this study. The 10-assay grouped data were plotted on the best-fit curve, and its K_m and V_{max} were estimated. In the MCT-1 mediated lactate influx, the apparent K_m and V_{max} were 220.1 ± 35.33 mM and 15877 ± 968.1 nmol/ml of RBC/min, respectively. The main findings of the present study were that 1) no interindividual variations were observed in the total lactate influxes and MCT1-mediated lactate influx across RBC membrane in the local Chinese population; 2) human MCT1 system exhibited a low affinity but high capacity transport mechanism for the transport of lactate into RBC; and 3) the T allele of 1470 T>A (Asp490Glu) polymorphism may have a defective effect in the transport activity of MCT1.

4.1 MATERIALS AND METHODS

4.1.1 Subjects

A total of 10 subjects participated in this study. All subjects had been recruited previously in accordance with requirements (Institutional Review Board, National University Hospital, Singapore) and provided written informed consent. The mean age is 24.7 ± 2.4 (21 to 29). The male:female sex ratio is 7:3. Ethnicity was defined through self-declaration by the donors of similar ethnicity through three generations. All DNA samples were rendered anonymous by removing links with specific individual information, i.e., any ID, name, or address.

4.1.2 Erythrocytes Lactate Influx Assay

4.1.2.1 Preparation of RBCs for Lactate Influx Assay

Techniques for RBC preparation and lactate influx measurement were adopted from previously published methods [72, 107, 162, 164]. Five milliliters of venous blood were drawn from each subject into heparinized vacutainers. An initial hematocrit (Hct) and hemoglobin concentration were determined for all blood samples. Three milliliters of blood sample were transferred to a 50 ml conical tube. The remaining portion of the blood sample was refrigerated at 4°C and saved for repeat measurements if required. The RBCs were isolated by centrifugation at room temperature (25°C, 10 min, 2000g). The plasma and buffy coat were removed by aspiration, leaving only the RBC pellet. The pellet was mixed by inversion with 30 volumes of chloride buffer (150 mM NaCl, 10 mM Na-tricine, pH 8.0 at 37°C, osmolality ~ 315mosmol/kg H₂O) and incubation in water bath for

30 min at 37°C. This step was to ensure removal of endogenous lactate [102]. At the end of the incubation, the RBCs were sedimented at room temperature (25°C, 10 min, 2000g) and the supernatant was removed by aspiration. The cell pellet was then washed two times. For each washing, four volumes of chloride buffer were added to the cell pellets, the pellet was mixed by inversion and then centrifuged (25°C, 10 min, 2000g). The supernatant was removed after each wash. Lactate depletion from the RBCs (~0.20 mM in 30% hematocrit solution) was confirmed by analysis via the spectrophotometric technique (BioVison; MV, California). After the final wash, the RBC pellet was suspended in HEPES buffer (90 mM NaCl, 50 mM HEPES, pH 7.4, 37°C, osmolality ~ 267 mosmol/kgH₂O) equivalent to a 30% hematocrit (packed cell volume) to obtain the stock cell solutions for influx measurements. This suspension was divided into two aliquots, each containing one milliliter. One of the two stock cell suspensions contained no lactate transport inhibitors. Five millimolar α -cyano-4-hydroxycinnamic acid (CHC) was added to the second stock cell suspension to inhibit the MCT1-mediated pathway. The two aliquots were incubated in a water bath for 30 min at 37°C, and Hct was determined in a sample of each stock cell suspension.

4.1.2.2 Total Lactate Influx

A 25 μ l sample of stock cell solution was incubated in 75 μ l of HEPES influx buffer for 20 s at 37°C. The HEPES buffer containing [¹⁴C]-lactate (0.2 μ Ci/ml) at thirteen unlabeled [La] values of 2.5, 6.2, 12.3, 24.7, 49.3, 98.7, 123.3, 246.7, 370.0, 493.3, 616.7, 740.0 and 863.3 mM. All HEPES influx buffers were adjusted to a pH 7.4. Because of dilution with the stock cell solution, the actual final [La]

values were 2, 5, 10, 20, 40, 80, 100, 200, 300, 400, 500, 600 and 700 mM, respectively. The incubation was stopped with 2 ml of ice-cold stop solution [150 mM NaCl, 10 mM MES, pH 6.5] and tubes were immediately iced. The sample was spun by centrifugation (4°C, 10 min, 2000 g) and was washed twice to eliminate extracellular radioactivity. After the final wash, the RBC pellet was lysed and deproteinized with 0.5 ml of 4.2% perchloric acid followed by centrifugation of the sample (4°C, 10 min, 2000 g). Finally, 0.4 ml of the supernatant was pipetted into scintillation vials containing 5 ml of scintillation liquid (Amersham Bioscience; Amersham, UK) and the radioactivity of the supernatant was measured with a liquid scintillation counter (Beckman Coulter, Kraemer Boulevard, USA). All measurements were made in triplicate.

4.1.2.3 MCT1-mediated Lactate Influx

The cells were suspended in HEPES containing CHC to block the MCT1 pathway. The samples were treated exactly as for the total lactate influx assay.

4.1.2.4 Calculation of Lactate Influx

To express the data as influx of lactate per milliliter of cells, the 25 µl sample of stock solution was multiplied by its haematocrit fraction (0.30) to obtain a packed cell volume. The lactate influx per microliter is then mathematically converted to a per milliliter value. Lactate influx through MCT1 transport system was estimated as follows. The difference between the uninhibited flux and the CHC-inhibited flux was taken to estimate the flux through MCT1. Because CHC is not specific to the MCT only, this value somewhat overestimates the role of the MCT1.

4.1.2.5 Data Analysis

For kinetic studies, the Michaelis-Menten constant (K_m) and maximum uptake rate (V_{max}) of L-lactic acid were estimated using GraphPad Prism 5 software.

4.1.3 DNA Amplification

4.1.3.1 DNA extraction

Genetic materials used in this study were obtained from a previously-developed cell repository from healthy volunteers of Chinese and Indian descent. 45 ml of Buffer A (0.32 M sucrose, 10 mM Tris HCl pH 7.4, 5 mM MgCl₂, and 1 % Triton-X-100) was added to the white cell pellet and mixed by inversion. The solution was spun (4°C, 20 min, 1500 g) and the supernatant was removed by aspiration. The same procedure was repeated once. The pellet was resuspended in 5 ml of Buffer B (25 mM EDTA pH 8.0 and 75 mM NaCl). This is followed by the addition of 250 µl of 10 % Sodium Dodecyl Sulfate (SDS) and 20 µl of 20 mg/ml proteinase K. The contents were vortexed briefly and incubated overnight at 37°C with shaking in an oven. At the end of incubation, 1.4 ml of saturated NaCl (6 M) was added to the mixture and the mixture was vortexed vigorously for 15 seconds. The solution was spun (15 min, 1500 g) and the supernatant was transferred to a new 50 ml falcon tube containing 15 ml of absolute ethanol. The mixture was mixed gently by inversion to precipitate DNA. The mixture was spun (20 min, 1500 g) and the supernatant was removed. The DNA pellet was washed with 5 ml of 70% ethanol and was spun (15 min, 1500 g). The supernatant was removed and the pellet for air-dried for 30 minutes. The recovered DNA was dissolved in 200 µl of

TE solution (10 mM Tris HCl pH 7.5 and 1 mM EDTA pH 7.5) and was dissolved at 4°C overnight. The DNA was transferred to an Eppendorf tube and stored at -20°C. The isolated DNA was quantified using μ Quant Universal Microplate Spectrophotometer (ITS) and absorbance readings were taken at 260 nm wavelength. Optical Density (OD), which determines the purity of the DNA, was obtained by measuring the ratio of 260 nm/280 nm (DNA maximum absorbance = 260 nm wavelength). OD readings between 1.7 – 1.8 were accepted as a lower or higher ratio indicates protein or ribonucleic acid contamination respectively. Finally, the DNA was diluted with DNase-free water to a concentration of 20 ng/ μ l.

4.1.3.2 Polymerase Chain Reaction Amplification

The polymerase chain reaction (PCR) amplifications were performed in a total volume of 30 μ l containing 1 X Master Mix (Promega, Madison, WI, USA), 0.4 μ M of each primer (Sigma-Aldrich, St. Louis, MI, USA) and 60 ng of DNA on the MJ Research Peltier Thermal Cycle (DNA Engine Dyad; MJ Research Inc, Waltham, MA, USA). The PCR conditions were pre-denaturation at 95°C for 5 min, followed by 35 cycles of denaturation at 95°C for 1 min, annealing for 1 min, and extension at 72°C for 1 min, and then a final extension at 72°C for 10 min. The annealing temperatures for the fragments of MCT1 and MCT4 genes are summarized in **Table 8** and **Table 9**, respectively. Cycle sequencing was performed on the MJ Research Peltier Thermal Cycler using the following conditions: initial denaturation at 96°C for 10 seconds, 50°C for 5 seconds, and 60°C for 4 minutes.

4.1.3.3 Agarose Gel Electrophoresis

After PCR amplifications, the PCR products obtained were verified by electrophoresis through 1% agarose gels stained with 0.2 µg/ml ethidium bromide. They were subjected to electrophoresis at 100 V for 1 hour and visualized under UV illumination. PCR amplifications that were found to produce poor DNA yield were discarded and repeated because it would lead to downstream problems such as ambiguous results from DNA sequencing.

4.1.4 DNA Sequencing

4.1.4.1 PCR Product Clean Up

Prior to sequencing, PCR products were cleaned up to remove excess primers and unincorporated dNTPs. 12 µl of PCR products were being added to one unit of Shrimp Alkaline Phosphatase (Promega) and two units of Exonuclease I (New England Biolabs, Beverly, MA, USA). The reaction mix was incubated at 37°C for 15 minutes and followed by enzyme deactivation at 80°C for 20 minutes.

4.1.4.2 Cycle Sequencing

In this study, all PCR products were subjected to DNA sequencing. Mutational analysis of the candidate genes was performed using BigDye Terminator v3.1 Cycle Sequencing Kit. Extension reactions were performed in a total volume of 20 µl containing 10 µl of purified PCR products, 0.5 µl of BigDye Terminator reagent, 2 µl of 5x sequencing buffer, 2 µl of oligonucleotide primer (5 pmole/µl) and 3.5 µl of water. Primers for cycle sequencing were similar to the primers for PCR (**Table 8** and **Table 9**). Amplification of cycle sequencing products was generated

using MJ Research Peltier Thermal Cycle with cycling profile: denaturation at 96°C for 1 min, 25 cycles of denaturation at 96°C for 10 seconds, annealing at 50°C for 5 seconds, extension at 60°C for 4 minutes. The extension products were stored at 4°C for maximum of 3 days or immediately proceed to DNA precipitation.

4.1.4.3 DNA Precipitation

After cycle sequencing, the 96-well reaction plate was removed from the thermal cycler and briefly spun. The sequencing products in each well were added with 2 µl of 125 mM EDTA, followed by 2 µl of 3 M sodium acetate. The contents were mixed and added with 50 µl of absolute ethanol. The contents were gently mixed and incubated in the dark at room temperature for 25 minutes. After the incubation, the samples were spun at 3000 g for 30 minutes. The supernatant was discarded by inverting the plate and spun at up to 185 g for 1 minute. This was followed by adding 70 µl of 70 % ethanol to each well, and spinning at 1650 g for 15 minutes. The supernatant was discarded and the DNA pellets were dried at 72°C for 10 minutes. The plate was covered with aluminum foil and stored at 4°C for a period of 2 weeks prior to sequencing analysis. Alternatively, 12 µl of HiDi was added to into each well containing DNA pellet and run on the automated ABI Prism Model 3100 Avant Genetic Analyzer (Applied Biosystems, Foster City, CA, USA).

4.1.4.4 Mutational Analysis of DNA Sequences

The sequences were analyzed with a Mutation SurveyorTM v2.61 (Softgenetics, State College, PA, USA) and Chromas (Techelysium software). All mutations

flagged by the software were checked by visual inspection to avoid any false positives. PCR was repeated and bidirectional sequencing performed on all detected variants to rule out PCR-induced mutations and sequencing artefacts.

4.1.5 Statistical Analysis

Unless otherwise indicated, all data are expressed as mean \pm SEM. Mann Whitney U tests were performed to analyze the differences between TA and AA genotypes of the polymorphism for all the lactate variables, Michaelis-Menten coefficients (K_m) and maximal lactate transport capacity (V_{max}) in total and MCT1-mediated lactate influx. Statistical significance was defined as $P < 0.05$.

4.2 RESULTS

4.2.1 Total and MCT1-mediated Lactate Influx into Human Erythrocytes

The 10-assay grouped data were plotted on the best-fit curve, and its K_m and V_{max} were estimated (**Fig. 16a** and **Fig. 16b**). In the total L-lactate influx assay, the uptake increased with the increase in external [La], but did not reach saturation at highest concentration (**Fig. 16a**). We could not further increase the external lactate concentration as red cell haemolysis occurs at external lactate concentration higher than 700 mM. Therefore, the K_m and V_{max} of total L-lactate uptake into human RBC cannot be estimated. The MCT1-mediated lactate influxes also increased with external [La] and reached plateau at high concentration (**Fig. 16b**). The apparent K_m and V_{max} for MCT1-mediated lactate influx were 220.1 ± 35.33 mM and 15877 ± 968.1 nmol/ml of RBC/min, respectively. The mean (\pm s.d.) and Coefficient of Variation (%) of L-lactate influx into RBC are summarized in **Table 41** and **Table 42**. For the uptake data of individual subject, please refer to **Appendix I**.

Figure 16a. Total lactate influx into RBC of local Chinese population ($n = 10$). Values are presented as mean \pm SEM.

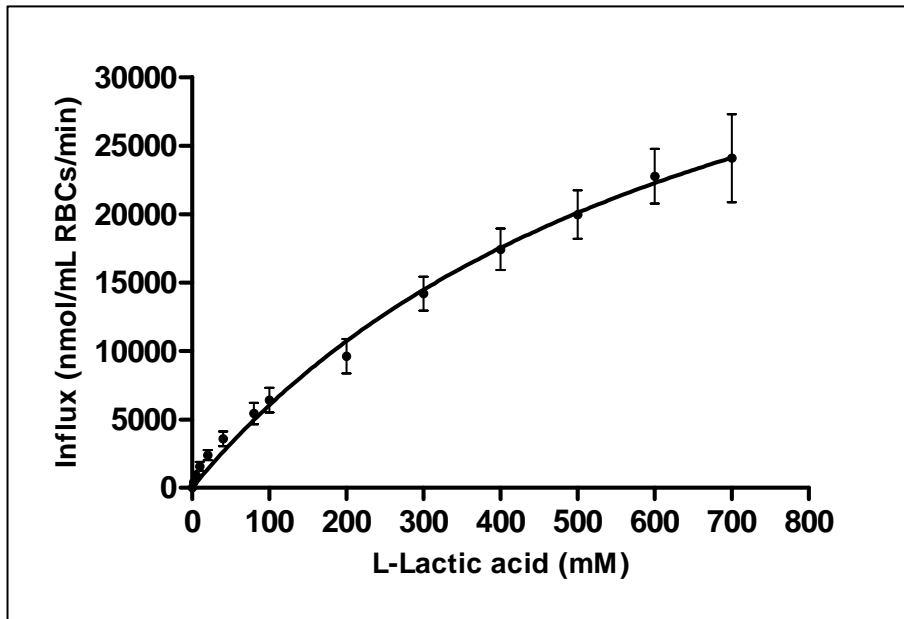


Figure 16b. Monocarboxylate transporter 1- mediated lactate influx into RBC of local Chinese population ($n = 10$). Values are presented as mean \pm SEM.

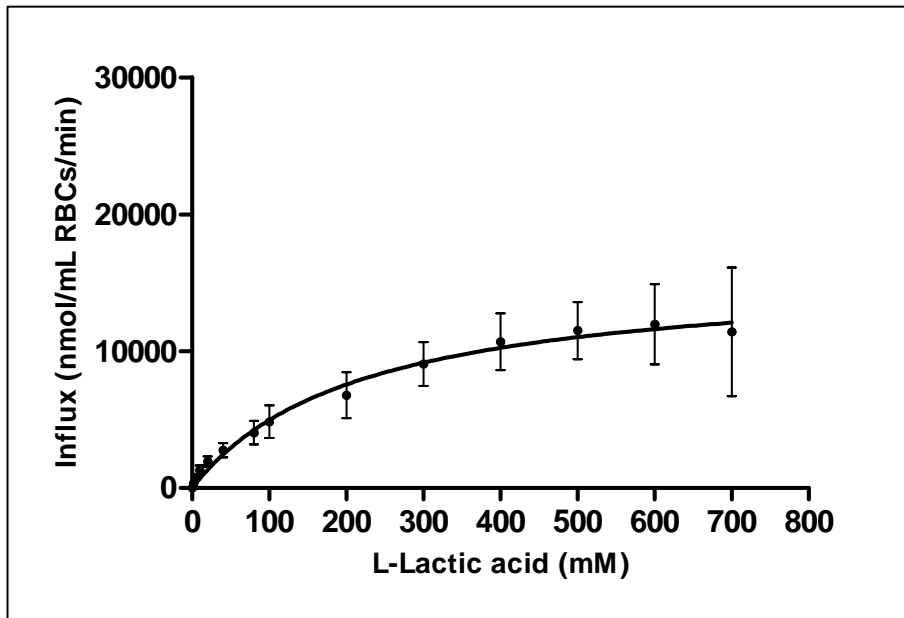


Table 41. *The total lactate influx into RBC of local Chinese population (n = 10)*

| L-lactate concentration (mM) | 2 | 5 | 10 | 20 | 40 | 80 | 100 | 200 | 300 | 400 | 500 | 600 | 700 |
|------------------------------|-------|-------|-------|-------|-------|-------|-------|-------|-------|-------|-------|-------|-------|
| Mean (nmol/mL RBC/min) | 405 | 922.2 | 1560 | 2386 | 3579 | 5433 | 6417 | 9615 | 14178 | 17423 | 19965 | 22761 | 24076 |
| Std. Deviation | 122.7 | 219.2 | 327 | 368.6 | 537.2 | 790.7 | 907.5 | 1255 | 1246 | 1518 | 1774 | 2006 | 3216 |
| Std. Error | 38.8 | 69.32 | 103.4 | 116.6 | 169.9 | 250.1 | 287 | 396.8 | 393.9 | 480 | 560.9 | 634.4 | 1017 |
| Coefficient of Variation (%) | 30.30 | 23.77 | 20.96 | 15.45 | 15.01 | 14.55 | 14.14 | 13.05 | 8.79 | 8.71 | 8.89 | 8.81 | 13.36 |

Table 42. *The Monocarboxylate transporter 1- mediated lactate influx into RBC of local Chinese population (n = 10)*

| L-lactate concentration (mM) | 2 | 5 | 10 | 20 | 40 | 80 | 100 | 200 | 300 | 400 | 500 | 600 | 700 |
|------------------------------|-------|-------|-------|-------|-------|-------|-------|-------|-------|-------|-------|-------|-------|
| Mean (nmol/mL RBC/min) | 356.5 | 793 | 1311 | 1936 | 2765 | 4048 | 4841 | 6786 | 9056 | 10690 | 11504 | 11967 | 11408 |
| Std. Deviation | 119 | 218.3 | 322.1 | 364.8 | 534.5 | 870.4 | 1186 | 1670 | 1594 | 2083 | 2079 | 2923 | 4706 |
| Std. Error | 37.64 | 69.04 | 101.8 | 115.4 | 169 | 275.2 | 374.9 | 528 | 504 | 658.6 | 657.5 | 924.3 | 1488 |
| Coefficient of Variation (%) | 33.38 | 27.53 | 24.57 | 18.84 | 19.33 | 21.50 | 24.50 | 24.61 | 17.60 | 19.49 | 18.07 | 24.43 | 41.25 |

4.2.2 Polymorphism-phenotype association of *SLC16A1* gene

In this study, the effect of a common MCT1 polymorphism, 1470 T>A (Asp490Glu), was examined. Among the eight Chinese samples studied, none of the samples were homozygous wildtype, 4 (50%) samples were heterozygous mutants and 4 (50%) were homozygous mutants. The DNA samples of two subjects were contaminated with PCR inhibitors. We were unable to amplify the PCR fragments after several attempts. Therefore, the genotyping data of these two subjects were missing and were excluded from the analysis.

The influence of genetic polymorphism in total lactate influx and MCT1-mediated lactate influx were compared at 2, 5, 10 and 20 mM of external L-lactate concentrations. Mann Whitney U tests were performed to analyze the differences between TA and AA genotypes of the 1470 T>A (Asp490Glu) polymorphism for all the lactate variables, Michaelis-Menten coefficients (K_m) and maximal lactate transport capacity (V_{max}) in total and MCT1-mediated lactate influx.. The TA group appeared to have lower values of the total influx into erythrocyte than the AA group at 2, 5 and 20 mM of lactate concentrations (**Fig. 17**). However, the differences in lactate influx were not statistically significant. Similarly, the MCT1-mediated lactate influx in TA group was lower than the AA group at external lactate concentration of 2, 5, 10 and 20 mM. The differences, however, were not significantly different at all lactate concentrations (**Fig. 18**). The K_m and V_{max} values of TA and AA groups in the total and MCT1-mediated uptakes were compared. There were no significant differences for the K_m and V_{max} between two genotype groups in the total and MCT1-mediated lactate influx (**Fig.19** and

Fig.20). Nonetheless, a higher K_m value was observed in the TA group as compared to the AA group.

Figure 17. The total lactate influx into RBC at four external L-lactate concentration in TA and AA groups of SLC16A1 gene. There were no significant differences between groups at all four external lactate concentration (**Table 43**).

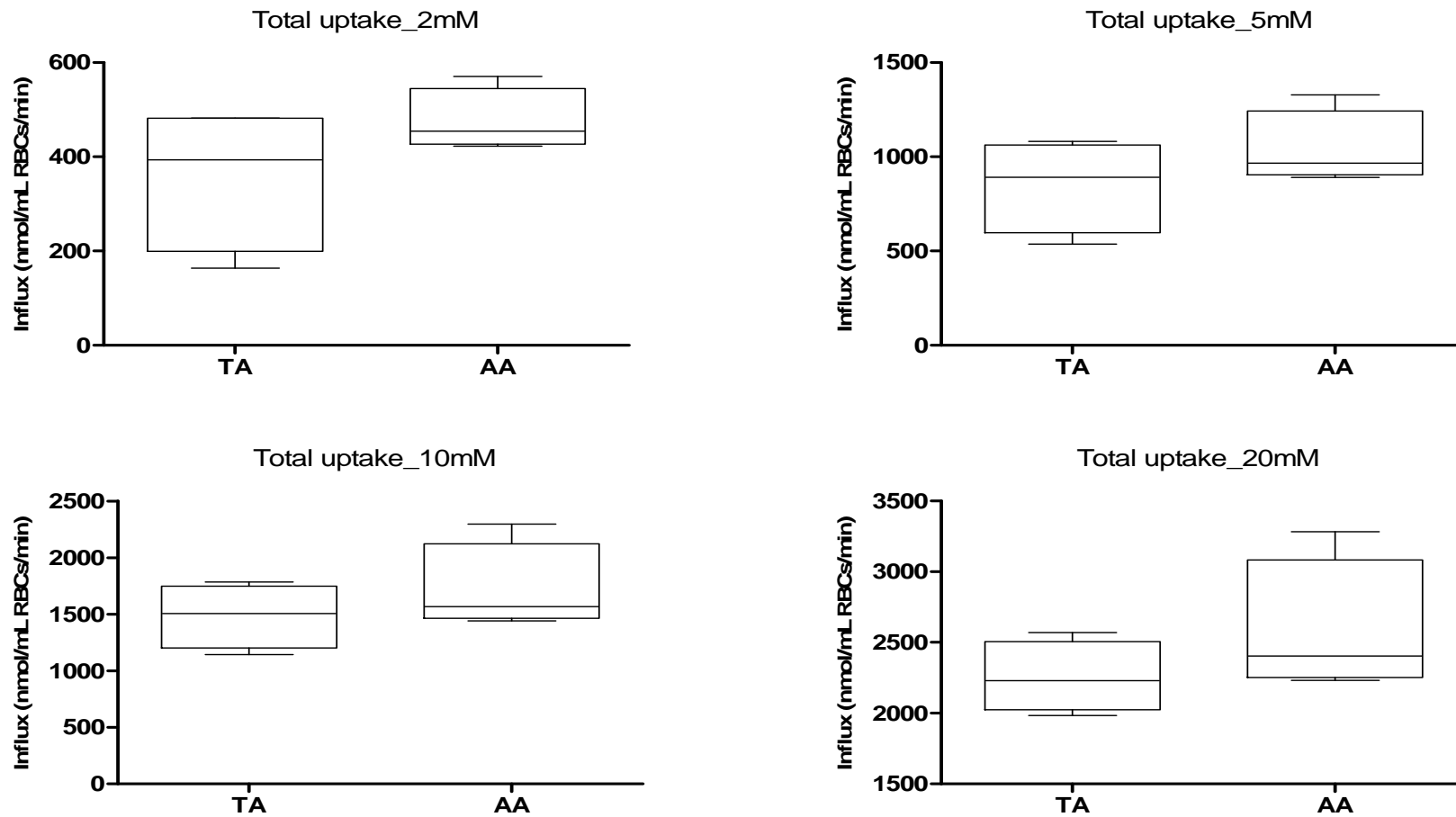


Table 43. The Mann Whitney U tests were performed to analyze the differences between TA and AA genotypes of the 1470 T>A (Asp490Glu) polymorphism in total lactate influx. Statistical significance was defined as $P < 0.05$.

| | TA versus AA | | | |
|---------------------------------------|------------------------|--------|--------|--------|
| | Total L-lactate Uptake | | | |
| | 2mM | 5mM | 10mM | 20mM |
| P value | 0.6857 | 0.6857 | 0.6857 | 0.3429 |
| Significant different? ($P < 0.05$) | No | No | No | No |

Figure 18. The MCT1-mediated lactate influx into RBC at four external L-lactate concentration in TA and AA groups of SLC16A1 gene. There were no significant differences between groups at all four external lactate concentration (**Table 44**).

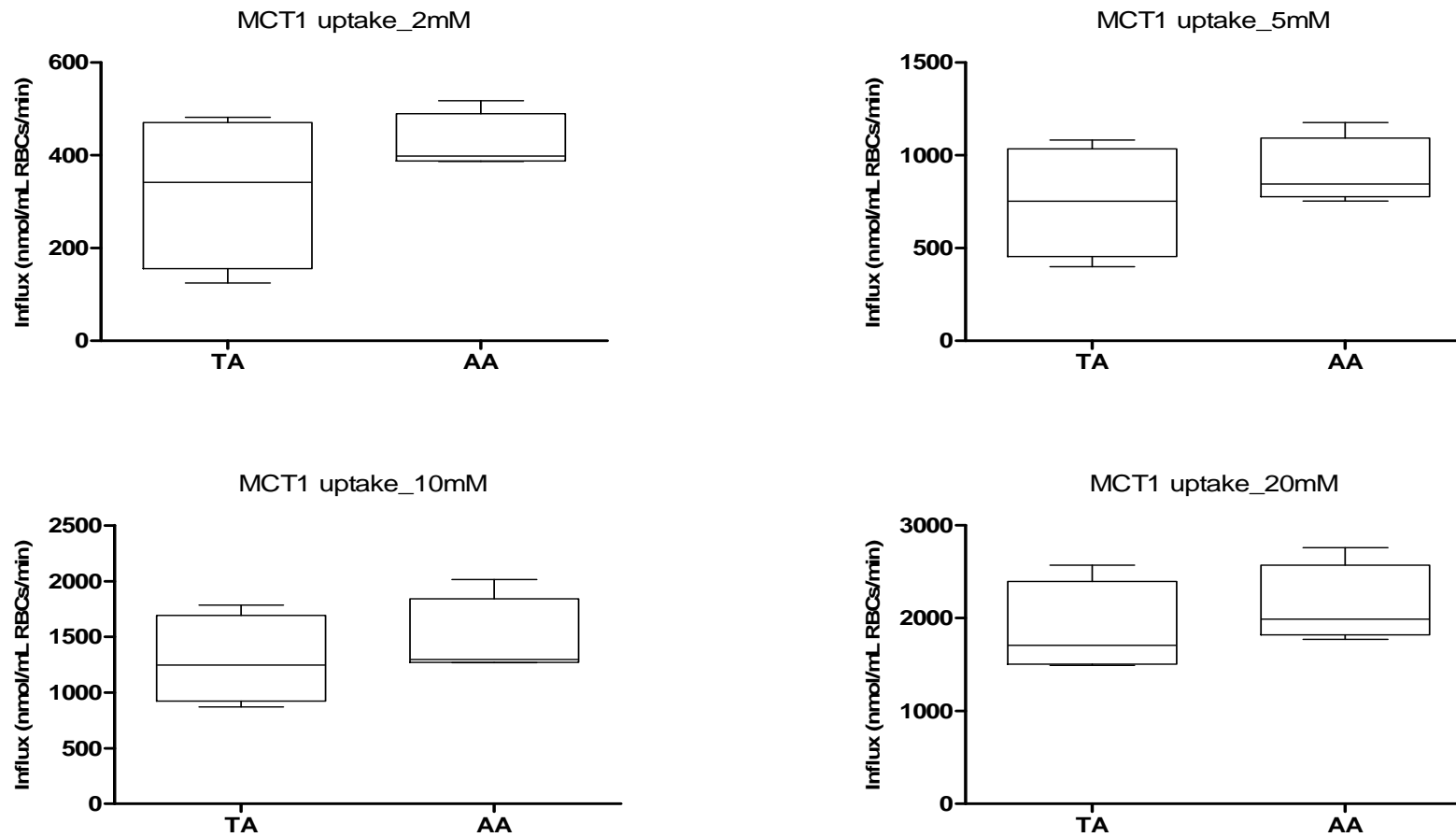


Table 44. The Mann Whitney U tests were performed to analyze the differences between TA and AA genotypes of the 1470 T>A (Asp490Glu) polymorphism in MCT1-mediated lactate influx. Statistical significance was defined as $P < 0.05$.

| | TA versus AA | | | |
|---------------------------------------|-----------------------|--------|--------|--------|
| | MCT1 L-lactate Uptake | | | |
| | 2mM | 5mM | 10mM | 20mM |
| P value | 0.6857 | 0.6857 | 0.6857 | 0.3429 |
| Significant different? ($P < 0.05$) | No | No | No | No |

Figure 19. The constant of Michaelis-Menten (K_m) for the total and MCT1-mediated lactate influx in in TA and AA groups of SLC16A1 gene. There were no significant differences between groups (**Table 45**).

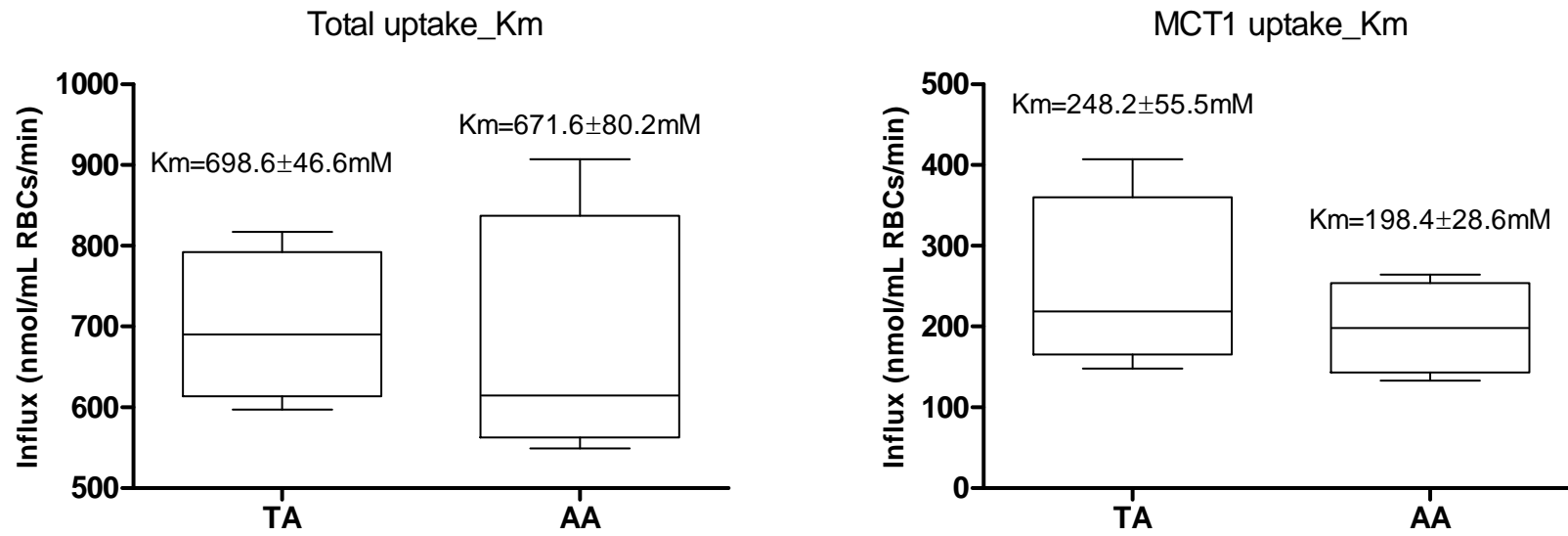


Table 45. The Mann Whitney U tests were performed to analyze the differences of the Km between TA and AA genotypes of the 1470 T>A (Asp490Glu) polymorphism. Statistical significance was defined as $P < 0.05$.

| | TA versus AA | |
|---------------------------------------|----------------------|------------------------------|
| | Total lactate influx | MCT1-mediated lactate influx |
| P value | 0.6857 | 0.8857 |
| Significant different? ($P < 0.05$) | No | No |

Figure 20. The maximal lactate transport capacity (V_{max}) for the total and MCT1-mediated lactate influx in in TA and AA groups of SLC16A1 gene. There were no significant differences between groups (**Table 46**).

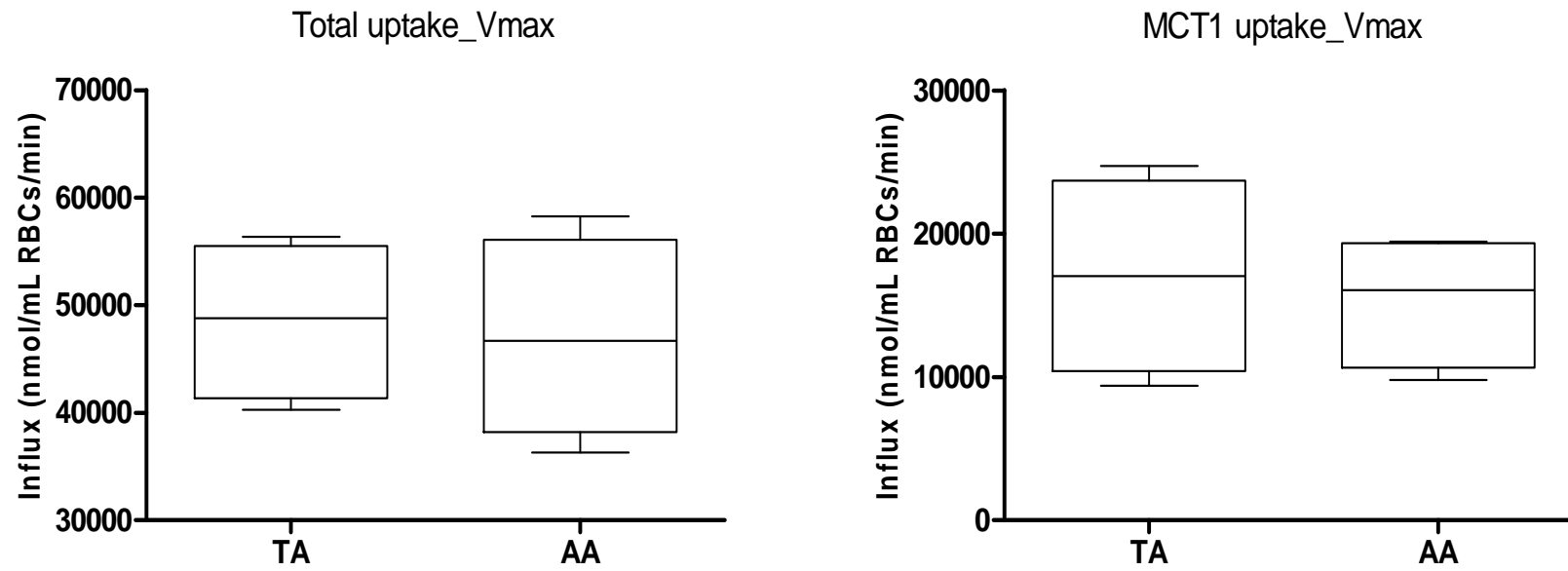


Table 46. The Mann Whitney U tests were performed to analyze the differences of the Vmax between TA and AA genotypes of the 1470 T>A (Asp490Glu) polymorphism. Statistical significance was defined as $P < 0.05$.

| | TA versus AA | |
|---------------------------------------|----------------------|------------------------------|
| | Total lactate influx | MCT1-mediated lactate influx |
| P value | 0.8857 | 0.6857 |
| Significant different? ($P < 0.05$) | No | No |

4.3 DISCUSSION

Transport of lactate across the erythrocyte membrane is mediated by three distinct pathways: 1) nonionic diffusion of lactic acid, 2) inorganic anion exchange (band 3), and 3) a monocarboxylate-specific carrier mechanism [94, 162, 163]. The significance of each of these pathways with regard to lactate transport is varied among species [72, 94]. The monocarboxylate-specific carrier is the major pathway for lactate transport in the RBC of humans, rabbits, and rats. However, the band 3 system is the preferred pathway in ox's RBC, which contributed in 53% of lactate transport. In humans, MCT1 is the only MCT isoform expressed on the RBC membrane. The MCT1 mechanism accounts for 90% of lactate flux across human erythrocyte membrane, while band 3 system and passive diffusion contribute for the remaining 10% of the lactate influx [162].

The first objective of this study was to examine the interindividual variation in total and MCT1-mediated lactate influx into human erythrocytes in the local Chinese population. We have previously genotyped the MCT1 gene in the ethnic Chinese and Indian groups of Singapore population and a common nonsynonymous polymorphism, 1470 T>A (Asp490Glu) had been identified in MCT1 gene (**Table 10**). With knowledge that MCT1 responsible up to 90% of lactate influx into RBC, it would be intriguing to correlate the *in vitro* uptake assay with the MCT1 polymorphism. Therefore, the second objective of this study was to examine the polymorphism-phenotype association of MCT1 gene.

4.3.1 Interindividual variation in Total and MCT1-mediated lactate influx

Low interindividual variability was observed in the total lactate influx in the ten Chinese subjects as the Coefficient of Variation (CV) of total lactate influx at all external lactate levels were lower than 30% (**Table 41**). The MCT1-mediated lactate influx exhibits higher interindividual variability as compared to the total lactate influx (**Table 41** and **Table 42**). Nonetheless, the CVs of lactate influx are lower than 30% at all external lactate levels except at 2 mM and 700 mM.

Therefore, the variability in L-lactate influx into RBC is low in this 10-grouped data. In this study, the uptake measurements were performed by incubating the erythrocytes with lactate concentrations up to 700 mM. Even though incubation times were short (20 seconds), this is a hypertonic medium and might affect uptake the measurements. Unfortunately, we could not find a suitable control to elucidate this experimental limitation. However, as explain in **Section 3.3.1**, it is essential to estimate the K_m and V_{max} on the range of substrate concentrations over which the transport activity reaches saturation to prevent erroneous. Therefore, we further extended the exogenous L-lactate concentrations up to 700 mM. The K_m value reported in this study was much higher than the K_m values reported by previous study but in accordance to our previous finding (**Fig. 13**). The possible explanations of these disparities have been explained in **Section 3.3.1**. Nonetheless, the finding of this study suggests that lactate transport across RBC membrane is a low affinity but high capacity transport process. Low interindividual variability was observed in the total and MCT-1 mediated lactate influx in the ten Chinese subjects.

4.3.2 Polymorphism-phenotype association of MCT1 gene

The second objective was to examine the relationship of 1470 T>A (Asp490Glu) variant with erythrocyte lactate transport activity. In this study, we examined the effect of this polymorphism on lactate influx into human erythrocytes. Among the eight Chinese samples studied, 0 (0%) samples were homozygous wildtype (TT), 4 (50%) samples were heterozygous mutants (TA) and 4 (50%) were homozygous mutants (AA). The influence of genetic polymorphism in total lactate influx and MCT1-mediated lactate influx were compared at 2, 5, 10 and 20 mM of external L-lactate concentrations. The total and MCT1-mediated lactate influx appeared to be lower in TA group (**Fig. 17** and **Fig. 18**) as compared to AA group at all external lactate concentrations, but the differences were not statistically significant. In addition, a higher K_m value was observed in the TA group as compared to the AA group in MCT1-mediated lactate influx (**Fig. 19**). However, no statistical difference was observed between two genotypic groups. Nonetheless, the finding of this data suggested that T allele may have a defective effect in transport function and appear to have a lower transport activity. The data in our study is supported by previous study[206]. Recently, the influence of 1470 T>A (Asp490Glu) polymorphism in high intensity circuit training has been studied [206]. The authors concluded that the carriers of T allele seem to exhibit a lower lactate transport activity [206], which is consistent with our finding. This finding contradicts with the result obtained using PolyPhen and SIFT algorithms, which predicted the 1470 T>A (Asp490Glu) polymorphism to be benign. Nishimura and Balch reported that a di-acidic signal (asp-x-glu; where x represents any amino acid) on the cytoplasmic tail of vesicular stomatitis virus glycoprotein (VSV-G) and other cargo molecules is required for selective release from the endoplasmic reticulum [205].

The glutamate residue at position 490 is located in the signal sequence (asp-x-glu; aa 488-490) for release from the endoplasmic reticulum when downstream from a tyr-x-x-φ motif [205]. Although glutamic acid and aspartic acid are both amino acids with similar physical-chemical properties, it is likely that aspartic acid may not be as effective as the preferred glutamate. However, as the MCT1 expression level on RBC membrane was not quantified in this study, we could not conclude that a substitution from glutamate to aspartate at position 490 of MCT1 protein will reduce the MCT1 membrane expression, and resulting in lower lactate transport activity.

Linkage disequilibrium analysis revealed a complete disequilibrium between the 1470 T>A (Asp490Glu) and 2917 C>T polymorphisms. Therefore, the genotype distribution of 2917 C>T was screened to study the haplotype-phenotype association of *SLC16A1* gene. The genotyping data revealed that the “T” allele of 1470 T>A (Asp490Glu) polymorphism was consistently inherited with the “C” allele of 2917 C>T variant. From our observation, the ATC haplotype predicted from haplotype analysis of *SLC16A1* gene (**Table 17**) may be associated with the lower lactate transport activity in the erythrocyte. Therefore, the apparent higher K_m for this particular ATC haplotype shows that the T allele may be associated with the reduced activity of MCT1, which is supported by previous study [206].

The differences found between TA and AA genetic groups were found to be not statistically significant. As only ten subjects were recruited in this study, the lack of statistical significance may be due to the small sample size. Besides, all the subjects recruited in this study were the carriers of A allele (TA or AA genotype).

No homozygous wildtype (TT genotype) subjects were identified. As result of it, the gene dose effect of TT genotype cannot be examined in this study. Therefore, additional studies involving larger samples will be required to establish the clinical impact of genetic polymorphism in *SLC16A1* gene.

4.3.3 Summary

The main findings of the present study were that 1) low interindividual variations were observed in the total lactate influxes and MCT1-mediated lactate influx across RBC membrane in the local Chinese population; 2) human MCT1 system exhibited a low affinity but high capacity transport mechanism for the transport of lactate into RBC; and 3) the T allele of 1470 T>A (Asp490Glu) polymorphism may have a defective effect in the transport activity of MCT1.

CHAPTER 5

**A RANDOMIZED CROSSOVER STUDY TO EVALUATE THE
POTENTIAL INFLUENCE OF MCT1 AND ITS INHIBITOR,
DIFLUNISAL, ON THE DISTRIBUTION OF LACTATE
IN PLASMA AND ERYTHROCYTE IN HEALTHY MALE ADULTS**

OVERVIEW

The objective of this study was to clinically examine the effect of monocarboxylate transporter 1 inhibitor, diflunisal, on lactate distribution in plasma and erythrocyte. This was a single-centre, randomized, 2 period crossover drug interaction study conducted in 10 healthy adult male volunteers. In this study, a single dose infusion of sodium lactate was given to each eligible subject at infusion rate of 5.6 mg/kg/min for 30 min. A dose regimen of 500 mg of diflunisal or placebo was administered to the subjects twice daily 2 days prior to the day of dosing and in the morning on the day of dosing. Blood for L-lactate analyses was sampled at predose, 10, 20, 30, 40, 50, and 60 min after sodium lactate infusion. We observed small differences between placebo RBC and diflunisal RBC lactate levels. The $\text{RBC:Plasma [La]}^{\text{Diflunisal}}$ ratios were constantly lower than $\text{RBC:Plasma [La]}^{\text{Placebo}}$ ratios after 20 min of the onset of infusion. These differences, however, were not statistically significant. In conclusion, the results from this study show that therapeutic recommended dose of diflunisal is insufficient to inhibit lactate transport in blood. The reason of this may due to the high protein binding property of diflunisal.

5.1 MATERIALS AND METHODS

5.1.1 Study Design

This was a single-center (Investigated Medicine Unit, National University Health System, designated IMU), randomized, 2 period crossover drug interaction study conducted in 12 healthy male volunteers. The subjects were randomly divided into two groups: A and B, with 6 in each group. The 12 subjects underwent the following treatments in 2 periods:

Period 1: administered a single dose infusion of sodium lactate (5.6 mg/kg/min for 30 min). Diflunisal (Apo-Diflunisal, Apotec Inc. Canada, 500 mg) or placebo was administered to the subjects twice daily 2 days prior to the day of dosing and in the morning on the day of dosing.

Period 2: administered a single dose infusion of sodium lactate (5.6 mg/kg/min for 30 min). Diflunisal (Apo-Diflunisal, Apotec Inc Canada, 500 mg) or placebo was administered to the subjects twice daily 2 days prior to the day of dosing and in the morning on the day of dosing.

Subjects were asked to fast from all food and drink (except water) for at least 10 hours prior to dosing with study medication until 1 hour after dosing. Each oral medication was administered with 250mL of water. Subjects were asked not to break, crush, or chew the diflunisal tablet before swallowing. Blood samples were collected at regular intervals as indicated in **Table 47** and **Table 48**. A washout period of 7 days was incorporated between the study periods to avoid the influence of previously administered drug(s).

Table 47. Study Plan- Period 1

| Time relative to dose | 1st Screening visit | Subject admission / Pretreatment | | | | | Pharmacokinetic study duration | | | | | | | | | | Final evaluation |
|--|---------------------|----------------------------------|--------|--------|--------|--------|--------------------------------|---------|---|--------|--------|--------|--------|--------|--------|--------|------------------|
| | Day -15 | -Day 2 | | -Day 1 | | | Day 1 | | | | | | | | | | > 60 min |
| | | -50 hr | -38 hr | -26 hr | -14 hr | -11 hr | -2 hr | -10 min | 0 | 10 min | 20 min | 30 min | 40 min | 50 min | 60 min | | |
| Informed consent | • | | | | | | | | | | | | | | | | |
| Review eligibility | • | • | | | | | | • | | | | | | | | | |
| Inpatient at study unit | | | | | ← | | | | | | | | | | | → | |
| Medical/Drug history | • | • | | | | | | | | | | | | | | | |
| Seated vital signs | • | • | | | | | | • | | | | | | | | • | |
| Physical examination | •complete | •brief | | | | | | • | | | | | | | | •brief | |
| Clinical lab tests | • | | | | | | | | | | | | | | | | |
| Regulated food and water intake | | | | | | • | | | | | | | | | | | |
| Administration of Sodium lactate infusion | | | | | | | | • | | | | | | | | | |
| Administered with Diflunisal (A) or Placebo (B) | | • | • | • | • | | • | | | | | | | | | | |
| Venous blood sampling for lactate measurement | | | | | | | | • | | • | • | • | • | • | • | | |
| Venous blood sampling for pH and CO ₂ measurement | | | | | | | | • | | | | • | | | • | | |
| AEs/SAEs monitoring | | • | • | • | • | • | • | • | • | • | • | • | • | • | • | • | |

Table 48. Study Plan- Period 2

| Time relative to dose | Subject admission / Pretreatment | | | | | Pharmacokinetic study duration | | | | | | | | | | Final evaluation |
|--|----------------------------------|--------|--------|--------|--------|--------------------------------|---------|---|--------|--------|--------|--------|--------|--------|----------|------------------|
| | Day 8 | | Day 9 | | | Day 10 | | | | | | | | | | |
| | -50 hr | -38 hr | -26 hr | -14 hr | -11 hr | -2 hr | -10 min | 0 | 10 min | 20 min | 30 min | 40 min | 50 min | 60 min | > 60 min | |
| Review eligibility | • | | | | | | • | | | | | | | | | |
| Inpatient at study unit | | | | ← | | | | | | | | | | | | → |
| Medical/Drug history | • | | | | | | | | | | | | | | | |
| Seated vital signs | • | | | | | | • | | | | | | | | | • |
| Physical examination | • brief | | | | | | • | | | | | | | | | • brief |
| Clinical lab tests | | | | | | | | | | | | | | | | |
| Regulated food and water intake | | | | | • | | | | | | | | | | | |
| Administration of Sodium lactate infusion | | | | | | | | • | | | | | | | | |
| Administered with Diflunisal (B) or Placebo (A) | • | • | • | • | | • | | | | | | | | | | |
| Venous blood sampling for lactate measurement | | | | | | | • | | • | • | • | • | • | • | | |
| Venous blood sampling for pH and CO ₂ measurement | | | | | | | • | | | | • | | | | • | |
| AEs/SAEs monitoring | • | • | • | • | • | • | • | • | • | • | • | • | • | • | • | • |

5.1.2 Subject Selection

Twelve male healthy volunteers aged 32.5 ± 4.5 years old (mean \pm s.d.) and weighing 78.3 ± 6.8 kg (mean \pm s.d.) entered the study. One subject was dropped from the study due to medical condition (high blood pressure). Another subject was excluded from analysis due to blood clotting which affected the actual lactate concentration. Hence, a total of 10 subjects were included in the study. All were nonsmokers with no history of serious illness. Subjects with a medical history of psychiatric disorders or allergy to diflunisal and other NSAIDs were excluded from the study. Their health to be judged to be normal following a physical examination and routine biochemical tests of hepatic and renal function. No medications were permitted for at least 2 weeks immediately before and during each study period. The volunteers were also told to abstain from alcohol 48 hours before and throughout the study period. The study was approved by the DSRB, National Healthcare Group. The written informed consent was obtained from each subject prior to the study. For the inclusion/exclusion criteria and other details of the trial, please refer to the full clinical study protocol in **Appendix II**.

5.1.3 Sample Size Calculations

A total of twelve subjects were recruited in this study. The sample size was calculated based on a 80% power analysis estimates that a minimum number of $N=8$ is required to detect a minimum difference of 30% in plasma, whole blood and RBCs lactate levels (mean plasma lactate = 16.7 ± 3.81 mmol/l; mean erythrocyte lactate = 8.0 ± 2.42 mmol/l; mean whole blood lactate = 12.4 ± 2.42 mmol/l), at a level of significance of $p=0.05$. In case of discontinuing, loss to

follow-up, or any other cause for the subjects not to accomplish this study, the number of subject was increased to N=12.

5.1.4 Blood Sampling

Blood for L-lactate analyses was sampled at predose, 10, 20, 30, 40, 50, and 60 min after sodium lactate infusion (**Table 36 and Table 37**). For each pharmacokinetics time point, 10 ml of blood was drawn into 3 heparinized tubes. Blood sample were immediately submerged in ice-ethanol slurry (-20°C) for 60 seconds and then placed on ice (Note: The equilibration of L-lactate across the erythrocyte occurred quickly at 37°C (~10 minutes), but the equilibration is greatly slowed at 0°C, taking as long as 100 hours). One tube of blood sample was centrifuged at 4000 rpm for 10 min at 4°C. We transferred 100 µL of plasma, erythrocyte and whole blood to each of the Eppendof tubes containing 400 µL of Lactate Assay Buffer (BioVision, Mountain View, CA, USA). The lyzed samples were transferred to a 10kD spin column (Merck Millipore, Billerica, Massachusetts, USA) and spun at 4000 rpm for 10 min at 4°C. The plasma, whole blood and erythrocyte extracts were sent immediately for lactate analysis.

5.1.5 Lactate Analysis

Lactate concentrations were measured in duplicate using a lactate kit (BioVision, Mountain View, CA, USA). The test samples were prepared at 50 µL per well with Lactate Assay Buffer in a 96-well plate. 10 µL of sample was added into each well individually and the volume was adjusted to 50 µL per well. For each well, Reaction Mix (containing 46 µL Lactate Assay Buffer, 2 µL Lactate Substrate Mix

and 2 μL Lactate Enzyme Mix) was added and mixed well. The reaction mix was incubated for 30 min at room temperature and measured at OD 450 nm wavelength using μQuant Universal Microplate Spectrophotometer (ITS). The background was corrected by subtracting the value derived from the zero lactate control and calculated the lactate concentrations of the test sample using the formula:

$$C = \text{La/Sv} * D \text{ (nmol/}\mu\text{L or mM)}$$

Where: **La** is the lactate amount (nmol) of test sample from standard curve.

Sv is the sample volume (μL) added into the well.

D is the dilution factor.

5.1.6 Statistical analysis

Unless otherwise indicated, all data are expressed as mean \pm SEM. Student's *t*-test was used to determine the significance of differences between placebo and treatment group means. Statistical significance was defined as $P < 0.05$.

5.2 RESULTS

5.2.1 Plasma and Erythrocyte Lactate Levels

Figure 13 shows the mean concentration of plasma and erythrocyte lactate over time in response to exogenous lactate infusion in ten subjects pre-treated with diflunisal or placebo. For the plasma and erythrocyte lactate level of individual subjects, please refer to **Appendix III**. An exogenous lactate infusion rate of 5.6 mg/kg/min was given to each eligible subject for 30 minutes. As shown in **Fig. 21** the plasma and erythrocyte lactate levels were elevated from the start of infusion and reached maximum at 30 minutes, and gradually returned to normal resting level at 60 minutes after the start of lactate infusion. The mean lactate level was statistically significantly elevated from 1.00 to 2.31 mmol/L H₂O⁻¹ in placebo plasma, 1.05 to 2.32 mmol/L H₂O⁻¹ in diflunisal plasma, 0.80 to 1.65 mmol/LH₂O⁻¹ in placebo RBC and 0.76 to 1.59 mmol/L H₂O⁻¹ in diflunisal RBC. No significant differences were observed between the plasma lactate levels of placebo- and diflunisal-treated groups (**Table 49**). The difference between the RBC lactate levels of placebo- and diflunisal-treated groups is not statistically significant different at all time points except at 60 min (**Table 49**).

The plasma and erythrocyte AUC_{0-1h} values were calculated by trapezoidal rule integration (**Fig. 22** and **Table 50**). There were no significant alterations in the plasma AUC_{0-1h} values between the placebo and diflunisal groups (111.9 ± 5.04 vs. 111.4 ± 1.17). The value of RBC AUC_{0-1 hr} in the placebo-treated group is slightly higher than the AUC_{0-1 hr} of the diflunisal-treated group (85.30 ± 2.92 vs. 82.20 ± 6.53). This difference, however, is not statistically significant. The mean peak plasma and RBC concentration was occurred at 30 min after the onset of

lactate infusion for both placebo-treated and diflunisal-treated groups (**Table 50**).

The peak plasma concentration was not significantly altered in the diflunisal-treated group as compared to the placebo-controlled group. Similarly, no difference was observed in the peak RBC L-lactate concentration in both groups.

Figure 21. The plasma and RBC compartmental profiles (mean \pm S.E.M.) of L-lactate in the subjects pretreated with placebo and diflunisal during lactate infusion (0 to 30 min) and during recovery (30 to 60 min) The mean plasma and RBC lactate levels were significantly increased above the rest value (zero time point) at 30 min in placebo and diflunisal groups. The statistical comparison was performance using paired student's t-test (Table 49). The mean plasma lactate concentration values were not significantly different between two treatment groups at all time points. The mean RBC lactate concentration values were not significantly different between two treatment groups at all time points except at 60 min. Values are presented as mean \pm SEM.

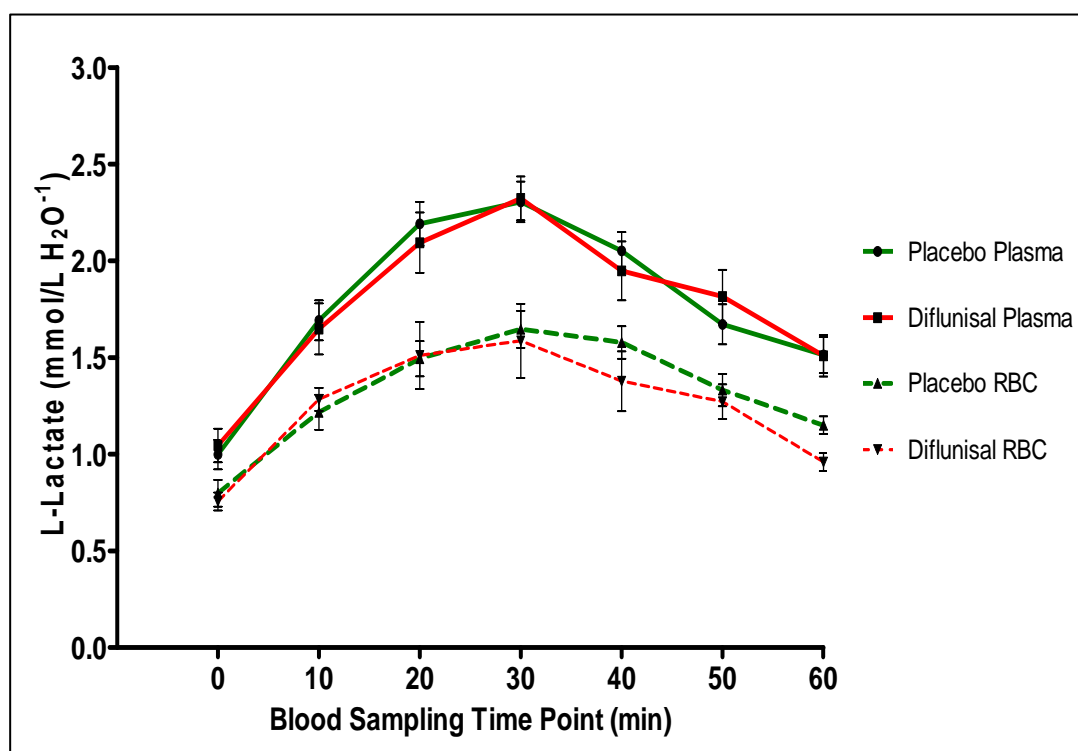


Table 49. The paired t tests were performed to test for the effect of diflunisal in L-lactate distribution in plasma and RBC. The statistical significance was defined as $p < 0.05$.

| Time point (min) | Placebo versus Diflunisal | | | | | | |
|------------------|---------------------------|--------|--------|--------|--------|--------|---------|
| | 0 | 10 | 20 | 30 | 40 | 50 | 60 |
| Plasma | 0.6370 | 0.8013 | 0.5745 | 0.8996 | 0.6310 | 0.4184 | 0.9023 |
| RBC | 0.7175 | 0.4465 | 0.8411 | 0.6077 | 0.2985 | 0.8589 | 0.0224* |

Figure 22. The total area under the curve (AUC) of plasma and RBC lactate levels in the subjects pretreated with placebo and diflunisal. The plasma and RBC values were not significantly different between two treatment groups. Values are represented as mean \pm S.E.M. * $p < 0.05$, statistically significant

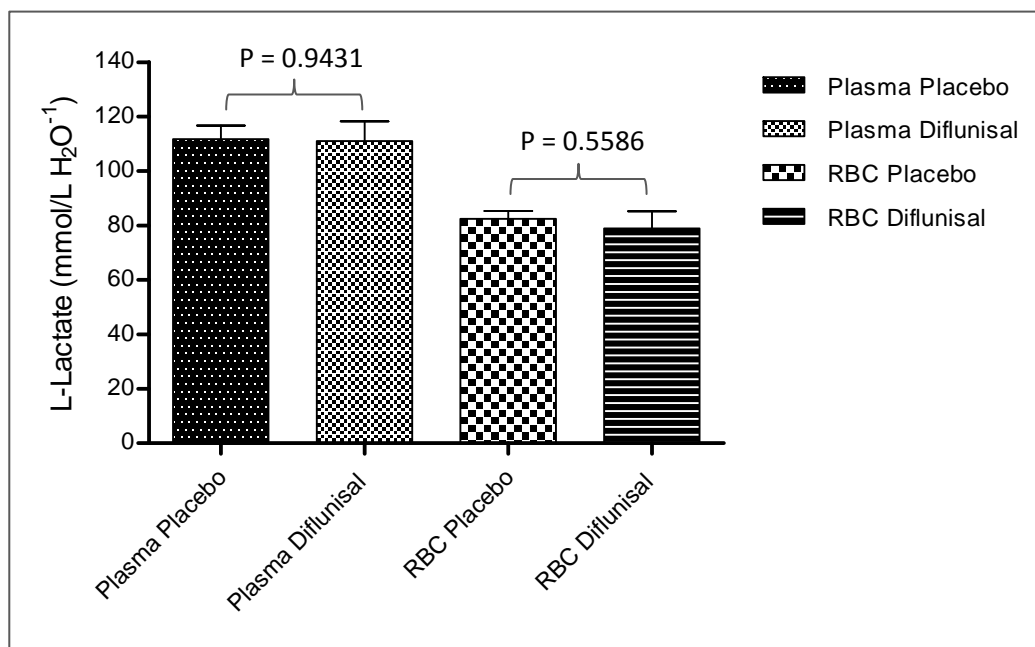


Table 50. Pharmacokinetic parameters for L-lactate in placebo- and diflunisal-treated groups (mean \pm S.E.M)

| | Placebo plasma | Diflunisal plasma | Placebo RBC | Diflunisal RBC |
|--|-------------------|-------------------|-------------------|-------------------|
| AUC _{0-1 hr} (mmol/L H ₂ O ⁻¹ Hr) | 111.9 \pm 5.04 | 111.4 \pm 1.17 | 85.30 \pm 2.92 | 82.20 \pm 6.53 |
| Cmax (mmol/L H ₂ O ⁻¹) | 2.300 \pm 0.105 | 2.320 \pm 0.114 | 1.660 \pm 0.096 | 1.580 \pm 0.191 |
| Tmax (min) | 30 | 30 | 30 | 30 |

5.2.2 Plasma to RBC Lactate Ratio

Figure 23 shows the ratio of plasma to erythrocyte lactate over time in response to exogenous lactate infusion in ten subjects pre-treated with diflunisal or placebo. The RBC:Plasma $[La]^{Placebo}$ ratio was relatively constant throughout the infusion and recovery period (ranging from 0.72 ± 0.07 to 0.82 ± 0.06). The RBC:Plasma $[La]^{Diflunisal}$ ratio was lower than the RBC:Plasma $[La]^{Placebo}$ ratio at rest (zero time point). However, the RBC:Plasma $[La]^{Diflunisal}$ ratio elevated above the RBC:Plasma $[La]^{Placebo}$ ratio at 10 minutes and decreased again and eventually dropped below the RBC:Plasma $[La]^{Placebo}$ ratio at 30 minutes. Although the RBC:Plasma $[La]^{Diflunisal}$ ratio was constantly lower than the RBC:Plasma $[La]^{Placebo}$ ratio at all time points except 10 and 20 min, the differences were not statistically significant for all time points (**Table 51**).

Figure 23. Plasma to RBC lactate ratio during exogenous lactate infusion (0 to 30 min) and during recovery period (30 to 60 min). The differences were not statistically significant for all time points. Values are presented as mean \pm SEM.

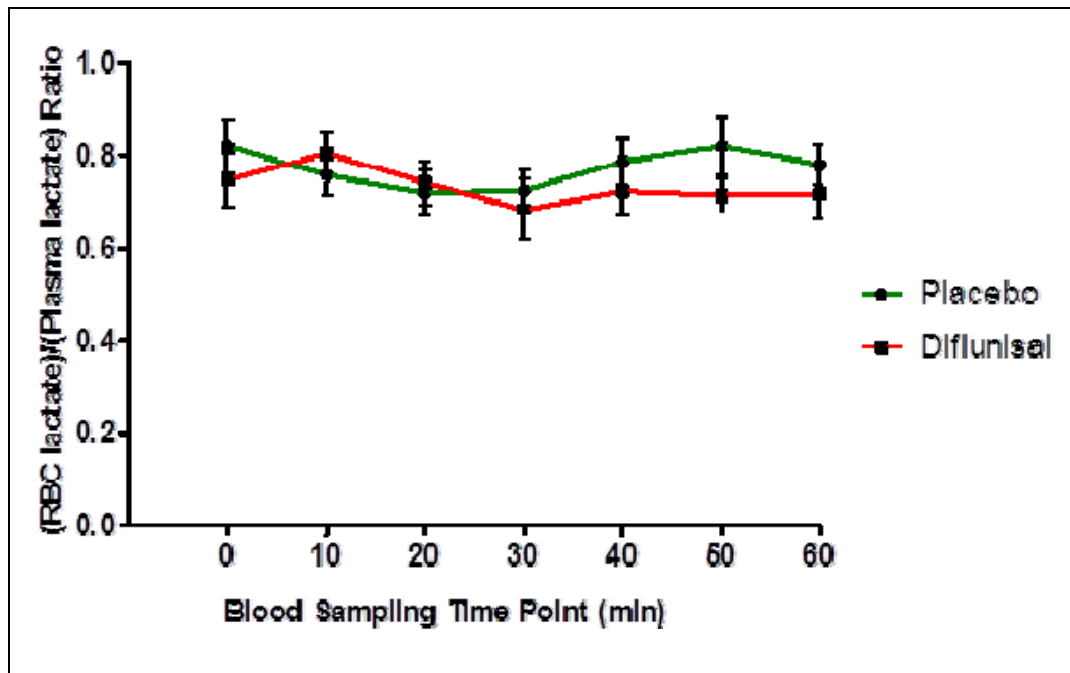


Table 51. The paired *t* tests were performed to analyze the differences of plasma to RBC lactate ratio between placebo and diflunisal groups. The statistical significance was defined as $p < 0.05$.

| Time point (min) | Placebo versus Diflunisal | | | | | | |
|--|---------------------------|--------|--------|--------|--------|--------|--------|
| | 0 | 10 | 20 | 30 | 40 | 50 | 60 |
| <i>p</i> -value | 0.0977 | 0.6522 | 0.8262 | 0.3785 | 0.2717 | 0.2294 | 0.2277 |
| Significant different? ($P < 0.05$) | no | no | no | no | no | no | no |

5.3 DISCUSSION

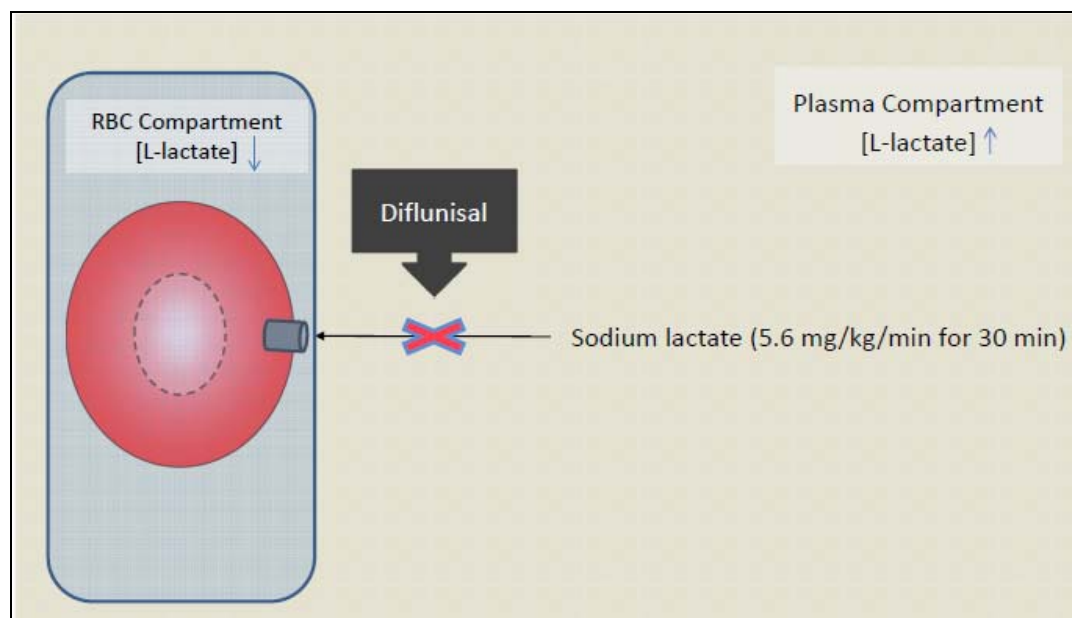
The bulk of evidence suggests that lactate is an important intermediary in numerous metabolic processes. It was previously considered as the dead-end waste product of glycolysis [233], the primary cause of the O₂ debt following exercise [234], a major cause of muscle fatigue [146], and a key factor in acidosis-induced tissue damage. However, the role of lactate has been redefined since the introduction of the lactate hypothesis by George Brooks [235]. The bulk of evidence suggests that lactate is an important mobile fuel for main organs (such as heart, active muscle and brain) and is also involved in the process of wound repair and regeneration.

The blood constitutes a key component in the lactate shuttle because of its role in distributing lactate throughout the body's different tissues. During exercise, lactate is transported out from the active muscle into the plasma. From plasma, lactate is further transported into the red cell compartment and subsequently distributed to different tissues in the body. Given that the MCT1-specific carrier system has been shown to be the predominant route for lactate transport in human erythrocytes, any impairment in MCT1 activity may have far-reaching consequences. The defect in MCT1 transport activity could be due to genetic variations or blocking of transport function by inhibitors. In fact, the defect in MCT1 has been associated with lactate transport deficiency in red cells and muscle tissues by Fishbein back in 1986 [171]. Although several potent MCT1 inhibitors have been reported [109, 110, 236], the *in vivo* effects of these inhibitors have not been investigated. Therefore, it will be beneficial to clinically examine the physiological effect of MCT1-mediated lactate influx from plasma to erythrocyte.

5.3.1 The influence of diflunisal on L-lactate distribution in blood

In this study, the *in vitro* inhibitory effects of several pharmaceutical and dietary compounds were investigated (Table 38 and Fig. 10). Of which, diflunisal exhibited potent inhibitory effect and therefore was chosen as the inhibitor to block RBC lactate influx. It was hypothesized that diflunisal will block the *in vivo* L-lactate influx into human erythrocytes and therefore confer higher plasma L-lactate and lower erythrocyte L-lactate concentrations (Fig. 24). The new information provided by the present study consists of the lactate concentration of the plasma versus RBC fractions of the blood during exogenous L-lactate infusion with or without the influence of MCT1 inhibitor, diflunisal.

Figure 24. The illustration figure of diflunisal in inhibiting the L-lactate influx into human RBC. It is hypothesized that diflunisal will block the influx of L-lactate into human RBC and resulting in higher plasma lactate and lower RBC lactate concentrations.



In this study, a single dose infusion of sodium lactate was given to each eligible subject at infusion rate of 5.6 mg/kg/min for 30 minutes. The plasma lactate level was expected to increase to approximately 3-4 mmol/L H₂O⁻¹ based on the reference provided for several studies. However, the plasma lactate level was only increased by up to approximately 2.3 mmol/L H₂O⁻¹ in both groups. This could be due to the difference in the infusion period. In the study done by van Hall *et al.*, the subjects were given sodium lactate intravenous infusion at infusion rate of 5.6 mg/kg/min for 20 minutes, followed by infusion of 4.3 mg/kg/min for another 100 min. However, an infusion rate of 30 instead of 120 minutes was selected in this study because we were concerned that the infusion may cause discomfort and the amount of sodium lactate infused may increase the blood pressure of the subjects. Besides, the previous studies were designed for athletes who are physically trained. Therefore, a mild infusion rate was selected for the safety of the subjects. Nonetheless, the plasma lactate concentrations were significantly increased and reached maximum at the end of infusion (30 minutes) in both treatment groups (**Fig. 21**).

In this study, diflunisal was used to block MCT1 activity. A dose regimen of 500 mg was selected based on an assumption that the mean diflunisal plasma concentration following administration of 500 mg single oral dose is sufficient to inhibit MCT1 transport activity. Diflunisal exhibits a strong inhibitory effect on the uptake of L-lactate with a K_i value of 29.56 μM, which is equivalent to 7.4 μg/ml (**Table 39**). A pharmacokinetics study of diflunisal indicated that the peak plasma concentration of diflunisal is 87 μg/mL following a single 500 mg oral dose. A dose regimen of 1000 mg daily in divided doses has been approved for

maintenance therapy of rheumatoid and osteoarthritis. Therefore, a 1000 mg daily regimen was selected in order to achieve the maximum suppression on MCT1 activity.

We expected to see a decrease in RBC:Plasma [La] ratio in the diflunisal treatment group. As diflunisal blocks MCT1 activity, this will prevent lactate from entering RBCs. Consequently, the plasma lactate may increase as the influx into RBCs is blocked. In this study, we did not observe a higher plasma lactate level in the diflunisal group (**Fig. 22**). The diflunisal plasma lactate levels were not significantly different from the placebo plasma lactate levels at all time points (**Fig. 21** and **Table 49**). However, we observed small differences between placebo RBC and diflunisal RBC lactate concentrations. The diflunisal RBC lactate levels were constantly lower than placebo RBC lactate levels after 20 min of the onset of infusion. However, these differences were not statistically significant at all time point except at 60 minutes. The RBC:Plasma [La]^{Diflunisal} ratio was lower than the RBC:Plasma [La]^{Placebo} ratio at rest (zero time point). But the RBC:Plasma [La]^{Diflunisal} ratio elevated above the RBC:Plasma [La]^{Placebo} ratio at 10 minutes and decreased again and eventually dropped below the RBC:Plasma [La]^{Placebo} ratio at 30 minutes (**Fig. 23**). These differences, however, were not statistically significant (**Table 51**).

Although diflunisal has been reported as a potent MCT1 inhibitor and its inhibitory effect is achievable at clinically relevant concentrations, we did not observe a significant inhibitory effect in this study. To some extent, this finding is not unexpected. As diflunisal is highly protein bound in the plasma, the unbound

plasma concentration of diflunisal may be below its K_i value and therefore insufficient to inhibit lactate transport on RBC. The main limitation of this study is that the plasma diflunisal concentration was not quantified. Therefore, we could not conclude that the negative finding is due to insufficient unbound diflunisal concentration in the plasma.

The sample size was calculated based on a 80% power analysis estimates that a minimum number of $N = 8$ is required to detect a minimum difference of 30% in plasma, whole blood and RBCs lactate levels (mean plasma lactate = 16.7 ± 3.81 mmol/l; mean erythrocyte lactate = 8.0 ± 2.42 mmol/l; mean whole blood lactate = 12.4 ± 2.42 mmol/l) [237]. It is possible that this is an overestimation of the actual inhibitory effect of diflunisal on the transport activity of human MCT1 *in vivo*.

Nonetheless, the 30% change in RBC plasma level may be apparent if the sample size is increased. In this study, an infusion period of 30 minutes instead of 120 minutes was selected because we were concerned of the safety of the subjects. This infusion rate might be too short and the extending of the infusion period could have caused a positive result. Last but not least, there might be another rescue pathways or transporters that mediating L-lactate transport into human erythrocyte when the MCT1 pathway is blocked. Therefore, the observed inhibitory effect of diflunisal on human MCT1 activity is smaller.

In this study, the PCR amplification of three subjects was unsuccessful despite several attempts were made to purify and improve the DNA quality. Therefore, the effect of 1470 T>A (Asp490Glu) was not examined in this study because it is likely that power may have limited the interpretation of key findings when $n = 7$.

Several potent MCT1 inhibitors have been identified in our lab. These inhibitors, namely diclofenac, meclofenamic acid and tolfenamic acid have stronger inhibitory effects than diflunisal (**Table 38**). The peak plasma level of diclofenac achieved from multiple doses (oral 50 mg was administered 3 times daily for 7 days) was 2.3 µg/mL [218], while the K_i value of diclofenac is 6.17 µM (~1.96 µg/mL). Although the inhibitory concentration of diclofenac is achievable from the oral intake, the peak plasma concentration is only slightly higher than its K_i value. Therefore, diclofenac was not selected in this study. Meclofenamate and tolfenamate were not selected as study drugs because these inhibitors had only been identified a few weeks before the initiation of the trial. However, these two inhibitors can be considered as potential MCT1 inhibitors for future studies.

The second objective of the study was to evaluate the impact of the genetic variation in *SLC16A1* gene on the distribution of lactate and on drug interaction with diflunisal. However, the genotyping was unsuccessful in three out of ten subjects due to the substandard quality of DNA samples. Therefore, the genotype-phenotype association of MCT1 was not evaluated in this study.

5.3.2 Summary

In conclusion, the results from this study show that therapeutic recommended dose of diflunisal was insufficient to inhibit lactate transport on RBC. The reason for this may be due to high protein binding property of diflunisal. The unbound plasma concentration of diflunisal may be below its K_i value and therefore insufficient to inhibit lactate transport on RBC. However, this assumption cannot be verified because the plasma diflunisal level was not measured in this study. Nevertheless, we observed small differences between placebo RBC and diflunisal RBC lactate levels. The RBC:Plasma $[La]^{Diflunisal}$ ratios were constantly lower than RBC:Plasma $[La]^{Placebo}$ ratios after 20 min of the onset of infusion. These differences, however, were not statistically significant.

CHAPTER 6
CONCLUSION

6.1 Conclusion

The monocarboxylate transporter 1 and 4 mediate the transport of metabolically important monocarboxylates, such as lactate, pyruvate and butyrate. Given that MCT1 and MCT4 have been implicated in lactate shuttle transport, any impairment in transport activity may have far reaching consequences. The changes in transporter kinetics (e.g. genetic polymorphisms, food/drug-transporter interactions and disease-altered expression) may potentially lead to large shifts in the efficacy-toxicity relationship of a drug. Therefore, the impacts of pharmacogenetics and food/drug-transporter interactions on monocarboxylate transports were examined in this study. A summary of findings was summarized in **Table 52**.

For the past decades, no significant progress has been made in the discovery of MCT1 and MCT4 polymorphisms and the assessment of allelic frequencies. Therefore, the first objective of this project was therefore to describe the genetic polymorphism in the promoter, exons, and exon-intron junctions of *SLC16A1* and *SLC16A3* genes that may be present in the ethnic Chinese and Indian groups of Singapore population. To our knowledge, this is the first report on the comprehensive analysis of *SLC16A1* and *SLC16A3* genes in any population. Although genotyping were carried out on both *SLC16A1* and *SLC16A3* genes, this thesis focuses only on the functional characterization of MCT1.

A total of 21 genetic variations, including 14 novel ones, were found in *SLC16A1* gene. Of the 3 nonsynonymous variants, only 303T>G (Ile101Met) was predicted by PolyPhen and SIFT as having a potentially damaging effect on protein function, whereas 1282 G>A (Val428Ile) and 1470 T>A (Asp490Glu) were speculated to be

benign. Three reported SNPs, namely IVS3-17A>C, 1470T>A (Asp490Glu) and 2917(1414) C>T are the common polymorphisms found in the coding region of *SLC16A1* gene in Chinese and Indian populations. Linkage disequilibrium analysis revealed strong association between these common variants in both ethnic groups.

A total of 46 genetic variants were detected in *SLC16A3* gene, of which 33 are novel. Of the 5 nonsynonymous variants, only 44C>T (Ala15Val) was predicted by PolyPhen and SIFT as having a potentially damaging effect on protein function, whereas 55G>A (Gly19Ser), 574G>A (Val192Met) and 916G>A (Gly306Ser) had conflicting results between the SIFT and PolyPhen algorithms. Finally, 641C>T (Ser214Phe) was predicted to be tolerated variant.

MCT1 is the only MCT isoform found in the human erythrocyte and contributes up to 90% of lactate influx. In this study, we examined the interindividual variation in total and MCT1-mediated lactate influx into human erythrocytes in local Chinese population. However, low interindividual variability was observed in the total and MCT1-mediated lactate influx. In the MCT-1 mediated lactate influx, the apparent K_m and V_{max} were 220.1 ± 35.33 mM and 15877 ± 968.1 nmol/ml of RBC/min, respectively. The finding of this study suggests that lactate transport across human erythrocyte membrane is low affinity but high capacity transport process. We have previously genotyped the MCT1 gene in the ethnic Chinese and Indian groups of Singapore population and a common nonsynonymous polymorphism, 1470 T>A (Asp490Glu) had been identified in MCT1 gene. With knowledge that MCT1 is responsible for up to 90% of lactate influx into RBC, it would be intriguing to correlate the *in vitro* uptake assay with the MCT1 polymorphism. The findings of

this study suggest that T allele of 1470 T>A (Asp490Glu) may have a defective effect in transport function and appear to have a lower transport activity. However, additional studies involving larger samples are required to verify the impact of 1470 T>A (Asp490Glu) polymorphism in MCT1 transport activity.

The diet-interaction via MCT1 inhibition may affect lactate shuttling and drug disposition. Therefore, the effects of various dietary and pharmacological agents on MCT1 were evaluated. Of these, diflunisal, diclofenac, mefenamic acid, meclofenamic acid, tolfenamic acid, luteolin, etodalac, phloretin and morin were the most potent with IC₅₀ values of 40.24 ± 1.10, 1.33 ± 1.17, 11.83 ± 1.24, 9.68 ± 1.10, 5.95 ± 1.12, 2.71 ± 1.28, 13.30 ± 1.06, 47.98 ± 1.11 and 44.53 ± 1.08 μM, respectively. The inhibitory concentrations of tested NSAIDs (diflunisal, mefenamic acid, meclofenamic acid, flufenamic acid and tolfenamic acid) are in the range of physiologically relevant concentrations that are achievable from the oral intake. However, due to high protein binding of the tested NSAIDs, the actual unbound plasma concentrations of tested NSAIDs may be below the K_i values reported in this study. The tested NSAIDs may not contribute significantly to the *in vivo* inhibition of MCT1 activity. Therefore, we examined the inhibitory effects of NSAID on MCT1 *in vivo*.

The fourth objective of this study was to clinically examine the effect of MCT1 inhibitor, diflunisal, on lactate distribution in plasma and erythrocyte. We observed small differences between placebo RBC and diflunisal RBC lactate levels. The RBC:Plasma [La]^{Diflunisal} ratios were constantly lower than RBC:Plasma [La]^{Placebo} ratios after 20 min of the onset of infusion. These differences, however, were not

statistically significant. In conclusion, the results from this study show that therapeutic recommended dose of diflunisal is insufficient to inhibit lactate transport in blood. The reason of this may due to high protein binding property of diflunisal, short lactate infusion period and the presence of rescue pathways that mediating lactate influx into human erythrocyte when MCT1 pathway is inhibited. Nonetheless, the findings of this study will increase our understanding of the clinical relevance of MCT1 transporter-based drug interactions.

Table 52. Summary of data

| PHARMACOGENETICS OF TRANSPORTER | |
|---|---|
| Objective | Summary of data |
| <p>Population genetics studies in <i>SLC16A1</i> and <i>SLC16A3</i></p> | <p><i>SLC16A1 (MCT1)</i></p> <ul style="list-style-type: none"> ▪ A total of 21 genetic variations were found, of which 14 are novel ▪ Three nonsynonymous variants were found <ul style="list-style-type: none"> ➢ 303 T>G (Ile101Met) - predicted as having detrimental effect ➢ 1282 G>A (Val428Ile) - predicted to be benign ➢ 1470 T>A (Asp490Glu) - predicted to be benign ▪ Genotyping data was in accordance to HWE for all loci, except for -363-100 C>G ▪ LD analysis revealed strong association between three common polymorphism, namely IVS3-17A>C, 1470T>A (Asp490Glu) and 2917(1414)C>T in both Chinese and Malay ethnic groups <p><i>SLC16A3 (MCT4)</i></p> <ul style="list-style-type: none"> ▪ A total of 46 genetic variants were detected, of which 33 are novel ▪ Five nonsynonymous variants were found <ul style="list-style-type: none"> ➢ 44C>T (Ala15Val) ➢ 55G>A (Gly19Ser) ➢ 574G>A (Val192Met) ➢ 916G>A (Gly306Ser) ➢ 641C>T (Ser214Phe) ▪ Genotyping data was in accordance to HWE for all loci, except for IVS2-149 G>T ▪ Three common SNPs, namely -139-1105 C>T, -139-804 C>T and -139del(-727-795), were detected in the promoter region of transcript variant 2 ▪ Three common polymorphisms, namely -118-554 A>T, -118-130 A>C and -86 A>G were detected in the promoter and 5'UTR region of transcript variant 4 |

| | |
|--|---|
| <p>Interindividual variation in lactate influx</p> <p>Polymorphism-phenotype association of MCT1 polymorphism, 1470 T>A (Asp490Glu)</p> | <ul style="list-style-type: none"> ▪ Low interindividual variability was observed in the total- and MCT1-mediated L-lactate into human erythrocytes ▪ Human MCT1 system exhibited a low affinity but high capacity transport mechanism for the transport of L-lactate into RBC <ul style="list-style-type: none"> ➢ $K_m = 123.9 \pm 24.6$ mM ➢ $V_{max} = 12079.0 \pm 722.3$ nmol/ml of RBCs/min ▪ The total and MCT1-mediated L-lactate influxes are lower in TA group as compared to AA group at 2, 5, 10 and 20 mM of external L-lactate concentrations ▪ The differences found between TA and AA genetic groups are not statistically significant ▪ The T allele of 1470 T>A (Asp490Glu) variant may have a defective effect in MCT1 protein function and appear to have a lower transport activity |
|--|---|

DRUG/FOOD-TRANSPORTER INTERACTION

| Objective | Summary of data |
|--|--|
| <p>Biochemical kinetic studies of MCT1</p> | <ul style="list-style-type: none"> ▪ MCT1 is a low affinity high capacity process for the transport of L-lactate into human erythrocytes <ul style="list-style-type: none"> ➢ $K_m = 123.9 \pm 24.6$ mM ➢ $V_{max} = 12079.0 \pm 722.3$ nmol/ml of RBCs/min ▪ Several MCT1 inhibitors have been identified <ul style="list-style-type: none"> ➢ NSAID: diflunisal, diclofenac, mefenamic acid, meclofenamic acid, flufenamic acid, tolfenamic acid, etodalac ➢ Phytochemical: luteolin, phloretin and morin ▪ Five NSAIDs are in the range of physiologically relevant concentrations that are achievable from the oral intake <ul style="list-style-type: none"> ➢ diflunisal, diclofenac, mefenamic acid, meclofenamic acid, flufenamic acid, tolfenamic acid |
| <p>Clinical study of MCT1</p> | <ul style="list-style-type: none"> ▪ At rest, no significant differences were observed in the RBC:Plasma lactate ratio between placebo and diflunisal group <ul style="list-style-type: none"> ➢ Placebo = 0.82 ± 0.09 ➢ Diflunisal = 0.75 ± 0.09 ▪ The diflunisal RBC lactate level were constantly lower |

| | |
|--|---|
| | <p>than placebo RBC lactate level after 20 min of the onset of infusion. These differences were not statistically significant</p> <ul style="list-style-type: none">▪ The RBC:Plasma [La]Diflunisal ratio was constantly lower than the RBC:Plasma [La]Placebo ratio at all time points except at 10 and 20 min. The differences were not statistically significant for all time points▪ The results from this study show that therapeutic recommended dose of diflunisal was insufficient to inhibit lactate transport on RBC |
|--|---|

CHAPTER 7
FUTURE WORK

7.1 FUTURE DIRECTIONS

We hope that this study has shed some light on the functional implications of the pharmacogenetics of monocarboxylate transporter and the role of such transporters in drug actions. For future work, it would be intriguing to characterize functional effects of MCT1 and MCT4 variants reported in this study. Although the relationship of a MCT1 variant, 1470 T>A (Asp490Glu), with erythrocyte activity has been investigated in this study, additional studies involving larger sample sizes will be required to establish the clinical impact of this variant in MCT1 transport kinetics. Three reported SNPs, namely IVS3-17 A>C, 1470 T>A (Asp490Glu) and 2971 (1414) C>T are the common polymorphisms found in the coding region of *SLC16A1* gene in Chinese and Indian populations. Haplotype estimation shows that haplotype ATC was most common in both ethnic groups. Therefore, haplotype-phenotype analysis can be performed to investigate the relationship of ATC haplotype in MCT1 transport activity.

Although population genotyping were performed on both *SLC16A1* and *SLC16A3* gene, this thesis focuses only on the functional characterization of MCT1.

Therefore, more work can be done to clarify the transport kinetics of MCT4 and the effects of various potential inhibitors on its transport activity. There are several challenges in constructing the MCT4 functional assay model: 1) absence of cell-lines which have little or no background activity of other MCT isoforms; 2) absence of MCT isoform-specific substrates; and 3) absence of MCT isoform-specific inhibitors. A suitable model is therefore necessary to characterize the functional consequence of MCT4 transporter.

The influence of MCT1 inhibitor, diflunisal, on lactate distribution in human plasma and erythrocyte has been investigated. Although there were small differences in RBC lactate level between placebo- and diflunisal- treated groups, these differences were not statistically significant. One of the most probable explanations could be the insufficient power of the study. In addition, an infusion period of 30 minutes might be too short to detect differences. Therefore, a clinical study with larger sample size and longer infusion period can be designed to further investigate the clinical impact of diflunisal on MCT1 activity. In the current study, two potent inhibitors, meclofenamate and tolfenamate, were recognized. Meclofenamate and tolfenamate have more potent inhibitory effect than diflunisal (**Table 39**). These two inhibitors were not selected as the study drug because they had only been identified a few weeks before the initiation of the trial. Nonetheless, these two compounds could be considered as potential blockers for future studies.

REFERENCES:

- 1 Singer SJ and Nicolson GL. The fluid mosaic model of the structure of cell membranes. *Science* 1972;175(23):720-31.
- 2 Crane RK. Hypothesis for mechanism of intestinal active transport of sugars. *Fed Proc* 1962;21(891-5).
- 3 Hediger MA, Ikeda T, Coady M, Gundersen CB and Wright EM. Expression of size-selected mRNA encoding the intestinal Na⁺/glucose cotransporter in *Xenopus laevis* oocytes. *Proc Natl Acad Sci U S A* 1987;84(9):2634-7.
- 4 Juliano RL and Ling V. A surface glycoprotein modulating drug permeability in Chinese hamster ovary cell mutants. *Biochim Biophys Acta* 1976;455(1):152-62.
- 5 Thiebaut F, Tsuruo T, Hamada H, Gottesman MM, Pastan I and Willingham MC. Cellular localization of the multidrug-resistance gene product P-glycoprotein in normal human tissues. *Proc Natl Acad Sci U S A* 1987;84(21):7735-8.
- 6 Nishimura M and Naito S. Tissue-specific mRNA expression profiles of human ATP-binding cassette and solute carrier transporter superfamilies. *Drug Metab Pharmacokinet* 2005;20(6):452-77.
- 7 Nishimura M and Naito S. Tissue-specific mRNA expression profiles of human solute carrier transporter superfamilies. *Drug Metab Pharmacokinet* 2008;23(1):22-44.
- 8 Higgins CF. ABC transporters: From microorganisms to man. *Annu Rev Cell Biol* 1992;8(67-113).
- 9 Ames GF, Mimura CS, Holbrook SR and Shyamala V. Traffic ATPases: A superfamily of transport proteins operating from *Escherichia coli* to humans. *Adv Enzymol Relat Areas Mol Biol* 1992;65(1-47).
- 10 Rees DC, Johnson E and Lewinson O. ABC transporters: The power to change. *Nat Rev Mol Cell Biol* 2009;10(3):218-27.
- 11 Borst P and Elferink RO. Mammalian ABC transporters in health and disease. *Annu Rev Biochem* 2002;71(537-92).
- 12 Dean M and Annilo T. Evolution of the ATP-binding cassette (ABC) transporter superfamily in vertebrates. *Annu Rev Genomics Hum Genet* 2005;6(123-42).
- 13 Harland DN, Garmory HS, Brown KA and Titball RW. An association between ATP binding cassette systems, genome sizes and lifestyles of bacteria. *Res Microbiol* 2005;156(3):434-42.
- 14 Ross JI, Eady EA, Cove JH, Cunliffe WJ, Baumberg S and Wootton JC. Inducible erythromycin resistance in staphylococci is encoded by a member of the ATP-binding transport super-gene family. *Mol Microbiol* 1990;4(7):1207-14.
- 15 Lee EJ, Lean CB and Limentani LM. Role of membrane transporters in the safety profile of drugs. *Expert Opin Drug Metab Toxicol* 2009;5(11):1369-83.
- 16 Davidson AL, Dassa E, Orelle C and Chen J. Structure, function, and evolution of bacterial ATP-binding cassette systems. *Microbiol Mol Biol Rev* 2008;72(2):317-64, table of contents.
- 17 He L, Vasiliou K and Nebert DW. Analysis and update of the human solute carrier (SLC) gene superfamily. *Hum Genomics* 2009;3(2):195-206.
- 18 Zimmermann C, Gutmann H, Hruz P, Gutzwiller JP, Beglinger C and Drewe J. Mapping of multidrug resistance gene 1 and multidrug resistance-associated protein isoform 1 to 5 mRNA expression along the human intestinal tract. *Drug Metab Dispos* 2005;33(2):219-24.
- 19 Seithel A, Karlsson J, Hilgendorf C, Bjorquist A and Ungell AL. Variability in mRNA expression of ABC- and SLC-transporters in human intestinal cells: Comparison between human segments and Caco-2 cells. *Eur J Pharm Sci* 2006;28(4):291-9.

- 20 Lown KS, Mayo RR, Leichtman AB, Hsiao HL, Turgeon DK, Schmedlin-Ren P et al. Role of intestinal p-glycoprotein (mdr1) in interpatient variation in the oral bioavailability of cyclosporine. *Clin Pharmacol Ther* 1997;62(3):248-60.
- 21 Drescher S, Glaeser H, Murdter T, Hitzl M, Eichelbaum M and Fromm MF. P-glycoprotein-mediated intestinal and biliary digoxin transport in humans. *Clin Pharmacol Ther* 2003;73(3):223-31.
- 22 Schinkel AH, Smit JJ, van Tellingen O, Beijnen JH, Wagenaar E, van Deemter L et al. Disruption of the mouse mdr1a p-glycoprotein gene leads to a deficiency in the blood-brain barrier and to increased sensitivity to drugs. *Cell* 1994;77(4):491-502.
- 23 Schinkel AH, Wagenaar E, van Deemter L, Mol CA and Borst P. Absence of the mdr1a p-glycoprotein in mice affects tissue distribution and pharmacokinetics of dexamethasone, digoxin, and cyclosporin a. *J Clin Invest* 1995;96(4):1698-705.
- 24 Salama NN, Kelly EJ, Bui T and Ho RJ. The impact of pharmacologic and genetic knockout of p-glycoprotein on nelfinavir levels in the brain and other tissues in mice. *J Pharm Sci* 2005;94(6):1216-25.
- 25 Kim RB, Fromm MF, Wandel C, Leake B, Wood AJ, Roden DM et al. The drug transporter p-glycoprotein limits oral absorption and brain entry of hiv-1 protease inhibitors. *J Clin Invest* 1998;101(2):289-94.
- 26 Yamaguchi H, Yano I, Saito H and Inui K. Pharmacokinetic role of p-glycoprotein in oral bioavailability and intestinal secretion of grepafloxacin in vivo. *J Pharmacol Exp Ther* 2002;300(3):1063-9.
- 27 Wang JS, Taylor R, Ruan Y, Donovan JL, Markowitz JS and Lindsay De Vane C. Olanzapine penetration into brain is greater in transgenic abcb1a p-glycoprotein-deficient mice than fvb1 (wild-type) animals. *Neuropsychopharmacology* 2004;29(3):551-7.
- 28 Yokogawa K, Takahashi M, Tamai I, Konishi H, Nomura M, Moritani S et al. P-glycoprotein-dependent disposition kinetics of tacrolimus: Studies in mdr1a knockout mice. *Pharm Res* 1999;16(8):1213-8.
- 29 Uhr M, Grauer MT and Holsboer F. Differential enhancement of antidepressant penetration into the brain in mice with abcb1ab (mdr1ab) p-glycoprotein gene disruption. *Biol Psychiatry* 2003;54(8):840-6.
- 30 Williams RT. Detoxication mechanisms. New York: John Wiley & Sons, Inc.; 1959.
- 31 You G. Structure, function, and regulation of renal organic anion transporters. *Med Res Rev* 2002;22(6):602-16.
- 32 Grover A and Benet LZ. Effects of drug transporters on volume of distribution. *AAPS J* 2009;11(2):250-61.
- 33 Huang SM and Lesko LJ. Drug-drug, drug-dietary supplement, and drug-citrus fruit and other food interactions: What have we learned? *J Clin Pharmacol* 2004;44(6):559-69.
- 34 Qiuping Gu MD, Ph.D.; Charles F. Dillon, M.D., Ph.D.; and Vicki L. Burt, Sc.M., R.N. Prescription drug use continues to increase: U.S. Prescription drug data for 2007-2008. *NCHS Data Brief* 2010;42(
- 35 Jaime Gahche MPhRB, Ph.D., R.D.; Vicki Burt, Sc.M., R.N.; Jeffery Hughes, M.P.H.; Elizabeth Yetley, Ph.D.; Johanna Dwyer, D.Sc., R.D.; Mary Frances Picciano, Ph.D.; Margaret McDowell, Ph.D., R.D.; and Christopher Sempos, Ph.D. Dietary supplement use among u.S. Adults has increased since nhanes iii (1988–1994). *NCHS Data Brief* 2011;62(
- 36 Endres CJ, Hsiao P, Chung FS and Unadkat JD. The role of transporters in drug interactions. *Eur J Pharm Sci* 2006;27(5):501-17.

- 37 Kumar YS, Adukondalu D, Sathish D, Vishnu YV, Ramesh G, Latha AB et al. P-glycoprotein- and cytochrome p-450-mediated herbal drug interactions. *Drug Metabol Drug Interact* 2010;25(1-4):3-16.
- 38 Sasongko L, Link JM, Muzi M, Mankoff DA, Yang X, Collier AC et al. Imaging p-glycoprotein transport activity at the human blood-brain barrier with positron emission tomography. *Clin Pharmacol Ther* 2005;77(6):503-14.
- 39 Cihlar T, Lin DC, Pritchard JB, Fuller MD, Mendel DB and Sweet DH. The antiviral nucleotide analogs cidofovir and adefovir are novel substrates for human and rat renal organic anion transporter 1. *Mol Pharmacol* 1999;56(3):570-80.
- 40 Lalezari JP, Stagg RJ, Kuppermann BD, Holland GN, Kramer F, Ives DV et al. Intravenous cidofovir for peripheral cytomegalovirus retinitis in patients with aids. A randomized, controlled trial. *Ann Intern Med* 1997;126(4):257-63.
- 41 Ho RH and Kim RB. Transporters and drug therapy: Implications for drug disposition and disease. *Clin Pharmacol Ther* 2005;78(3):260-77.
- 42 Ayrton A and Morgan P. Role of transport proteins in drug absorption, distribution and excretion. *Xenobiotica* 2001;31(8-9):469-97.
- 43 Dresser GK, Bailey DG, Leake BF, Schwarz UI, Dawson PA, Freeman DJ et al. Fruit juices inhibit organic anion transporting polypeptide-mediated drug uptake to decrease the oral availability of fexofenadine. *Clin Pharmacol Ther* 2002;71(1):11-20.
- 44 Takeda M, Khamdang S, Narikawa S, Kimura H, Hosoyamada M, Cha SH et al. Characterization of methotrexate transport and its drug interactions with human organic anion transporters. *J Pharmacol Exp Ther* 2002;302(2):666-71.
- 45 Sadeque AJ, Wandel C, He H, Shah S and Wood AJ. Increased drug delivery to the brain by p-glycoprotein inhibition. *Clin Pharmacol Ther* 2000;68(3):231-7.
- 46 Schwarz UI, Gramatte T, Krappweis J, Berndt A, Oertel R, von Richter O et al. Unexpected effect of verapamil on oral bioavailability of the beta-blocker talinolol in humans. *Clin Pharmacol Ther* 1999;65(3):283-90.
- 47 Milne RW, Larsen LA, Jorgensen KL, Bastlund J, Stretch GR and Evans AM. Hepatic disposition of fexofenadine: Influence of the transport inhibitors erythromycin and dibromosulphothalein. *Pharm Res* 2000;17(12):1511-5.
- 48 Hamman MA, Bruce MA, Haehner-Daniels BD and Hall SD. The effect of rifampin administration on the disposition of fexofenadine. *Clin Pharmacol Ther* 2001;69(3):114-21.
- 49 Fromm MF, Kim RB, Stein CM, Wilkinson GR and Roden DM. Inhibition of p-glycoprotein-mediated drug transport: A unifying mechanism to explain the interaction between digoxin and quinidine [see comments]. *Circulation* 1999;99(4):552-7.
- 50 Pauli-Magnus C, von Richter O, Burk O, Ziegler A, Mettang T, Eichelbaum M et al. Characterization of the major metabolites of verapamil as substrates and inhibitors of p-glycoprotein. *J Pharmacol Exp Ther* 2000;293(2):376-82.
- 51 Westphal K, Weinbrenner A, Giessmann T, Stuhr M, Franke G, Zschiesche M et al. Oral bioavailability of digoxin is enhanced by talinolol: Evidence for involvement of intestinal p-glycoprotein. *Clin Pharmacol Ther* 2000;68(1):6-12.
- 52 Wakasugi H, Yano I, Ito T, Hashida T, Futami T, Nohara R et al. Effect of clarithromycin on renal excretion of digoxin: Interaction with p-glycoprotein. *Clin Pharmacol Ther* 1998;64(1):123-8.
- 53 Boyd RA, Stern RH, Stewart BH, Wu X, Reyner EL, Zegarac EA et al. Atorvastatin coadministration may increase digoxin concentrations by inhibition of intestinal p-glycoprotein-mediated secretion. *J Clin Pharmacol* 2000;40(1):91-8.
- 54 Greiner B, Eichelbaum M, Fritz P, Kreichgauer HP, von Richter O, Zundler J et al. The role of intestinal p-glycoprotein in the interaction of digoxin and rifampin. *J Clin Invest* 1999;104(2):147-53.

- 55 Funk C, Ponelle C, Scheuermann G and Pantze M. Cholestatic potential of troglitazone as a possible factor contributing to troglitazone-induced hepatotoxicity: In vivo and in vitro interaction at the canalicular bile salt export pump (bsep) in the rat. *Mol Pharmacol* 2001;59(3):627-35.
- 56 Fattinger K, Funk C, Pantze M, Weber C, Reichen J, Stieger B et al. The endothelin antagonist bosentan inhibits the canalicular bile salt export pump: A potential mechanism for hepatic adverse reactions. *Clin Pharmacol Ther* 2001;69(4):223-31.
- 57 Stieger B, Fattinger K, Madon J, Kullak-Ublick GA and Meier PJ. Drug- and estrogen-induced cholestasis through inhibition of the hepatocellular bile salt export pump (bsep) of rat liver. *Gastroenterology* 2000;118(2):422-30.
- 58 Ho ES, Lin DC, Mendel DB and Cihlar T. Cytotoxicity of antiviral nucleotides adefovir and cidofovir is induced by the expression of human renal organic anion transporter 1. *J Am Soc Nephrol* 2000;11(3):383-93.
- 59 Tune BM. Nephrotoxicity of beta-lactam antibiotics: Mechanisms and strategies for prevention. *Pediatr Nephrol* 1997;11(6):768-72.
- 60 Petrovic V, Teng S and Piquette-Miller M. Regulation of drug transporters during infection and inflammation. *Mol Interv* 2007;7(2):99-111.
- 61 Nolin TD, Naud J, Leblond FA and Pichette V. Emerging evidence of the impact of kidney disease on drug metabolism and transport. *Clin Pharmacol Ther* 2008;83(6):898-903.
- 62 Lazarowski A, Czornyj L, Lubienieki F, Girardi E, Vazquez S and D'Giano C. Abc transporters during epilepsy and mechanisms underlying multidrug resistance in refractory epilepsy. *Epilepsia* 2007;48 Suppl 5(140-9).
- 63 Aszalos A. Drug-drug interactions affected by the transporter protein, p-glycoprotein (abcb1, mdr1) i. Preclinical aspects. *Drug Discov Today* 2007;12(19-20):833-7.
- 64 Neuvonen PJ, Niemi M and Backman JT. Drug interactions with lipid-lowering drugs: Mechanisms and clinical relevance. *Clin Pharmacol Ther* 2006;80(6):565-81.
- 65 Morris ME and Zhang S. Flavonoid-drug interactions: Effects of flavonoids on abc transporters. *Life Sci* 2006;78(18):2116-30.
- 66 Deferme S and Augustijns P. The effect of food components on the absorption of p-gp substrates: A review. *J Pharm Pharmacol* 2003;55(2):153-62.
- 67 Kawahara M, Sakata A, Miyashita T, Tamai I and Tsuji A. Physiologically based pharmacokinetics of digoxin in mdr1a knockout mice. *J Pharm Sci* 1999;88(12):1281-7.
- 68 Oswald S, Koll C and Siegmund W. Disposition of the cholesterol absorption inhibitor ezetimibe in mdr1a/b (-/-) mice. *J Pharm Sci* 2007;96(12):3478-84.
- 69 Kido Y, Tamai I, Ohnari A, Sai Y, Kagami T, Nezu J et al. Functional relevance of carnitine transporter octn2 to brain distribution of l-carnitine and acetyl-l-carnitine across the blood-brain barrier. *J Neurochem* 2001;79(5):959-69.
- 70 Meredith D and Christian HC. The slc16 monocarboxylate transporter family. *Xenobiotica* 2008;38(7-8):1072-106.
- 71 Halestrap AP and Denton RM. Specific inhibition of pyruvate transport in rat liver mitochondria and human erythrocytes by alpha-cyano-4-hydroxycinnamate. *Biochem J* 1974;138(2):313-6.
- 72 Deuticke B. Monocarboxylate transport in erythrocytes. *J Membr Biol* 1982;70(2):89-103.
- 73 Halestrap AP and Price NT. The proton-linked monocarboxylate transporter (mct) family: Structure, function and regulation. *Biochem J* 1999;343 Pt 2(281-99).
- 74 Merezinskaya N and Fishbein WN. Monocarboxylate transporters: Past, present, and future. *Histol Histopathol* 2009;24(2):243-64.

- 75 Broer S, Schneider HP, Broer A, Rahman B, Hamprecht B and Deitmer JW. Characterization of the monocarboxylate transporter 1 expressed in xenopus laevis oocytes by changes in cytosolic ph. *Biochem J* 1998;333 (Pt 1)(167-74.
- 76 Wilson MC, Jackson VN, Heddle C, Price NT, Pilegaard H, Juel C et al. Lactic acid efflux from white skeletal muscle is catalyzed by the monocarboxylate transporter isoform mct3. *J Biol Chem* 1998;273(26):15920-6.
- 77 Kirk P, Wilson MC, Heddle C, Brown MH, Barclay AN and Halestrap AP. Cd147 is tightly associated with lactate transporters mct1 and mct4 and facilitates their cell surface expression. *EMBO J* 2000;19(15):3896-904.
- 78 Philp NJ, Wang D, Yoon H and Hjelmeland LM. Polarized expression of monocarboxylate transporters in human retinal pigment epithelium and arpe-19 cells. *Invest Ophthalmol Vis Sci* 2003;44(4):1716-21.
- 79 Wilson MC, Meredith D, Fox JE, Manoharan C, Davies AJ and Halestrap AP. Basigin (cd147) is the target for organomercurial inhibition of monocarboxylate transporter isoforms 1 and 4: The ancillary protein for the insensitive mct2 is embigin (gp70). *J Biol Chem* 2005;280(29):27213-21.
- 80 Garcia CK, Goldstein JL, Pathak RK, Anderson RG and Brown MS. Molecular characterization of a membrane transporter for lactate, pyruvate, and other monocarboxylates: Implications for the cori cycle. *Cell* 1994;76(5):865-73.
- 81 Garcia CK, Li X, Luna J and Francke U. Cdna cloning of the human monocarboxylate transporter 1 and chromosomal localization of the slc16a1 locus to 1p13.2-p12. *Genomics* 1994;23(2):500-3.
- 82 Garcia CK, Brown MS, Pathak RK and Goldstein JL. Cdna cloning of mct2, a second monocarboxylate transporter expressed in different cells than mct1. *J Biol Chem* 1995;270(4):1843-9.
- 83 Perez de Heredia F, Wood IS and Trayhurn P. Hypoxia stimulates lactate release and modulates monocarboxylate transporter (mct1, mct2, and mct4) expression in human adipocytes. *Pflugers Arch* 2010;459(3):509-18.
- 84 Philp NJ, Yoon H and Lombardi L. Mouse mct3 gene is expressed preferentially in retinal pigment and choroid plexus epithelia. *Am J Physiol Cell Physiol* 2001;280(5):C1319-26.
- 85 Philp NJ, Yoon H and Grollman EF. Monocarboxylate transporter mct1 is located in the apical membrane and mct3 in the basal membrane of rat rpe. *Am J Physiol* 1998;274(6 Pt 2):R1824-8.
- 86 Price NT, Jackson VN and Halestrap AP. Cloning and sequencing of four new mammalian monocarboxylate transporter (mct) homologues confirms the existence of a transporter family with an ancient past. *Biochem J* 1998;329 (Pt 2)(321-8.
- 87 Vellonen KS, Hakli M, Merezhinskaya N, Tervo T, Honkakoski P and Urtti A. Monocarboxylate transport in human corneal epithelium and cell lines. *Eur J Pharm Sci* 2010;39(4):241-7.
- 88 Friesema EC, Ganguly S, Abdalla A, Manning Fox JE, Halestrap AP and Visser TJ. Identification of monocarboxylate transporter 8 as a specific thyroid hormone transporter. *J Biol Chem* 2003;278(41):40128-35.
- 89 Kim DK, Kanai Y, Chairoungdua A, Matsuo H, Cha SH and Endou H. Expression cloning of a na⁺-independent aromatic amino acid transporter with structural similarity to h⁺/monocarboxylate transporters. *J Biol Chem* 2001;276(20):17221-8.
- 90 Kim DK, Kanai Y, Matsuo H, Kim JY, Chairoungdua A, Kobayashi Y et al. The human t-type amino acid transporter-1: Characterization, gene organization, and chromosomal location. *Genomics* 2002;79(1):95-103.
- 91 Halestrap AP and Meredith D. The slc16 gene family-from monocarboxylate transporters (mcts) to aromatic amino acid transporters and beyond. *Pflugers Arch* 2004;447(5):619-28.

- 92 Broer S, Broer A, Schneider HP, Stegen C, Halestrap AP and Deitmer JW. Characterization of the high-affinity monocarboxylate transporter mct2 in xenopus laevis oocytes. *Biochem J* 1999;341 (Pt 3):529-35.
- 93 Manning Fox JE, Meredith D and Halestrap AP. Characterisation of human monocarboxylate transporter 4 substantiates its role in lactic acid efflux from skeletal muscle. *J Physiol* 2000;529 Pt 2(285-93).
- 94 Poole RC and Halestrap AP. Transport of lactate and other monocarboxylates across mammalian plasma membranes. *Am J Physiol* 1993;264(4 Pt 1):C761-82.
- 95 Poole RC, Cranmer SL, Halestrap AP and Levi AJ. Substrate and inhibitor specificity of monocarboxylate transport into heart cells and erythrocytes. Further evidence for the existence of two distinct carriers. *Biochem J* 1990;269(3):827-9.
- 96 Lin RY, Vera JC, Chaganti RS and Golde DW. Human monocarboxylate transporter 2 (mct2) is a high affinity pyruvate transporter. *J Biol Chem* 1998;273(44):28959-65.
- 97 Broer S, Rahman B, Pellegrini G, Pellerin L, Martin JL, Verleysdonk S et al. Comparison of lactate transport in astroglial cells and monocarboxylate transporter 1 (mct 1) expressing xenopus laevis oocytes. Expression of two different monocarboxylate transporters in astroglial cells and neurons. *J Biol Chem* 1997;272(48):30096-102.
- 98 Kobayashi M, Fujita I, Itagaki S, Hirano T and Iseki K. Transport mechanism for l-lactic acid in human myocytes using human prototypic embryonal rhabdomyosarcoma cell line (rd cells). *Biol Pharm Bull* 2005;28(7):1197-201.
- 99 Carpenter L and Halestrap AP. The kinetics, substrate and inhibitor specificity of the lactate transporter of ehrlich-lette tumour cells studied with the intracellular pH indicator bcecf. *Biochem J* 1994;304 (Pt 3):751-60.
- 100 Hosoya K, Kondo T, Tomi M, Takanaga H, Ohtsuki S and Terasaki T. Mct1-mediated transport of l-lactic acid at the inner blood-retinal barrier: A possible route for delivery of monocarboxylic acid drugs to the retina. *Pharm Res* 2001;18(12):1669-76.
- 101 Halestrap AP. Transport of pyruvate and lactate into human erythrocytes. Evidence for the involvement of the chloride carrier and a chloride-independent carrier. *Biochem J* 1976;156(2):193-207.
- 102 Dubinsky WP and Racker E. The mechanism of lactate transport in human erythrocytes. *J Membr Biol* 1978;44(1):25-36.
- 103 Hadjiagapiou C, Schmidt L, Dudeja PK, Layden TJ and Ramaswamy K. Mechanism(s) of butyrate transport in caco-2 cells: Role of monocarboxylate transporter 1. *Am J Physiol Gastrointest Liver Physiol* 2000;279(4):G775-80.
- 104 Utoguchi N and Audus KL. Carrier-mediated transport of valproic acid in bewo cells, a human trophoblast cell line. *Int J Pharm* 2000;195(1-2):115-24.
- 105 Wu X, Whitfield LR and Stewart BH. Atorvastatin transport in the caco-2 cell model: Contributions of p-glycoprotein and the proton-monocarboxylic acid co-transporter. *Pharm Res* 2000;17(2):209-15.
- 106 Wang Q, Lu Y and Morris ME. Monocarboxylate transporter (mct) mediates the transport of gamma-hydroxybutyrate in human kidney hk-2 cells. *Pharm Res* 2007;24(6):1067-78.
- 107 Deuticke B. Monocarboxylate transport in red blood cells: Kinetics and chemical modification. *Methods Enzymol* 1989;173(300-29).
- 108 Choi JS, Jin MJ and Han HK. Role of monocarboxylic acid transporters in the cellular uptake of NSAIDs. *J Pharm Pharmacol* 2005;57(9):1185-9.
- 109 Shim CK, Cheon EP, Kang KW, Seo KS and Han HK. Inhibition effect of flavonoids on monocarboxylate transporter 1 (mct1) in caco-2 cells. *J Pharm Pharmacol* 2007;59(11):1515-9.

- 110 Wang Q and Morris ME. Flavonoids modulate monocarboxylate transporter-1-mediated transport of gamma-hydroxybutyrate in vitro and in vivo. *Drug Metab Dispos* 2007;35(2):201-8.
- 111 Jackson VN, Price NT, Carpenter L and Halestrap AP. Cloning of the monocarboxylate transporter isoform mct2 from rat testis provides evidence that expression in tissues is species-specific and may involve post-transcriptional regulation. *Biochem J* 1997;324 (Pt 2)(447-53.
- 112 Yoon H, Fanelli A, Grollman EF and Philp NJ. Identification of a unique monocarboxylate transporter (mct3) in retinal pigment epithelium. *Biochem Biophys Res Commun* 1997;234(1):90-4.
- 113 Grollman EF, Philp NJ, McPhie P, Ward RD and Sauer B. Determination of transport kinetics of chick mct3 monocarboxylate transporter from retinal pigment epithelium by expression in genetically modified yeast. *Biochemistry* 2000;39(31):9351-7.
- 114 Philp NJ, Ochrietor JD, Rudoy C, Muramatsu T and Linser PJ. Loss of mct1, mct3, and mct4 expression in the retinal pigment epithelium and neural retina of the *5a11/basigin*-null mouse. *Invest Ophthalmol Vis Sci* 2003;44(3):1305-11.
- 115 Fishbein WN, Merezhinskaya N and Foellmer JW. Relative distribution of three major lactate transporters in frozen human tissues and their localization in unfixed skeletal muscle. *Muscle Nerve* 2002;26(1):101-12.
- 116 Pilegaard H, Terzis G, Halestrap A and Juel C. Distribution of the lactate/h⁺ transporter isoforms mct1 and mct4 in human skeletal muscle. *Am J Physiol* 1999;276(5 Pt 1):E843-8.
- 117 Dimmer KS, Friedrich B, Lang F, Deitmer JW and Broer S. The low-affinity monocarboxylate transporter mct4 is adapted to the export of lactate in highly glycolytic cells. *Biochem J* 2000;350 Pt 1(219-27.
- 118 Meredith D, Bell P, McClure B and Wilkins R. Functional and molecular characterisation of lactic acid transport in bovine articular chondrocytes. *Cell Physiol Biochem* 2002;12(4):227-34.
- 119 Bergersen L, Rafiki A and Ottersen OP. Immunogold cytochemistry identifies specialized membrane domains for monocarboxylate transport in the central nervous system. *Neurochem Res* 2002;27(1-2):89-96.
- 120 Bonen A. The expression of lactate transporters (mct1 and mct4) in heart and muscle. *Eur J Appl Physiol* 2001;86(1):6-11.
- 121 Hatta H, Tonouchi M, Miskovic D, Wang Y, Heikkila JJ and Bonen A. Tissue-specific and isoform-specific changes in mct1 and mct4 in heart and soleus muscle during a 1-yr period. *Am J Physiol Endocrinol Metab* 2001;281(4):E749-56.
- 122 Sepponen K, Koho N, Puolanne E, Ruusunen M and Poso AR. Distribution of monocarboxylate transporter isoforms mct1, mct2 and mct4 in porcine muscles. *Acta Physiol Scand* 2003;177(1):79-86.
- 123 Bonen A, Heynen M and Hatta H. Distribution of monocarboxylate transporters mct1-mct8 in rat tissues and human skeletal muscle. *Appl Physiol Nutr Metab* 2006;31(1):31-9.
- 124 Pierre K and Pellerin L. Monocarboxylate transporters in the central nervous system: Distribution, regulation and function. *J Neurochem* 2005;94(1):1-14.
- 125 Kido Y, Tamai I, Okamoto M, Suzuki F and Tsuji A. Functional clarification of mct1-mediated transport of monocarboxylic acids at the blood-brain barrier using in vitro cultured cells and in vivo bui studies. *Pharm Res* 2000;17(1):55-62.
- 126 Gerhart DZ, Enerson BE, Zhdankina OY, Leino RL and Drewes LR. Expression of monocarboxylate transporter mct1 by brain endothelium and glia in adult and suckling rats. *Am J Physiol* 1997;273(1 Pt 1):E207-13.

- 127 Leino RL, Gerhart DZ and Drewes LR. Monocarboxylate transporter (mct1) abundance in brains of suckling and adult rats: A quantitative electron microscopic immunogold study. *Brain Res Dev Brain Res* 1999;113(1-2):47-54.
- 128 Leino RL, Gerhart DZ, Duelli R, Enerson BE and Drewes LR. Diet-induced ketosis increases monocarboxylate transporter (mct1) levels in rat brain. *Neurochem Int* 2001;38(6):519-27.
- 129 Smith JP and Drewes LR. Modulation of monocarboxylic acid transporter-1 kinetic function by the camp signaling pathway in rat brain endothelial cells. *J Biol Chem* 2006;281(4):2053-60.
- 130 Pellerin L. Brain energetics (thought needs food). *Curr Opin Clin Nutr Metab Care* 2008;11(6):701-5.
- 131 Pellerin L and Magistretti PJ. Food for thought: Challenging the dogmas. *J Cereb Blood Flow Metab* 2003;23(11):1282-6.
- 132 Fernandes J, Berger R and Smit GP. Lactate as energy source for brain in glucose-6-phosphatase deficient child. *Lancet* 1982;1(8263):113.
- 133 Hawkins RA, Mans AM and Davis DW. Regional ketone body utilization by rat brain in starvation and diabetes. *Am J Physiol* 1986;250(2 Pt 1):E169-78.
- 134 Gjedde A and Crone C. Induction processes in blood-brain transfer of ketone bodies during starvation. *Am J Physiol* 1975;229(5):1165-9.
- 135 Nybo L and Secher NH. Cerebral perturbations provoked by prolonged exercise. *Prog Neurobiol* 2004;72(4):223-61.
- 136 Maddock RJ, Casazza GA, Buonocore MH and Tanase C. Vigorous exercise increases brain lactate and glx (glutamate+glutamine): A dynamic 1h-mrs study. *Neuroimage* 2011;57(4):1324-30.
- 137 Magistretti PJ, Pellerin L, Rothman DL and Shulman RG. Energy on demand. *Science* 1999;283(5401):496-7.
- 138 van Hall G, Stromstad M, Rasmussen P, Jans O, Zaar M, Gam C et al. Blood lactate is an important energy source for the human brain. *J Cereb Blood Flow Metab* 2009;29(6):1121-9.
- 139 Hillary FG, Liu WC, Genova HM, Maniker AH, Kepler K, Greenwald BD et al. Examining lactate in severe tbi using proton magnetic resonance spectroscopy. *Brain Inj* 2007;21(9):981-91.
- 140 Schnaberth G, Brunner G and Scheiber V. [lactate acidosis in the cerebrospinal fluid as a prognostic parameter of malacic cerebral insult (author's transl)]. *Wien Klin Wochenschr* 1981;93(12):388-93.
- 141 Rehncrona S and Kagstrom E. Tissue lactic acidosis and ischemic brain damage. *Am J Emerg Med* 1983;1(2):168-74.
- 142 Paljarvi L, Rehncrona S, Soderfeldt B, Olsson Y and Kalimo H. Brain lactic acidosis and ischemic cell damage: Quantitative ultrastructural changes in capillaries of rat cerebral cortex. *Acta Neuropathol* 1983;60(3-4):232-40.
- 143 Coon AL, Arias-Mendoza F, Colby GP, Cruz-Lobo J, Mocco J, Mack WJ et al. Correlation of cerebral metabolites with functional outcome in experimental primate stroke using in vivo 1h-magnetic resonance spectroscopy. *AJNR Am J Neuroradiol* 2006;27(5):1053-8.
- 144 Uhernik AL, Tucker C and Smith JP. Control of mct1 function in cerebrovascular endothelial cells by intracellular ph. *Brain Res* 2011;1376(10-22).
- 145 Singer SJ. A fluid lipid-globular protein mosaic model of membrane structure. *Ann N Y Acad Sci* 1972;195(16-23).
- 146 Hermansen L. Effect of metabolic changes on force generation in skeletal muscle during maximal exercise. *Ciba Found Symp* 1981;82(75-88).
- 147 Choi CS, Kim YB, Lee FN, Zabolotny JM, Kahn BB and Youn JH. Lactate induces insulin resistance in skeletal muscle by suppressing glycolysis and

- impairing insulin signaling. *Am J Physiol Endocrinol Metab* 2002;283(2):E233-40.
- 148 Liu C, Wu J, Zhu J, Kuei C, Yu J, Shelton J et al. Lactate inhibits lipolysis in fat cells through activation of an orphan g-protein-coupled receptor, gpr81. *J Biol Chem* 2009;284(5):2811-22.
- 149 Hashimoto T, Hussien R, Oommen S, Gohil K and Brooks GA. Lactate sensitive transcription factor network in l6 cells: Activation of mct1 and mitochondrial biogenesis. *FASEB J* 2007;21(10):2602-12.
- 150 Samuvel DJ, Sundararaj KP, Nareika A, Lopes-Virella MF and Huang Y. Lactate boosts tlr4 signaling and nf-kappab pathway-mediated gene transcription in macrophages via monocarboxylate transporters and md-2 up-regulation. *J Immunol* 2009;182(4):2476-84.
- 151 Brooks GA. Lactate: Glycolytic product and oxidative substrate during sustained exercise in mammals the lactate shuttle., vol A). Berlin: Springer; 1985a. p. 208218.
- 152 Gladden LB. A lactatic perspective on metabolism. *Med Sci Sports Exerc* 2008;40(3):477-85.
- 153 Brooks GA. Intra- and extra-cellular lactate shuttles. *Med Sci Sports Exerc* 2000;32(4):790-9.
- 154 Bergman BC, Horning MA, Casazza GA, Wolfel EE, Butterfield GE and Brooks GA. Endurance training increases gluconeogenesis during rest and exercise in men. *Am J Physiol Endocrinol Metab* 2000;278(2):E244-51.
- 155 Kelley KM, Hamann JJ, Navarre C and Gladden LB. Lactate metabolism in resting and contracting canine skeletal muscle with elevated lactate concentration. *J Appl Physiol* 2002;93(3):865-72.
- 156 Mazzeo RS, Brooks GA, Schoeller DA and Budinger TF. Disposal of blood [1-13c]lactate in humans during rest and exercise. *J Appl Physiol* 1986;60(1):232-41.
- 157 Gladden LB. Lactate metabolism: A new paradigm for the third millennium. *J Physiol* 2004;558(Pt 1):5-30.
- 158 Juel C and Halestrap AP. Lactate transport in skeletal muscle - role and regulation of the monocarboxylate transporter. *J Physiol* 1999;517 (Pt 3)(633-42.
- 159 Dubouchaud H, Butterfield GE, Wolfel EE, Bergman BC and Brooks GA. Endurance training, expression, and physiology of ldh, mct1, and mct4 in human skeletal muscle. *Am J Physiol Endocrinol Metab* 2000;278(4):E571-9.
- 160 Lindinger MI, McKelvie RS and Heigenhauser GJ. K⁺ and lac⁻ distribution in humans during and after high-intensity exercise: Role in muscle fatigue attenuation? *J Appl Physiol* 1995;78(3):765-77.
- 161 Vaihkonen LK and Poso AR. Interindividual variation in total and carrier-mediated lactate influx into red blood cells. *Am J Physiol* 1998;274(4 Pt 2):R1025-30.
- 162 De Bruijne AW, Vreeburg H and Van Steveninck J. Kinetic analysis of l-lactate transport in human erythrocytes via the monocarboxylate-specific carrier system. *Biochim Biophys Acta* 1983;732(3):562-8.
- 163 Deuticke B, Beyer E and Forst B. Discrimination of three parallel pathways of lactate transport in the human erythrocyte membrane by inhibitors and kinetic properties. *Biochim Biophys Acta* 1982;684(1):96-110.
- 164 Skelton MS, Kremer DE, Smith EW and Gladden LB. Lactate influx into red blood cells of athletic and nonathletic species. *Am J Physiol* 1995;268(5 Pt 2):R1121-8.
- 165 Kobayashi M, Otsuka Y, Itagaki S, Hirano T and Iseki K. Inhibitory effects of statins on human monocarboxylate transporter 4. *Int J Pharm* 2006;317(1):19-25.

- 166 Poole RC, Sansom CE and Halestrap AP. Studies of the membrane topology of the rat erythrocyte h⁺/lactate cotransporter (mct1). *Biochem J* 1996;320 (Pt 3)(817-24.
- 167 Kim CM, Goldstein JL and Brown MS. Cdna cloning of mev, a mutant protein that facilitates cellular uptake of mevalonate, and identification of the point mutation responsible for its gain of function. *J Biol Chem* 1992;267(32):23113-21.
- 168 Rahman B, Schneider HP, Broer A, Deitmer JW and Broer S. Helix 8 and helix 10 are involved in substrate recognition in the rat monocarboxylate transporter mct1. *Biochemistry* 1999;38(35):11577-84.
- 169 Manoharan C, Wilson MC, Sessions RB and Halestrap AP. The role of charged residues in the transmembrane helices of monocarboxylate transporter 1 and its ancillary protein basigin in determining plasma membrane expression and catalytic activity. *Mol Membr Biol* 2006;23(6):486-98.
- 170 Galic S, Schneider HP, Broer A, Deitmer JW and Broer S. The loop between helix 4 and helix 5 in the monocarboxylate transporter mct1 is important for substrate selection and protein stability. *Biochem J* 2003;376(Pt 2):413-22.
- 171 Fishbein WN. Lactate transporter defect: A new disease of muscle. *Science* 1986;234(4781):1254-6.
- 172 Merezhinskaya N, Fishbein WN, Davis JI and Foellmer JW. Mutations in mct1 cdna in patients with symptomatic deficiency in lactate transport. *Muscle Nerve* 2000;23(1):90-7.
- 173 Otonkoski T, Jiao H, Kaminen-Ahola N, Tapia-Paez I, Ullah MS, Parton LE et al. Physical exercise-induced hypoglycemia caused by failed silencing of monocarboxylate transporter 1 in pancreatic beta cells. *Am J Hum Genet* 2007;81(3):467-74.
- 174 Bonen A, Miskovic D, Tonouchi M, Lemieux K, Wilson MC, Marette A et al. Abundance and subcellular distribution of mct1 and mct4 in heart and fast-twitch skeletal muscles. *Am J Physiol Endocrinol Metab* 2000;278(6):E1067-77.
- 175 Green H, Halestrap A, Mockett C, O'Toole D, Grant S and Ouyang J. Increases in muscle mct are associated with reductions in muscle lactate after a single exercise session in humans. *Am J Physiol Endocrinol Metab* 2002;282(1):E154-60.
- 176 Narumi K, Furugen A, Kobayashi M, Otake S, Itagaki S and Iseki K. Regulation of monocarboxylate transporter 1 in skeletal muscle cells by intracellular signaling pathways. *Biol Pharm Bull* 2010;33(9):1568-73.
- 177 Perrini S, Henriksson J, Zierath JR and Widegren U. Exercise-induced protein kinase c isoform-specific activation in human skeletal muscle. *Diabetes* 2004;53(1):21-4.
- 178 Chahine KG, Baracchini E and Goldman D. Coupling muscle electrical activity to gene expression via a camp-dependent second messenger system. *J Biol Chem* 1993;268(4):2893-8.
- 179 Furugen A, Kobayashi M, Narumi K, Watanabe M, Otake S, Itagaki S et al. Amp-activated protein kinase regulates the expression of monocarboxylate transporter 4 in skeletal muscle. *Life Sci* 2011;88(3-4):163-8.
- 180 Cuff MA, Lambert DW and Shirazi-Beechey SP. Substrate-induced regulation of the human colonic monocarboxylate transporter, mct1. *J Physiol* 2002;539(Pt 2):361-71.
- 181 Borthakur A, Saksena S, Gill RK, Alrefai WA, Ramaswamy K and Dudeja PK. Regulation of monocarboxylate transporter 1 (mct1) promoter by butyrate in human intestinal epithelial cells: Involvement of nf-kappab pathway. *J Cell Biochem* 2008;103(5):1452-63.
- 182 Saksena S, Theegala S, Bansal N, Gill RK, Tyagi S, Alrefai WA et al. Mechanisms underlying modulation of monocarboxylate transporter 1 (mct1) by

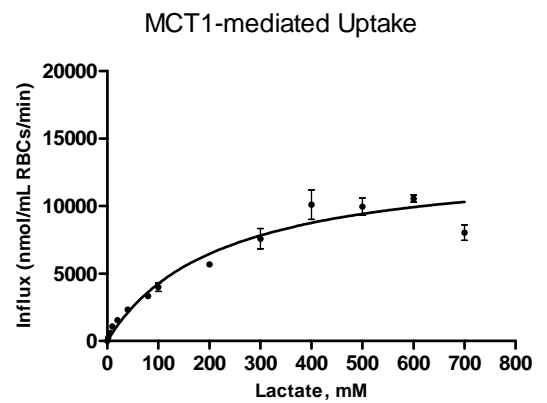
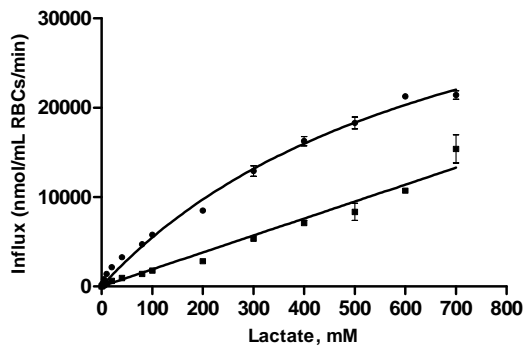
- somatostatin in human intestinal epithelial cells. *Am J Physiol Gastrointest Liver Physiol* 2009;297(5):G878-85.
- 183 Gyr KE and Meier R. Pharmacodynamic effects of sandostatin in the gastrointestinal tract. *Digestion* 1993;54 Suppl 1(14-9).
- 184 Lewin MJ. The somatostatin receptor in the gi tract. *Annu Rev Physiol* 1992;54(455-68).
- 185 Ullah MS, Davies AJ and Halestrap AP. The plasma membrane lactate transporter mct4, but not mct1, is up-regulated by hypoxia through a hif-1alpha-dependent mechanism. *J Biol Chem* 2006;281(14):9030-7.
- 186 Nagasawa K, Nagai K, Ishimoto A and Fujimoto S. Transport mechanism for lovastatin acid in bovine kidney nbl-1 cells: Kinetic evidences imply involvement of monocarboxylate transporter 4. *Int J Pharm* 2003;262(1-2):63-73.
- 187 Nagasawa K, Nagai K, Sumitani Y, Moriya Y, Muraki Y, Takara K et al. Monocarboxylate transporter mediates uptake of lovastatin acid in rat cultured mesangial cells. *J Pharm Sci* 2002;91(12):2605-13.
- 188 Tsuji A, Saheki A, Tamai I and Terasaki T. Transport mechanism of 3-hydroxy-3-methylglutaryl coenzyme a reductase inhibitors at the blood-brain barrier. *J Pharmacol Exp Ther* 1993;267(3):1085-90.
- 189 Tamai I, Sai Y, Ono A, Kido Y, Yabuuchi H, Takanaga H et al. Immunohistochemical and functional characterization of ph-dependent intestinal absorption of weak organic acids by the monocarboxylic acid transporter mct1. *J Pharm Pharmacol* 1999;51(10):1113-21.
- 190 Bhattacharya I and Boje KM. Ghb (gamma-hydroxybutyrate) carrier-mediated transport across the blood-brain barrier. *J Pharmacol Exp Ther* 2004;311(1):92-8.
- 191 Takanaga H, Maeda H, Yabuuchi H, Tamai I, Higashida H and Tsuji A. Nicotinic acid transport mediated by ph-dependent anion antiporter and proton cotransporter in rabbit intestinal brush-border membrane. *J Pharm Pharmacol* 1996;48(10):1073-7.
- 192 Enerson BE and Drewes LR. Molecular features, regulation, and function of monocarboxylate transporters: Implications for drug delivery. *J Pharm Sci* 2003;92(8):1531-44.
- 193 Tamai I, Takanaga H, Maeda H, Sai Y, Ogihara T, Higashida H et al. Participation of a proton-cotransporter, mct1, in the intestinal transport of monocarboxylic acids. *Biochem Biophys Res Commun* 1995;214(2):482-9.
- 194 Wang Q and Morris ME. The role of monocarboxylate transporter 2 and 4 in the transport of gamma-hydroxybutyric acid in mammalian cells. *Drug Metab Dispos* 2007;35(8):1393-9.
- 195 Wang X, Levi AJ and Halestrap AP. Substrate and inhibitor specificities of the monocarboxylate transporters of single rat heart cells. *Am J Physiol* 1996;270(2 Pt 2):H476-84.
- 196 Skelton MS, Kremer DE, Smith EW and Gladden LB. Lactate influx into red blood cells from trained and untrained human subjects. *Med Sci Sports Exerc* 1998;30(4):536-42.
- 197 Sara F, Connes P, Hue O, Montout-Hedreville M, Etienne-Julan M and Hardy-Dessources MD. Faster lactate transport across red blood cell membrane in sickle cell trait carriers. *J Appl Physiol* 2006;100(2):427-32.
- 198 Koho NM, Hyyppa S and Poso AR. Monocarboxylate transporters (mct) as lactate carriers in equine muscle and red blood cells. *Equine Vet J Suppl* 2006(36):354-8.
- 199 Koho NM, Raekallio M, Kuusela E, Vuolle J and Poso AR. Lactate transport in canine red blood cells. *Am J Vet Res* 2008;69(8):1091-6.
- 200 Koho NM, Vaihkonen LK and Poso AR. Lactate transport in red blood cells by monocarboxylate transporters. *Equine Vet J Suppl* 2002(34):555-9.

- 201 Tesch PA, Daniels WL and Sharp DS. Lactate accumulation in muscle and blood during submaximal exercise. *Acta Physiol Scand* 1982;114(3):441-6.
- 202 Hodoglugil U, Williamson DW, Huang Y and Mahley RW. Common polymorphisms of atp binding cassette transporter a1, including a functional promoter polymorphism, associated with plasma high density lipoprotein cholesterol levels in turks. *Atherosclerosis* 2005;183(2):199-212.
- 203 Tregouet DA, Ricard S, Nicaud V, Arnould I, Soubigou S, Rosier M et al. In-depth haplotype analysis of abca1 gene polymorphisms in relation to plasma apoa1 levels and myocardial infarction. *Arterioscler Thromb Vasc Biol* 2004;24(4):775-81.
- 204 Teo YY, Sim X, Ong RT, Tan AK, Chen J, Tantoso E et al. Singapore genome variation project: A haplotype map of three southeast asian populations. *Genome Res* 2009;19(11):2154-62.
- 205 Nishimura N and Balch WE. A di-acidic signal required for selective export from the endoplasmic reticulum. *Science* 1997;277(5325):556-8.
- 206 Cupeiro R, Benito PJ, Maffulli N, Calderon FJ and Gonzalez-Lamuno D. Mct1 genetic polymorphism influence in high intensity circuit training: A pilot study. *J Sci Med Sport* 2009.
- 207 Cuff MA and Shirazi-Beechey SP. The human monocarboxylate transporter, mct1: Genomic organization and promoter analysis. *Biochem Biophys Res Commun* 2002;292(4):1048-56.
- 208 Faber PW, van Rooij HC, Schipper HJ, Brinkmann AO and Trapman J. Two different, overlapping pathways of transcription initiation are active on the tata-less human androgen receptor promoter. The role of sp1. *J Biol Chem* 1993;268(13):9296-301.
- 209 Kollmar R, Sukow KA, Sponagle SK and Farnham PJ. Start site selection at the tata-less carbamoyl-phosphate synthase (glutamine-hydrolyzing)/aspartate carbamoyltransferase/dihydroorotase promoter. *J Biol Chem* 1994;269(3):2252-7.
- 210 Ng PC and Henikoff S. Accounting for human polymorphisms predicted to affect protein function. *Genome Res* 2002;12(3):436-46.
- 211 Sunyaev S, Ramensky V, Koch I, Lathe W, 3rd, Kondrashov AS and Bork P. Prediction of deleterious human alleles. *Hum Mol Genet* 2001;10(6):591-7.
- 212 Chasman D and Adams RM. Predicting the functional consequences of non-synonymous single nucleotide polymorphisms: Structure-based assessment of amino acid variation. *J Mol Biol* 2001;307(2):683-706.
- 213 Saunders CT and Baker D. Evaluation of structural and evolutionary contributions to deleterious mutation prediction. *J Mol Biol* 2002;322(4):891-901.
- 214 Johnson MM, Houck J and Chen C. Screening for deleterious nonsynonymous single-nucleotide polymorphisms in genes involved in steroid hormone metabolism and response. *Cancer Epidemiol Biomarkers Prev* 2005;14(5):1326-9.
- 215 Ramensky V, Bork P and Sunyaev S. Human non-synonymous snps: Server and survey. *Nucleic Acids Res* 2002;30(17):3894-900.
- 216 Xi T, Jones IM and Mohrenweiser HW. Many amino acid substitution variants identified in DNA repair genes during human population screenings are predicted to impact protein function. *Genomics* 2004;83(6):970-9.
- 217 Copeland R. *Enzymes : A practical introduction to structure, mechanism and data analysis*. New York: Wiley-VCH; 2000.
- 218 Kienzler JL, Gold M and Nollevaux F. Systemic bioavailability of topical diclofenac sodium gel 1% versus oral diclofenac sodium in healthy volunteers. *J Clin Pharmacol* 2010;50(1):50-61.
- 219 Pentikainen PJ, Neuvonen PJ and Backman C. Human pharmacokinetics of tolfenamic acid, a new anti-inflammatory agent. *Eur J Clin Pharmacol* 1981;19(5):359-65.

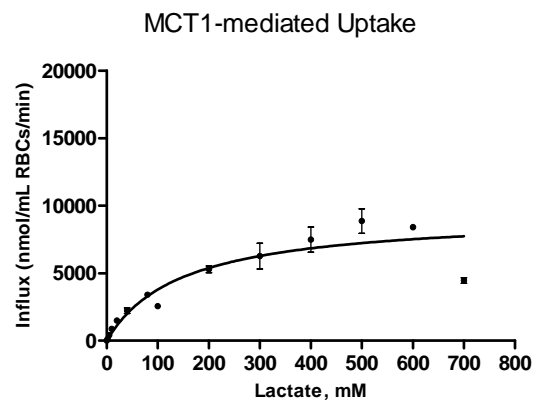
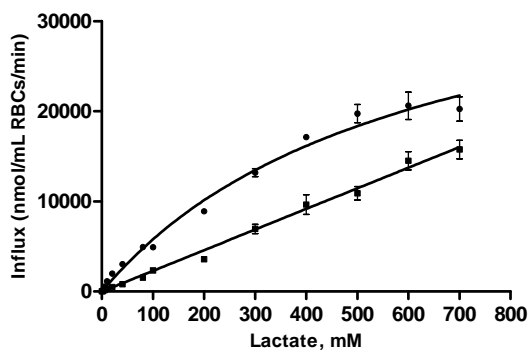
- 220 Schjerning Olsen AM, Fosbol EL, Lindhardsen J, Folke F, Charlot M, Selmer C et al. Duration of treatment with nonsteroidal anti-inflammatory drugs and impact on risk of death and recurrent myocardial infarction in patients with prior myocardial infarction: A nationwide cohort study. *Circulation* 2011;123(20):2226-35.
- 221 Brophy JM. Cardiovascular effects of cyclooxygenase-2 inhibitors. *Curr Opin Gastroenterol* 2007;23(6):617-24.
- 222 Gislason GH, Jacobsen S, Rasmussen JN, Rasmussen S, Buch P, Friberg J et al. Risk of death or reinfarction associated with the use of selective cyclooxygenase-2 inhibitors and nonselective nonsteroidal antiinflammatory drugs after acute myocardial infarction. *Circulation* 2006;113(25):2906-13.
- 223 Gislason GH, Rasmussen JN, Abildstrom SZ, Schramm TK, Hansen ML, Fosbol EL et al. Increased mortality and cardiovascular morbidity associated with use of nonsteroidal anti-inflammatory drugs in chronic heart failure. *Arch Intern Med* 2009;169(2):141-9.
- 224 Solomon SD, McMurray JJ, Pfeffer MA, Wittes J, Fowler R, Finn P et al. Cardiovascular risk associated with celecoxib in a clinical trial for colorectal adenoma prevention. *N Engl J Med* 2005;352(11):1071-80.
- 225 Brophy JM, Levesque LE and Zhang B. The coronary risk of cyclo-oxygenase-2 inhibitors in patients with a previous myocardial infarction. *Heart* 2007;93(2):189-94.
- 226 Jeong D, Kim TS, Lee JW, Kim KT, Kim HJ, Kim IH et al. Blocking of acidosis-mediated apoptosis by a reduction of lactate dehydrogenase activity through antisense mRNA expression. *Biochem Biophys Res Commun* 2001;289(5):1141-9.
- 227 Li YH, Ito K, Tsuda Y, Kohda R, Yamada H and Itoh T. Mechanism of intestinal absorption of an orally active beta-lactam prodrug: Uptake and transport of carindacillin in caco-2 cells. *J Pharmacol Exp Ther* 1999;290(3):958-64.
- 228 Semenza GL. Tumor metabolism: Cancer cells give and take lactate. *J Clin Invest* 2008;118(12):3835-7.
- 229 Sonveaux P, Vegrn F, Schroeder T, Wergin MC, Verrax J, Rabbani ZN et al. Targeting lactate-fueled respiration selectively kills hypoxic tumor cells in mice. *J Clin Invest* 2008;118(12):3930-42.
- 230 Kang KW, Im YB, Go WJ and Han HK. C-myc amplification altered the gene expression of abc- and slc-transporters in human breast epithelial cells. *Mol Pharm* 2009;6(2):627-33.
- 231 Kang KW, Jin MJ and Han HK. Igf-I receptor gene activation enhanced the expression of monocarboxylic acid transporter 1 in hepatocarcinoma cells. *Biochem Biophys Res Commun* 2006;342(4):1352-5.
- 232 Froberg MK, Gerhart DZ, Enerson BE, Manivel C, Guzman-Paz M, Seacotte N et al. Expression of monocarboxylate transporter mct1 in normal and neoplastic human CNS tissues. *Neuroreport* 2001;12(4):761-5.
- 233 Wasserman K. The anaerobic threshold measurement in exercise testing. *Clin Chest Med* 1984;5(1):77-88.
- 234 Margaria R EH, and Dill DB. The possible mechanisms of contracting and paying the oxygen debt and the role of lactic acid in muscular contraction. *Am J Physiol* 1933;106:689-715.
- 235 Brooks GA. Lactate: Glycolytic product and oxidative substrate during sustained exercise in mammals the lactate shuttle. Berlin: Springer; 1985a.
- 236 Wang X, Wang Q and Morris ME. Pharmacokinetic interaction between the flavonoid luteolin and gamma-hydroxybutyrate in rats: Potential involvement of monocarboxylate transporters. *AAPS J* 2008;10(1):47-55.
- 237 Harris RT and Dudley GA. Exercise alters the distribution of ammonia and lactate in blood. *J Appl Physiol* 1989;66(1):313-7.

APPENDIX I.

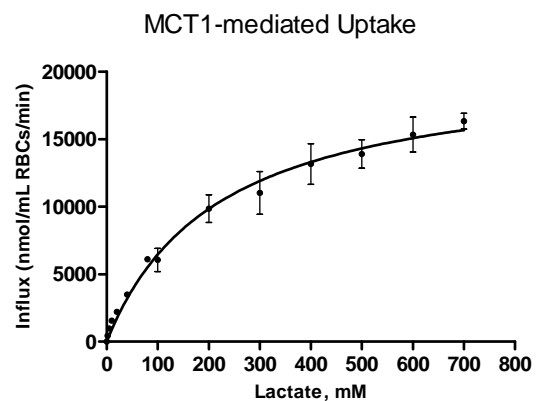
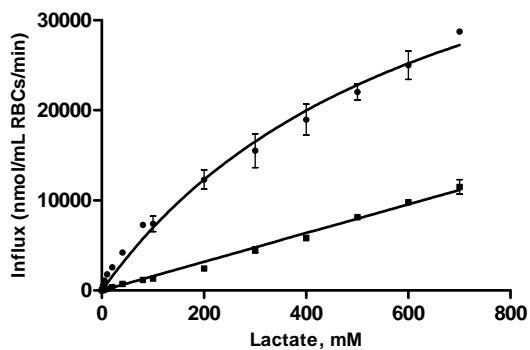
Subject ID: S001



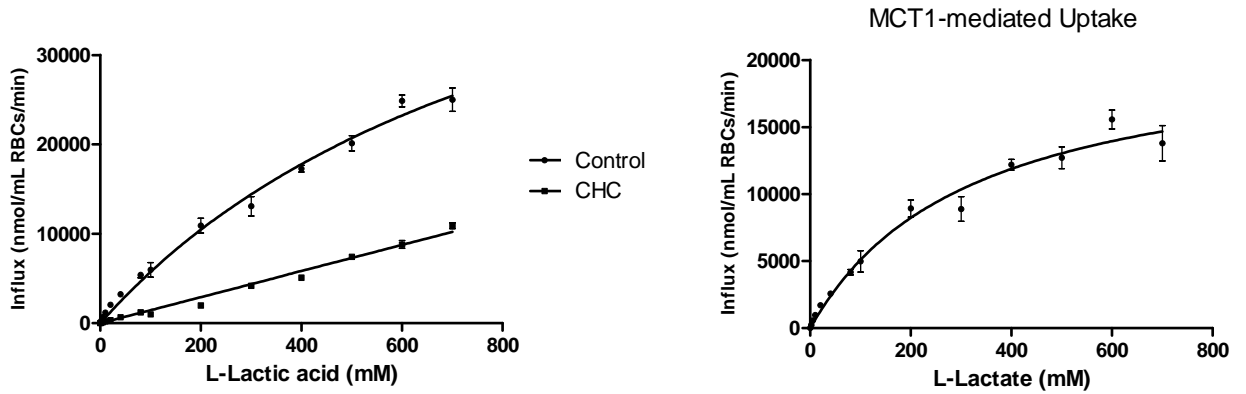
Subject ID: S002



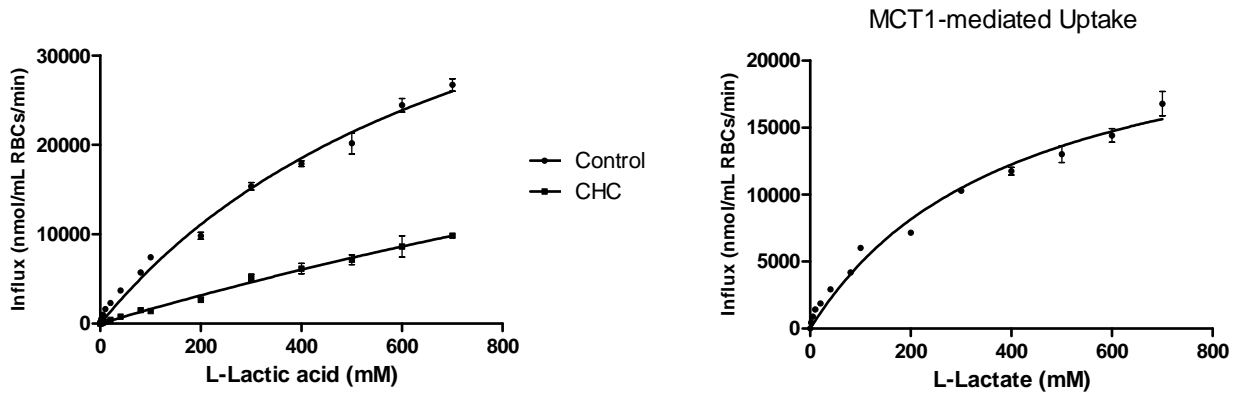
Subject ID: S003



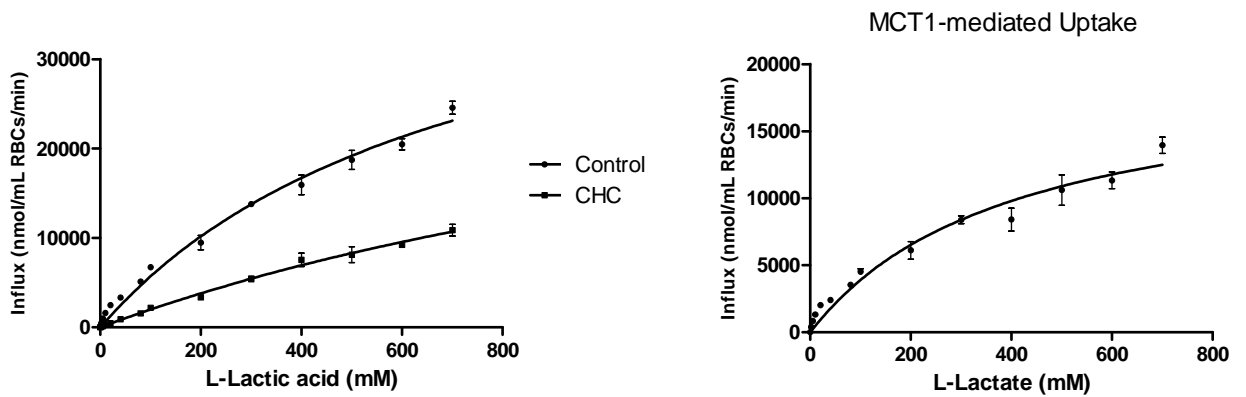
Subject ID: S004



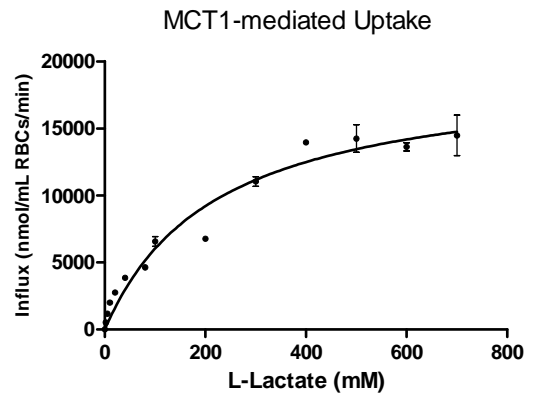
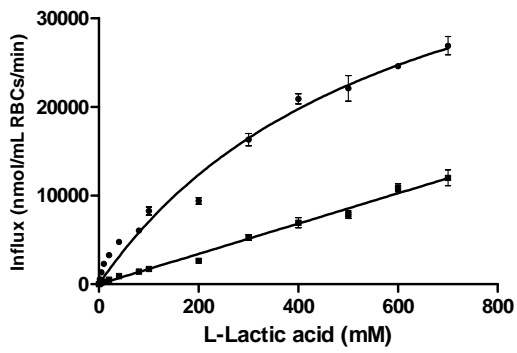
Subject ID: S005



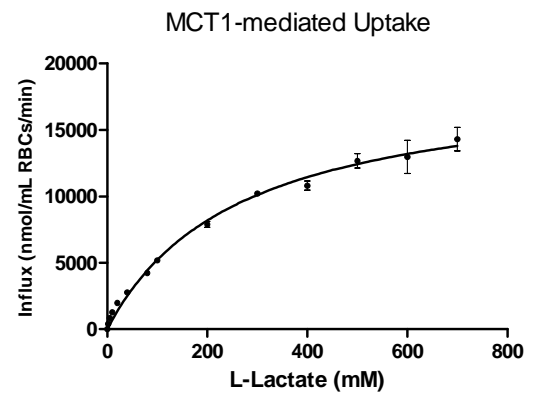
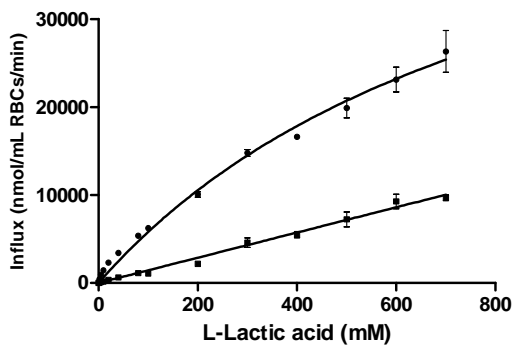
Subject ID: S006



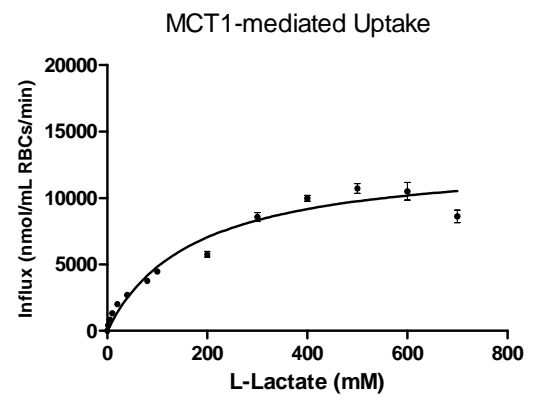
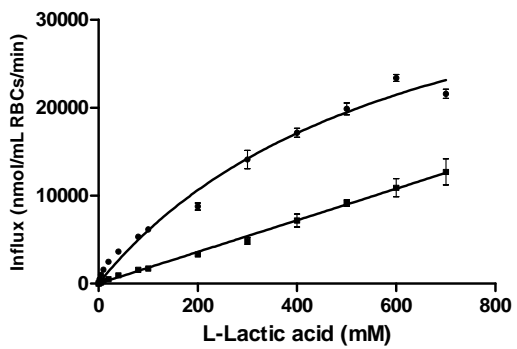
Subject ID: S007



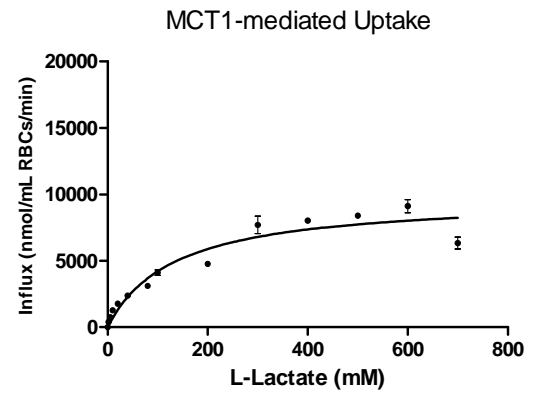
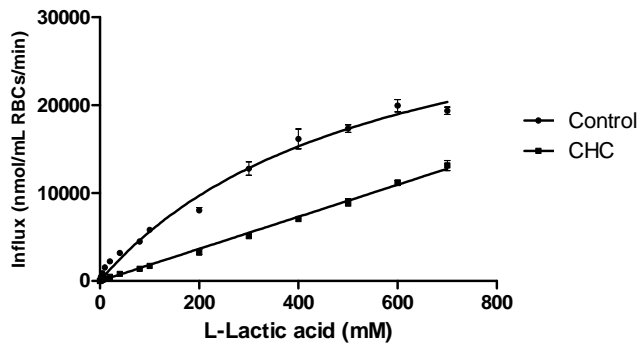
Subject ID: S008



Subject ID: S009



Subject ID: S010



APPENDIX II.

ADMINISTRATIVE INFORMATION

Protocol Title: A Randomized Crossover Study to Evaluate the Potential Influence of MCT1 and Its Inhibitor, Diflunisal, on the Distribution of Lactate in Plasma, Whole Blood and Erythrocyte in Healthy Male Adults.

Protocol Number: PGL2009MCT1

Development Phase: Not Applicable

Investigational drug name: Sodium Lactate, Diflunisal

Primary Study Contact:

Study timelines:

Protocol Synopsis

Protocol Title: An Randomized Crossover Study to Evaluate the Potential Influence of MCT1 and Its Inhibitor, Diflunisal, on the Distribution of Lactate in Plasma, Whole Blood and Erythrocyte in Healthy Male Adults.

Principal Investigator

Edmund JD Lee

Professor

Pharmacology Department / Pharmacogenetics Laboratory

National University of Singapore, Singapore

Study centre, type and number of subjects planned

12 healthy male subjects will be enrolled at a single study centre (Investigational Medicine Unit, National University Health System, designated IMU).

Study period

Estimated date of first subject enrolled Beginning of March 2011

Estimated date of last subject completed End of June 2011

Phase of development

Phase I Pharmacokinetic

Objective

The primary objectives of the study are to evaluate the potential influence of MCT1 and its Inhibitor, diflunisal, on the distribution of lactate in plasma, whole blood and erythrocyte. The secondary objectives of the study are to evaluate the impact of the genetic variation in MCT1 on the distribution of lactate and on the drug interaction with diflunisal.

Study design

This will be a single-center, randomized, 2 periods crossover drug interaction study conducted in 12 healthy adult male volunteers. Twelve subjects will be randomly divided into two groups: A and B, with 6 in each group. The 12 subjects will undergo the following treatments in 2 periods: in Period 1: Single dose infusion of sodium lactate (5.6 mg/kg/min for 30 min) + Diflunisal (500 mg) multiple oral doses to group A subjects; Placebo multiple oral does to group B; in Period 2: the two groups will be crossed over. Blood samples will be collected at regular interval and will be analyzed for the study drug by validated methods. Post hoc examination of polymorphisms in *SLC16A1* (MCT1) gene and possibly others will be conducted.

Investigational product, dosage and mode of administration

Each subject will undergo the following treatments in 2 periods in the following sequence:

Period 1: be administered a single dose infusion of sodium lactate (5.6 mg/kg/min for 30 min). Diflunisal (**Apo-Diflunisal**, Apotec Inc Canada, 500 mg) or placebo will be administered to the subjects twice daily 2 days prior to the day of dosing and in the morning on the day of dosing.

Period 2: be administered a single dose infusion of sodium lactate (5.6 mg/kg/min for 30 min). Diflunisal (**Apo-Diflunisal**, Apotec Inc Canada, 500 mg) or placebo will be administered to the subjects twice daily 2 days prior to the day of dosing and in the morning on the day of dosing.

Duration of treatment

This will be a single-centre, randomized, 2 periods, drug-interaction study. A washout period of 7 days is incorporated between the study periods.

Outcome variables

- Pharmacokinetic

The primary endpoint for the study will be the plasma and erythrocyte lactate distribution in the absence or presence of diflunisal.

- Pharmacogenetics

Blood samples will be obtained from each subject and will be used to study genetic polymorphisms of monocarboxylate transporter 1 (MCT1, *SLC16A1*). Post hoc examination of polymorphisms in this gene will be conducted using DNA extracted from all the participants for pharmacokinetic study.

1. Introduction

1.1 Background

Monocarboxylate transporter 1: The monocarboxylate transporter (MCT) family currently comprises 14 members, but only the first 4 members (MCT1-MCT4) have been experimentally proven to mediate the transportation of metabolically important endogenous monocarboxylates such as pyruvate, lactate, acetate and ketone bodies (1-2). These monocarboxylate anions are transported across the plasma membrane via active or facilitated transporter down their concentration gradients due to their highly charged chemical structures. MCT1 is the first member of the family and it is found in the great majority of tissue including skeletal muscle, brain endothelium (blood-brain barrier (BBB)), intestine, erythrocyte and heart (2-3). MCT1 plays a very vital role in the energy metabolism and pH regulation of the cells and its impairment might provide an explanation for some pathophysiological conditions.

MCT1, together with other MCTs, are involved in the pH regulation and metabolism of the cells. As large amounts of lactic acid are constantly produced in anaerobic glycolytic tissues (such as white skeletal muscle, red blood cells and tumor cells), the efflux of lactic acid must keep pace with its production to prevent a drop in intracellular pH (1-2). In other tissues (such as red skeletal muscle, brain and heart), lactic acid is transported into the cell and is utilized as a respiratory fuel (1-2). This cell-to-cell lactate shuttle hypothesis has been proposed in at least 4 tissues- skeletal muscle, brain, retina and testis (4). The overall pattern of lactate transport is quite similar in the aforementioned tissues, by which the organ is subdivided into glycolytic and oxidative cell types, with the latter cell type utilizing the “waste products” produced by the former cell type as energy source. This mechanism provides the most efficient energy utilization and therefore is adapted by tissues of which energy demand is high.

It is now clear that lactate is an intermediary in numerous metabolic process, a mobile fuel for aerobic metabolism, and perhaps a mediator for redox state among various compartments both within and between cells (5). Blood (both plasma and RBCs) constitutes a key component in the lactate shuttle because of its role in distributing lactate throughout the body’s different tissues. Plasma carries ~70% of the lactate released from muscle lactate output and RBCs provides an additional space for translocation ~30% of lactate and hydrogen ions from the plasma (6). Transport of these metabolites away from the exercising muscle and into the blood by the MCT pathway may reduce the potential for muscle acidosis and fatigue.

Lactic acid exists predominantly in the form of lactate at physiological pH due to its low pKa value. Lactic acid may diffuse across the cell membrane, but, for the transport of lactate anion, a transporter is required. In mammalian erythrocytes, three parallel pathways of lactate influx are present: 1) nonionic diffusion of the undissociated acid; 2) inorganic-anion exchange system; and 3) monocarboxylate-specific carrier system (7-9). The significance of each of these pathways with regard to lactate transport is known to vary among species(9-10). Interestingly, the monocarboxylate-specific carrier system has been shown to be the predominant route for lactate influx in human erythrocytes and MCT1 has been shown to be the only monocarboxylate transporter expressed in human RBC (11-12). Therefore, any impairment (due to genetic defects or MCT inhibitors) in the activity of MCT1 is likely to have far-reaching consequences. In fact, the defect in MCT1 has been associated with lactate transport deficiency in red blood cells and muscle tissues by Fishbein back in 1986 (13).

1.2 Rationale

1.2.1 Lactate as a probe substrate for MCT1: Transport of lactate across erythrocyte membrane is mediated by MCT1 via a proton-mediated manner (1,2,4,7-12). Exogenous lactate infusion had been used in several studies to raise the blood lactate levels in human (15-18). Sodium lactate is administered by intravenous route as an electrolyte replenisher and systemic alkalizer. Adverse effects of sodium lactate are essentially limited to overdosage of either sodium or lactate ions.

1.2.2 Diflunisal as an inhibitor for MCT1: Various NSAIDs have been shown to strongly inhibit the MCT1 uptake of benzoic acid in Caco-2 cells and diflunisal was shown to be the most potent inhibitor among the tested NSAIDs (19). Therefore, diflunisal will be chosen to investigate the impact of MCT1 inhibition on drug distribution.

1.3 Significance

MCT1 plays a very significant role in the energy metabolism and pH regulation of the cells and blood constitutes a key component in the lactate shuttle because of its role in distributing lactate throughout the body's different tissues. It will therefore be beneficial to clinically examine the physiological effect of MCT1-mediated lactate influx from plasma to erythrocyte. Hence, the purpose of this study is to evaluate the potential influence of MCT1 on the distribution of lactate in plasma and erythrocyte and the effects of the MCT1 inhibitor, diflunisal, on lactate distribution in blood. The results of this study will increase our understanding of the clinical relevance of MCT1 transporter-based drug interactions.

2. Study Objectives

2.1 Primary

The primary objectives of the study are to evaluate the potential influence of MCT1 and its Inhibitor, diflunisal, on the distribution of lactate in plasma, whole blood and erythrocyte.

2.2 Secondary

The secondary objectives of the study are to evaluate the impact of the genetic variation in MCT1 on the distribution of lactate in blood and on the drug interaction with diflunisal.

3. Study Endpoint(s)

3.1 Primary

- Pharmacokinetics

The primary endpoint for the study will be the plasma and erythrocyte lactate distribution in the absence or presence of diflunisal.

3.2 Secondary

- Pharmacogenetics

Blood samples will be obtained from each subject and will be used to study specific genetic polymorphisms of monocarboxylate transporter 1 (MCT1, *SLC16A1*). Post hoc examination of polymorphisms in this gene will be conducted using DNA extracted from all the participants for pharmacokinetic study.

4. Study Design

4.1 Overall study design

This will be a single-center, randomized, 2 periods crossover drug interaction study conducted in 12 healthy adult male volunteers. Twelve subjects will be randomly divided into two groups: A and B, with 6 in each group. The 12 subjects will undergo the following treatments in 2 periods: in Period 1: Single dose infusion of sodium lactate (5.6 mg/kg/min for 30 min) + Diflunisal (500 mg) multiple oral doses to group A subjects; Placebo multiple oral doses to group B; in Period 2: the two groups will be crossed over.

For **Period 1**, subjects will be admitted to the unit in the evening prior of the dosing day and will stay until 2 hours after dosing for the collection of blood samples for measurement of drug content (Table 1).

For **Period 2**, subjects will be admitted to the unit in the evening prior of the dosing day and will stay until 2 hours after dosing for the collection of blood samples for measurement of drug content (Table 2).

Subjects will fast from all food and drink (except water) for at least 10 hours prior to dosing with study medication until 1 hour after dosing. Each oral medication will be administered with 250mL of water. Subjects will be asked not to break, crush, or chew the diflunisal tablet before swallowing. Blood samples will be collected at regular intervals as indicated in Table 1 and Table 2. A washout period of 7 days is incorporated between the study periods to avoid the influence of previously administered drug(s). Post hoc examination of polymorphisms in MCT1 gene will be conducted.

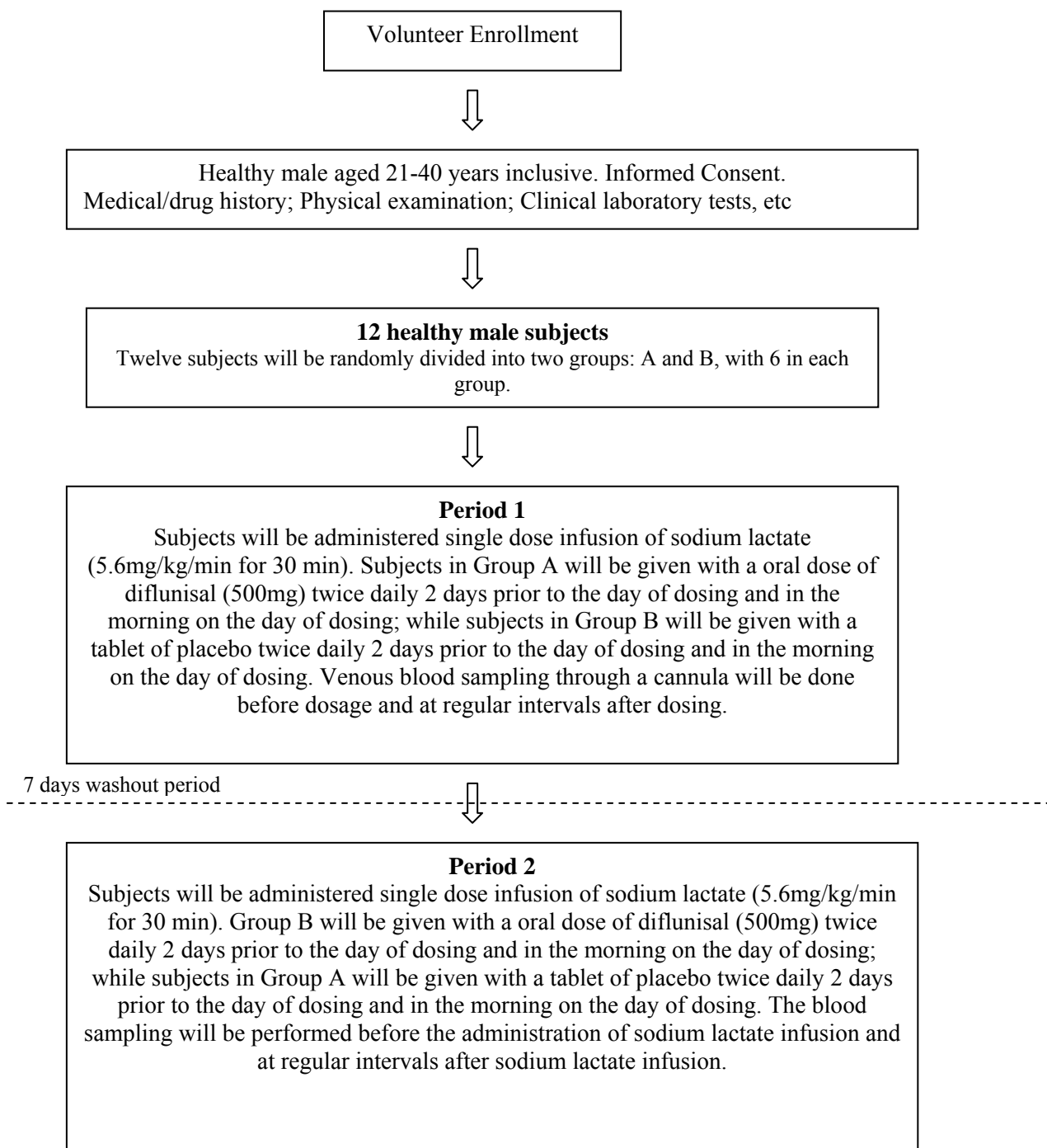
Table 1. Study Plan- Period 1

| Time relative to dose | 1st Screening visit | Subject admission / Pretreatment | | | | | Pharmacokinetic study duration | | | | | | | | | | Final evaluation |
|--|---------------------|----------------------------------|--------|--------|--------|--------|--------------------------------|---------|---|--------|--------|--------|--------|--------|--------|----------|------------------|
| | Day -15 | -Day 2 | | -Day 1 | | | Day 1 | | | | | | | | | | |
| | | -50 hr | -38 hr | -26 hr | -14 hr | -11 hr | -2 hr | -10 min | 0 | 10 min | 20 min | 30 min | 40 min | 50 min | 60 min | > 60 min | |
| Informed consent | • | | | | | | | | | | | | | | | | |
| Review eligibility | • | • | | | | | | • | | | | | | | | | |
| Inpatient at study unit | | | | | ← | | | | | | | | | | | → | |
| Medical/Drug history | • | • | | | | | | | | | | | | | | | |
| Seated vital signs | • | • | | | | | | • | | | | | | | | • | |
| Physical examination | •complete | •brief | | | | | | • | | | | | | | | •brief | |
| Clinical lab tests | • | | | | | | | | | | | | | | | | |
| Regulated food and water intake | | | | | | • | | | | | | | | | | | |
| Administration of Sodium lactate infusion | | | | | | | | • | | | | | | | | | |
| Administered with Diflunisal (A) or Placebo (B) | | • | • | • | • | | • | | | | | | | | | | |
| Venous blood sampling for lactate measurement | | | | | | | | • | | • | • | • | • | • | • | | |
| Venous blood sampling for pH and CO ₂ measurement | | | | | | | | • | | | | • | | | • | | |
| AEs/SAEs monitoring | | • | • | • | • | • | • | • | • | • | • | • | • | • | • | • | |

Table 2. Study Plan- Period 2

| Time relative to dose | Subject admission / Pretreatment | | | | | Pharmacokinetic study duration | | | | | | | | | | Final evaluation |
|--|----------------------------------|--------|--------|--------|--------|--------------------------------|---------|---|--------|--------|--------|--------|--------|--------|----------|------------------|
| | Day 8 | | Day 9 | | | Day 10 | | | | | | | | | | |
| | -50 hr | -38 hr | -26 hr | -14 hr | -11 hr | -2 hr | -10 min | 0 | 10 min | 20 min | 30 min | 40 min | 50 min | 60 min | > 60 min | |
| Review eligibility | • | | | | | | • | | | | | | | | | |
| Inpatient at study unit | | | | ← | | | | | | | | | | | → | |
| Medical/Drug history | • | | | | | | | | | | | | | | | |
| Seated vital signs | • | | | | | | • | | | | | | | | | • |
| Physical examination | • brief | | | | | | • | | | | | | | | | • brief |
| Clinical lab tests | | | | | | | | | | | | | | | | |
| Regulated food and water intake | | | | | • | | | | | | | | | | | |
| Administration of Sodium lactate infusion | | | | | | | | • | | | | | | | | |
| Administered with Diflunisal (B) or Placebo (A) | • | • | • | • | | • | | | | | | | | | | |
| Venous blood sampling for lactate measurement | | | | | | | • | | • | • | • | • | • | • | | |
| Venous blood sampling for pH and CO ₂ measurement | | | | | | | • | | | | • | | | • | | |
| AEs/SAEs monitoring | • | • | • | • | • | • | • | • | • | • | • | • | • | • | • | • |

Figure 1: Study Flow Charts



5. Selection of Study Population

5.1 Number of subjects

This study will screen approximately 30 subjects to get enough 12 healthy volunteers.

5.2 Study selection record

In order to establish that the subject population was selected without bias, a record will be kept of subjects who were considered for enrolment and the reasons why they were not enrolled will be recorded in the subject screening log.

5.3 Eligibility criteria

5.3.1 Inclusion criteria

1. The subject is healthy, as judged by a responsible physician, with no clinically significant abnormality identified on the laboratory or medical evaluation, including 12-lead ECG, at screening. A subject with a clinical laboratory or laboratory parameter outside the reference range (adjusted for age, if appropriate), may be included only if the Investigator considers that the abnormal finding does not pose additional risk and will not interfere with the study procedures.
2. Male aged 21-40 years inclusive.
3. Body weight \geq 50kg (110 lbs) and body mass index (BMI) of 18.5 to 29.9 kg/m² inclusive (BMI will be calculated as weight in kg/[height in m²]).
4. Have normal renal function as evident by a normal creatinine clearance and normal serum creatine levels.
5. The subject is capable of giving informed consent, which includes compliance with the requirements and restrictions listed in the consent form.

5.3.2 Exclusion criteria

1. A positive urine test for drugs of abuse or alcohol at screening or prior to the start of dosing in treatment period 1.
2. Subjects with a clinical history or current alcohol or illicit drug use which, in the opinion of the investigator, would interfere with the subject's ability to comply with the dosing schedule and protocol-specified evaluations. A history of regular alcohol consumption averaging $>$ 14 drinks/week (1 drink (12 g alcohol) = 5 ounces (150 mL) of wine or 12 ounces (360 mL) of beer or 1.5 ounces (45 mL) of 80 proof distilled spirits) within 6 months of screening.

3. The subject has received an investigational drug or participated in any other research trial within 30 days, 5 half-lives, or twice the duration of the biological effect of any drug (whichever is longer) prior to the first dose of current study medication.
4. Use of any prescription or non-prescription drugs, vitamins, herbal and dietary supplements within seven days (or 14 days if the drug is a potential enzyme inducer, such as St. John's Wort) or 5 half-lives (whichever is longer) prior to the first dose of study medication, unless in the opinion of the Investigator and sponsor the medication will not interfere with the study procedures or compromise subject safety.
5. Has a history of regular use of tobacco- or nicotine-containing products within 3 months of the screening visit.
6. Subjects with a pre-existing condition interfering with normal gastrointestinal anatomy or motility, hepatic and/or renal function, that could interfere with the absorption, metabolism, and/or excretion of the study drugs. Examples of conditions that could interfere with normal gastrointestinal anatomy or motility include gastrointestinal bypass surgery, partial or total gastrectomy, small bowel resection, vagotomy, malabsorption, Crohn's disease, ulcerative colitis, intestinal or urinary obstruction, or celiac sprue.
7. History of hypersensitivity to sodium lactate or diflunisal or other NSAIDs; or history of drug or other allergy that, in the opinion of the physician responsible, contraindicates their participation.
8. Subjects with a history of clinically significant hepatic disease or hepatic dysfunction.
9. Subjects with congestive heart failure or recently had or will be having bypass heart surgery.
10. Subjects with severe renal insufficiency (with calculated creatinine clearance < 60mL/min) and in clinical states in which there exists edema with sodium retention.
11. Subjects with a history of stomach or bowel problems (e.g., bleeding, perforation, ulcers).
12. Subjects with a history of swelling or fluid buildup, asthma, growths in the nose (nasal polyps), or mouth inflammation.
13. Subjects with a history of psychiatric disorder or panic attack.
14. Subjects with known pancreatitis.
15. Subjects with bleeding, low platelet count and coagulation problems.
16. Anuria or oliguria.

17. Subjects with anoxia, beriberi or diabetes

6. Study Assessment and Procedures

6.1 Enrolment procedures

The screening will take place approximately 28 days before the start of the study. Recruitment of volunteers will be executed by the IMU staff of National University Health System in compliance with GCP guidelines. Approximately 30 male subjects between 21 and 40 years of age will be recruited after providing informed written consent. Candidates that satisfy all inclusion/exclusion criteria, pass a routine physical examination and have acceptable screening laboratory results will be enrolled into the pharmacokinetic study. A final number of 12 healthy male volunteers are expected to participate in the study.

6.2 Screening visit procedures

Screening will be conducted after the DSRB-approved informed consent has been signed but within the 28 days preceding study drug administration. Each subject will undergo enrolment evaluations and procedures during consecutive screening periods, according to the Study Plan (Table 1).

The following activities will occur during this Screening Visit:

1st Screening

- Informed consent;
- Demography, including date of birth, sex, and race/ethnicity;
- Determination of eligibility based on inclusion/exclusion criteria;
- Complete Medical/Drug history;

A complete medical and drug history will be recorded for each subject. Significant medical conditions that have occurred within the past 2 years or conditions that are ongoing (ie, headache, backache, indigestion) are to be recorded in the CRF. The drug history must identify any known drug allergies (history of hypersensitivity to diflunisal or other NSAIDs; or history of drug or other allergy that, in the opinion of the physician responsible, contraindicates their participation), presence of history of drug abuse and use of chronic medications. Medications taken within 2 weeks of Day 1 of the inpatient period are to be recorded in the CRF.

- Alcohol/Smoking history;
- Vital signs- blood pressure, heart rate and temperature, taken after resting at a sitting position for at least 5 minutes;

- Complete physical examination;
- 12-lead ECG;
- Clinical (safety) laboratory tests;

6.3 Treatment phase procedures

6.3.1 Day -2 pre-dose procedures

Subjects will be asked to make a separate visit to the unit twice daily on Day-2 for pre-treatment with diflunisal or placebo;

- Administration of diflunisal or placebo at 7am (window period: 7 to 9 am);
- Administration of diflunisal or placebo at 7pm (window period: 7 to 9 pm);

6.3.2 Day -1 pre-dose procedures

Subjects will be asked to make a separate visit to the unit at 0700 hour in the morning for the administration of diflunisal or placebo. At approximately 1700 hour, subjects will be asked to admit to the unit.

- Administration of diflunisal or placebo at 7 am (window period: 7 to 9 am);

On admission to the Investigational Medicine Unit (IMU) at 1700 hour on Day -1, subjects will be reminded of study restrictions and undergo the following assessments:

- Interim medical history;
- Interim concomitant medication history;
- Seated vital signs;
- Brief physical examination;
- Administration with diflunisal or placebo at 7 pm (window period: 7 to 9 pm);

6.3.3 Day 1 procedures

Blood pressure, heart rate and temperature, taken after resting at a sitting position for at least 5 minutes (Pre-dose);

- Brief physical examination (Pre-dose);
- Interim concomitant medications;

- AE assessment;
- Administration of diflunisal or placebo at -2 hour pre-dose;
- Collection of pre-dose PK blood sample;
- Collection of blood sample for blood gas analysis.
- Administration of sodium lactate infusion (subjects should be fasted for at least ten hours prior to and one hour following administration of study medication)
- Collection of PK blood samples at 10, 20, 30 minute post-dose;
- Collection of blood sample for blood gas analysis.
- Collection of PK blood samples at 40, 50, 60 minute post-dose;
- Collection of blood sample for blood gas analysis.
- Subjects may be discharged from the IMU 2 hours after the collection of 60 minute PK blood sample;

6.4.3 Day 8 pre-dose procedures

Subjects will be asked to make a separate visit to the unit twice daily on Day 8 for pre-treatment with diflunisal or placebo;

- Administration of diflunisal or placebo at 7am (window period: 7 to 9 am);
- Administration of diflunisal or placebo at 7pm (window period: 7 to 9 pm);

6.3.5 Day 9 pre-dose procedures

Subjects will be asked to make a separate visit to the unit at 0700 hour in the morning for the administration of diflunisal or placebo. At approximately 1700 hour, subjects will be asked to admit to the unit.

- Administration of diflunisal or placebo at 7 am (window period: 7 to 9 am);

On admission to the Investigational Medicine Unit (IMU) at 1700 hour on Day 9, subjects will be reminded of study restrictions and undergo the following assessments:

- Interim medical history;
- Interim concomitant medication history;

- Seated vital signs;
- Brief physical examination;
- Administration with diflunisal or placebo at 7 pm (window period: 7 to 9 pm);

6.3.6 Day 10 procedures

Blood pressure, heart rate and temperature, taken after resting at a sitting position for at least 5 minutes (Pre-dose);

- Brief physical examination (Pre-dose);
- Interim concomitant medications;
- AE assessment;
- Administration of diflunisal or placebo at -2 hour pre-dose;
- Collection of pre-dose PK blood sample;
- Collection of blood sample for blood gas analysis.
- Administration of sodium lactate infusion (subjects should be fasted for at least ten hours prior to and one hour following administration of study medication)
- Collection of PK blood samples at 10, 20, 30 minute post-dose;
- Collection of blood sample for blood gas analysis.
- Collection of PK blood samples at 40, 50, 60 minute post-dose;
- Collection of blood sample for blood gas analysis.
- Subjects may be discharged from the IMU 2 hours after the collection of 60 minute PK blood sample;

6.4 Follow-up visit procedures

- Interim concomitant medication history;
- AE assessment;
- Brief physical examination;

6.5 Safety measurements

Measurement used to evaluate safety include clinical laboratory tests, vital signs, 12-lead ECGs, physical examination and monitoring for adverse events.

6.5.1 Clinical laboratory tests

Clinical (safety) tests will be performed including clinical chemistry, hematology and urinalysis. Blood and urine samples will be taken during the screening at the times stated in the Study Plan (Table 1 and Table 2). The date of collection will be recorded on the appropriate CRF.

- Samples will be collected in the following tubes and at the volumes specified:

| | |
|--------------------|---|
| Clinical chemistry | 5 ml in a serum separator tube (SST) |
| Hematology | 3 ml in a tube containing EDTA |
| Urinalysis | 10 ml midstream sample in a urine specimen tube |
| Blood gas analysis | 3 ml in tube containing EDTA |

- The following variables will be measured:

| | |
|--------------------|---|
| Clinical chemistry | ALP, ALT, AST, albumin, chloride, creatinine, glucose, potassium, sodium, total protein, total & direct bilirubin, urea nitrogen, uric acid |
| Hematology | Erythrocyte count, hemoglobin, hematocrit, leukocyte cell count, platelet count |
| Urinalysis | Bilirubin, RBC count, glucose, ketone bodies, pH, protein, specific gravity |
| Blood gas analysis | Carbon dioxide (CO ₂) gases, pH (hydrogen ion concentration) |

6.5.2 Vital signs

Vital signs consist of oral temperature, heart rate and blood pressure. Assessment of vital signs should be performed after resting in a sitting position for at least 5 minutes.

6.5.3 Physical examinations

- Complete physical examination

The complete physical examination consists of an assessment of the eyes, ears, nose, throat, lymph nodes, heart, abdomen, lungs/thorax, extremities (including spines), skin, and neurologic (reflexes). Physical examination data to be recorded on the CRF will include: 1) normal/abnormal/not done, and 2) a description of any abnormalities.

- Brief physical examination

The brief physical examination includes the assessment of the abdomen, heart, and lungs/thorax. If the subject states changes have occurred related to systems not assessed, then these systems should also be examined. Brief physical examination data to be recorded on the CRF will include: 1) normal/abnormal/not done, and 2) a description of any abnormalities.

6.5.4 Adverse event assessments

Possible side effects of sodium lactate:

- Adverse effects of sodium lactate are essentially limited to overdosage of either sodium or lactate ions;

Possible side effects of diflunisal:

- Gastrointestinal discomfort (nausea, vomiting, heartburn, gas, dyspepsia, gastrointestinal pain, diarrhea, constipation, and flatulence);
- Any sign of allergic reaction (pruritus, urticaria, rash etc);
- Dizziness, drowsiness, headache, fatigue/tiredness.
- Somnolence, insomnia.

The Product Prescribing Information will be consulted for detailed information on safety monitoring and management of adverse events.

6.6 Genetic Sampling, Labelling, Storage, and Shipping

Post hoc examination of polymorphisms in MCT1 gene will be conducted. Blood samples will be obtained from each subject to identify the genotypes of MCT1. DNA extracted from the participants for pharmacokinetic study might also be used to identify the genetic variants of other drug transporters. The results of genetic testing will be kept confidential, but de-identified genetic data may be reviewed with research collaborators and published. Otherwise, no genetic data will be provided to the subject, the subject's family, the investigator, or any other physician who is treating the subject or who may treat the subject in the future. Neither the subject's insurance company nor the subject's employer will have any access to these test results. There will be no direct benefit to the subject in having DNA testing performed.

6.6.1 Collection and Labelling of Genetic Samples

Approximately 10 ml of blood will be collected from each subject into EDTA-coated polypropylene tubes on the day of enrollment screening according to the Study Plan (Table 1 and 2). The blood should be mixed by gentle inversion of the tube. Tubes should be labelled with the following information only: "Genotyping Sample", date of sample, study number and subject number.

6.7 Volume of Blood Sampling

The total volume of blood that will be drawn from each subject in this study is as follows:

Table 3 Volume of blood to be drawn from each subject

| Assessment | Samples volume (ml) | n of samples | Total volume (ml) |
|--|---------------------|--------------|-------------------|
| Pharmacokinetic sampling (Lactate assay) | 10 | 14 | 140 |
| Genetic Analysis | 10 | 1 | 10 |
| Safety Clinical chemistry | 5 | 3 | 15 |
| Hematology | 3 | 1 | 3 |
| Blood gas test | 3 | 3 | 9 |
| Total | | | 177 |

6.8 Pharmacokinetic samples

6.8.1 Blood samples for pharmacokinetic measurements

For timing of individual sample collections refer to the Study Plan (Table 1 and 2). The collection and processing of blood samples, and the labelling and storage of plasma for bioanalysis are described below. The plasma and whole blood samples will be analyzed for study drug by validated methods. Enzymatic method (BioVision, Inc) will be used to determine the plasma and whole blood lactate levels. All bioanalytical assays will be performed by trained technical personnel in compliance with good laboratory practice (GLP) guidelines.

6.8.2 Collection of blood samples (PK)

Blood samples (10ml) for the determination of lactate concentrations will be collected in EDTA-containing tubes at time specified in the Study Plan (Table 1 and Table 2) and immediately cooled on ice. Samples will be clearly labelled. The date and time of collection will be recorded on the CRF.

6.8.3 Processing of blood samples (PK)

The blood sample will be split into 2 tubes. One tube will be centrifuged at 1800g for 10 mins at +4°C. The resulting plasma and erythrocyte samples will be stored separately in below -80°C and at +4°C, respectively, until assay. The remaining tube of whole blood sample will be stored at +4°C.

6.8.4 Labelling of blood samples (PK)

Labels must be applied to the plasma, erythrocyte and whole blood sample tubes; they will include the following information:

Plasma sample

Study number:

Subject number:

Study Day:

Protocol time:

Matrix: PLASMA

Analyte: Lactate

Erythrocyte sample

Study number:

Subject number:

Study Day:

Protocol time:

Matrix: ERYTHROCYTE

Analyte: Lactate

Whole blood sample

Study number:

Subject number:

Study Day:

Protocol time:

Matrix: WHOLE BLOOD

Analyte: Lactate

6.8.5 Storage of blood samples (PK)

All frozen samples to be stored in below -20°C freezer, prior to shipment.

All erythrocyte and whole blood samples to be stored at +4°C, prior to shipment.

All samples should **NOT** be allowed, at any time, to thaw during storage and subsequent delivery to **Pharmacogenetics Laboratory of NUS (PGL)**.

6.8.6 Shipment of blood samples (PK)

Plasma samples will be shipped frozen using dry ice in an insulated container while erythrocyte samples will be transported on ice in an icebox.

All blood samples will be delivered to the Pharmacogenetics Laboratory of NUS (PGL) for analysis.

7. Lifestyle and/or Dietary Restrictions

Subjects will fast from food and drink (except water) for at least ten hours prior to dosing until one hour after dosing.

Standard meals will be served as outlined below. At all mealtimes, food will be served after completion of protocol-specified procedures.

- An evening snack will be allowed until 10:00 pm.
- Breakfast will not be provided on the morning of dosing.
- Standard and identical meals will be provided during PK study.

7.1 Caffeine, Alcohol and Tobacco Restrictions

Caffeine

During each dosing period, subjects will abstain from ingesting caffeine containing products for 24 hours prior to the start of dosing until collection of the final pharmacokinetic sample during each period.

Alcohol

During each dosing period, subjects will abstain from alcohol for 24 hours prior to the start of dosing until collection of the final pharmacokinetic sample during each period.

Tobacco

The use of tobacco or nicotine-containing products is not permitted during this study.

8. Investigational products

8.1 Study Medication/Formulation

- Sodium Lactate Solution 5.6 mg/kg/min Intravenous Infusion (Hospira Inc. USA)
- Diflunisal 500 mg Regular Release Tablets (Apo-Diflunisal, Apotex Inc. Canada)

8.2 Dose Rationale

A single dose infusion of sodium lactate will be given to each eligible subject at infusion rate of 5.6 mg/kg/min for 30 mins. Blood lactate level is expected to increase to approximately 3-4 mM based on the references provided for several studies (15-18).

In the study done by van Hall *et al.*, the subjects were given sodium lactate intravenous infusion at infusion rate of 5.6 mg/kg/min for 20 mins, followed by infusion of 4.3 mg/kg/min for another 100 mins. In the study, no adverse effects had been reported (15). Coco M *et al.* reported that the increase of blood lactate is associated with a worsening of attentional processes. However, the effect of blood lactate on attentional processes is reversible and attention efficacy will be restored upon reversion of blood lactate to normal resting levels (18). This is a transient event and blood lactate level will be returned to normal within 20 minutes after the lactate infusion (18).

A dose regimen of 500 mg diflunisal has been selected based on an assumption that the mean diflunisal plasma concentration following administration of 500 mg single oral dose is sufficient to inhibit MCT1 transport activity. Diflunisal exhibits a strong inhibitions effect in the uptake of benzoic acid with an IC₅₀ value of 50 µM, which equivalent to 12.51 µg/mL (19). Pharmacokinetics study of diflunisal indicated that the mean plasma diflunisal level is approximately 23 µg/mL following a single does of diflunisal 250 mg in non-fasting state (20). However, 500 mg dose regimen is selected in order to achieve the maximum suppression on MCT1 transport activity. A dose regimen of 1000 mg daily in divided doses has been approved for maintenance therapy of rheumatoid arthritis and osteoarthritis. Maintenance doses higher than 1500 mg a day are not recommended.

8.3 Dosage and Administration

During each treatment period, subjects will receive the following treatments. A washout period of 7 days is incorporated between the study periods to avoid the influence of previously administered drug(s).

Period 1: Single dose infusion of sodium lactate (5.6 mg/kg/min for 30 min) + Diflunisal (500 mg) multiple oral doses to group A subjects; Placebo multiple oral does to group B

Period 2: the two groups will be crossed over.

Subjects will be asked to fast at least ten hours prior to and one hour following administration of study medication. Each oral medication will be administered with 250mL of water. Subjects will be asked not to break, crush, or chew the diflunisal tablet before swallowing.

8.4 Blinding

This study is single-blinded study.

8.5 Packaging and Labeling

Commercially-available products will be purchased by site for use in this study.

8.6 Preparation

No specific preparation of study medication is required prior to administration.

8.7 Handling and Storage

Investigational product must be dispensed or administered according to procedures described herein. Only subjects enrolled in the study may receive investigational product, in accordance with all applicable regulatory requirements. Only authorized site staff may supply or administer investigational product. All investigational products must be stored in a secure area with access limited to the investigator and authorized site staff and under physical conditions that are consistent with investigational product-specific requirements.

Investigational products will be stored at a controlled room temperature of 20-25°C (68-77°F); excursions between 15-30°C (59-86°F) are permissible.

8.8 Product Accountability

The medication provided for this study is for use only as directed in the protocol. All unused drugs will be accounted for and destroyed appropriately by site personnel. The site personnel will account for all drugs dispensed.

9. Treatment Discontinuation And Subject Withdrawals

9.1 Treatment Discontinuation

Subjects may be discontinued early from study treatment and assessments at any time, at the discretion of the investigator. Specific reasons for discontinuing a subject from this study are:

- eligibility criteria not fulfilled,
- occurrence of SAE or other safety reasons as judged by the investigator,

- development of study specific discontinuation criteria, e.g., protocol non-compliance (any protocol non-compliance will be assessed by the investigator to determine if it is severe enough to merit withdrawal),
- voluntary discontinuation by the subject, who is at any time free to discontinue his or her participation in the study without prejudice to further treatment,
- subject lost to follow-up.

9.2 Subject Withdrawals

Subjects who withdraw from the study should always be asked about the reason(s) for their discontinuation and about the presence of any AEs. The full assessments that are specified at the final follow up visit should also be carried out wherever possible. If possible, they should be seen and assessed by the investigator. AEs should be followed up and any investigational products should be returned by the subject. The reason for discontinuation of a subject must be documented into the CRF provided.

Discontinuation of any subject should be communicated to the IMU/PI. All withdrawals due to SAE must be reported to the IMU/PI within 24 hours. Withdrawals due to the occurrence of non-SAE must be reported to the IMU/PI within 15 calendar days.

Discontinued or withdrawn subjects must be followed up after the last dose of investigational product, to the extent possible. All deaths and all SAEs that occur during the follow up must be reported to the IMU/PI within 24 hours. All AEs and SAEs reported during the subjects' participation in the study should be followed until resolution as far as practicable.

9.3 Subjects replacement

In case of dropouts/withdrawals, there will be no replacements during study period 1 and 2.

10. Adverse Events (Ae) and Serious Adverse Events (Sae)

The investigator is responsible for the detection and documentation of events meeting the criteria and definition of an AE or SAE, as provided in this protocol. During the study when there is a safety evaluation, the investigator or site staff will be responsible for detecting, documenting and reporting AEs and SAEs, as detailed in this section of the protocol.

10.1 Definition of an AE

Any untoward medical occurrence in a patient or clinical investigation subject, temporally associated with the use of a medicinal product, whether or not considered related to the medicinal product.

An AE can therefore be any unfavorable and unintended sign (including an abnormal laboratory finding), symptom, or disease (new or exacerbated) temporally associated with the use of a medicinal product. For marketed medicinal products, this also includes failure to produce expected benefits (i.e. lack of efficacy), abuse or misuse.

Examples of an AE **include**:

- Exacerbation of a chronic or intermittent pre-existing condition including either an increase in frequency and/or intensity of the condition.
- New conditions detected or diagnosed after investigational product administration even though it may have been present prior to the start of the study.
- Signs, symptoms or the clinical sequelae of a suspected interaction.
- Signs, symptoms or the clinical sequelae of a suspected overdose of either investigational product or a concomitant medication (overdose per se will not be reported as an AE/SAE).

Examples of an AE **do not include** a/an:

- Medical or surgical procedure (e.g., endoscopy, appendectomy); the condition that leads to the procedure is an AE
- Situations where an untoward medical occurrence did not occur (social and/or convenience admission to a hospital)
- Anticipated day-to-day fluctuations of pre-existing disease(s) or condition(s) present or detected at the start of the study that do not worsen
- The disease/disorder being studied, or expected progression, signs or symptoms of the disease/disorder being studied, unless more severe than expected for the subject's condition.

10.2 Items to be assessed for an AE

- Seriousness
- Severity

Adverse events will be graded on a three-point scale (mild, moderate, severe) and reported in the detail indicated on the Case Report Form. The definitions are as follows:

MILD Discomfort noticed, but no disruption of normal daily activity

MODERATE Discomfort sufficient to reduce or affect normal daily activity

SEVERE Incapacitating, with inability to work or to perform normal daily activity

- Treatment
- Outcome
- Causality (Not related, Possibly related, Probably related, Related)

10.3 Definition of a SAE

A serious adverse event is any untoward medical occurrence that, at any dose:

- Results in death
- Is life-threatening

NOTE: The term 'life-threatening' in the definition of 'serious' refers to an event in which the subject was at risk of death at the time of the event. It does not refer to an event, which hypothetically might have caused death, if it were more severe.

- Requires hospitalization or prolongation of existing hospitalization

NOTE: In general, hospitalization signifies that the subject has been detained (usually involving at least an overnight stay) at the hospital or emergency ward for observation and/or treatment that would not have been appropriate in the physician's office or out-patient setting. Complications that occur during hospitalization are AEs. If a complication prolongs hospitalization or fulfills any other serious criteria, the event is serious. When in doubt as to whether "hospitalization" occurred or was necessary, the AE should be considered serious.

Hospitalization for elective treatment of a pre-existing condition that did not worsen from baseline is not considered an AE.

- Results in disability/incapacity, or

NOTE: The term disability means a substantial disruption of a person's ability to conduct normal life functions. This definition is not intended to include experiences of relatively minor medical significance such as uncomplicated headache, nausea, vomiting, diarrhea, influenza, and accidental trauma (e.g.

sprained ankle) which may interfere or prevent everyday life functions but do not constitute a substantial disruption.

- Is a congenital anomaly/birth defect

Medical or scientific judgement should be exercised in deciding whether reporting is appropriate in other situations, such as important medical events that may not be immediately life-threatening or result in death or hospitalization but may jeopardize the subject or may require medical or surgical intervention to prevent one of the other outcomes listed in the above definition. These should also be considered serious. Examples of such events are invasive or malignant cancers, intensive treatment in an emergency room or at home for allergic bronchospasm, blood dyscrasias or convulsions that do not result in hospitalization, or development of drug dependency or drug abuse.

10.4 Clinical Laboratory Abnormalities and Other Abnormal Assessments as AEs and SAEs

Abnormal laboratory findings (e.g., clinical chemistry, hematology, and urinalysis) or other abnormal assessments (e.g., ECGs, X-rays, and vital signs) that are judged by the investigator as **clinically significant** will be recorded as AEs or SAEs if they meet the definition of an AE or SAE. Clinically significant abnormal laboratory findings or other abnormal assessments that are detected during the study or are present at baseline and significantly worsen following the start of the study will be reported as AEs or SAEs. However, clinically significant abnormal laboratory findings or other abnormal assessments that are associated with the disease being studied, unless judged by the investigator as more severe than expected for the subject's condition, or that are present or detected at the start of the study and do not worsen, will **not** be reported as AEs or SAEs.

10.5 Time Period, and Frequency of Detecting AEs and SAEs

Any pre-existing condition or signs and/or symptoms present in a subject prior to the start of the study (i.e., before informed consent has been given) should be recorded as Medical/ Surgical History.

From the time a subject consents to participate in the study until he or she has completed the study (including any follow-up period), all SAEs assessed as related to study participation (e.g., protocol-mandated procedures, invasive tests, or change in existing therapy) will be reported.

All AEs/SAEs occurring after the administration of study medication and on or before the Follow-up Visit must be reported as Adverse Events/Serious Adverse Events. All AEs/SAEs must be recorded irrespective of whether they are considered drug related. AEs will be evaluated by the investigator and recorded.

Any AEs already documented at a previous assessment and designated as ongoing, should be reviewed at subsequent visits as necessary. If these have resolved, this should be documented. If an AE changes in intensity/frequency then this should be recorded as a separate event (i.e., a new record started).

10.6 Reporting of SAEs

When the investigator becomes aware of an SAE during the course of the study, the SAE must be reported to the PI or his representative within one day.

All SAEs have to be reported, whether or not considered causally related to the investigational product. All SAEs will be recorded in the Case Report Form. The investigator is responsible for informing the DSRB and/or the HAS

11. Data Analysis and Statistical Considerations

11.1 Pharmacokinetic Analysis.

Plasma/whole blood/RBC concentration-time data for lactate will be tabulated and graphically displayed for each subject. Mean plasma/whole blood/RBC concentration-time data will also be calculated for study drug.

Whole-blood and plasma lactate concentrations will be measured in duplicate using an enzymatic method (BioVision Research Products, Mountain View, CA, USA). Whole-blood and plasma lactate levels will be corrected for water content and expressed as mmol.L^{-1} of water. Intererythrocyte lactate concentrations will be calculated from whole-blood and plasma concentrations as follows:

$$C_c = [Cb - Cp(1 - Hct)] / Hct$$

Where C_c is the erythrocyte lactate concentration, Cb is the measured venous blood lactate concentration and Cp is the measured plasma lactate concentration, and Hct is the measured haematocrit.

Data will be collected and averaged, and compared by using paired Student's t-test. Significance will be set at $p > 0.05$ and all data will report as mean \pm standard deviation.

11.2 Safety Data Analysis

Safety data, including adverse events and clinical laboratory evaluations, will be summarized by treatment. No formal statistical comparisons will be made for safety data.

11.3 Statistical Considerations

Sample size assumptions. A 80% powered analysis estimates that a minimum number of N=8 is required to detect a minimum difference of 30% in plasma, whole blood and RBCs lactate levels, at a level of significance of $p=0.05$ (mean plasma lactate = 16.7 ± 3.81 mmol/l; mean erythrocyte lactate = 8.0 ± 2.42 mmol/l; mean whole blood lactate = 12.4 ± 2.42 mmol/l). In case of discontinuing, loss of follow-up, or any other cause for the subjects not to accomplish this study, the number of subject increase to N=12.

12. Study Management

12.1 Monitoring

The monitoring of this study will be performed in accordance with the principle of Good Clinical Practice (GCP) as laid out in the International Conference on Harmonisation (ICH) document "Good Clinical Practice: Consolidated Guideline", by staff of the IMU.

12.2 Training of Staff

The principal investigator and IMU Manager will maintain a record of all individuals involved in the study (medical, nursing and other staff). He or she will ensure that appropriate training relevant to the study is given to all of these staff, and that any new information of relevance to the performance of this study is forwarded to the staff involved.

12.3 Changes to the Protocol

Study procedures will not be changed without the approval of the principal investigator.

If it is necessary for the study protocol to be amended, the amendment and/or a new version of the study protocol must be notified to the DSRB and HSA.

12.4 Study Timetable and Termination

The first subject is expected to enroll in beginning of 2010 and all subjects are expected to complete the study by early March 2010.

12.5 Data Management

12.5.1 Case Report Form

Case report form (CRF) will be used to record all data not captured electronically. The actual date and time of each dose and each blood sample will be recorded on a

Case Report Form. Data should be recorded legibly onto the CRFs in blue or black ball-point pen. Correction fluid or covering labels must not be used.

Brief CRFs will be completed for subjects who sign a consent form to participate but who are not entered into the study.

12.5.2 Pharmacogenetic Data

The samples and data for genetic analysis in this study will be coded. The samples will be labelled with a clinical study subject number that can be traced back to the subject only by the investigator. The samples and data will not carry a personal identifier. Pharmacogenetic data will be managed by the Pharmacogenetics Lab NUS.

12.5.3 Safety Measurements

Safety will be assessed by adverse events, physical examination, blood pressure, heart rate, pulse, clinical chemistry, hematology, and urinalysis in order to assure the health and well being of subjects participating in this trial as well as provide beginning information regarding the safety profile of the administered drugs.

13. Ethics

13.1 Ethics Review

The final study protocol and the final version of the Written Informed Consent Form must be approved or given a favorable opinion in writing by the DSRB as appropriate. The principal investigator is responsible for informing the DSRB of any amendment to the protocol in accordance with local requirements. In addition, the DSRB must approve all advertising used to recruit subjects for the study. The protocol must be re-approved by the DSRB annually, as local regulations require.

The principal investigator must submit progress reports to the DSRB according to local regulations and guidelines. The principal investigator must also provide the DSRB with any reports of serious adverse events from the study site.

13.2 Ethical Conduct of the Study

The study will be performed in accordance with the ethical principles that have their origin in the Declaration of Helsinki and are consistent with Good Clinical Practice, applicable regulatory requirements.

13.3 Subject Information and Consent

The principal investigator at each centre will ensure that the subject is given full and adequate oral and written information about the nature, purpose, possible risk and benefit of the study. Subjects must also be notified that they are free to discontinue from the study at any time. The subject should be given the opportunity to ask questions and allowed time to consider the information provided.

The subject's signed and dated informed consent must be obtained before conducting any procedure specifically for the study.

The principal investigator must store the original, signed Written Informed Consent Form. A copy of the Written Informed Consent Form must be given to the subject.

13.4 Subject Data Protection

The Written Informed Consent Form will explain that study data will be stored in a computer database. The Written Informed Consent Form will also explain that for data verification purposes, authorized representatives of a regulatory authority, DSRB may require direct access to parts of the hospital or practice records relevant to the study, including subjects' medical history.

Reference:

1. Halestrap AP, Meredith D. The SLC16 gene family-from monocarboxylate transporter (MCTs) to aromatic amino acid transporters and beyond. *Eur. J. Physiol.* 2004;447:619-628.
2. Meredith D and Christian HC. The SLC16 monocarboxylate transporter family. *Xenobiotica* 2008;38:1072-1106.
3. Enerson BE, Drewes LR. Molecular features, regulation, and function of monocarboxylate transporters: implications for drug delivery. *J Pharm Sci* 2003; 92(8):1531-44.
4. Merezhinskaya N, Fishbein WN. Monocarboxylate transporters: past, present, and future. *Histol Histopathol* 2009;24(2):243-64.
5. Gladden LB. Is there an intracellular lactate shuttle in skeletal muscle? *J Physiol.* 2007;582(Pt 3):899.
6. De Bruijne AW, Vreeburg H, Van Steveninck J. Kinetic analysis of L-lactate transport in human erythrocytes via the monocarboxylate-specific carrier system. *Biochim Biophys Acta.* 1983;732(3):562-8.
7. McKelvie RS, Lindinger MI, Heigenhauser GJ, Jones NL. Contribution of erythrocytes to the control of the electrolyte changes of exercise. *Can J Physiol Pharmacol.* 1991;69(7):984-93.
8. Deuticke B, Beyer E, Forst B. Discrimination of three parallel pathways of lactate transport in the human erythrocyte membrane by inhibitors and kinetic properties. *Biochim Biophys Acta.* 1982;684(1):96-110.
9. Poole RC, Halestrap AP. Transport of lactate and other monocarboxylates across mammalian plasma membranes. *Am J Physiol.* 1993;264(4 Pt 1):C761-82. Review.
10. Deuticke B. Monocarboxylate transport in red blood cells: kinetics and chemical modification. *Methods Enzymol.* 1989;173:300-29.
11. Skelton MS, Kremer DE, Smith EW, Gladden LB. Lactate influx into red blood cells of athletic and nonathletic species. *Am J Physiol.* 1995;268(5 Pt2):R1121-8.

12. Halestrap AP, Price NT. The proton-linked monocarboxylate transporter (MCT) family: structure, function and regulation. *Biochem J.* 1999;343 Pt 2:281-99. Review.
13. Fishbein WN. Lactate transporter defect: a new disease of muscle. *Science* 1986 ;234(4781):1254-6.
14. Poole RC, Sansom CE, Halestrap AP. Studies of the membrane topology of the rat erythrocyte H⁺/lactate cotransporter (MCT1). *Biochem J.* 1996;320 (Pt 3):817-24.
15. Coco M, Di Corrado D, Calogero RA, Perciavalle V, Maci T, Perciavalle V. Attentional processes and blood lactate levels. *Brain Res.* 2009;1302:205-11.
16. Miller BF, Fattor JA, Jacobs KA, Horning MA, Navazio F, Lindinger MI, Brooks GA. Lactate and glucose interactions during rest and exercise in men: effect of exogenous lactate infusion. *J Physiol.* 2002;544(Pt 3):963-75.
17. Miller BF, Fattor JA, Jacobs KA, Horning MA, Suh SH, Navazio F, Brooks GA. Metabolic and cardiorespiratory responses to "the lactate clamp". *Am J Physiol Endocrinol Metab.* 2002;283(5):E889-98.
18. van Hall G, Strømstad M, Rasmussen P, Jans O, Zaar M, Gam C, Quistorff B, Secher NH, Nielsen HB. Blood lactate is an important energy source for the human brain. *J Cereb Blood Flow Metab.* 2009 ;29(6):1121-9.
19. Choi JS, Jin MJ, Han HK. Role of monocarboxylic acid transporters in the cellular uptake of NSAIDs. *J Pharm Pharmacol.* 2005;57(9):1185-9.
20. Tempero KF, Cirillo VJ, Steelman SL. Diflunisal: a review of pharmacokinetic and pharmacodynamic properties, drug interactions, and special tolerability studies in humans. *Br J Clin Pharmacol.* 1977;4 Suppl 1:31S-36S. Review.

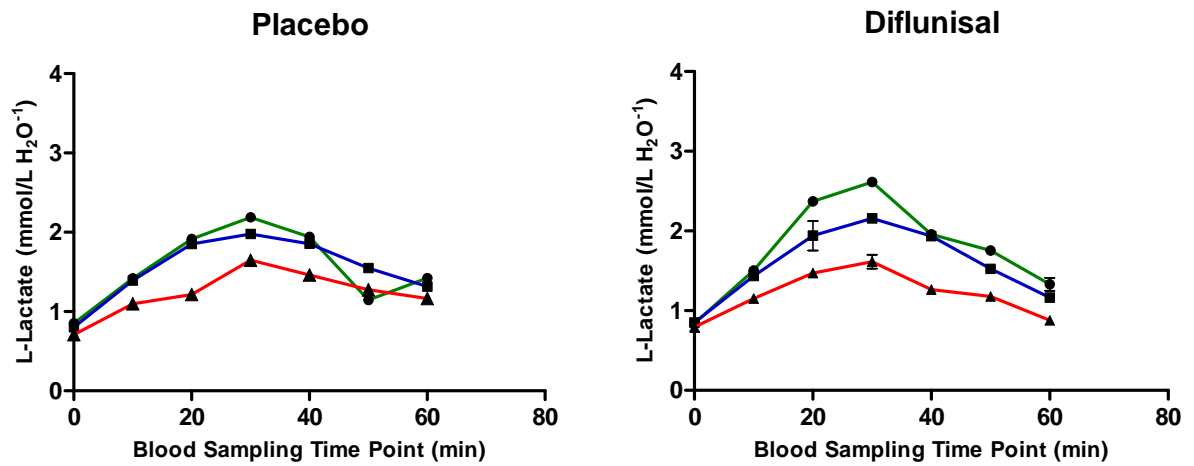
APPENDIX III.

Legend: Green line: Plasma Lactate Concentration

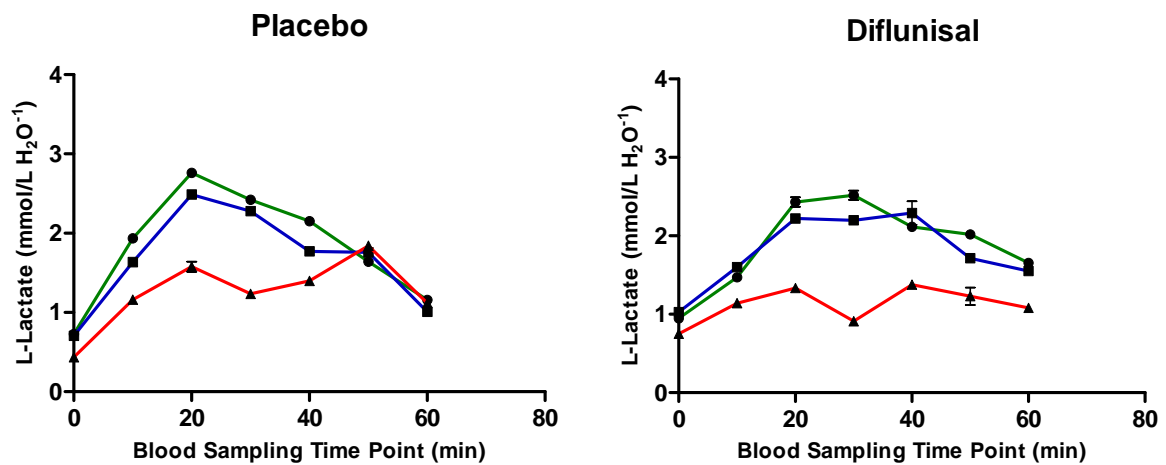
Blue line: Whole Blood Lactate Concentration

Red line: Erythrocyte Lactate Concentration

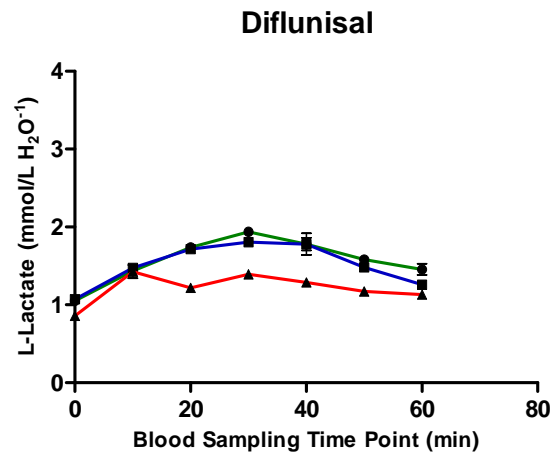
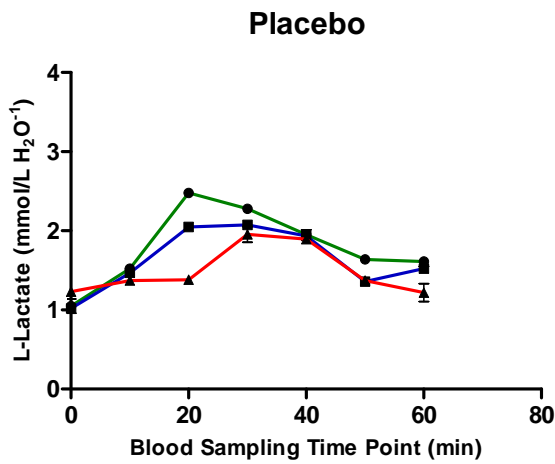
Subject Initial: CGY



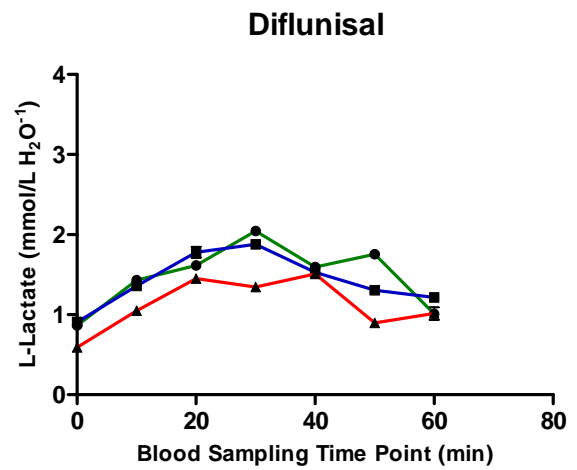
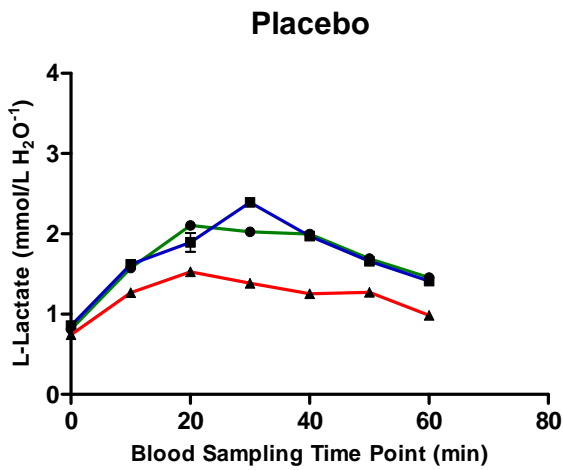
Subject Initial: LCK



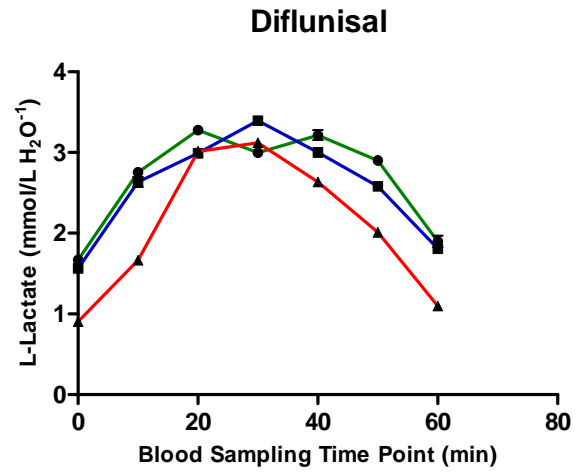
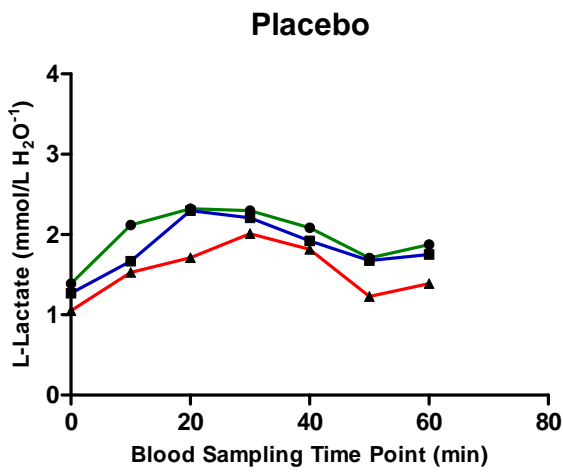
Subject Initial: DDJ



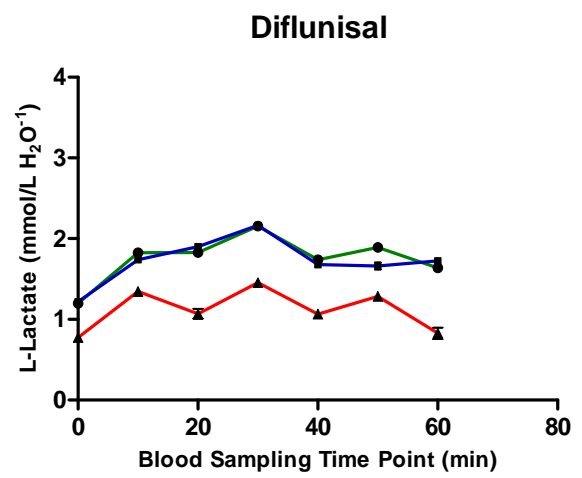
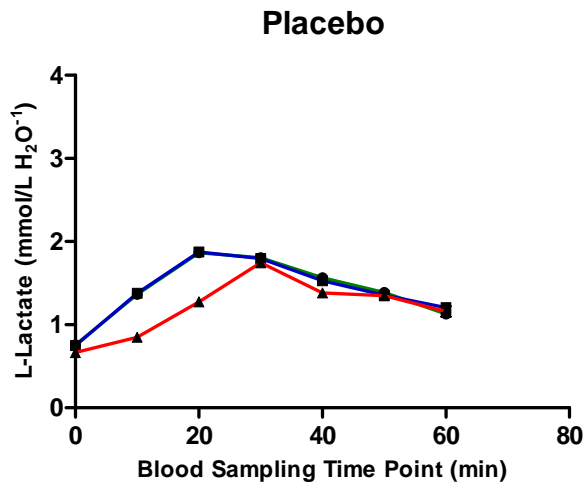
Subject Initial: KPL



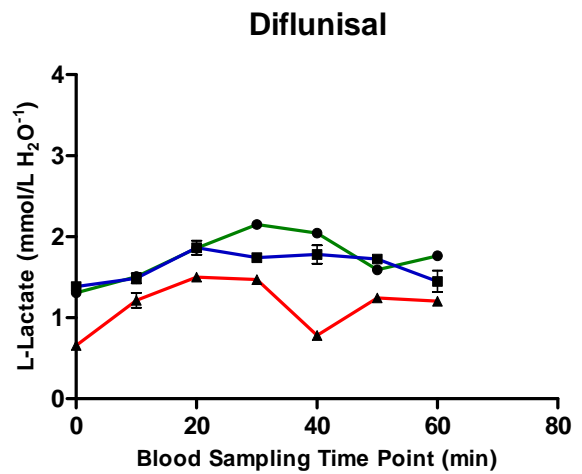
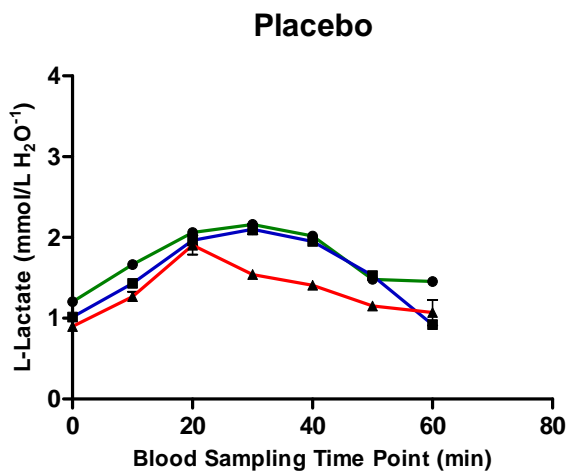
Subject Initial: LCY



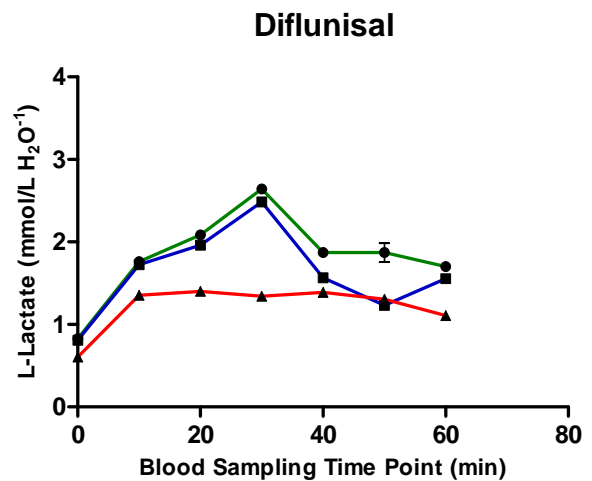
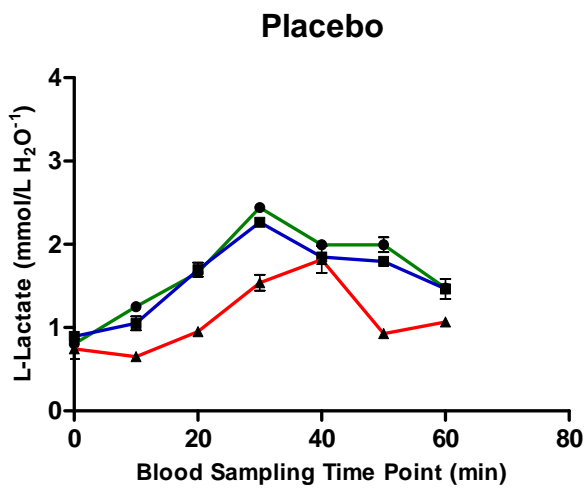
Subject Initial: TYC



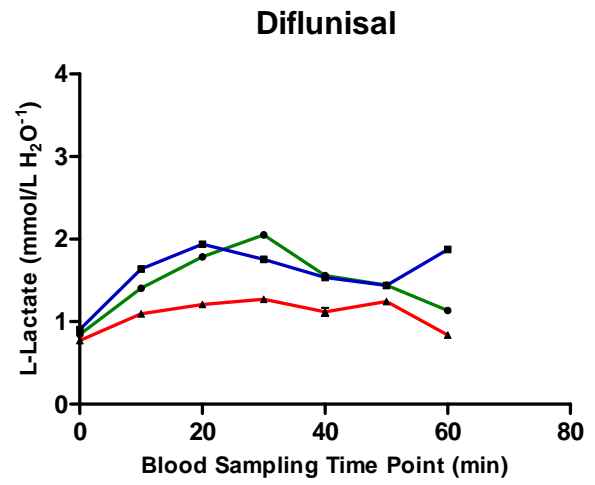
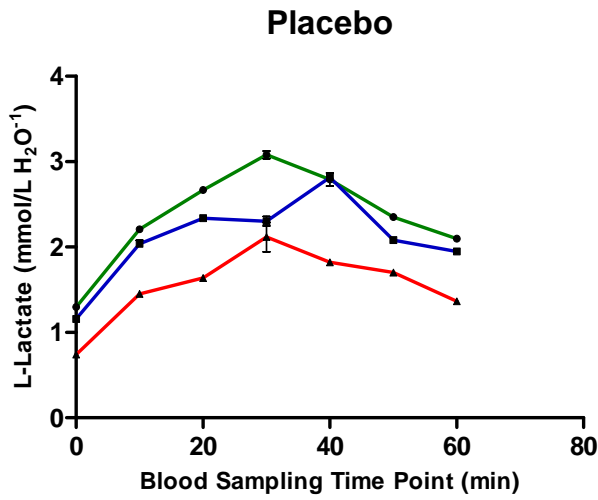
Subject Initial: TSM



Subject Initial: TKW



Subject Initial: TSH



Subject Initial: TKC

